UNIVERSIDAD DE GRANADA

DEPARTAMENTO DE INGENIERÍA DE LA CONSTRUCCIÓN Y PROYECTOS DE INGENIERÍA

UNIVERSIDAD
DE GRANADA

DESARROLLO DE ELEMENTOS ELÁSTICOS SOSTENIBLES E INTELIGENTES PARA LA MONITORIZACIÓN DE VÍAS DE FERROCARRIL

LÍNEA DE INVESTIGACIÓN DEL PROGRAMA EN LA QUE SE INSCRIBE: INGENIERÍA DE LA CONSTRUCCIÓN Y DEL TERRENO

TESIS DOCTORAL

JUAN MANUEL CASTILLO MINGORANCE

Para la obtención del

GRADO DE DOCTOR POR LA UNIVERSIDAD DE GRANADA

Programa Oficial de Doctorado en Ingeniería Civil (B23.56.1)

Granada, enero 2025

UNIVERSIDAD DE GRANADA

DEPARTAMENTO DE INGENIERÍA DE LA CONSTRUCCIÓN Y PROYECTOS DE INGENIERÍA

UNIVERSIDAD
DE GRANADA

DESARROLLO DE ELEMENTOS ELÁSTICOS SOSTENIBLES E INTELIGENTES PARA LA MONITORIZACIÓN DE VÍAS DE FERROCARRIL

TESIS DOCTORAL

D. Juan Manuel Castillo Mingorance

Ingeniero de Caminos, Canales y Puertos

Directores de tesis:

D. Miguel Del Sol Sánchez

Dr. Ingeniero de Caminos, Canales y Puertos

D. Fernando M Moreno Navarro

Dr. Ingeniero de Caminos, Canales y Puertos

Granada, enero 2025

Editor: Universidad de Granada. Tesis Doctorales
Autor: Juan Manuel Castillo Mingorance
ISBN: 978-84-1195-850-9
URI: https://hdl.handle.net/10481/106413

Agradecimientos

Quisiera aprovechar este espacio para mostrar mi agradecimiento a todas aquellas personas que directa o indirectamente han puesto su grano de arena para que haya alcanzado esta meta tan importante para mí.

En primer lugar, agradecer a mis directores de tesis, tanto a Miguel del Sol Sánchez, como a Fernando Moreno Navarro por el entusiasmo y el ímpetu con el que me han trasmitido sus conocimientos y sus consejos, así como la paciencia y generosidad prestada a lo largo de toda esta etapa.

En segundo lugar, quisiera agradecer a mis compañeros del Laboratorio de Ingeniería de la Construcción de la Universidad de Granada, LabIC.UGR, (Gema, Raúl, Mari Carmen, Tom, Rafa, Ana Elena, Manolo, …) todo el apoyo prestado, así como su colaboración a lo largo de todo el trabajo. En especial, quisiera agradecer a la directiva del LabIC.UGR, en especial a Mayca, la oportunidad que me han dado de formar parte de esa gran familia de los cuales más que compañeros, puedo asegurar que para mí ya son amigos/as.

Dentro del plano personal, quiero dedicar esta tesis doctoral a mis padres y hermana, quienes en ningún momento han dejado de apoyarme y darme fuerzas en los momentos de más debilidad para no abandonar, ya que para mí compaginar mi trabajo y dedicación en la empresa familiar con mi última etapa como estudiante de doctorado ha sido una gran carrera de fondo.

A mi mujer María del Mar, siendo la más grande razón en mi vida encaminada al triunfo, fue el ingrediente ideal para poder conseguir lograr esta dichosa y muy digna victoria en la vida, el poder haber culminado esta tesis. Te agradezco por tantas ayudas y muchos aportes no solo para el avance de mi tesis, sino además para mi vida; eres mi inspiración y mi razón.

A mi hijo Juanma, que, con su sonrisa y simpatía, me ha dado las fuerzas para darle el último empujón a este proyecto personal y poder llegar a la meta de convertirme en Dr. Ingeniero de Caminos, Canales y Puertos, de lo cual, sé que estará muy orgulloso.

A todos, gracias.

Declaración

Memoria presentada por D. Juan Manuel Castillo Mingorance para la obtención al grado de Doctor por la Universidad de Granada.

El doctorando D. Juan Manuel Castillo Mingorance, y los directores de tesis D. Miguel Del Sol Sánchez y D. Fernando M. Moreno Navarro, declaran al firmar este documento, que el trabajo presentado para la obtención del grado de Doctor ha sido realizado en su totalidad por el doctorando bajo la dirección de ambos directores, y hasta donde su conocimiento alcanza, durante el desarrollo del trabajo se han respetado los derechos de otros autores citados en la sección de bibliografía, cuando sus resultados o publicaciones han sido utilizadas.

Granada, 15 de enero de 2025

Directores de la Tesis:

Fdo.: Miguel del Sol Sánchez

Fdo.: Fernando M. Moreno Navarro

Doctorando:

Fdo.: Juan Manuel Castillo Mingorance

Tesis como agrupación de publicaciones

La Tesis Doctoral se basa en la agrupación de artículos publicados por el Doctorando en revistas científicas internacionales, relevantes en el área de conocimiento en el que se enmarca la tesis. Para el reconocimiento de Tesis por Compendio de Publicaciones se han cumplido los siguientes requerimientos:

- La tesis consiste en la agrupación de cuatro artículos científicos en la presente memoria. El doctorando es autor de los cuatro trabajos de investigación publicados en revistas de relevante impacto internacional dentro del campo de conocimiento de los materiales y tecnologías para la infraestructura ferroviaria, siendo esta la línea de investigación en la que queda enmarcada la Tesis Doctoral.
- Los artículos han sido aceptados con fecha posterior a la obtención del título de grado y de máster por parte del doctorando. Dichas fechas se corresponden con el 5 de julio de 2017 y el 25 de septiembre de 2019, respectivamente, mientras que los artículos han sido publicados a partir de noviembre del 2020.
- Las publicaciones recogidas en este Tesis Doctoral no han sido utilizadas en ninguna tesis anterior.
- Los coautores de los artículos declaran no haber presentado dichas publicaciones en otra tesis, y renuncian a hacerlo en tesis posteriores. El trabajo y contribución del doctorando ha sido indicado y declarado en los documentos administrativos correspondientes.
- La Tesis Doctoral integra las publicaciones como anexos dentro de la presente memoria.

Los artículos científicos en los que se basa la agrupación de publicaciones de la Tesis Doctoral son los siguientes:

Castillo-Mingorance, J.M.; Sol-Sánchez, M.; Moreno-Navarro, F., Rúbio Gámez; M.C. *A Critical Review of Sensors for the Continuos Monitoring of Smart and Suistainable Railway Infraestructures*. Sustainability, 12 (2020) 9428. (Índice de Impacto 3,3 en 2.023, Q2 en ENVIRONMENTAL SCIENCES en 2.023).
https://doi.org/10.3390/su12229428

Castillo-Mingorance, J.M.; Sol-Sánchez, M.; Mattinzioli, T.; Moreno-Navarro, F., Rúbio Gámez; *Development of rail pads from recycled polymers for ballasted railway tracks.* Constr. Build. Mater. 337 (2022) 127479. (Índice de Impacto 7,4 en 2.023, Q1 en CIVIL ENGENIERING,

MATERIALS SCIENCE (MULTIDISCIPLINARY), y CONSTRUCTION & BUILDING TECHNOLOGY en 2.023).

https://doi.org/10.1016/j.conbuildmat.2022.127479

Sol-Sánchez, M.; **Castillo-Mingorance, J.M.**; Moreno-Navarro, F.; Rubio-Gámez, M.C. *Smart rail pads for the continuos monitoring of sensored railway tracks: Sensor analysis.* Autom. Constr. 132 (2021) 103950. (Índice de Impacto 9,6 en 2.023, Q1 en CIVIL ENGENIERING y CONSTRUCTION & BUILDING TECHNOLOGY en 2.023). https://doi.org/10.1016/j.autcon.2021.103950

Sol-Sánchez, M.; **Castillo-Mingorance, J.M.**; Moreno-Navarro, F.; Mattinzioli, T.; Rubio-Gámez, M.C. *Piezolectric-sensored sustainable pads for smart railway traffic and track state monitoring: Full-scale laboratory test. Constr. Build. Mater.* 301 (2021) 124324. (Índice de Impacto 7,4 en 2.023, Q1 en CIVIL ENGENIERING, MATERIALS SCIENCE (MULTIDISCIPLINARY), y CONSTRUCTION & BUILDING TECHNOLOGY en 2.023). https://doi.org/10.1016/j.conbuildmat.2021.124324

Índice

Índice de Figuras

Índice de Tablas

Resumen

Las necesidades del transporte, tanto de personas como de mercancías, así como la competencia existente entre modos de transporte ha provocado, para poder satisfacer las necesidades del posible consumidor, un importante incremento en las velocidades de circulación de los trenes y de su capacidad de carga de mercancías. En los últimos años, la movilidad ha experimentado un crecimiento exponencial y con ello, la sobre-explotación de las infraestructuras sobre las que circulan los vehículos, requiriendo mayores inversiones en conservación para así poder asegurar su funcionalidad y seguridad.

En este marco, actualmente existe la necesidad y tendencia hacia el desarrollo de materiales y tecnologías que permitan mejorar la operatividad y eficiencia del ferrocarril a través de la optimización de los tiempos, recursos y costes derivados de las actividades de mantenimiento (cada vez más altos debido a la sobre explotación de las infraestructuras). Por esta razón, el mantenimiento predictivo es una herramienta con una demanda creciente debido al gran potencial que presenta, permitiendo transformar las actividades de mantenimiento correctivo (generalmente más costosas) en mantenimiento preventivo (el cuál es posible realizar en las horas valle de uso de la infraestructura).

El reto actual se centra en predecir estos fallos para establecer estrategias de mantenimiento preventivo. Para ello, es necesario el desarrollo de elementos que permitan llevar a cabo una monitorización continua de la vía a través de la implementación de elementos inteligentes que permitan transformar las actuaciones correctivas en predictivas, logrando así posicionar al sector del ferrocarril entre los principales modos de transporte, todo ello, sin olvidar la importancia de apostar por un desarrollo sostenible a través de la reducción en el consumo de materias primas y la apuesta por la reutilización y reciclaje de materiales. Es por ello, que la presente tesis tiene como objetivo principal el desarrollo de elementos elásticos sostenibles mediante el uso de materiales reciclados e inteligentes a través de la inclusión de sensores.

Para la consecución de estos objetivos se han llevado a cabo una serie de etapas de trabajo que comprenden (i) el desarrollo y caracterización de materiales poliméricos reciclados para ser empleados en la fabricación de placas de asiento sostenibles, (ii) el diseño de placas de asiento con diferentes materiales reciclados y geometrías con el fin de obtener una amplia gama de soluciones elásticas sostenibles con distintas propiedades que puedan dar respuesta a las necesidades de la vía, (iii) la selección y calibración de los sensores más adecuados para su uso en las placas de asiento inteligentes y funcionales, (iv) el diseño placas de asiento sostenibles e

inteligentes mediante la inclusión de sensores que permitan la monitorización de la vía y (v) la prueba y validación de la funcionalidad de los elementos elásticos sostenibles e inteligentes a través de ensayos a escala real.

1. Introducción

En los últimos años, la movilidad de personas y mercancías ha experimentado un crecimiento exponencial y con ello, la utilización de la infraestructura, aumentando el número de trenes que circulan por las vías [1]. Este hecho, junto con el aumento de las exigencias de calidad y seguridad del transporte viene requiriendo mayores inversiones en conservación y mantenimiento de las infraestructuras para así poder asegurar su funcionalidad y seguridad. En este contexto, el ferrocarril presenta algunas ventajas frente a los otros modos de transporte como pueden ser la reducción de las emisiones de CO_2 alrededor del 30% frente a otros modos como el coche o el avión, el empleo de una menor cantidad de energía por pasajero-km que el autobús, el coche o el avión (llevando 3 veces más de pasajeros con la misma cantidad de energía), una ocupación del espacio tres veces menor que las autovías o la reducción de los costes externos asociados a factores como pueden ser los accidentes o el cambio climático [2].

Sin embargo, con el objetivo de continuar con el posicionamiento del ferrocarril como medio de transporte de referencia, es necesario seguir desarrollando un sistema moderno, inteligente y medioambientalmente sostenible que permita garantizar un buen uso de los recursos disponibles. En este contexto, con el fin de asegurar una buena operatividad del sistema, existe la necesidad de transformar el modelo de mantenimiento correctivo, en el cual una vez aparece una deficiencia en el sistema, ésta se corrige, hacia un modelo predictivo, el cual permite disminuir considerablemente los impactos sociales y económicos [3] [4].

En este marco, actualmente existe la necesidad y tendencia hacia el desarrollo de materiales y tecnologías que permitan mejorar la operatividad y eficiencia del ferrocarril a través de la optimización de los tiempos, recursos y costes derivados de las actividades de conservación. Por esta razón, el mantenimiento predictivo es una herramienta con una demanda creciente debido al gran potencial que presenta, permitiendo transformar las actividades correctivas (generalmente más costosas) en preventivas (las cuales son posible realizarlas en las horas valle de uso de la infraestructura) [5].

El avance de las nuevas tecnologías y el desarrollo de nuevos sensores ha permitido mejorar la capacidad en el conocimiento del estado de la vía, permitiendo una mejor programación de las actividades de conservación de la vía y dando respuesta así a las necesidades de mantenimiento. El circuito inventado por William Robinson en 1872 pudo ser considerado como el primer sistema de vigilancia y control de la vía con el fin de prevenir accidentes [6]. Desde entonces, numerosas técnicas de seguimiento y variedad de sensores han

sido desarrollados para ser aplicados tanto en elementos móviles como en secciones de vía, con el fin de controlar el tráfico y las condiciones de la infraestructura ferroviaria. Para ello, se han empleado multitud de sensores tales como acelerómetros, galgas extensiométricas, correlación digital de imágenes, geófonos, sensores magnéticos y deflectómetros entre otros [7]. Sin embargo, muchos de estos sensores convencionales no son prácticos para la monitorización de la vía a largo plazo, debido a que presentan una configuración compleja, falta de precisión en las medidas en situaciones adversas, posibilidad de deterioro y/o robo debido a su uso externo en la vía, y un precio elevado, entre otros inconvenientes. De este modo, en los últimos años se está apostando por el uso de sensores embebidos en componentes de la vía que permitan mitigar parte de estos inconvenientes, aunque actualmente sigue siendo una técnica en vías de desarrollo.

Por otro lado, para dar respuesta al incremento de las cargas al cual están sometidas las vías de ferrocarril, es fundamental la inclusión de materiales elásticos, tales como placas de asiento, que permitan amortiguar las cargas y adaptar la rigidez de la vía a la tipología de tráfico a la cual va estar sometida. Una rigidez de la vía alta podría incrementar las cargas dinámicas y la presión sobre la subestructura, mientras que una rigidez baja, produciría daños en las vías del ferrocarril, al no ser capaz de amortiguar los impactos producidos por los trenes durante su circulación. Es por ello, que, durante los últimos años, se estén desarrollando diferentes soluciones con el fin de optimizar la rigidez de la vía para conseguir un sistema que combine estabilidad y capacidad de amortiguamiento de cargas [8] [9] [10] [11]. Además, con el fin de dotar de carácter sostenible a este componente, habitualmente fabricado a partir de polímeros derivados del petróleo, surge la oportunidad de emplear materiales reciclados en su producción, lo que permitiría reducir los impactos económicos y ambientales asociados a estos componentes de vía.

Así, dentro de estas soluciones, cobra especial relevancia la posibilidad de integrar ambas líneas de investigación en un sólo elemento funcional. Por un lado, el desarrollo de elementos elásticos sostenibles a partir de materiales reciclados que permitan optimizar el comportamiento y durabilidad de la vía desde el punto de vista de la sostenibilidad, y, por otro lado, la inclusión de sensores para la monitorización de la vía. Así, esta Tesis Doctoral se centra en el estudio y desarrollo de elementos elásticos sostenibles que incluyan sensores para la monitorización de vía, desde un punto de vista funcional, eficiente y respetuoso con el medioambiente.

2. Estado del Arte

En este apartado se recoge un resumen y conclusiones del estudio del Estado del Arte de la presente Tesis Doctoral, el cual está recogido en el primer artículo de la agrupación de publicaciones (Anexo I - *A Critical Review of Sensors for the Continuos Monitoring of Smart and Suistainable Railway Infraestructures*).

A partir del estudio del Estado del Arte, las siguientes conclusiones pueden ser extraídas:

La evolución de los sistemas de ensayos mediante métodos de monitorización continua de la vía permite, mediante el uso de sensores, la detección temprana de los principales modos de fallo que sufren y degradan la infraestructura. Las operaciones de mantenimiento predictivo permiten optimizar los recursos existentes, obteniendo un sistema más inteligente y sostenible [5]. Los avances producidos en los últimos años en el desarrollo de los sensores han permitido obtener componentes cada vez más pequeños, más precisos y más económicos. Este aumento de la viabilidad técnica y económica en el uso de dichos dispositivos ha propiciado su interés en diversos campos como puede ser el monitoreo ambiental [12], de puentes [13] o incluso, de infraestructuras lineales [14]. Gracias a ello, el ferrocarril podría seguir siendo considerado un referente para el transporte moderno, inteligente y eficiente, lo que lo convierte en uno de los medios más competitivos a la vez que se disminuyen los costes de conservación y explotación al permitir un mantenimiento predictivo continuo de la vía. Por tanto, conseguir un sistema de monitorización capaz de detectar y predecir los principales modos de fallo de la vía férrea, como deformaciones permanentes, cambios en la sección estructural, fallos por fatiga de los materiales o vibraciones o ruido.

El control de los principales modos de fallo de las vías ferroviarias sobre balasto se puede realizar mediante el uso de sensores avanzados pero simples capaces de medir parámetros de la vía como deformaciones, vibraciones, oscilaciones de la vía o incluso las fuerzas dinámicas producidas por el tráfico ferroviario. En este sentido, se ha demostrado que los sensores de fibra óptica se encuentran entre los más versátiles, pudiendo monitorizar propiedades tales como deformaciones, tensiones, vibraciones o incluso temperaturas con un único componente. Sin embrago, hay que tener en cuenta el elevado precio de esta tecnología que, en comparación con otras alternativas, requerirán de un mayor grado de investigación y desarrollo que permita un uso más generalizado. Por otro lado, el uso de galgas extensiométricas permitirían registrar las micro deformaciones producidas en el material, sin embargo, presenta ciertas desventajas, tales como su fragilidad, son susceptibles a las interferencias electromagnéticas y se ven

afectadas por los cambios de temperatura. Por otro lado, también se ha visto que se podría monitorizar el estado de la vía a través de la medición de la transmisión de tensiones y vibraciones, donde diversas experiencias demostraron que los piezoeléctricos y los acelerómetros presentan un buen potencial para esta aplicación. Esto se destaca especialmente en el caso de los piezoeléctricos por sus diversas ventajas, como su alta linealidad y su bajo coste, al tiempo que permite un registro claro de la dinámica de cargas (intensidad y frecuencia).

Por todo ello, de las conclusiones obtenidas del estudio del estado del arte, ha propiciado que la presente tesis doctoral se haya centrado en el desarrollo de elementos elásticos sostenibles e inteligentes, focalizándose en el desarrollo de placas de asiento inteligentes mediante la inclusión de sensores piezoeléctricos de bajo coste, gracias a su susceptibilidad para ser embebidos en las placas, por dimensiones y propiedades físicas.

3. Objetivos

3.1. Objetivo general

A partir de las conclusiones extraídas en el estudio del estado del Arte se han identificado las necesidades en el avance de materiales para un ferrocarril más eficaz y eficiente. Así, el objetivo de la presente tesis doctoral consiste en el desarrollo de placas de asiento sostenibles, mediante el uso de materiales reciclados, e inteligentes a través de la inclusión de sensores, que permitan llevar a cabo la monitorización continua de la vía.

3.2. Objetivos específicos

Para el desarrollo de las placas de asiento sostenibles a partir de materiales reciclados e inteligentes mediante la inclusión de sensores se plantean los siguientes objetivos específicos:

- Desarrollar y caracterizar materiales poliméricos reciclados para ser empleados en la fabricación de placas de asiento sostenibles. (artículo 2)

- Diseñar placas de asiento con diferentes materiales reciclados y geometrías con el fin de obtener una gama de soluciones elásticas sostenibles con distintas propiedades que puedan dar respuesta a las necesidades de la vía (artículo 2).

- Seleccionar y calibrar los sensores más adecuados para su uso en las placas de asiento inteligentes y funcionales y diseñar dichas éstas mediante la inclusión de estos componentes que permitan la monitorización de la vía (artículo 3)

- Evaluar y validar la funcionalidad de los elementos elásticos sostenibles e inteligentes (artículo 4).

4. Metodología

Para la consecución de los objetivos marcados en la presente tesis doctoral, la metodología seguida para el desarrollo de los elementos elásticos sostenibles (mezcla de polímeros reciclados y partículas de caucho procedentes de neumáticos fuera de uso) e inteligentes mediante la inclusión de sensores que permitan la monitorización continua de la vía, tras el estudio del estado del arte, se puede dividir en tres etapas principales:

(i) Se han desarrollado diferentes materiales a partir de polímeros reciclados los cuales han permitido elaborar placas de asiento con diferentes comportamientos mecánicos.

(ii) Una vez validado y conocido el comportamiento de las mismas, se ha llevado a cabo la inclusión de distintos tipos de sensores en estos elementos elásticos con el fin de seleccionar el tipo de sensor más apropiado para el conseguir el objetivo de monitorizar el comportamiento de la vía a partir de sus señales. Para ello, se han realizado diferentes ensayos de laboratorio que han permitido conocer la sensibilidad y viabilidad de cada tipo de sensor, así como su aptitud ante los principales procesos de fallo que presentan esta tipología de elementos elásticos.

(iii) Finalmente, una vez estudiado los materiales, la morfología de las placas y los sensores, se han validado las placas de asiento mediante ensayos de laboratorio a escala real.

Con el fin de describir con mayor profundidad las metodologías seguida en las citadas fases de investigación, este cuarto capítulo se estructura primero, en describir los materiales empleados a lo largo de la tesis doctoral, para seguidamente describir el plan de ensayos y métodos de laboratorio.

4.1. Materiales

Esta sección recoge un resumen de los materiales utilizados en las distintas fases de la Tesis Doctoral, mostrando mayor detalle en los artículos recogidos en los anexos.

4.1.1. Materiales empleados para el diseño y desarrollo de las placas sostenibles (artículo 2)

Para el desarrollo de las placas de asiento se han empleado cuatro materiales diferentes. Tres de ellos fueron usados como material aglomerante (R-HDPE, R-PP/PE and Resin) cuyas especificaciones se definen a continuación, los cuales fueron mezclados con partículas de caucho procedentes de neumáticos fuera de uso (CR) en diferentes proporciones y

granulometrías. En este caso CR fue usado como modificador de la rigidez de las placas de asiento. Hay estudios previos que demuestran que la inclusión de CR puede modificar la rigidez global de la vía, como, por ejemplo, mediante el proceso del Stone blowing [15].

Los materiales empleados como aglomerantes se describen a continuación:

Figura 1. Materiales empleados en la fabricación de placas de asiento

- R-HDPE. Se trata de polietileno de alta densidad procedente de cajas de plástico fuera de uso. Su densidad se encuentra sobre 980 kg/m3. El proceso de reciclaje de este material consiste en la recolección, limpieza y triturado en partículas de un tamaño menor a 5 mm.

- R-PP/PE. Se trata de material procedente del residuo de geomembranas utilizadas para impermeabilización, el cual está formado por dos capas diferentes. La capa impermeabilizante esta principalmente formada por polietileno de baja densidad (LDPE), aunque contiene otros polímeros como el polipropileno (PP). Además, la geomembrana también contiene fibras de poliéster (trazas blancas), con fines protectores. En la capa más superficial del mismo, puede contener diferentes aditivos,

tales como, tintes, antioxidantes y estabilizadores térmicos y de radiación UV Este material tiene una densidad media de 930 kg/m^3.

- Resin. Resina industrial polimérica bicomponente compuesta de poliuretano, con propiedades elásticas. Este material tiene una dureza de 60 a 7 días (DIN 53505) y una Resistencia a la abrasión de 65 mg a 14 días (ASTM D 4060). Este material ha sido elegido como material industrial de referencia, el cual nos permite validar el comportamiento de los materiales reciclados.

Por otro lado, las partículas de caucho procedentes de neumáticos fuera de vida útil, fueron empleadas como modificadores de la rigidez de las placas de asiento con el fin de proporcionar una amplia gama de soluciones elásticas para su uso en distintos tipos de vías. Para ello, se emplearon tres granulometrías distintas, específicamente, menores de 0,6 mm (R0.6), entre 0.6 y 2 mm (R2) y entre 2 y 4 mm. La Figura 2 muestra la curva granulométrica de las partículas de caucho empleadas. La densidad media de este material es de 1,170 kg/m3.

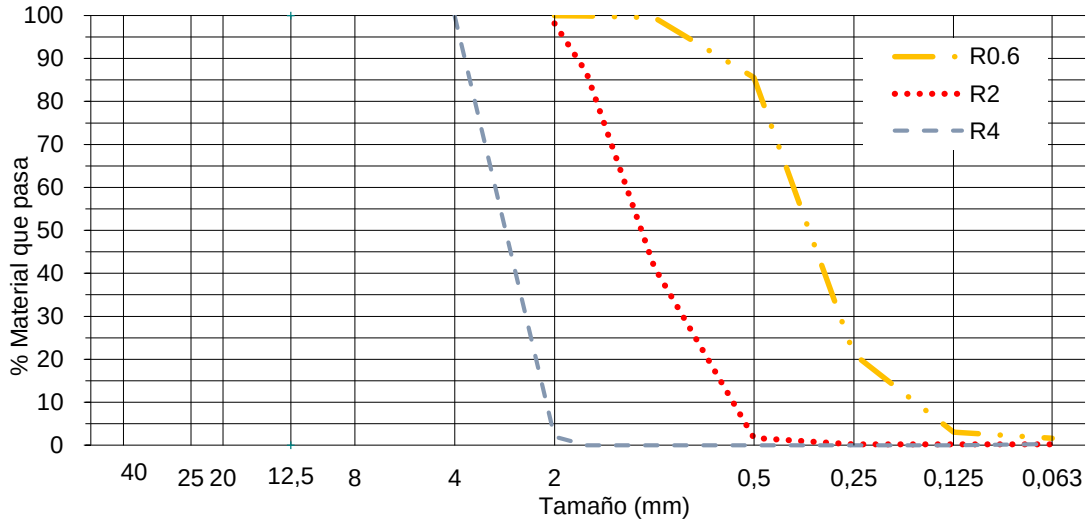

Figura 2. Granulometría partículas de caucho

4.1.2. Materiales utilizados en la fase de estudio y selección de sensores (artículo 3)

Durante el estudio, tres tipos de sensores fueron seleccionados: 1) acelerómetros para controlar los cambios en las oscilaciones; 2) paneles de presión (sensores piezoresistivos) para medir los cambios de presión sobre las placas de asiento; y 3) piezoeléctricos para controlar los

cambios en el comportamiento de la vía a partir de las variaciones en las propagaciones de las ondas en el material.

Acelerómetros

Durante el proceso de estudio de las diferentes tipologías de sensores dos tipos de acelerómetros fueron seleccionados, los cuales son comúnmente usados en industrias como dispositivos de navegación, instrumentación médica, juegos, etc.

El primero, referenciado en esta tesis como ACC1 (Figura 3), es un acelerómetro capaz de registrar datos en las tres direcciones del plano (X,Y,Z), con una resolución de (13 bit), capaz de medir hasta ± 16g. Este dispositivo incluye un sistema de gestión de la memoria. El segundo, a pesar de ser capaz de medir aceleraciones en las tres dimensiones y tener una resolución de 14 bit solamente es capaz de medir aceleraciones entre ±2g hasta ±8g. El tamaño de ACC1 es de 25 mm x 19 mm x 3,1 mm, mientras que ACC2 tiene 20,5 mm x 14,5 mm x 2,8 mm.

El precio de los acelerómetros ACC1 y ACC2, se sitúa en torno a 20 € y 5€, respectivamente. Este parámetro también es considerado a la hora de seleccionar un tipo de sensor que sea efectivo para el objetivo de la investigación desde un punto de vista técnico y económico.

Sensores Piezoresistivos

En esta tipología, dos modelos de sensor fueron estudiados (Figura 3).

Por un lado, un sensor circular (PR1) fabricado en poliéster con un espesor de 0.208 mm y un área de contacto de 25.4 mm. Este tiene un coste aproximado de 25 €. El radio de medida recomendado por el fabricante es de 0-30 kN, el cual puede verse incrementado variando las resistencias eléctricas empleadas en el circuito. Es por ello, que este sensor ha sido calibrado empleando resistencias desde 1 kΩ hasta 10 kΩ.

Por otro lado, otro cuadrado (nombrado como PR2 en Figura 3) fue analizado. Se trata de un sensor de geometría cuadrada con un espesor de 0,42mm, 43,7 mm de ancho y 43,7 mm de largo. Este componente tiene un coste cercano a los 10 €.

En ambos casos, los sensores piezoeléctricos han sido calibrados con diferentes resistencias.

Piezoeléctricos

Se trata de un sensor (nombrado como PI en la Figura 3) de bajo coste cuyo precio oscila los 0,10 €. La base circular metálica que lo compone tiene un diámetro exterior de 35 mm, mientras que el de lámina de cuarzo es de 24 mm. Los piezoeléctricos empleados tienen un espesor de 0,3 mm. Estos sensores utilizan el efecto piezoeléctrico, un fenómeno en el que ciertos materiales generan una carga eléctrica cuando se someten a una deformación mecánica (como presión o tensión).

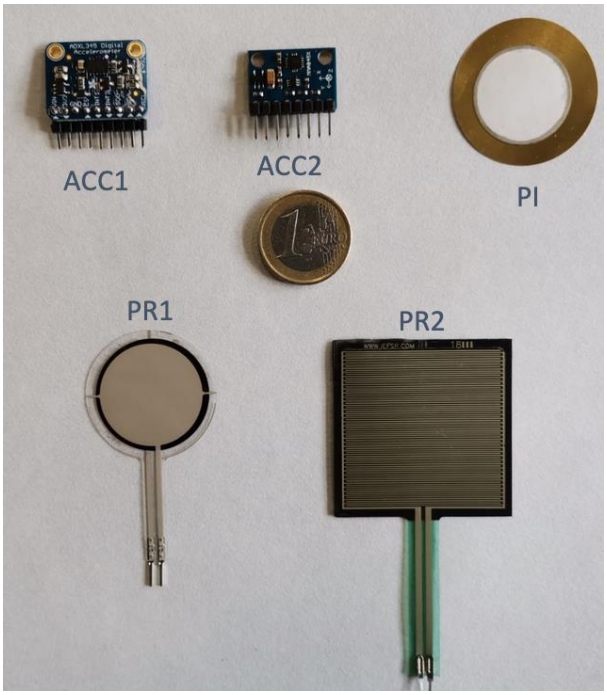

Figura 3. Sensores analizados

En todos los casos, las medidas han sido registradas con un microcontrolador de bajo coste como es el microcontrolador de ARDUINO UNO (Figura 4 y Figura 5) .

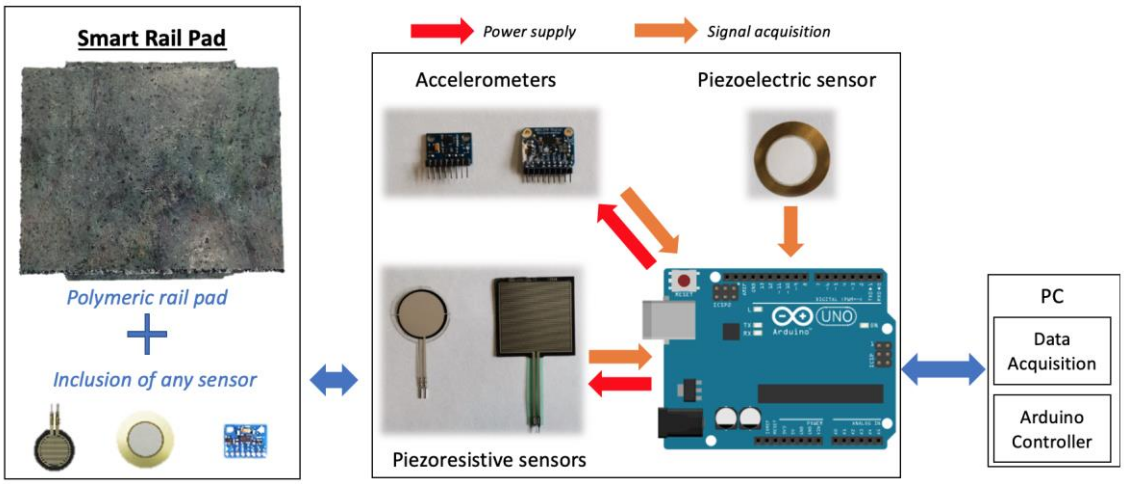

Figura 4. Diagrama conceptual de las Placas de Asiento Inteligentes, y configuración del sistema de adquisición de datos.

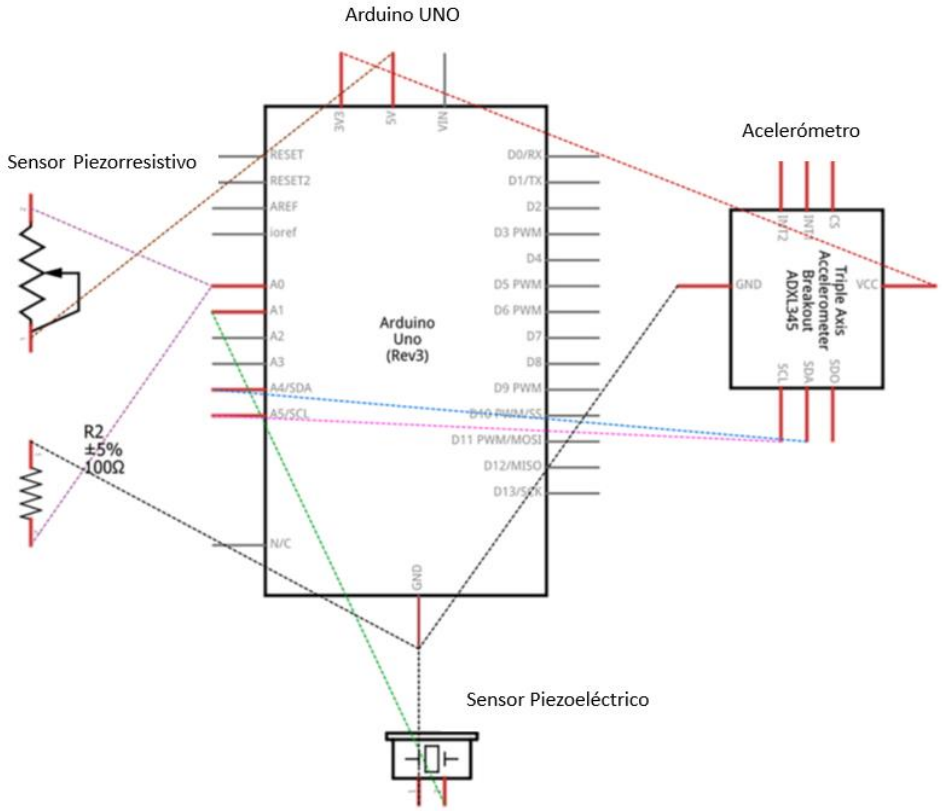

Figura 5. Diagrama de conexiones entre cada tipo de sensor y el microcontrolador Arduino.

Para el ensayo y validación de estos sensores, se emplearon placas fabricadas con diferentes polímeros con el objetivo de estudiar la aplicabilidad de los mismos cuando varían sus propiedades como puede ser la rigidez estática (parámetro fundamental en esta tipología de elementos). Más concretamente, tres placas cuadradas de 100 mm x 100 mm x 7 mm fueron usados para estudiar la viabilidad de los sensores para ser incluidos en los diferentes materiales.

Estas fueron fabricadas con HDPE (Polietileno de alta densidad), una combinación de PP/PE (polipropileno y polietileno de baja densidad) y resina industrial de poliuretano con propiedades elásticas. La rigidez elástica, ensayadas según la norme EN 13146-9, es de 575 kN/mm, 250 kN/mm y cercana a los 150 kN/mm, respectivamente.

Adicionalmente, dos placas con dimensiones de 140mm x 180 mm x 7 mm de espesor fueron empleadas durante la investigación con el objetivo de comprobar la aplicabilidad de los sensores en elementos elásticos fabricados con las dimensiones requeridas para su aplicación como placas de asiento. Estas, fabricadas con HDPE y Resin, fueron estudiadas simulando diferentes estados de la vía con el fin de determinar la aplicabilidad del sensor ante los diferentes condicionantes a los cuales están sometidos la vía (estado de la vía y condiciones del tráfico). Figura 6 muestra un ejemplo de placas de asiento fabricadas con materiales reciclados con la geometría convencional e incluyendo sensores: (a) sensor piezorresistivo en la superficie, (b) sensor piezoeléctrico embebido en la cara inferior.

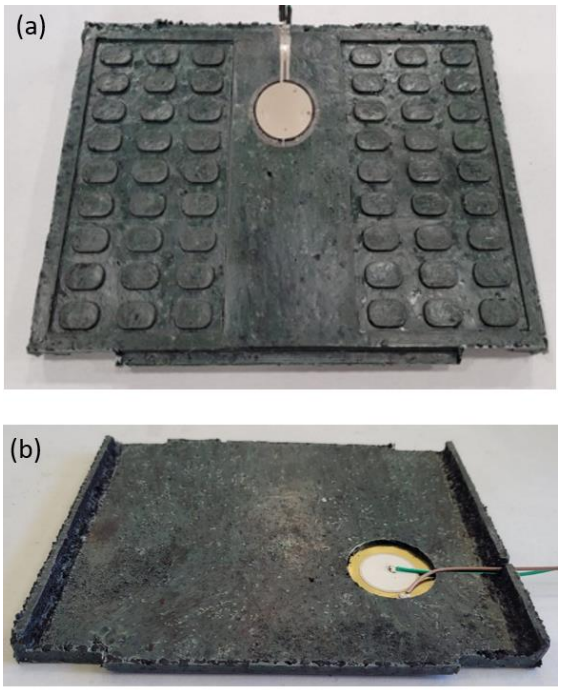

Figura 6. Ejemplo visual de la apariencia de las placas de asiento inteligentes. (a) sensor piezorresistivo en la superficie, (b) sensor piezoeléctrico embebido en la cara inferior de la placa.

4.1.3. Materiales de la fase de validación (artículo 4)

Esta fase de la investigación se ha centrado en la validación del empleo de sensores piezoeléctricos, descritos anteriormente, embebidos en placas fabricadas a partir de polímeros reciclados, con el objetivo de validar la aplicabilidad de esta tipología de sensores al estudio del comportamiento del tráfico y de la vía tras el paso de los ferrocarriles. En esta fase, las placas fueron fabricadas con la combinación de 50% HDPE y 50 % partículas de caucho con un tamaño de partículas que oscila entre 2-4 mm.

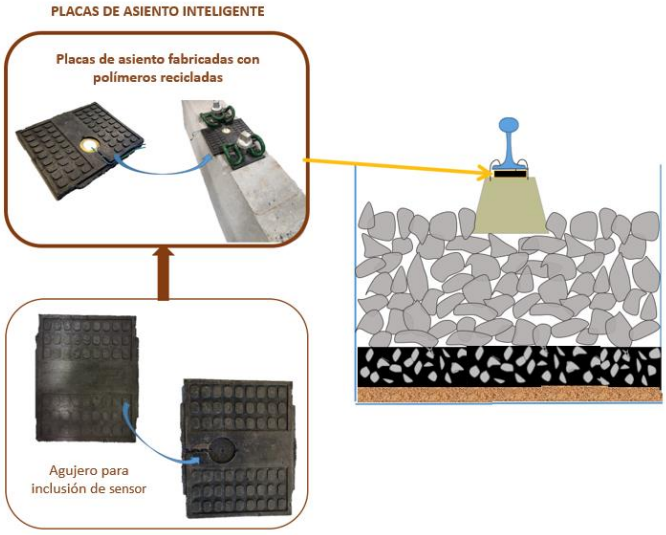

Figura 7. Esquema colocación placa de asiento

4.2. Plan de ensayos y métodos

La metodología de esta tesis doctoral, se estructura en cuatro etapas de trabajo de acuerdo a la Tabla 1. El resultado de cada una de las etapas ha sido recogido en cada uno de los artículos publicados según se muestra en la tabla anteriormente mencionada.

	ETAPA	Artículo
0	Estudio del estado del arte	**Castillo-Mingorance, J.M.;** Sol-Sánchez, M.; Moreno-Navarro, F., Rúbio Gámez; M.C. A Critical Review of Sensors for the Continuos Monitoring of Smart and Suistainable Railway Infraestructures. Sustainability, 12 (2020) 9428.

1	Desarrollo de materiales elásticos sostenibles a partir de polímeros reciclados y partículas de caucho procedentes de NFU	**Castillo-Mingorance, J.M.;** Sol-Sánchez, M.; Mattinzioli, T.; Moreno-Navarro, F., Rúbio Gámez; *Development of rail pads from recycled polymers for ballasted railway tracks.* Constr. Build. Mater. 337 (2022) 127479.
2	Desarrollo de placas de asiento sostenibles e inteligentes mediante la inclusión de sensores	Sol-Sánchez, M.; **Castillo-Mingorance, J.M.**; Moreno-Navarro, F.; Rubio-Gámez, M.C. *Smart rail pads for the continuos monitoring of sensored railway tracks: Sensor analysis.* Autom. Constr. 132 (2021) 103950.
3	Prueba y validación de las placas de asiento sostenibles e inteligentes a través de ensayos a escala real	Sol-Sánchez, M.; **Castillo-Mingorance, J.M.**; Moreno-Navarro, F.; Mattinzioli, T.; Rubio-Gámez, M.C. *Piezolectric-sensored sustainable pads for smart railway traffic and track state monitoring: Full-scale laboratory test. Constr. Build. Mater.* 301 (2021) 124324.

Tabla 1. Etapas de plan de trabajo y publicaciones asociadas

En primer lugar, se ha llevado a cabo una revisión bibliográfica sobre los sistemas de monitorización continua disponibles aplicados a las líneas de ferrocarril, identificando las ventajas e inconvenientes de cada uno de ellos y los principales casos de estudio, cuyos resultados principales se han expuesto en el capítulo 2 de la presente tesis. Estos resultados, fueron recogidos en un artículo tipo revisión bibliográfica (Review), titulado ***A Critical Review of Sensor for the Continuos Monitoring of Smart and Suistainable Railway Infraestructuras*** publicado en la revista *Sustainability* (Sustainability 2020, 12, 9428; doi:10.3390/su12229428). A partir de las conclusiones extraídas en el estudio del estado del arte, se han llevado cabo 3 etapas:

4.2.1. Desarrollo de materiales elásticos sostenibles a partir de polímeros reciclados y partículas de caucho procedentes de NFU

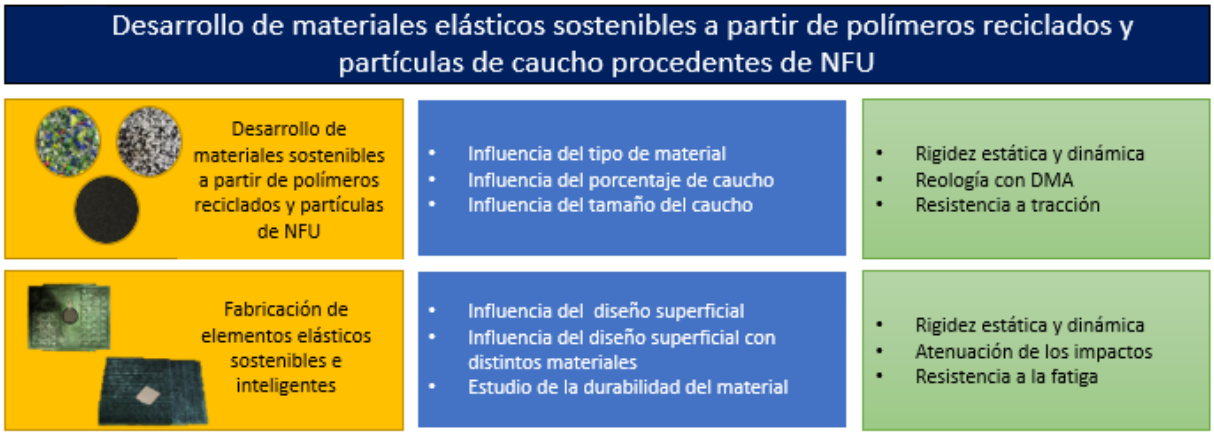

En primer lugar, se han desarrollado los materiales sostenibles que serán empleados en la fabricación de las placas de asiento. Para ello, cuatro materiales diferentes fueron utilizados, tres de ellos empleados como agentes aglutinantes mientras que el cuarto se utilizó como modificador de la rigidez. Para este propósito, se mezclaron los materiales aglutinantes (R-HDPE, R-PP/PE y Resin), junto con las partículas de caucho en diferentes tamaños y proporciones, obteniendo un amplio abanico de posibles materiales susceptibles de ser empleados en la fabricación de placas de asiento. Para evaluar las características físicas y mecánicas de los diferentes materiales obtenidos, se determinó su rigidez vertical secante 20-90 kN para placas de asiento (UNE EN 13146-9), su capacidad de atenuación mediante el uso de un dispositivo DMA (metodología descrita en el ARTICULO 2) y su resistencia a tracción (ISO 37).

Una vez estudiados los diferentes materiales susceptibles de ser empleados en la fabricación de placas de asiento, se pasó a evaluar la influencia de la geometría superficial de la placa con el fin de diseñar elementos elásticos aptos para su uso en distintos tipos de vías. Las placas de asiento fueron fabricadas acorde a las dimensiones requeridas para ser empleadas en un carril tipo UIC 54 [16] (140x180x7 mm), analizándose 4 geometrías diferentes:

G1: Placa de asiento lisa, usada como referencia.

G2: Placa de asiento con un patrón similar a la empeladas en las vías de alta velocidad españolas [17] [18], siguiendo un patrón de oblongos según se muestra en la Figura 8.

G3: Prototipo. Placa de asiento con protuberancias lineales de 6,6 mm de ala una profundidad de 2mm, separadas a la misma distancia. En la parte central, dicha protuberancia tiene un ancho de 54 mm

G4: Prototipo. Placa de asiento que sigue el mismo patrón que la G3 en su parte superior e inferior.

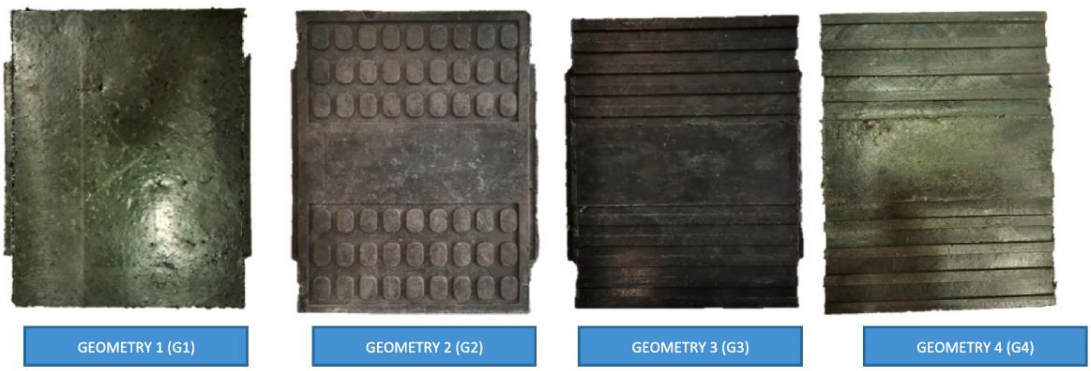

Figura 8. Diferentes geometrías aplicables a placas de asiento ensayadas.

Con el fin de poder analizar el comportamiento de estos materiales y la influencia de las distintas variables estudiadas, se realizaron los ensayos recogidos en la Tabla 2. La descripción de dichos ensayos se detalla en el artículo recogido en el anexo de la presente tesis, ***Development of rail pads from recycled polymers for ballasted railway tracks.*** (Constr. Build. Mater. 337 (2022) 127479).

Tabla 2. Ensayos realizados en la fase de desarrollo de las placas sostenibles

<table>
<tr><th>Etapa</th><th>Fase</th><th>Material</th><th>Variables</th><th>Ensayo</th></tr>
<tr><td rowspan="3">(1) Influencia de la composición del material</td><td>1.1 Influencia del tipo de material</td><td>R-HDPE
Resin
R-PP/PE</td><td>Tipo de Material</td><td rowspan="3">- Rigidez Estática 20/95
-Rigidez dinámica
-Capacidad de amortiguamiento
-Ensayo a Tracción</td></tr>
<tr><td>1.2 Influencia del porcentaje de caucho</td><td>R-HDPE + R2
R-PP/PE + R2
Resin + R2</td><td>Porcentaje partículas de caucho
-0%
-25%
-50%
-75%</td></tr>
<tr><td>1.3 Influencia del tamaño de las particulas de caucho</td><td>R-HDPE + 25/50/75% CR</td><td>Tamaño de las particulas de caucho
-R0.6
-R2
-R4</td></tr>
<tr><td rowspan="3">(2) Definición de la geometría</td><td>2.1 Influencia de la geometria superficial</td><td>R-HDPE + 50% R2</td><td>-Geometria 1
-Geometria 2
-Geometria 3
-Geometria 4</td><td>-Rigidez estática 20/95
-Rigidez dinámica</td></tr>
<tr><td rowspan="2">2.2. Influencia del diseño superficial en diferentes materiales</td><td rowspan="2">R-HDPE + 50% R2
R-HDPE + 50% R4
Resin + 50% R2
R-PP/PE + 50% R2</td><td>Geometría menos influyente</td><td rowspan="2">- Rigidez estática 20/95
-Rigidez dinámica
-Atenuación de impactos</td></tr>
<tr><td>Geometría más influyente</td></tr>
</table>

(3) Estudio de la durabilidad del material	3.1 Resistencia a la fatiga *Geometria 1*	R-HDPE + 50% R2 R-HDPE + 50% R4 Resin + 50% R2 R-PP/PE + 50% R2	Tipo de material	-Fatiga
(4) Analisis de la huella de carbono	4.1 Analisis de la huella bruta y neta	R-HDPE (25, 50, 75% CR) Resin (50,75% CR) PP-LDPE (25, 50, 75% CR)	Tipo de material	-Analisis Cradle-to-Gate de la huella de carbono

4.2.2. Desarrollo de placas de asiento sostenibles e inteligentes mediante la inclusión de sensores.

Una vez estudiados los diferentes materiales susceptibles de ser empleados para la fabricación de las placas de asiento, los sensores descritos anteriormente fueron analizados, así como, la interacción de los mismos con respecto a las placas de asiento.

Para ello, la metodología de ensayos se dividió en tres etapas: (1) calibración de los sensores en correlación con los principales parámetros que influyen en las vías de ferrocarril y elección del más adecuado par para las siguientes etapas, (2) estudio de la respuesta de los sensores, cuando son empleados en los distintos tipos de placas de asiento, compuestas de diferentes materiales, que como resultado, obtenemos placas con diferentes rigideces, (3) evaluación de la capacidad de los sensores de registrar los diferentes estados de vía y estados de tráfico, y finalmente, (4) evaluación de la duración de los sensores ante cargas repetitivas.

La Tabla 3 recoge los ensayos realizados. Con el fin de conocer el comportamiento de los sensores como parte del componente de la vía, se han aplicado desplazamientos verticales y cargas a diferentes amplitudes, cargas y frecuencias, simulando el paso de los trenes. La metodología se puede ver con mayor detalle en el artículo recogido en el anexo de la presente tesis doctoral***, Smart rail pads for the continuos monitoring of sensored railway tracks: Sensor analysis***. (Autom. Constr. 132 (2021) 103950).

Tabla 3. Ensayos realizados con el fin de caractarizar los distintos sensores estudiados.

<table>
<tr><th>Etapa</th><th>Variable de Estudio</th><th>Ensayo</th></tr>
<tr><td rowspan="2">Estudio del piezoeléctrico como parte del componente de la vía</td><td rowspan="2">Influencia de la capacidad de soporte</td><td>Desplazamientos verticales a diferentes amplitudes y frecuencias</td></tr>
<tr><td>Cargas verticales a diferentes fuerzas y frecuencias</td></tr>
<tr><td rowspan="3">2. Uso de sensores en diferentes tipos de placas de asiento</td><td>R-HDPE
R-PP/PE Resin</td><td rowspan="3">Aplicación de diferentes niveles de presión sobre las placas de asiento que incluyen los sensores</td></tr>
<tr><td>R-HDPE
R-HDPE+25R2
R-HDPE+50R2
R-HDPE+75R2</td></tr>
<tr><td>R-HDPE+50R0.6
R-HDPE+50R2
R-HDPE+50R4</td></tr>
<tr><td>3. Análisis de los sensores antes diferentes comportamientos de la vía</td><td>Rigidez Alta:
R-HDPE+50R4

Rigidez Baja:
Resin+50R0.6</td><td>Simulación del paso de los trenes</td></tr>
</table>

4.2.3. Prueba y validación de las placas de asiento sostenibles e inteligentes a través de ensayos a escala real

Se trata de la última etapa de esta Tesis Doctoral, en la cual se pretende validar la viabilidad del uso de sensores piezoeléctricos en las placas de asiento con el objetivo de monitorizar el tráfico y las condiciones de la vía. Para ello, la metodología de ensayo se dividió en tres etapas: (1) Estudio de las señales registradas por los sensores piezoeléctricos, evaluando los diferentes escenarios para cada solución con el objetivo de calibrar los sensores para esta aplicación; (2) Análisis de la capacidad de los sensores de monitorizar las condiciones del tráfico (principalmente, cargas, peso del vehículo y detección de impactos debido a condiciones desfavorables que hacen que haya un mal contacto entre la rueda y la vía); (3) estudio de la capacidad de monitorización de las condiciones de vía mediante la medida de la distribución de las cargas en las superestructura. La Tabla 4 resume el plan de ensayos llevado a cabo, mostrando las tres etapas anteriormente mencionadas, las variables analizadas y los sensores utilizados, así como los ensayos realizados.

Tabla 4. Plan de ensayos

Etapa	Variable de Estudio	Sensor	Placa de asiento	Ensayo
1. Calibración y selección del sensor	Desplazamientos	Acelerómetro 1 (ACC1) Acelerometro 2 (ACC2)	--	Desplazamientos verticales a diferentes amplitudes y frecuencias
	Cargas	Press 1 (PR1) Press 2 (PR2)		Cargas verticales a diferentes fuerzas y frecuencias
		Piezoelectric (PI)		
2. Uso de sensores en diferentes tipos de placas de asiento	Tipo de material	ACC1 PR1 PI	R-HDPE R-PP/PE Resin	Aplicación de diferentes niveles de presión sobre las placas de asiento que incluyen los sensores
	Cantidad de caucho empleado en la fabricación de las placas de asiento	PR1 PI	R-HDPE R-HDPE+25R2 R-HDPE+50R2 R-HDPE+75R2	
	Tamaño de las particular de caucho empleado en la fabricación de las placas de asiento	PR1 PI	R-HDPE+50R0.6 R-HDPE+50R2 R-HDPE+50R4	
3. Análisis de los sensores antes diferentes comportamientos de la vía	Simulación de diferentes estados de vía	ACC1 PR1 PI	Rigidez Alta: R-HDPE+50R4 Rigidez Baja: Resin+50R0.6	Simulación del paso de los trenes
	Diferentes niveles de carga			

Para ello, un cajón de ensayos de dimensiones de 2 m de longitud, por 1 metro de ancho y 60 cm de espesor se usó, con el objetivo de estudiar la capacidad de los sensores para medir los cambios en el comportamiento de la vía. La sección tipo empleada para estos ensayos estaba formada por: (i) una capa de 8 cm de material granular simulando la base de la subestructura, con módulo de elasticidad superior a los 80 MPa, en consonancia con los valores de vías reales; (ii) una capa de 12 cm de subbaalasto bituminoso; (iii) una capa de balasto de 30 cm de material ofítico con propiedades acordes a lo expuesto en la EN 13450; (iv) una sección de traviesa de hormigón (85 cm de longitud) comúnmente usado en las vías de alta velocidad españolas; (v) sistema de fijación VM, incluyendo las placas de asiento sensorizadas y (vi) sección de carril tipo UIC-54 de 25 cm de longitud. La Figura 9 muestra el aspecto visual del ensayo llevado a cabo antes de la colocación del carril sobre el sistema formado por tres traviesas (a) y después de su colocación (b).

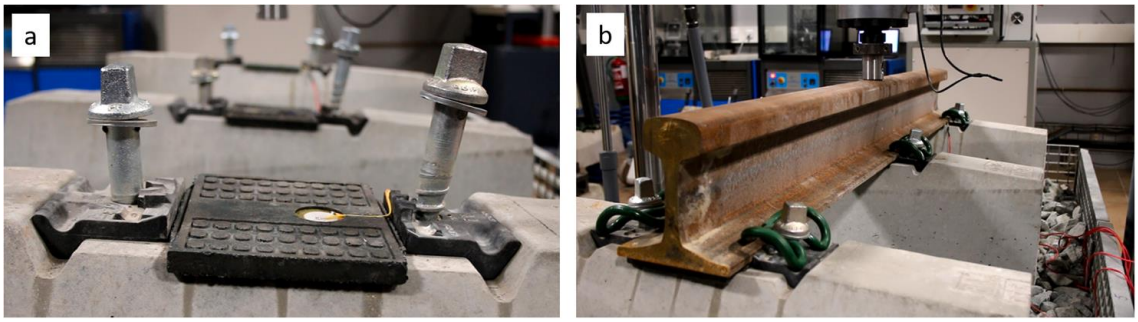

Figura 9. Ensayo a escala real formado por tres traviesas (a) placas de asiento inteligentes sobre traviesa; (b) configuración del ensayo.

5. Resultados

En este capítulo se recogen los resultados obtenidos a lo largo de la presente Tesis Doctoral, siendo el análisis realizado en consonancia con las diversas etapas de estudio descritas en el capítulo de metodología. Este apartado se trata de un resumen de resultados, los cuales se muestran con mayor profundidad en los anejos adjuntos al presente documento donde se recogen los artículos que conforman la agrupación de publicaciones de esta Tesis Doctoral.

5.1. Desarrollo de materiales elásticos sostenibles a partir de polímeros reciclados y partículas de caucho procedentes de NFU

La Figura. 10 muestra los resultados del ensayo de rigidez estática de las placas fabricadas con los diferentes materiales aglomerantes. Acorde con estos resultados, tres posibles soluciones podrían ser obtenidas de este estudio. Las placas fabricadas con R-PP/PE presentan valores de rigidez estática de entorno a 100KN/mm, mientras que, en los otros casos, dicho valor aumenta, llegando a valores de 800 KN/mm, en el caso de las placas fabricadas con R-HDPE, y 500 KN/mm, en el caso de las fabricadas con resina. De esta forma, se puede ver que el material usado como aglomerante juega un papel fundamental en el comportamiento de la placa de asiento, obteniendo elementos elásticos con diferentes propiedades para su uso en distintos tipos de vías de ferrocarril.

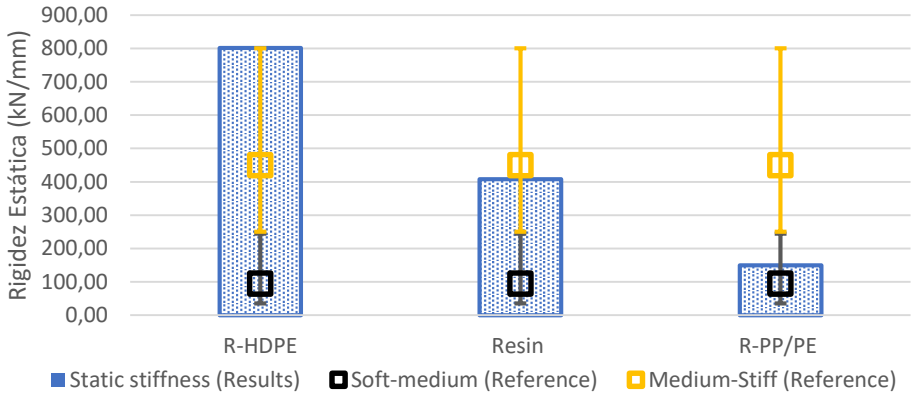

Figura. 10. Rigidez estática de las placas de asiento fabricadas con los materiales aglomerantes.

Partículas de caucho de diferentes concentraciones y tamaños fueron empleadas con el objetivo de poder modificar las propiedades de los materiales aglomerantes. La Figura 11 muestra la influencia de la cantidad de partículas de caucho (por volumen), sobre el total de material aglomerante, con partículas que oscilan entre el 0,6 y 2 mm (R2). Además, para uno de

ellos (R-HDPE), se muestra la influencia del tamaño de las partículas de caucho en la rigidez del conjunto.

De estos resultados se puede extraer que, aunque la rigidez de todos los materiales cambia con la inclusión de las partículas de caucho, en el caso de R-PP/PE varía en menor medida, llevando incluso a un ligero aumento de la rigidez de la placa. Esto puede estar relacionado en que ambos materiales presentan una rigidez del mismo orden, obteniendo valores algo superiores en el caso del caucho. Sin embargo, si comparamos R-HDPE y Resin, es posible observar como esta última es más susceptible de reducir su rigidez con la incorporación de partículas de caucho, lo que permitiría una mayor graduación de su comportamiento al realizar la combinación de ambos materiales.

Se puede ver que con un 50% de partículas de caucho R2 es posible reducir la rigidez estática en un 25% y 85% en placas de asiento fabricadas con R-HPE y Resin, respectivamente. Estos cambios indican que las partículas de caucho tienen un mayor impacto en las placas de asiento fabricadas con Resin, mientras que en las fabricadas con R-HDPE, el efecto es más limitado debido a la alta rigidez del plástico, y por tanto, requiriendo el uso de caucho.

En este sentido, se ha demostrado que el tamaño de las partículas de caucho puede optimizar la rigidez del material. Centrándonos en las placas de asiento fabricadas con R-HDPE, es posible observar como con el aumento del tamaño de las partículas de caucho es posible disminuir en mayor medida su rigidez. Por ejemplo, con la adición de un 50% de partículas de caucho de tamaño menor a 0.6 mm es posible reducir la rigidez estática entorno a un 20%, mientras que, si se utilizan partículas de tamaño entre 2 y 4 mm se obtiene una reducción en torno a un 40 %, pasando de una solución rígida a una solución de rigidez media. En la Figura 9 b se muestra la relación que existe entre la rigidez estática y la dinámica. Existen estudios previos que indican que, para obtener unas placas de asiento flexibles, dicho ratio debe encontrarse en torno a 3,5 [19]. Tanto R-HDPE como R-PP/PE han demostrado valores cercanos a este valor. Sin embargo, las placas de asiento fabricadas con Resin han presentado una ratio superior, lo cual indica una excesiva rigidización dinámica de este material debido a su comportamiento visco-elástico.

De acuerdo con estos resultados, se puede ver como con el uso de diferentes combinaciones de partículas de caucho es posible obtener un amplio abanico de soluciones, las cuales podrían ser empleadas en diversos tipos de vías, desde convencionales hasta Alta Velocidad.

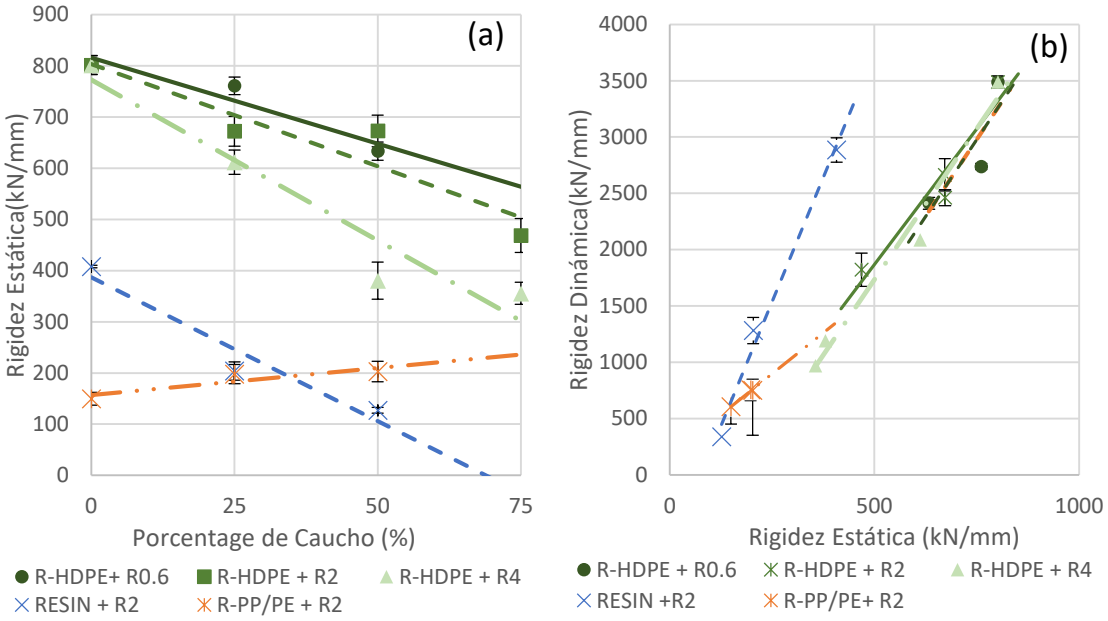

Figura 11. Rigidez estática de las placas de asiento fabricadas con diferentes materiales (a) y correlación de la rigidez para diferentes materiales (b)

Por otro lado, una vez caracterizados los posibles materiales susceptibles de ser usados en la fabricación de placas de asiento, diferentes geometrías fueron estudiadas. Para ello, se consideró un caso intermedio, analizando la influencia de la geometría en la rigidez de placas de asiento fabricadas con R-HDPE + 50 % R2. La Figura 12 muestra la rigidez estática y dinámica de las cuatro geometrías estudiadas. De estos resultados se observa como si reducimos la superficie de placa, disminuye, consiguientemente la rigidez. Si se compara G1 y G4, es posible disminuir en torno a un 50 y 70 %, respectivamente, la rigidez estática y dinámica de la placa de asiento. Es por ello, que se puede afirmar que uno de los parámetros fundamentales en el diseño geométrico de las placas de asiento es la superficie de contacto con el rail, y con ello, la variación de esta propiedad puede afectar a su rigidez.

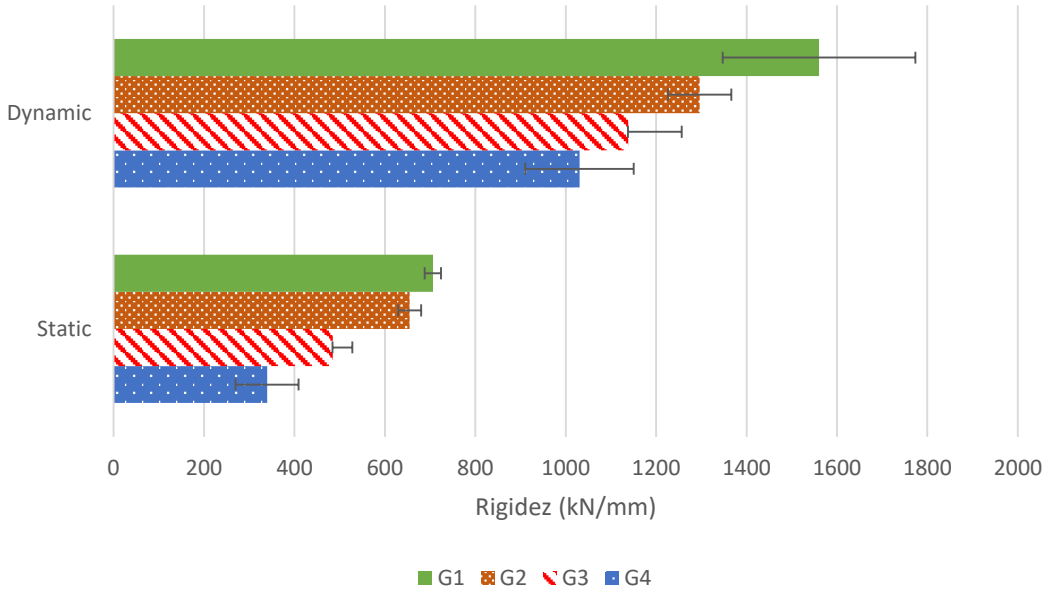

Figura 12. Rigidez estática y dinámica dependiendo de la geometría superficial de la placa de asiento.

Centrándonos en las placas de asiento con mayor y menor influencia de la geometría (G1 y G4), la Figura 13 muestra la capacidad de atenuación de impactos que presentan las placas de asiento estudiadas para diferentes combinaciones de materiales, con el fin de profundizar en el análisis de la influencia de estos parámetros de diseño de las placas (composición y geometría). Para este análisis se emplearon los materiales que, de acuerdo a los resultados previos, daban lugar a placas de rigidez media, variando el tipo de aglomerante para el caso de 50% de caucho con tamaño 2 mm. A su vez, se estudió el caso de la placa R-HDPE con 50% de caucho 4 mm para profundizar en el análisis de la influencia del caucho para este tipo de aglomerante que necesita mayor amortiguamiento por parte del caucho para reducir su rigidez, y obtener placas de rigidez media.

Todos ellos cumplieron con los requisitos establecidos por la normativa española, que establece un valor mínimo del 25% [16]. Para las placas de asiento Resin + 50% R2 y R-PP/PE + 50% R2, su geometría presentó limitada influencia en su resistencia de atenuación de impacto, obteniendo valores entre 78 % y 85%, independientemente del material y tipo de geometría. Sin embargo, en las placas de asiento fabricadas con R-HDPE el cambio en la geometría y la variación del tamaño de caucho llevó a mayor influencia en la capacidad de atenuación, al igual que ocurre con la rigidez de la placa. Quedó demostrado cómo el uso de un tamaño de partícula de caucho granulado mayor aumenta la capacidad de atenuación de impactos. Así, comparando R-HDPE +

50% R2 y R-HDPE + 50% R4, se observa que es posible incrementar la capacidad de atenuación de impactos en alrededor del 50% y 25% para G1 y G4 con el uso de R4, respectivamente.

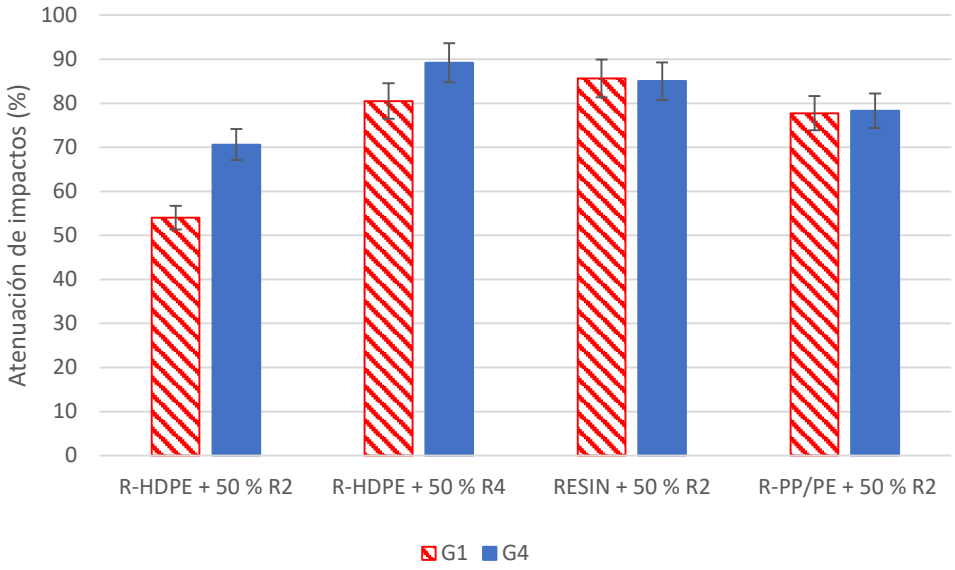

Figura 13. Capacidad de atenuación de impactos de las placas de asiento

La Figura 14 presenta la variación del desplazamiento del carril provocada por la fatiga (ensayo realizado según norma UNE-EN 13146–4). Los resultados se obtienen para Fmax (fuerza máxima igual a 83 kN) y para Fmin (fuerza mínima fuerza igual a 5 kN). En general, el desplazamiento encontrado tanto en la cabeza del carril y como en el patín serían compatibles para su uso en líneas de alta velocidad, según la normativa española [23], excepto las placas de asiento carril fabricadas con R-PP/PE + 50% R2. En este último caso, para Fmax, el desplacamiento supera los valores estándar en aproximadamente un 20% en la cabeza del carril y el 6% en el pie del carril, por lo que no se compatibiliza su uso para las líneas españolas de alta velocidad por su comportamiento plástico, según la norma española.

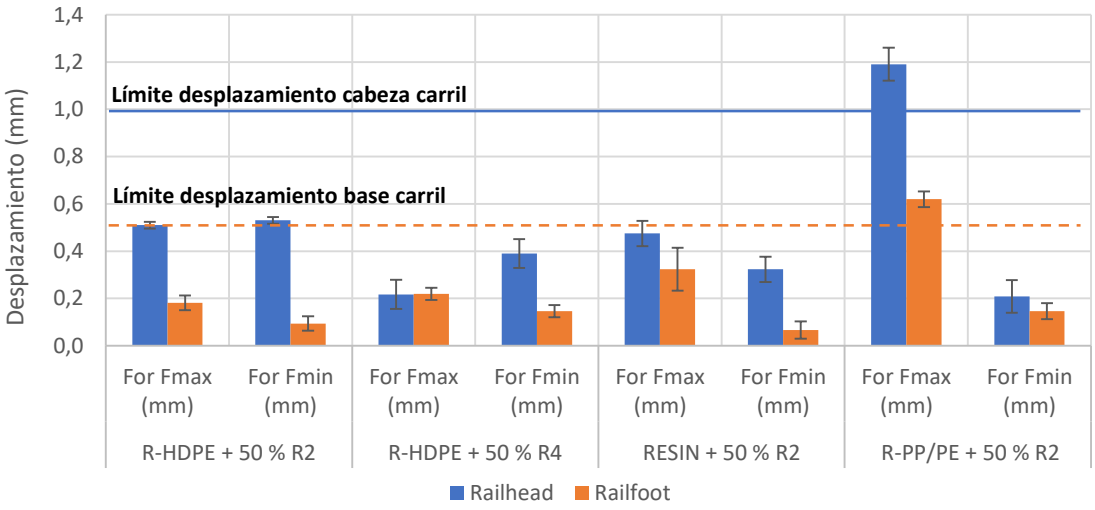

Figura 14. Desplazamientos del carril debidos al proceso de fatiga

La Figura 15 muestra los resultados del análisis de la huella de carbono para 11 posibles combinaciones de materiales viables, según resultados previos, para la fabricación de placas de asiento. A partir de estos resultados, se puede afirmar que el uso de polímeros reciclados (R-HDPE y R-PP/PE) proporciona un beneficio ambiental positivo. Sin embargo, el uso de la resina polimérica tiene un impacto ambiental superior en comparación con el uso de placas de asiento convenciones (12,6 veces superior), siendo este hecho disminuido al aumentar la cantidad de caucho reciclado incorporado a las placas, pero siempre resultando en mayores costes ambientales en el caso de la resina.

Si se comparan los impactos brutos y netos de los polímeros reciclados, se puede obsevar que el uso de ambos polimeros reciclados proporciona un ahorro medioambiental neto. Esto puede estar asociado a que la etapa de extracion de los plásticos reciclados, es decir, tratamiento y procesamiento de los residuos, tiene un menor impacto que la extracción de los componentes base que constituyen los polimeors vírgenes comúnmente empleados en placas de asiento comerciales.

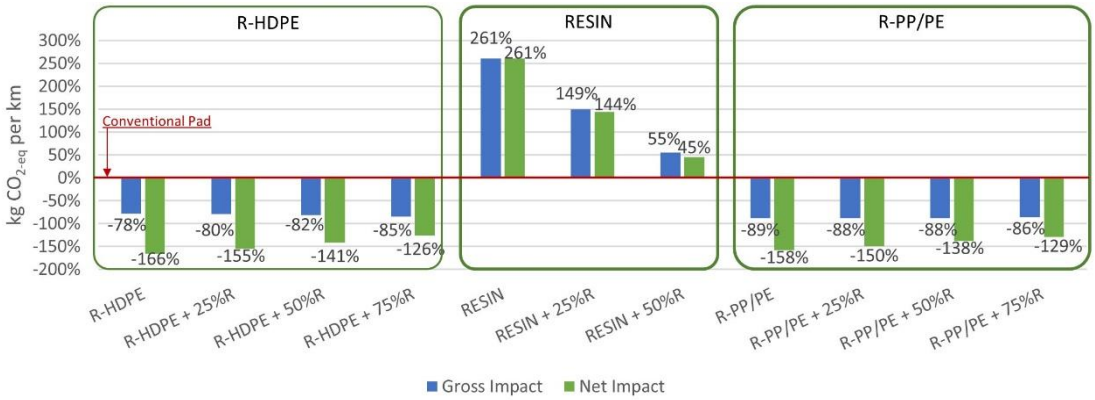

Figura 15. Huella de carbono de las placas de asiento fabricadas a partir de polímeros reciclados

5.2. Desarrollo de placas de asiento sostenibles e inteligentes mediante la inclusión de sensores.

En este apartado de la presente Tesis Doctoral se ha llevado a cabo el análisis de la aplicabilidad de cada tipo de sensor para su uso en la identificación de los diferentes comportamientos de la vía. La Figura 16 muestra las señales medidas por los acelerómetros en dos tipos de placas de asiento diferentes (una flexible y una rígida a base de diferentes componentes) y en dos subsistemas simulando dos superestructuras ferroviarias diferentes (una flexible y otra rígida). Los resultados muestran los cambios en la amplitud de aceleración registrados por los acelerómetros al reproducir diferentes niveles de carga. La figura b muestra un ejemplo de la evolución de la aceleración medida durante una secuencia de paso de tren, en comparación con los desplazamientos registrados por unos dispositivos LVDT (siglas en inglés para referirse a Transformador Diferencial de Variación Lineal), comúnmente empleados como instrumentación en ensayos de laboratorio.

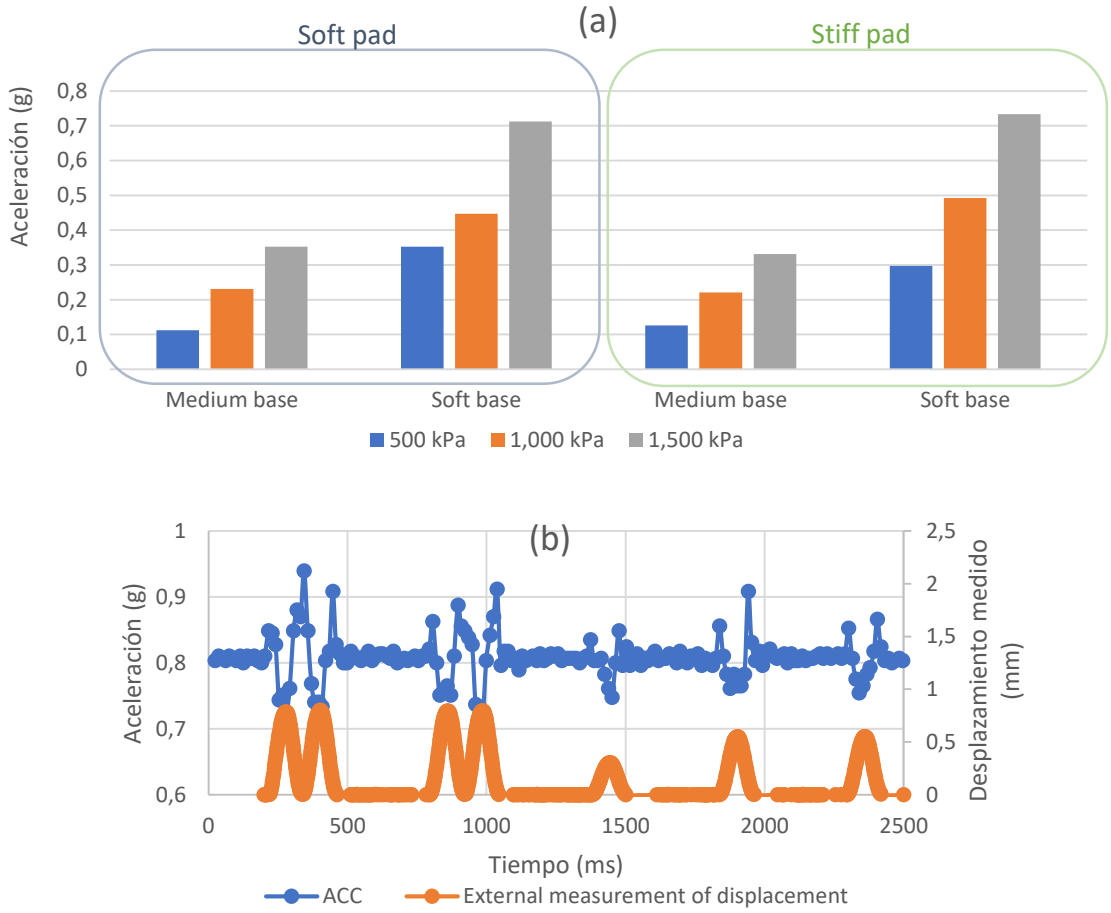

Figura 16. Resultados de los acelerómetros incluidos en las diferentes placas de asiento usadas sobre diferentes bases de ensayo. (a) influencia de la configuración del sistema sobre diferentes niveles de carga; (b) ejemplo de la correlación existente entre las medidas de aceleración y los desplazamientos generados bajo una secuencia de carga.

De manera similar, las Figura 17 y Figura 18 muestran los resultados registrados por los sensores piezorresistivo y los sensores piezoeléctricos cuando cada sistema de ensayo de vía está sometido a varios niveles de carga, simulando los diversos esfuerzos que sufre la vía durante el paso de los trenes. De estos resultados se puede observar que, al igual que lo visto en el caso de los acelerómetros, los valores máximos y mínimos del piezoeléctrico se encuentran desfasados con respecto a los picos de fuerza o desplazamiento, ya que las aceleraciones mínimas ocurren el valor máximo del desplazamiento del actuador. Eso se debe al hecho de que tales picos de desplazamiento representan un cambio en la dirección de la carga y, por tanto, provocando valores de aceleración mínimos. Por el contrario, en el caso de los sensores piezorresistivos, los valores más altos se alcanzan con la carga máxima del actuador y en los sensores piezoeléctricos, las cargas son registradas como pulsos eléctricos causados por la propagación de las vibraciones.

Los resultados demuestran que los acelerómetros (Figura 16) pueden identificar los diferentes niveles de carga producidos por el tráfico (simulando trenes con pesos), al mismo

tiempo que distingue las diferencias entre sistemas, ya que se midieron mayores aceleraciones para la base blanda donde se esperaban mayores movimientos. Cabe reseñar que la calidad de señal obtenida por este tipo de sensor es más baja que en el caso de los sensores piezoresistivos y sensores piezoeléctricos. Esto podría afectar a la idoneidad del uso de estos sensores, al no quedar registradas claramente las variaciones de las cargas.

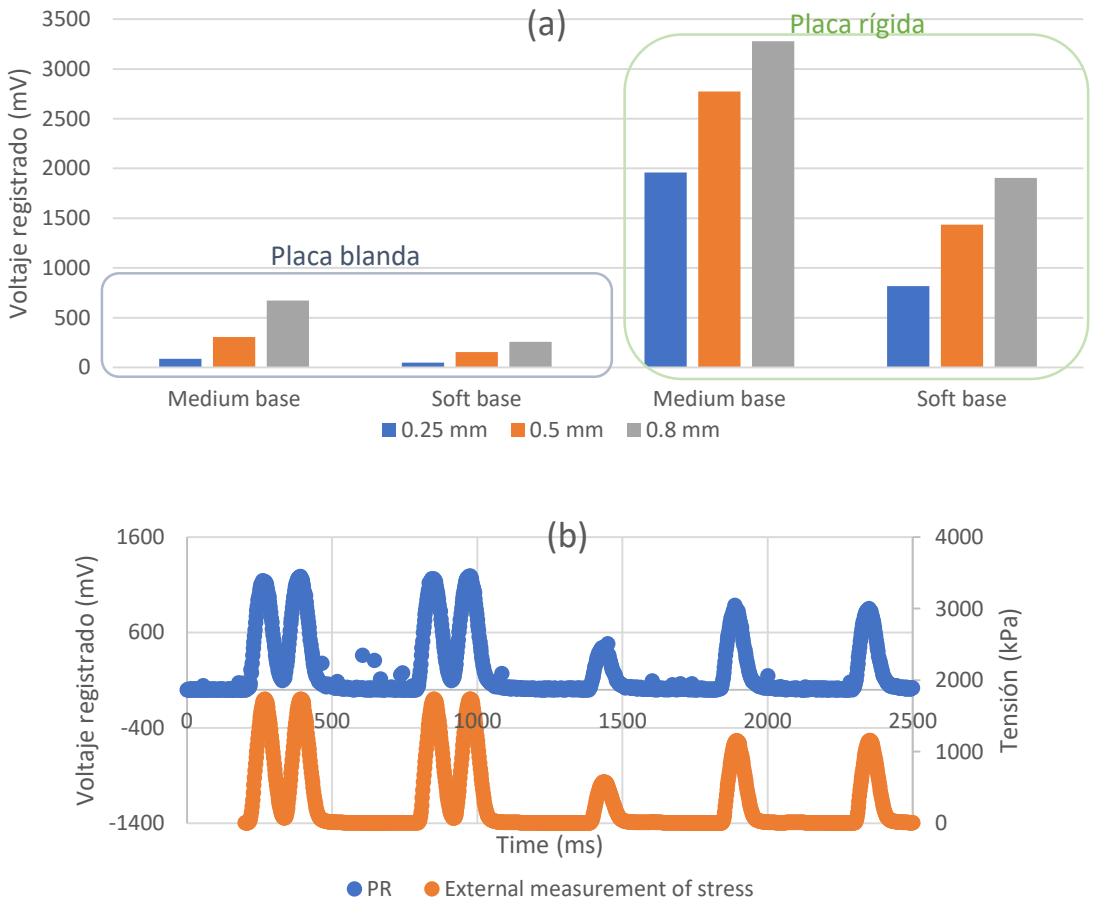

Figura 17. Resultados de los sensores piezoresistivos incluidos en placas sobre diferentes bases de ensayo. (a) influencia de la configuración del sistema sobre diferentes niveles de carga; (b) correlación entre medidas de los sensores y desplazamientos bajo una secuencia de carga.

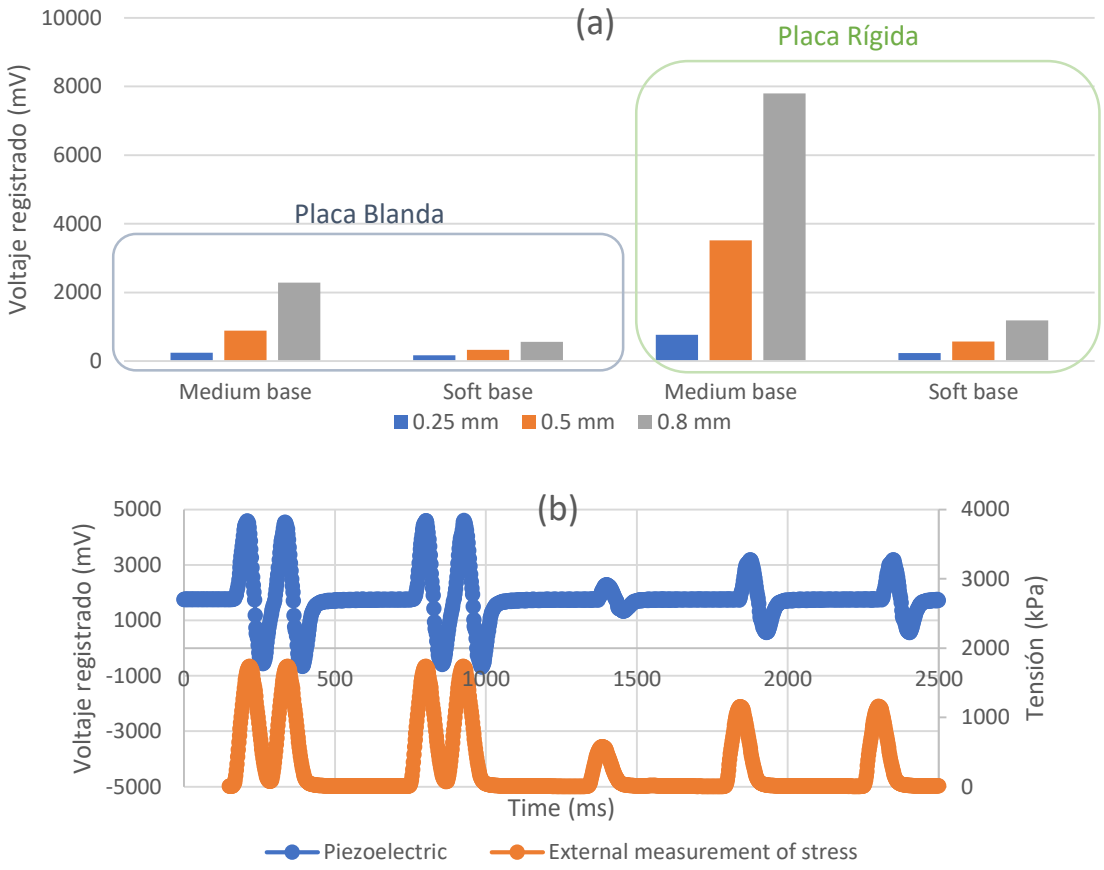

Figura 18. Resultados de los sensores piezoeléctricos incluidos en placas sobre diferentes bases de ensayo. (a) influencia de la configuración del sistema sobre diferentes niveles de carga; (b) correlación entre medidas de los sensores y desplazamientos bajo una secuencia de carga.

Por otro lado, como se indicó anteriormente, el uso de los sensores piezoresistivos y sensores piezoeléctricos permitieron una identificación clara de los ciclos de carga, que muestran ondas similares a las recogidas por los instrumentos de medida del equipo de ensayo, lo que demuestra el potencial de estas tecnologías para monitorear el comportamiento de la vía bajo el paso del tren. Ambos sensores (PR y PI) identificaron los diferentes niveles de esfuerzo necesarios para reproducir los diferentes desplazamientos a los cuales está sometida la vía (la Figura 17 y Figura 18, al tiempo que permite una distinción clara entre el tipo de sistema de vía (sobre una base media o blanda). Este último hecho fue más claro en el caso del piezoeléctrico donde las reducciones de señal fueron superiores al 50% cuando se pasó de base media a blanda, mientras que el PR mostró cambios menores.

Además, es importante señalar que, de acuerdo con resultados anteriores, los valores dependían del tipo de placa de asiento utilizada para incluir los sensores, obteniendo valores más altos para la placa compuesta de HDPE, la cual muestra una mayor rigidez.

Para una comprensión más profunda del funcionamiento de estos sensores, la Figura 19 representa ejemplos de cambios en el comportamiento de la vía monitoreado por sensores PR y PI a través de variaciones en el voltaje registrado cuando se usa en la placa de asiento rígida. Particularmente, el eje X representa las variaciones en la tensión aplicada sobre las placas de asiento debido a cambios en el soporte de la vía (simulando, por ejemplo, plataformas blandas o traviesas colgante, para disminuir la tensión en la traviesa central debajo de la rueda del tren) [20] [21] o debido a la variación en las cargas de tráfico. Por otro lado, el eje Y representa las variaciones producidas en los voltajes registrados debidos a una reducción en la carga del tráfico (de 1700 kPa a 850 kPa) o de 1700 kPa a 250 kPa por una reducción en la capacidad soporte de la vía.

Se puede observar cómo una variación del nivel de carga en una vía (asociada a cambios como el valor del peso del tren, la presencia de abolladuras en las ruedas o irregularidades en la vía, etc.) [22] podría ser claramente identificado por ambos tipos de sensores, lo que muestra el uso potencial de estas tecnologías para detectar fallos en la vía como se hizo con otros dispositivos en estudios anteriores [23] [24].

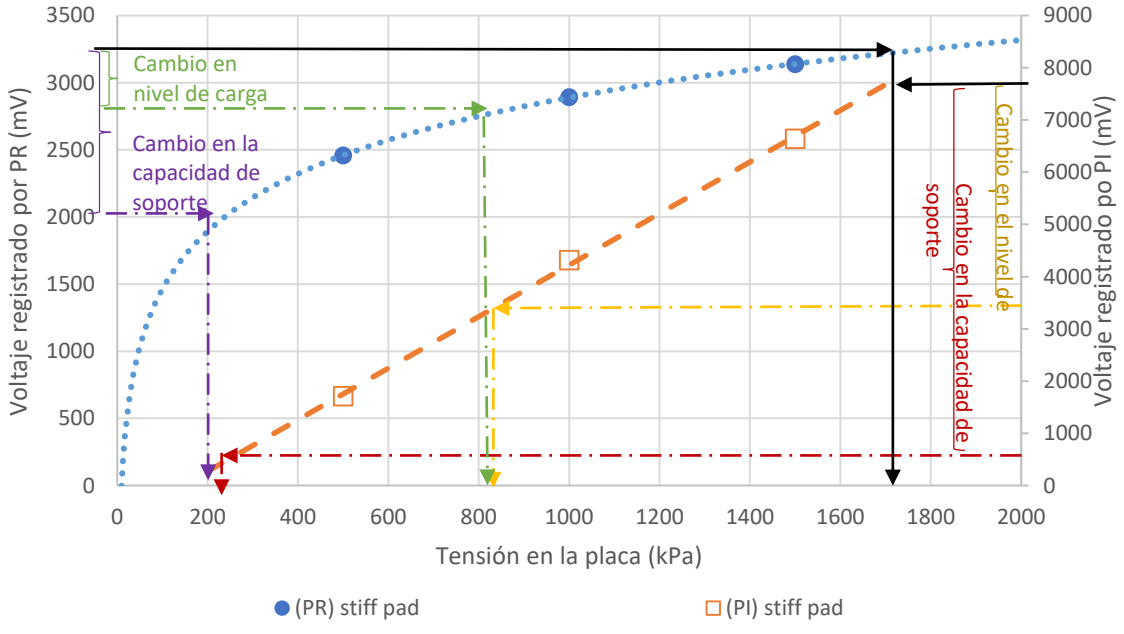

Figura 19. Correlación entre las medidas obtenidas por los sensores piezoresistivos (izquierda) y los sensores piezoeléctricos (derecha) con la variación de la carga aplicada sobre la placa de asiento ante diversos escenarios de ensayo.

5.3. Prueba y validación de las placas de asiento sostenibles e inteligentes a través de ensayos a escala real

Una vez conocidos y estudiados los sensores aplicables para la monitorización del estado de la vía y con el fin de poder validar las placas de asiento sostenibles e inteligentes aplicables a la vía del ferrocarril, se han llevado a cabo ensayos a escala real en el cajón de ensayos del Laboratorio de Ingeniería de la Construcción de la Universidad de Granada. La Figura 20a representa el diagrama de cargas por eje del tren y la gráfica en Figura 20b muestra los valores aplicados por la máquina de ensayos, reproduciendo el paso de los trenes a una velocidad cercana a los 100 km/h.

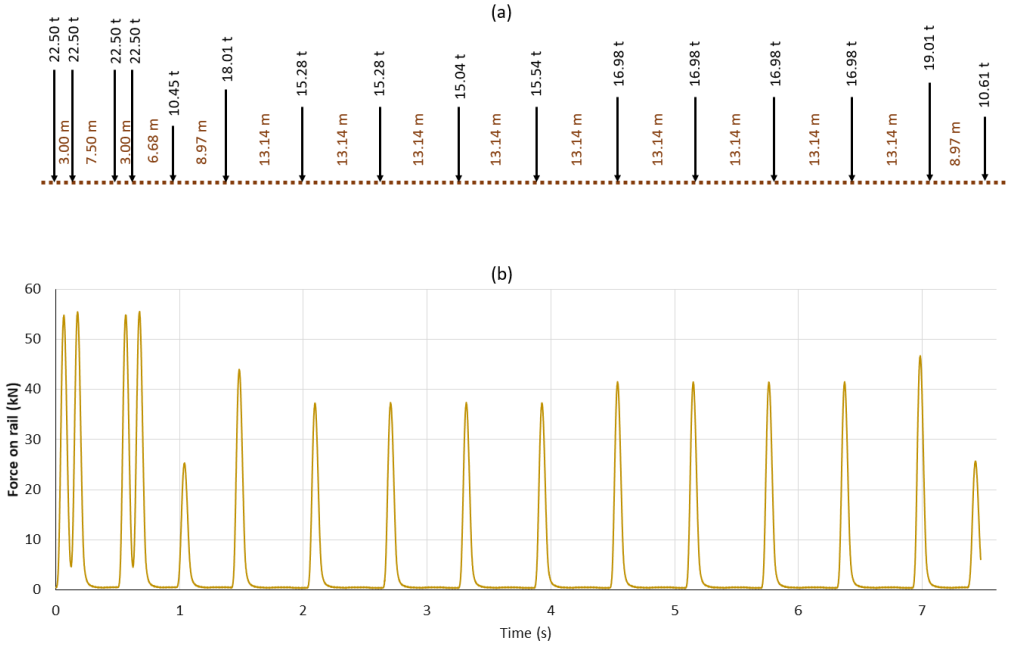

Figura 20. Diagrama de distribución de cargas: (a) distribución de cargas por eje; (b) distribución de las cargas sobre el carril durante el ensayo

La Figura 21 muestra las señales medidas por los piezoeléctricos durante la simulación de las diversas cargas representadas en la figura anterior. Se puede observar como el empleo de esta tecnología permite identificar los cambios en los niveles de carga, así como, identificar la secuencia de cargas aplicadas por la máquina de ensayo. La Figura 22 muestra la buena correlación existente entre la carga del tren y la señal medida por el piezoeléctrico. Con ello se demuestra que esta tipología de sensores podría ser adecuada para su uso en la identificación

de los niveles de carga, facilitando la monitorización continua de la vía (conteo de bogíes, pesaje dinámico de trenes, elaboración de modelos predictivos, etc.)

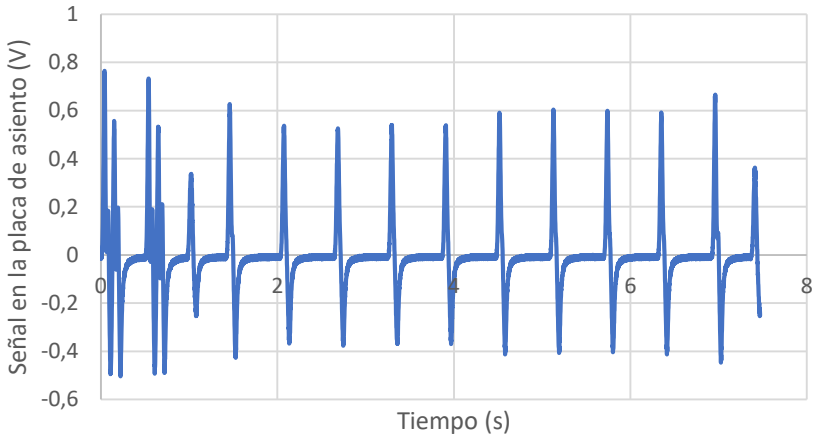

Figura 21. Diagrama de señales monitorizadas por las placas de asiento inteligentes.

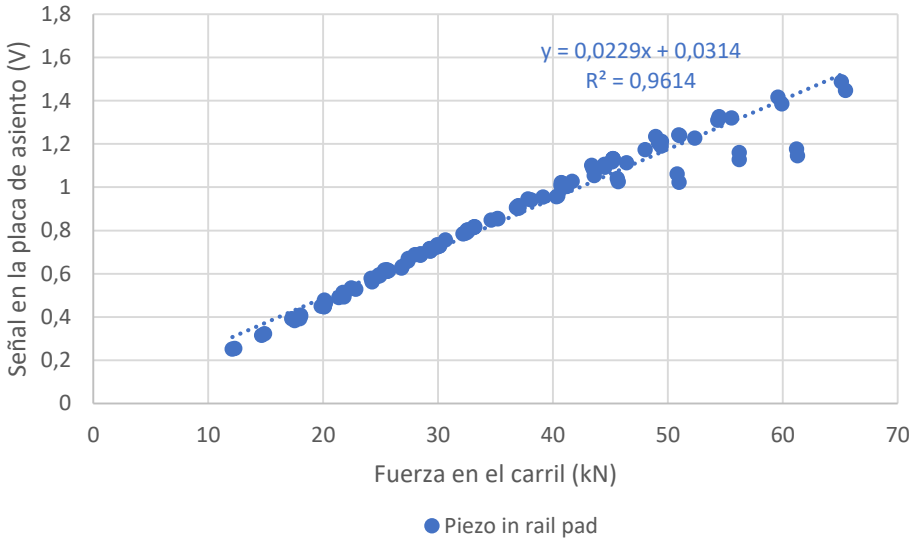

Figura 22. Correlación entre cargas aplicadas y señal registrada por componente inteligente.

La Figura 23 representa las variaciones (en %) entre las cargas aplicadas durante la simulación del paso de los trenes y los cambios de señal recogidos por los sensores.

Los resultados confirman la buena precisión de la placa de asiento inteligente, tal y como se muestra en la buena correlación lineal y valores de cambio porcentual de las cargas (observándose la superposición entre el valor teórico y los valores registrados).

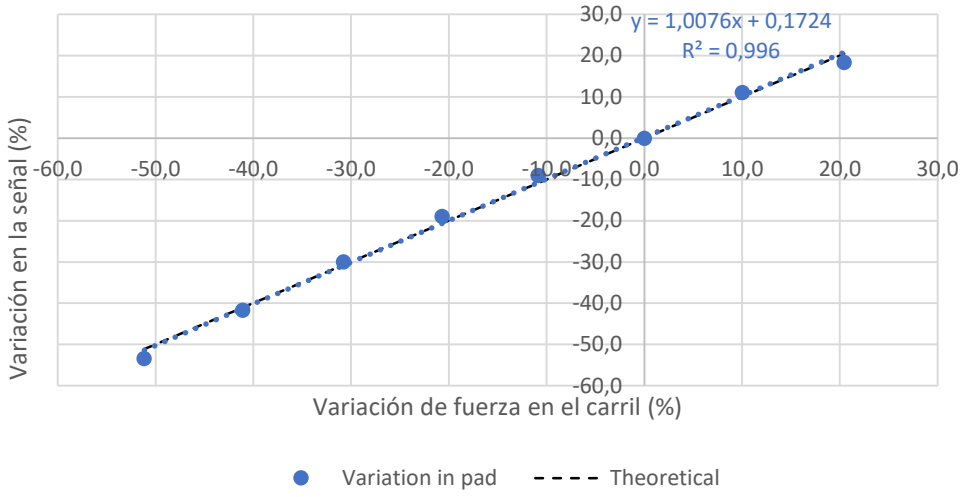

Figura 23. Correlación entre los cambios en las cargas de los trenes y los cambios registrados por los sensores.

La Figura 24 representa los valores medidos simulando un contacto regular e irregular entre las ruedas y el carril, donde los mayores impactos fueron aplicados en los ejes 7 y 10, simulando un desgaste excesivo en dichos bogies (identificado por los sensores). Ello demuestra que los piezoeléctricos podrían detectar la presencia irregularidades en el contacto rueda-carril, y con ello, su potencial aplicabilidad como elementos inteligentes para la monitorización de las condiciones del tráfico, así como de las cargas de los vehículos.

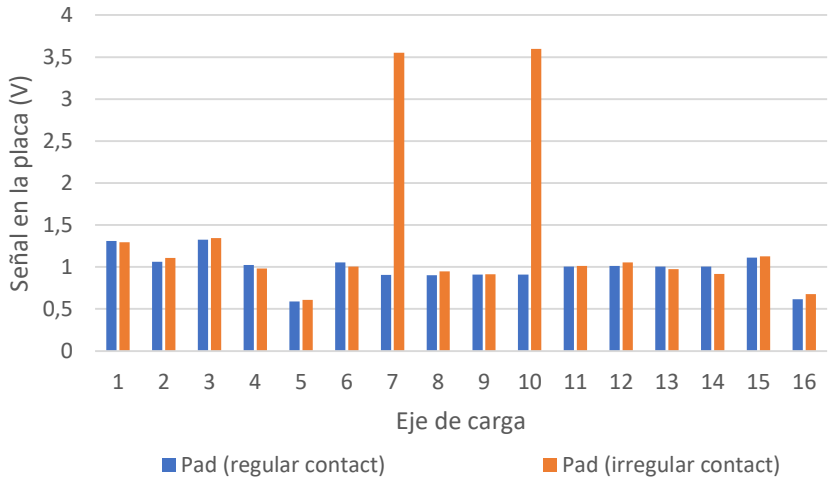

Figura 24. Resultado de la monitorización de un contacto irregular entre rueda y carril.

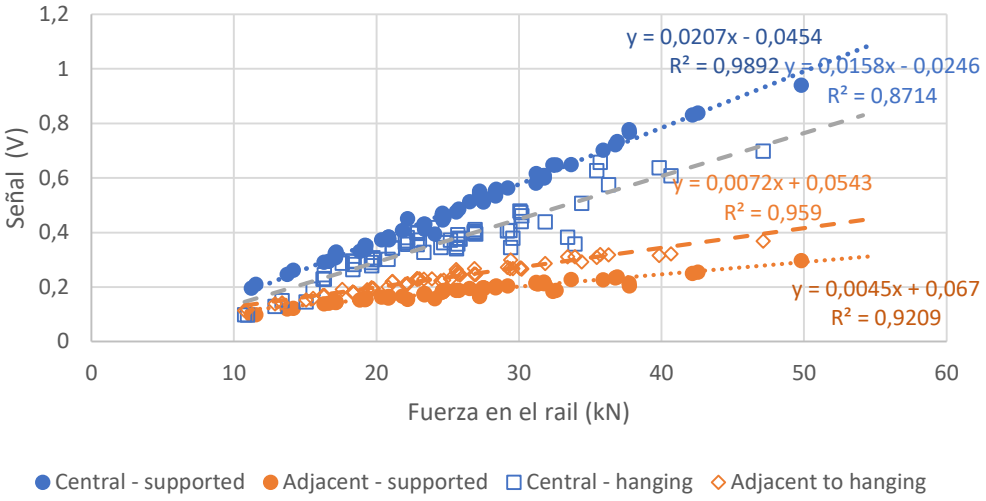

Figura 25. Resultados de la monitorización inteligente de la distribución de la carga de los carriles en diferentes traviesas, y la detección de traviesas colgantes.

6. Conclusiones

La presente Tesis Doctoral se centra en el desarrollo de placas de asiento sostenibles, fabricados a partir de polímeros reciclados e inteligentes, mediante la inclusión de sensores aplicados a vías de ferrocarril. Con ello se pretende conseguir elementos elásticos más competitivos desde el punto de vista medioambiental y a su vez, que permitan realizar un mantenimiento predictivo del estado del vehículo y de la vía.

Para conseguir este objetivo se ha realizado una investigación en la que, tras la realización del estudio del estado el arte, se ha llevado a cabo una serie de trabajos de laboratorio centrados en evaluar distintos polímeros reciclados y tipos de sensores para ser embebidos en placas de asiento. A partir de los resultados obtenidos, se pueden extraer las siguientes conclusiones:

- Se ha demostrado que el tipo de polímero reciclado usado como aglutinante juega un papel fundamental en la rigidez de la placa.
- Por lo general, un aumento en el porcentaje de partículas de caucho produce una disminución de la rigidez de la placa. Es por ello, que con la variación de la cantidad de caucho aportada y modificando el tamaño del mismo permite obtener un amplio abanico de soluciones.
- Siguiendo las conclusiones previas, se ha observado que, por ejemplo, al utilizar R-R-HDPE se obtienen placas con una rigidez de aproximadamente 800Kn/mm, mientras que con R-PP/PE se logran placas con una rigidez de alrededor de 100Kn/mm. Además, la incorporación de caucho permite ajustar la rigidez de las placas. Por ejemplo, al agregar hasta un 50% de caucho en partículas de aproximadamente 2mm, se puede reducir la rigidez entre un 25% y un 85%, dependiendo de las características de la mezcla.
- Se ha demostrado que la geometría de la placa tiene especial relevancia en la rigidez de la misma, la cual es posible reducir en más del 50% en algunos casos.
- Además, el empleo de materiales reciclados (R-HDPE y R-PP/PE) permite reducir en más de un 70% la huella de carbono en comparación con las placas de asiento convencionales.
- Por otro lado, los resultados obtenidos de la calibración de los sensores han demostrado que no todos los sensores son susceptibles de ser usados para la monitorización continua de las vías de ferrocarril.
- Los acelerómetros y piezoeléctricos muestran una relación lineal entre la señal obtenida y la fuerza/movimiento aplicado, pero mientras que el primero detecta los

cambios en las oscilaciones aplicadas, el segundo está centrado en el nivel de tensión aplicada a las placas de asiento. Los paneles piezoresistivos muestran una relación logarítmica entre ambos parámetros, por lo que su uso para detectar cambios de oscilación a altos niveles de carga es limitado.

- Los sensores piezoeléctricos presentan un mayor potencial para su en la monitorización dado que proporciona una señal clara cuando se mide el comportamiento de la vía.
- Además, se ha demostrado en ensayos a escala real que estas tipologías de sensores tienen la capacidad de detectar las variaciones del tráfico, las irregularidades en el contacto rueda-carril y las variaciones en el apoyo de las traviesas, mostrando claramente la capacidad de monitorear las variaciones de las cargas de los vehículos.

Por todo ello, la presente tesis doctoral demuestra que es posible confeccionar placas de asiento sostenibles, a través de la fabricación de las mismas con polímeros reciclados, obteniendo un gran abanico de soluciones que permiten adaptar la rigidez de la placa de asiento a las necesidades de la vía. Por otro lado, existe la necesidad de llevar a cabo una monitorización continua de la vía, que permita convertir las actuaciones de mantenimiento correctivas en actividades preventivas, reduciendo así los costes y tiempos de reparación. Para ello, el uso de sensores piezoeléctricos embebidos en las placas de asiento, puede ser una alternativa a los sistemas de monitorización convencional.

7. Futuras líneas de investigación

A partir de las conclusiones extraídas y de los trabajos de investigación realizados se han detectado las siguientes posibles futuras líneas de investigación:

- Desarrollo de la tecnología necesaria para la adquisición y registro de los datos proporcionados por los sensores de manera inalámbrica, los convierte en una herramienta más versátil para su empleo en vías de ferrocarril.
- Diseño de placas de asiento más versátiles que permitan la incorporación de distintos tipos de sensores, y que faciliten su sustitución, con el fin de ofrecer una solución adaptativa a las necesidades de la vía.
- Desarrollo de modelos predictivos que permitan identificar el momento óptimo para la realización de tareas de mantenimiento a partir de los datos aportados por los sensores.
- Estudios de durabilidad a largo plazo bajo condiciones extremas de temperatura y humedad.
- Influencia de las corrientes vagabundas en las medidas obtenidas por los sensores.

Bibliografía

[1] Eurostat, «Satical Officce of the European Comunties,» 2024.

[2] UIC- Union Internationale des Chemins de fer., High speed rail- Fast track to sustainable mobility., ISBN: 978-2-7461-1887-4., 2015.

[3] K. Odolinski y H. Boysen, «Railway line capacity utilization and its ipact on maintanance costs.,» *Journal of Rail Transport Planning & Management,* pp. 22-23, 2019.

[4] F. Peng, S. Kang, X. Li y Y. Ouyang, «A heuristic apporach to the railroad track maintenance shecduing problem,» *Comp. Aided Civil Infraestruc. Eng.,* vol. 26, nº 12, pp. 129-145, 2011.

[5] F. Calvo, J. De Oña, G. López, L. Garach y R. De Oña , «Rail track cost management for efficient railway charges,» *Proc. Inst. Civ. Eng. Transp.,* vol. 166, pp. 325-335, 2011.

[6] R. Williams, «Improvement in Electric-Signailng Apparaus for Railroad,» U.S. Patent US130661A, 1872.

[7] J. Castillo-Mingorance, M. Sol-Sánchez, F. Moreno-Navarro y M. Rubio-Gámez, «A Critical Review of Sensors for the Continuous Monitoring of Smart and Sustainable Railway Infraestuctures,» *Sustainability,* vol. 12, nº 9428, 2020.

[8] M. Sol-Sánchez, T. Mattinzili, F. Moreno-Navarro y M. Rubio-Gámez, «GRIDMAT- A Sustainable Material Combining Mat and Geogrid Concept for Ballasted Railways,» *Sustainability,* vol. 14, nº 11186, 2022.

[9] X. Lei y B. Zhang, «Analysis of Dynamic Behavior for Slab Track of High-Speed Rail Based on Vehicules and Tracks Element,» *Jorunal of Trasportation Engieneering,* vol. 134, nº 4, 2011.

[10] M. Sol-Sánchez, F. Moreno-Navarro y M. Rúbio-Gámez, «Viability analysis of deconstructed tires as material for rail pads in high speed railway.,» *Mater. Des,* vol. 64, pp. 407-414, 2014.

[11] M. Sol-Sánchez, L. Pirozzolo, F. Moreno-Navarro y M. Rúbio-Gámez, «A study into the mechanical performance of different configurations for the railway track section. A laboratorio aproach,» *Eng. Struct.,* vol. 119, pp. 13-2315, 2026.

[12] K. Brzowski, A. Rygula y A. Maczynski, «The use of low-cost sensor for aire quality analysis in road instersections.,» *Trasnsp. Res. Part D Transp. Envion,* vol. 77, pp. 198-211, 2019.

[13] K. Chilamkuri y V. Kone, «Monitoring of varadhi road bridge using acceleorometer sensor,» *Mater. Today Proc. ,* vol. 33, pp. 367-371, 2020.

[14] W. Xue, L. Wang, D. Wang y C. Druta , «Pavement Health Monitoring System Based on an Embedded Sensing Networ,» *J. Mater. Civ. Eng. ,* vol. 26, nº 04014072, 2014.

[15] M. Sol-Sánchez, A. Jiménez del Barco-Carrión, A. Hidalgo-Arroyo, L. Moreno-Navarro, L. Saiz y M. Rubio-Gámez, «Recycing waste rubber particles for the maintance of different states of railway tracks though a two-step stoneblowing process.,» *J. Clean. Prod,* vol. 244, nº 118570, 2020.

[16] ADIF (Spanish Railway Infraestructures manager). , ET 03.360.570.0 PLACAS ELASTICAS DE ASIENTO PARA SUJECCIÓN VM, Spain: Dirección técnica, 2005.

[17] D. Ferreño, J. Sainz-Aja, I. Carrascal, Cuartas, M, J. Pombo, Casado J y S. Diego, «Prediction of mechanical properties of rail pads under in-service condition through machine learning algormithms,» *Adv. Eng. Softw. ,* vol. 151, nº 1029727, 2021.

[18] L. Carrascal, A. Pérez, J. Casado, S. Diego, S. Polanco, D. Ferreño y J. Martín, «Eperimental studiy of metal cushion pads for high speed railways.,» *Const. Build. Mater.,* vol. 182, pp. 273-283, 2018.

[19] P. Bouvet y N. Vincent, «Laboratory characterization of rail pad dynamic properties.,» *Vibratec report,* nº 450.1998.004.RA.05.A, 1998.

[20] T. ç. Stark y S. Wilk , «Root case of differential movement at bridge transition zones,» *Proc. Insit. Mech. Eng. F J Rail Rapid Transit,* vol. 230, nº 4, 2015.

[21] T. Sussmant, «Field condition observed at a site with concrete tie base abrasion,» *Railw. Eng. Conf. Edinb,* 2017.

[22] H. Wang y V. Markine, «Dynamic behavior of the track in transitions zones considering the differential settlement.,» *J. Sound Vib. ,* vol. 419, nº 114863, 2019.

[23] D. Khairallah, J. Blanc, L. Cottineau, P. Hornych, J. Piau, S. Pouget, M. Hosseingholian, A. Ducreau y F. Sabin, «Monitoring of railway structures of the high speed line BPL whti bituminous and granular sublayers,» *Const. Build. Mater.,* vol. 211, pp. 337-348, 2019.

[24] S. Song, Y. Hou, M. Guo y L. Wang , «An investigations on the aggregate-shape embedded piezoeletric sensors for civil infraestructure health monitoring,» *Const. Build. Mater.,* vol. 131, pp. 57-65, 2017.

El resto de bibliografía consultada para el desarrollo de la presente tesis doctoral queda recogida en cada uno de los artículos incluidos en el Anexo I de este documento.

Anexo I

Se adjuntan como anexos los siguientes artículos, en los que se basa el compendio que compone la presente tesis doctoral.

Castillo-Mingorance, J.M.; Sol-Sánchez, M.; Moreno-Navarro, F., Rúbio Gámez; M.C. *A Critical Review of Sensors for the Continuos Monitoring of Smart and Suistainable Railway Infraestructures*. Sustainability, 12 (2020) 9428. (Factor de Impacto 3.889). https://doi.org/10.3390/su12229428

Castillo-Mingorance, J.M.; Sol-Sánchez, M.; Mattinzioli, T.; Moreno-Navarro, F., Rúbio Gámez; *Development of rail pads from recycled polymers for ballasted railway tracks.* Constr. Build. Mater. 337 (2022) 127479. (Factor de Impacto). https://doi.org/10.1016/j.conbuildmat.2022.127479

Sol-Sánchez, M.; **Castillo-Mingorance, J.M.**; Moreno-Navarro, F.; Rubio-Gámez, M.C. *Smart rail pads for the continuos monitoring of sensored railway tracks: Sensor analysis.* Autom. Constr. 132 (2021) 103950. (Factor de Impacto). https://doi.org/10.1016/j.autcon.2021.103950

Sol-Sánchez, M.; **Castillo-Mingorance, J.M.**; Moreno-Navarro, F.; Mattinzioli, T.; Rubio-Gámez, M.C. *Piezolectric-sensored sustainable pads for smart railway traffic and track state monitoring: Full-scale laboratory test. Constr. Build. Mater.* 301 (2021) 124324. (Factor de Impacto). https://doi.org/10.1016/j.conbuildmat.2021.124324

Castillo-Mingorance, J.M.; Sol-Sánchez, M.; Moreno-Navarro, F., Rúbio Gámez; M.C. *A Critical Review of Sensors for the Continuos Monitoring of Smart and Suistainable Railway Infraestructures*. Sustainability, 12 (2020) 9428. (Índice de Impacto 3,3 en 2.023, Q2 en ENVIRONMENTAL SCIENCES en 2.023).

https://doi.org/10.3390/su12229428

A Critical Review of Sensors for the Continuous Monitoring of Smart and Sustainable Railway Infrastructures

Juan Manuel Castillo-Mingorance[1], Miguel Sol-Sánchez[1]*, Fernando Moreno-Navarro[1] and María Carmen Rubio-Gámez[1]

[1] Laboratory of Construction Engineering, University of Granada, C/Severo Ochoa s/n, 18071 Granada, Spain; jumacami@ugr.es (J.M.C.-M.); fmoreno@ugr.es (F.M.-N.); mcrubio@ugr.es (M.C.R.-G.)

* Correspondence: msol@ugr.es

Received: date; Accepted: date; Published: date

Abstract: Real-time and continuous monitoring through smart sensors is considered to be the evolution of traditional track testing, enabling the earlier detection of the main failure modes that degrade railway tracks. Through carrying out preventive maintenance operations, infrastructure resources may be optimized, leading to smarter and more sustainable infrastructure. For this reason, under the larger goal of creating a synergy with various types of sensors for railway tracks, this article presents a critical review on the different, currently available sensors for smart and continuous monitoring. Specifically, the most appropriate monitoring technologies for each of the main railway track failure modes have been assessed and identified, thus deriving the advantages and capacities of each solution. Furthermore, this review presents some of the main experiences carried out to date in literature by using sensor technologies, such as strain gauges, piezoelectric sensors, fiber-optics, geophones and accelerometers. These technologies have proven to offer appropriate characteristics and accuracy for the continuous monitoring of a railway track's structural state, being capable of measuring different parameters, such as deflections, deformations, stresses or accelerations that would permit the technical tracking of various forms of degradation.

Keywords: real-time monitoring; rail track sensor; smart infrastructure; structural health monitoring; review

1. Introduction

The transport of both people and goods plays a fundamental role in the advancement of society and the economy. In recent years, mobility has greatly increased with an increased use of infrastructures, which in turn requires greater investments to conserve their functionality and safety

[1]. This is accentuated by the fact that train circulation speed and capacity is increasing too, with the aim to reduce travel time and increase railway efficiency [2]. For this reason, to guarantee good track operability it is necessary to optimize the time, resources and costs for maintenance activities (which are increasing in frequency due to increased use).

In this sense, predictive maintenance is a management tool increasing in demand, due its high potential. For this purpose, continuous rail track monitoring plays a fundamental role for efficiently and reliably tracking the condition of the infrastructure. The use of smart and cutting-edge sensors and technologies to monitor the railroad would permit its continuous tracking, and enable the anticipation of future possible pathologies, turning current corrective maintenance into predictive maintenance, thus minimizing associated maintenance costs [3]. Through this, any premature degradation would also be avoided and, therewith, a decrease in the possible costs associated to the renewal of some components of the infrastructure, obtaining a more sustainable solution.

The first monitoring systems date from 1872, when William Robinson invented the first track circuit used in a railway, which is still used nowadays. This system detects the presence of, or lack of, trains on the railway through the electric connections created between the wheels and rails [4]. Since then, sensor technology has evolved very quickly, further increasing in recent years. As a result, track deflection and change in railway stiffness, as well as other railway pathologies that could appear, in railroads can be monitored in different ways, from more simple systems (such as the traditional hydraulic jack-loading method, load cells or deflectometers) to the more sophisticated auscultator train [5]. However, this last solution, despite obtaining good results, is very expensive (one of them can cost more than EUR 45 million), and for this reason, its use is very limited. On the other hand, the use of traditional monitoring systems is limited to the punctual test in a specific area, and does not provide continuous monitoring. Therefore, the development and study of innovative technological solutions for real-time and continuous monitoring has great potential to improve the predictive maintenance possibilities of railways.

The high rate of development of sensor technologies in recent years has made sensors which are smaller, more accurate and cheaper. This increase in technical and economic viability has increased the interest of these devices in various fields such as environmental monitoring [6], bridge monitoring [7] or even testing lineal infrastructures [8]. Through their use, railway transportation could continue to be considered a reference for a modern, intelligent and efficient transportation, making it more competitive, and at the same time decreasing associated maintenance costs, via implementing continuous predictive maintenance.

Therefore, to achieve a smart monitoring system able to detect and predict the main modes of railway track failure, such as permanent deformations, change in the structural section, component fatigue failures and vibration or noise, it is necessary to determine the technology available in the market, its capacity and functionality, as well as, any case studies in which it has been used. Thus, this paper assesses the characteristics of the main types of smart sensors which have the potential to be used for the continuous monitoring of railway tracks, via studying their possible implementation in tracks per the main failure modes and providing understanding on the key parameters to measure in each mode.

For this purpose, the methodology followed consisted of, firstly, identifying and studying the main modes of railroad failure through the literature review of scientific indexed journals as well as technical reports. This revealed the principal factors that can accelerate track failure, and how they are commonly detected via conventional testing. Following on, the smart sensors with the highest potential for track monitoring were analyzed and compared using the current information available in scientific articles (collecting case studies from the last 5 years) as well as consulting technical guides from manufacturers. Finally, a discussion section provides an analysis of the information reviewed, assessing the suitability and potentiality of each sensor for the continuous monitoring of railway tracks per the main modes of railroad failures and the principal current demands.

2. The Main Modes of Track Failure and Their Traditional Monitoring

There are various different failure modes associated with railroads, which decrease the original quality of the tracks due to the degradation of the infrastructure. This depends on several factors such as railroad use, the environment or the possible failure of individual components that could occur during its service life. Despite there being other types of failure whereby the railroad could be rendered inoperable, this paper is focused on those to be carried out during the youth stage in ballasted tracks, given that this track typology is the most commonly used and where a higher level of monitorization is required. The most significant failures are explained in the following sections.

2.1. Permanent Deformation and Rail Track Settlement

Among the most typical failures in lineal infrastructures is related to the permanent deformations, which are more problematic than those with differential magnitudes due to changes in the resistant capacity of the bearing courses. With the continuous loading from thousands of trains, all these deformations are accumulated, giving way to differential rail track settlement. This problem is accentuated in the transition between two track areas with different stiffnesses, such as the transition from an embankment to a bridge or tunnel, or from transitioning between diverse geological areas. Transition zones could be considered as the most problematic areas for rail track settlement, where the rearrangements of the ballast would result in "hanging" sleepers, increasing the impact generated by the passing trains and thus, accentuating this problem increasingly over time. This failure mode could be considered as a vicious circle, where an increase in "hanging" sleeper problems generates a higher dynamic impact in the infrastructure from passing trains, and therewith, an increase in the rail track settlements.

Thus, this problem has traditionally been assessed by measuring the evolution of the track settlement in different sections along transition zones, as well as the height oscillations of the sleepers (referring back to the effect of "hanging" sleepers). Additionally, considering registering the acceleration, it is also possible to obtain the track deflections. For this purpose, the use of instrumentation such as Linear Variable Differential Transformers (LVDTs), high definition cameras and deflectometers is common [9–12]. For example, Mishra et al. [13] used a series of LVDTs to monitor a problematic section in a transition zone south of Philadelphia, USA. For this purpose, five LVDTs were used to collect the different settlements that were generated in each of the layers (Figure 1). Another example is Bowness et al. [14] who used remote video monitoring to assess track displacements. A webcam (with a higher resolution than conventional cameras) was attached to a telescope, which located all of the train structure layers, far away enough to avoid any possible impacts due to the deflection and vibration of the rail track. Particle image velocimetry was used to analyze the images taken during train circulation, with a resolution of 0.04 mm from a distance of 15 m. However, in both cases, in spite of these devices obtaining good results, they are both expensive to install, time consuming for data interpretation, and susceptible to being easily manipulated or even stolen.

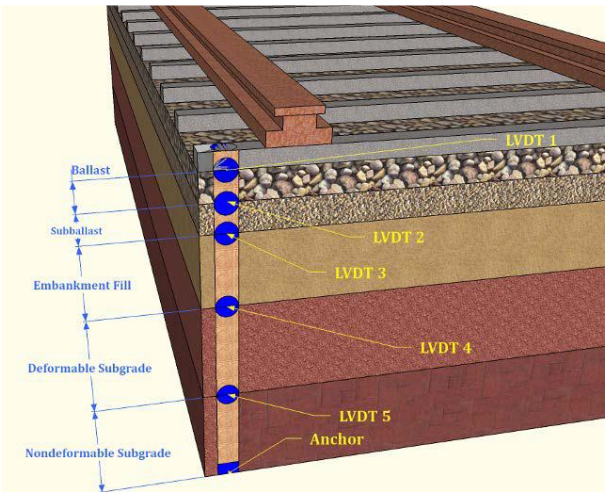

Figure 1. Schematic of track substructure used by Mishra et al. [13].

2.2. Component Fatigue Failure

Another factor that could significantly affect rail track operability is the fatigue failure of individual components. With increasing load capacities (freight trains) and speeds (passenger trains), the rail could suffer located defects due to the dynamic impacts received, where any irregular wheel-rail contact and slips between the wheels and rail would promote extra short-wave vibrations, as well as an increase in stresses. The railroad fasteners are also subjected to fatigue efforts due to cyclic elastic movements, further increasing with force-wave transmission and any noise from wheel-rail contact. In the sleepers, also affected by the passing train, different defects could appear depending on the material with which they are manufactured. In timber sleepers, bio-deteriorations and the climate affect them considerably [15,16]. On the other hand, concrete sleepers are mainly affected by wheel–rail impacts as well as rail–seat deterioration caused by frictional forces present between the pads and the sleepers, further increasing with the presence of any fine particles and/or water [17,18].

Regarding the ballast layer, its degradation can be associated with the abrasion between the corners of the aggregates or its crushing due to traffic overloads, along with ballast fouling, due to any fine particles that considerably affect water drainage, negatively influencing rail track stiffness regularity [19]. Aggregate degradation could be caused by climatic factors and freeze-thaw cycles [20], but mainly from the breaking of aggregates due to the passing traffic [21]. The variation in stiffness along the railway track induces a dynamic load between wheel–rail contact and sleeper–ballast, further increasing the fatigue problems in the rest of components [22], while also varying the bearing capacity of the track. Additionally, high overloading in the sleepers and ballast increases the settlement that could appear in the railroad structure.

Therefore, to minimize the degradation of the various components, it is essential to control and monitor the forces transmitted by the train to the track, as well as evaluate the evolution of the bearing capacity of the track and its deformations. To date, corrective maintenance has been mainly carried out for these components, detected through a visual exam carried out by a specialist or in some cases, with the aid of auscultators trains. However, with the applications of new technology systems is could be possible to detect this type of failure sooner—for example, through the use of axle-box acceleration analysis [23] or analyzing the displacement, accelerations and velocities via the electromagnetic waves in rails and sleepers [19].

2.3. Vibration and Noise

Among the more direct results of rail track settlements and fatigue failures are the deformations and irregularities along the track, which increase vibrations and noise levels. This problem is especially relevant in urbanized areas. According to Connolly et al. [24], there are two main track imperfections that contribute to track vibrations: (a) repeated loading at high frequencies, which can deform the wheels causing the loss of its initial geometry [25], and (b) the appearance of irregularities in the rail due to impacts or deformations associated with problems such as stiffness changes, settlements, welding, transition zones or excessive wear [26]. There are numerous mechanisms that influence rail track vibrations, which have a certain frequency whose ranges can be observed in Figure 2.

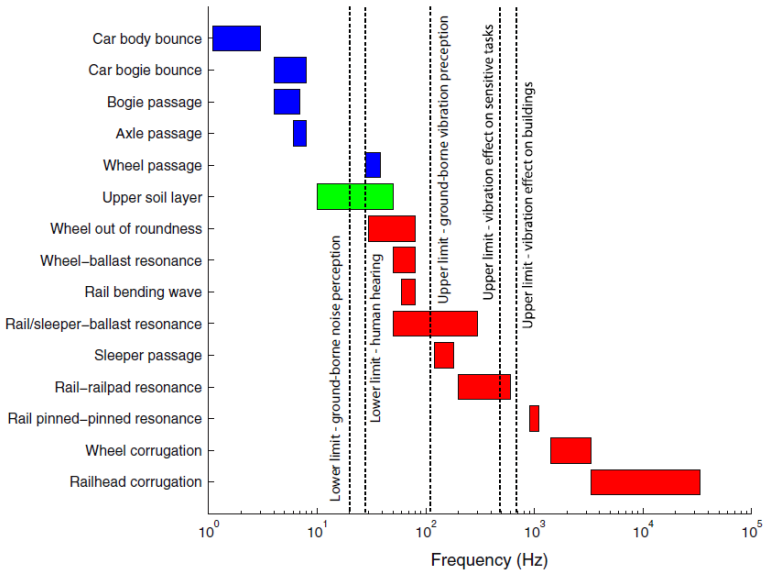

Figure 2. Typical frequency range excitation [24].

Furthermore, it is important to note during the monitoring of the track that throughout the noise (or vibration) spectrum, it is possible to predict the rail-sleeper-force [27], and therefore, it is possible to identify specific track failure types, and thus, the corresponding preventive maintenance operation. For this reason, a good knowledge of the vibrations (amplitudes and frequencies) makes it possible to identify specific problems on the rail track system, as well as quantify them. Traditionally, these vibrations are recorded with the help of accelerometers implanted in the auscultator trains.

2.4. Change in the Structural Section Influence of Stiffness

As mentioned above, the changes in the rail track's stiffness play a crucial role in the proper performance of the railroad. Given both the current and anticipated future trends for traffic (faster and higher loaded trains), a more rapid degradation of components is to be expected, particularly in the case of the ballast since this can be considered the weakest component in ballasted tracks (the most common track type). These facts cause stiffness variation in the rail track section, further accentuating its effect. A higher stiffness gives place to higher overloads in the rail track, causing corrugation and increasing the vibrations [28]. Meanwhile, a low stiffness directly influences the increase in ballast settlement and the fatigue of components [29]. This also increases the necessary power for the locomotives to cross the track, and thus, the level of vibration and noise. Nielsen showed that vertical stiffness variations induce differential track settlements, resulting in the accelerated deterioration of the railway track [30]. In addition, track stiffness considerably influences track geometry deterioration, rail fatigue and the deterioration of other components of the railway [31].

Figure 3 shows an example of how a difference between the stiffness that there is in the railway track and its optimum could cause a high vertical track geometry deterioration.

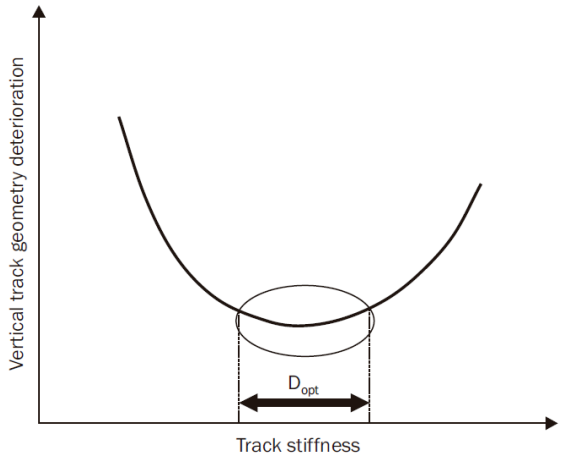

Figure 3. Illustrative display of optimum track stiffness [31].

For this reason, it is necessary to guarantee good stiffness regularity throughout the railway track, and hence, incorporate real-time continuous monitorization. Traditionally, the rail track stiffness is measured with a rail car system that applies a load and measures the track deformation. The China Academy of Railway Sciences (CARS) was among the first to develop a vehicle for the continuous measurement of the static stiffness. Since then, these type of devices have been developed in different countries, such as TU Delft's High Speed Deflectograph (HSD) in the Netherlands [32], Track Loading Vehicle (TLV) in the USA [33], Rolling Stiffness Measurement Vehicle (RSMV) in Sweden, Szybka Kolej Miejska w Trójmieście (SKMT) device developed by the Czech Technical University of Prague and the Commercial Railway Research Ltd. (KZV) in Czech Republic or Schweizerische Budesbahnen (SBB) in Switzerland [34]. However, all of these methods require track closure while the measurements are taken, and thus further increase the associated maintenance cost [35]. In addition, a limitation of these systems is that they do not provide the stiffness variation along the whole railway line.

Nowadays, there are other techniques to measure track stiffness, from the traditional hydraulic jack-loading methods, by applying a certain amount of load on the rail and measuring the displacement with a displacement meter [35], to the more sophisticated methods, using fiber optics [36–38], which still need to be developed in greater depth.

3. Monitoring Elements

Having covered the traditional failure modes and their traditional monitoring methods, this section will review the currently available sensor solutions. Within the different technologies available, this paper analyzes those that would allow the real-time and continuous monitoring of the rail track condition, instead of how it is currently conducted in a periodic manner.

3.1. Strain Gauges

3.1.1. Main Characteristics

Strain gauges are a type of sensor able to measure micro-deformations through its piezo-resistive properties. Piezo resistive properties provide a material with the capability to change electrical resistance when a certain load or pressure is applied to its surface, deforming it in the mechanical-axis directions. Thus, in the case of the strain gauges, as the length of the material increases, its resistivity decreases due to the reduction in the cross-section [39]. It is necessary to determine the elastic modulus of the gauge, due to the fact that it is not possible to use it outside of its elastic limits.

Typically, the strain gauge is manufactured with a metallic foil pattern which is formed by photoengraving a film that has previously been mounted onto a flexible resin plastic base [40]. The dimensions of metallic gauges can vary between 0.4 and 150 mm, and its resistance between 120 and 350 Ω. Specialized gauges are also available with a resistance of 1000 Ω, specially designed to be used

with polymer materials [41]. Gauges are able to register micro-deformations around 0.005. Normally, these devices require a voltage of 2 to 20 V, and through measuring their change in electrical properties the deformation in the material can be calculated.

In the market, it is possible to find a multitude of strain gauge types, from gauges designed to be glued over a surface (i.e., on a rail or a sleeper), to gauges to be embedded into a material (i.e., in concrete or bituminous mixtures). With little changes in resistance it is possible to detect applied loads, but readings are highly susceptible to temperature changes; thus, the Wheatstone bridge (Figure 4) is typically adopted for its assembly. This arrangement is formed by 4 resistors, which increase the sensitivity of the sensor, while compensating the undesired effect of its temperature sensitivity [42].

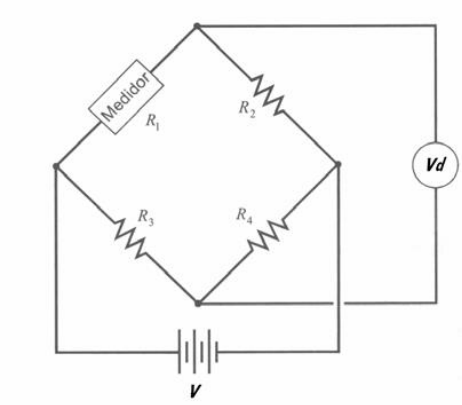

Figure 4. Example of Wheatstone bridge, where medidor refers to the strain gauge [42].

Strain gauge sensors were initially considered as a good way to detect dynamic loads and train speeds, by determining the deformation of a rail due to a passing train, which could also monitor the bearing capacity of the track and the deformation of its components. Nonetheless, it must be considered that they present certain disadvantages that are necessary to take into account such as its fragility, susceptibility to electromagnetic interference, excessive size and high sensitivity to temperature [12].

3.1.2. Case Studies

Most application of gauges are based on the hypothesis that the forces identified in rails could be considered as an indicator of the vehicle type on the rail. It is possible to characterize the forces through the deformations that occur from passing trains, via determining the strain measured and the properties of the material (i.e., Young's modulus E and Poisson ratio). Gauge positions play a fundamental role in data collection. An example of sensor setup is shown in Figure 5, where a sensor with four gauges, oriented at 45° (a, b, c, d), is positioned in the neutral axis of the rail's web to determine the vertical loading, P. Additionally, it is possible to measure the lateral shear force using two gauges (e and f) arranged with a vertical layout.

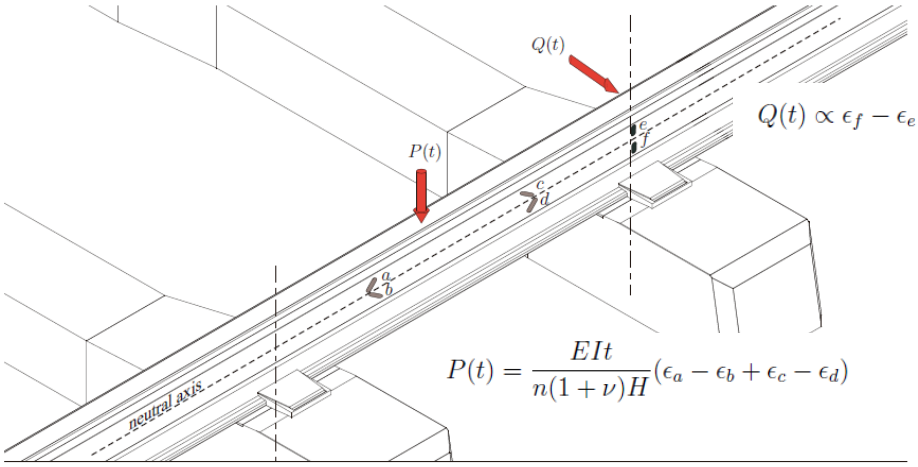

Figure 5. Gauges distribution to obtain forces P and Q [12].

Following this described layout, Askarinejad et al. [43] used strain gauges to detect the dynamic loads imposed by a train passing over insulated rail joints. Furthermore, Palo et al. [44] used strain distribution monitoring at the wheel/rail interference for decision-making support. However, these studies found that it was difficult to measure the forces because the data measuring period was not long enough, so that during the experiment there was not a linear wear pattern, and the trains which passed were different in nature causing different lateral forces. Other authors [45] used strain gauges to develop a new creep measurement technique by measuring internal rail stresses, considering the variation of rail temperature and the influence of straight and curved rails. Furthermore, the Multi-Purpose Q and Y load detector (MPQY) system developed by Delprete et al. [46] allowed the simultaneous measurement of the vertical forces (due to train weight), the lateral forces (primarily caused by dynamic and cinematic effects) and also, the longitudinal forces (generated by traction or braking actions) using strain gauges glued in an intermediate device, shown in Figure 6.

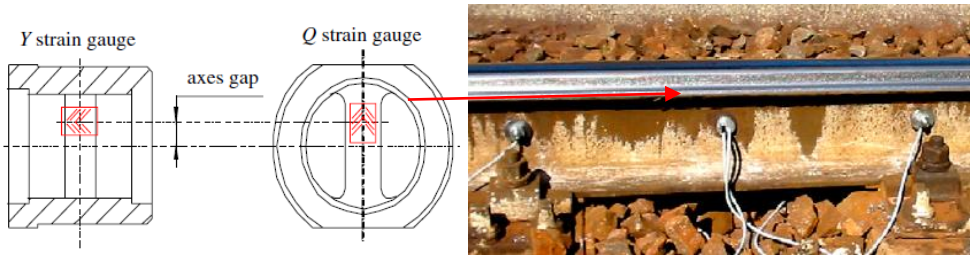

Figure 6. Multi-Purpose Q and Y load detector (MPQY) systems schema [46].

Conversely, INNOtec Systems GmbH, in Germany, developed the MONY system. This system uses pads equipped with force gauges in the middle, as is displayed in Figure 7. The MONY system

can measure dynamic loads by obtaining a good relation between the tread state, the rail-sleeper-force and the radiated noise [27].

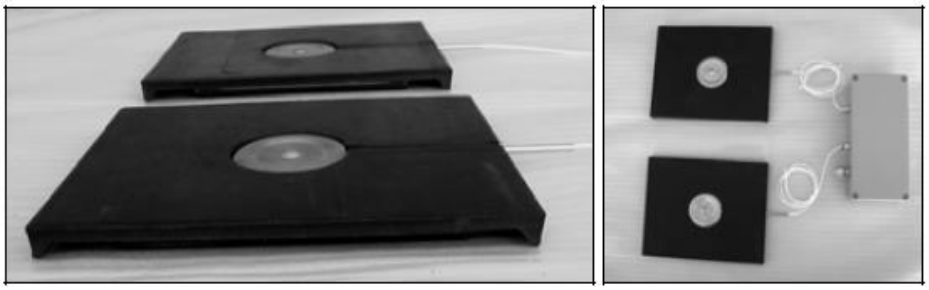

Figure 7. MONI ® measurement system [27].

Finally, there are also specific gauges (H-gauges) designed to be embedded in asphalt mixtures for bituminous sub-ballast. These H-gauges were used by Khairallah et al. [47] in order to determine the deformation that appeared in a bituminous layer located in an experimental section in the line Bretagne-Pays de la Loire, France. This is a high-speed line in which two different substructures were studied: bituminous and granular sublayers. This type of gauge has two anchors that register the movement in a single axis between two points in the asphalt mixture, as is showed in Figure 8. Additionally, this type of gauge is prepared to support the typical temperature and compaction loads of the asphalt mixture installation (reaching up to 160 °C).

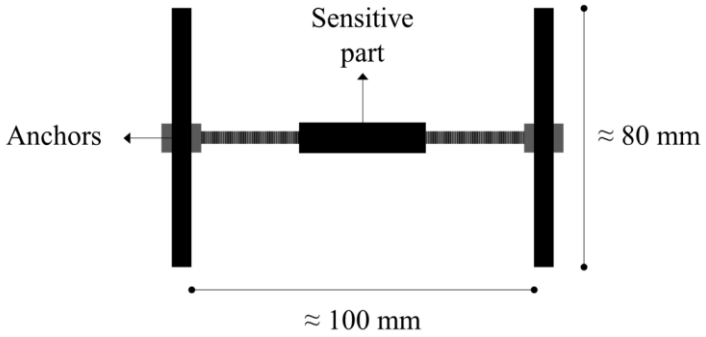

Figure 8. Schematics of a H-gauge [48].

3.2. Piezoelectric Sensors

3.2.1. Main Characteristics

The piezoelectric phenomenon, occurring in certain materials, consists of the capacity to generate an electric current as a result of a mechanical load or vibration. This can occur in certain naturally occurring materials such as quartz, Rochelle salt, tourmaline or topaz. Alternatively, these materials can also be synthetically produced. Among them, there is Lead Zirconate titanate (PZT), Polyvinylidene Fluoride Polymer (PVDF), Barium titanate and Zinc oxide. All of them have the capacity to generate a certain voltage when a compression load or vibration is applied. Furthermore, these types of materials, when in sensors, have a high accuracy due to their natural frequency being very high and having a good linearity in a wide range.

Piezoelectric sensors are available on the market in a wide range of types, ranging from smaller ones with a 20 mm diameter, all the way to large sheets with varying geometries. A piezoelectric sensor has the capacity to generate voltages in the range of a few milli-volts to tens of volts, depending on its construction. A disadvantage of their use is that it cannot be used to take a static reading, since they are activated by the variation of the compression load.

These sensors have many different uses in different fields, such as for hydraulic pressure measurement or in load cells. Meanwhile, in railway tracks, they could be used to monitor the stresses

transmitted by the traffic to the rail structure, and therefore, identify any failure modes depending on the magnitude of the amplitude and frequency recorded for the track oscillations. Nonetheless, to date, in the railway field, few experiences have been reported, which shows that there is potential to further deepen this research field.

3.2.2. Case Studies

Zhan et al. [49] developed a monitoring rail pad to detect damage caused by train wheels, which functions by measuring the vertical forces that act on the rail pads. To achieve this, they made a rail pad with a thin PVDF-based (polyvinylidene fluoride) multilayer sensing device under the rail pads. This type of material presents certain advantages as it has a large frequency bandwidth, a linear output over a wide dynamic range, is lightweight, flexible, available in large sheet, and is also relatively low in cost (around EUR 25 for each pad sensor). The calibration of this sensor was carried out by applying series of loads from 10 to 80 kN, obtaining a maximum voltage of 6 V. This device is shown in Figure 9.

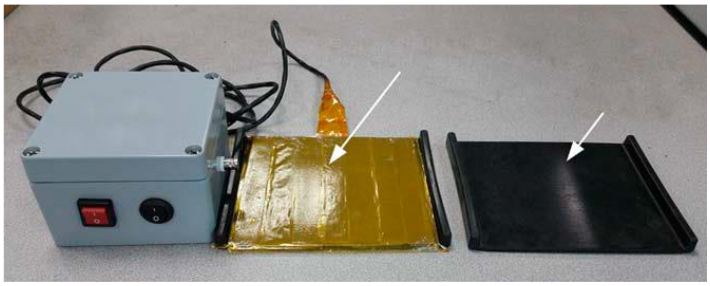

Figure 9. Signal conditioner, rail pad sensor and rail pad [49].

3.3. Fiber-Optic Sensor

3.3.1. Main Characteristics

Fiber optic sensors are based on the detection of variations of light-wave propagation in optical fibers, which are characterized by being able to span long distances and offer a long-term solution [38]. For measuring strain, fiber optic systems could be divided in two main categories (Table 1): fiber Bragg grating (FBG) sensors, where an optical interrogator is used to analyze an array of optical sensors inscribed into a fiber; a distributed optical fiber sensor (Brillion and Rayleigh scattering), where the optical fiber is used as a continuous sensor by itself [37]. Despite fiber Bragg gratins (FBG) having numerous advantages, thanks to their versatility, wide dynamic range and high measurement accuracy, it is only implementable in lengths of less than 1 km. Although FBG cannot provide a continuous map of temperature or strain, within them, around 100 sensors can be found, which could be implemented with a spatial resolution of 2 mm [50]. However, the distributed sensors do not present this problem, allowing it to be provided [51]. Meanwhile, the distributed optical fiber sensor has the potential to span various kilometers using low cost telecommunication fibers [53]. In railway monitoring case studies, it is possible to find the latter fiber optic type (i.e., based on Brillouin and Rayleigh scattering) having been used.

Sensors based on Brillouin scattering have the capability to provide information, such as axle counts, axle distance and train speeds, while also allowing for dynamic load estimations that could be used to understand the evolution of track degradation for preventive maintenance measures. However, this system requires access to both ends of the fiber, reducing the sensing range by half. Furthermore, this type of sensor has a lower strain sensitivity than Rayleigh-based fibers [53].

With this last scattering mode, it is possible to measure within a sensing range of 100 to 150 km [54] and a spatial resolution of 0.5 to 5 mm [55]. Moreover, in a Rayleigh-based distributed system, the acquisition bandwidth is 60 times stronger than the Brillouin scattering [56]. Within this typology, two different measurement technologies are available. The Optical Time Domain Reflectometer (OTDR) allows the measurement of the optical fiber length and characterization of the different

anomalies or possible changes that appear along the fiber, such as strain, temperature and vibration changes. With OTDR, is possible to measure a sensing range between 10 and 50 km [57] using a spatial resolution of 5 to 10 m [58]. On other hand, the Optical Frequency Domain Reflectometer (OFDR) allows strain and temperature to be obtained with a sensing range much lower than OTDR (50–70 m) [59] with a spatial resolution around 1 mm [60].

In general, fiber optic sensors present certain advantages such as high temperature capacity, multiplexing and no sensitivity to electromagnetic interferences [12].

Table 1. Comparison of various fiber optic sensing techniques applied to railway.

Sensor Type	Characteristics [38]	Advantages	Disadvantages
Fiber Bragg	• **Type:** Discrete/Quasi-distributed • **Sensing Range:** around 100 channels • **Spatial Range:** 2 mm • **Measurement parameters:** strain, stress and displacement	• Versatility • Wide dynamic range • High measurement accuracy	• Not continuous • Areas of implementation are limited (<1 km) • Thermal sensitivity • Expensive
Brillouin scattering	• **Type:** Distributed • **Sensing Range:** 100–150 km • **Spatial Range:** 0.5–5 mm • **Measurement parameters:** strain, stress and displacement	• Provide a continuous map of physical parameters such as temperature or strain • Capacity to measure some kilometers	• Require access to both ends of the fiber • Half sensor ranges • Lower strain sensitivity than Rayleigh-based distributed • Thermal sensitivity • Expensive
Rayleigh scattering-OTDR	• **Type:** Distributed • **Sensing Range:** 10–50 km • **Spatial Range:** 5–10 m • **Measurement parameters:** strain, temperature and vibration	• Provide a continuous map of physical parameters such as temperature or strain • Capacity to measure some kilometers • Bandwidth 60 times stronger than Brillouin	• Expensive
Rayleigh scattering-OFDR	• **Type:** Distributed • **Sensing Range:** 50–70 m • **Spatial Range:** around 1 mm • **Measurement parameters:** strain and temperature		

3.3.2. Case Studies

The first time that FBG was used in railway monitoring was in 2004, when this technology was used for axle counting and derailment detection [61]. From then on, this technology was developed in other areas of the railway, such as train wheel condition monitoring [62–64], train vibration and weight measurements [62–65] and the structural analysis of the railway track [5,66–68].

Sensorline developed a combination of several FBG sensors embedded into an elastic pad during the production process, allowing strain measurements to be obtained inside an elastic pad during the passage of trains as a base for material optimization [36], as shown in Figure 10. This sensor is used

for counting train axles or recording dynamic loads, as well as for obtaining a better understanding of the strain variations in a pad to improve its replacement interval.

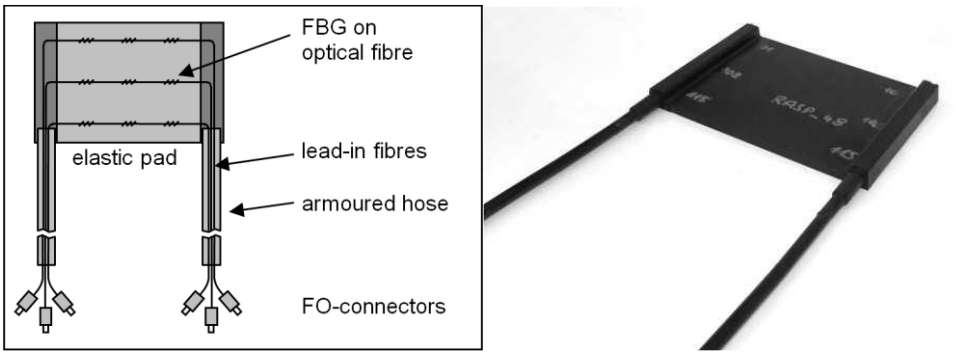

Figure 10. Schema and prototype of the rail-strain-pad [36].

Yoon et al. [69] developed another system based on the Brillouin correlation domain analysis to measure the longitudinal strain of a rail in real time, whose implementation is shown in Figure 11. On the other hand, Minardo et al. [53] used a Brillouin distributed sensor to obtain useful information, such as train identification, axle count, travel speed and dynamic load magnitude. This solution was implemented on the Italian regional line San Severo-Peschici, Italy, operated by Ferrovie del Gargano.

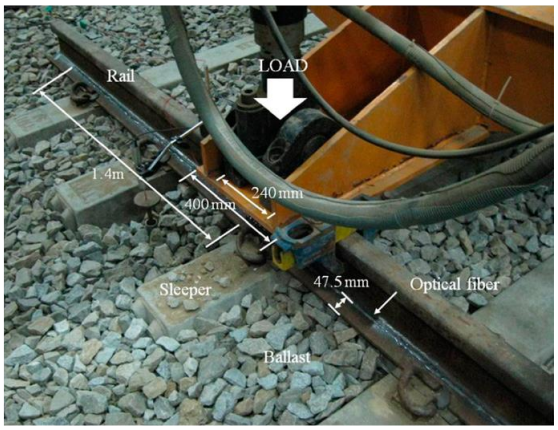

Figure 11. Schema of system developed by Yoon et al. [70].

Wheeler et al. [70] used a 7.5 m long rail section with an optical fiber to measure the strain during the passage of a freight train. However, despite Rayleigh backscatter fiber optic sensing allowing the measurement of dynamic strains, this measurement should be carried out at low speeds (8–11 km/h) due to this technology being highly sensitive to vibrations, hence limiting its use.

3.4. Geophone

3.4.1. Main Characteristics

Geophones are small seismic sensors that produce an output voltage proportional to its wave velocity when it vibrates [14]. The dynamic deflections and component movements are calculated by filtering and processing the velocities measured. Geophones have the capacity to only monitor frequencies higher than their natural frequency, up to a maximum known as spurious frequency. Commonly, the natural frequency of these devices is an order of 10 Hz, and the spurious frequency an order of 250 Hz [41], although it is possible to find geophones on the market with lower natural frequencies. For example, for LF 24 (among the most commonly used), the required voltage can vary between ±11 and ±25 V DC with a current from ±2 to ±6 mA. Additionally, the sensitivity of the geophones can range from 10 to 200 V/m/s. These devices present certain advantages such as their ability to measure large displacements (in millimeters) and being easily powered [35].

3.4.2. Case Studies

LF 24 (Low frequency velocity sensor) geophones were used by Bowness et al. [14] to measure peak to peak displacements (within 0.07 mm) for frequencies as low as 1 Hz in the sleepers. Milne et al. [71] used the same type of geophone to carry out a comparative study between LF 24 and Micro Electrical Mechanical System accelerometers, which showed little variations in their results. Figure 12 shows the accelerometer and the geophone setup over a sleeper, which are used to register the accelerations produced by the passing trains.

Crespo-Chacon et al. [72] obtained reliable readings for the vertical velocities and displacements of vibrating rails on the high-speed line that connects Madrid with Valladolid, Spain, through the use of 2 Hz geophones. To obtain reliable measurements when the train speeds were lower than 100 km/h, different corrections (phase and amplitude) were applied.

3.5. Accelerometer

3.5.1. Main Characteristics

Accelerometers, depending on their structure and operation, can be divided in two main types: piezo-resistive and capacitive based accelerometers [73]. In the piezo-resistive accelerometers, vibrations are detected and transformed into a voltage by a piezoelectric cantilever, a membrane or a thin film [74]. In contrast, capacitive sensors record acceleration changes between a slightly separated proof mass and a conductive electrode [73]. The typical operation frequency can be from 2 to 10 kHz, measuring accelerations that can vary between ±1 and ±250 g. Accelerometers are usually a low potency device, using an electrical current of the order of a micro-amp or a milli-amp, and a voltage of the order of 5 V or less.

In recent years, micro-electrical mechanical systems (MEMS) are also being developed. These are small-size, low-cost sensors used to measure accelerations. Typically, the sensors are embedded in a semiconducting chip. The cost of this type of accelerometer (considering the price of the cheapest, commercially available, conventional accelerometer (together with the signal conditioning unit)) can be around 1 to 10% [74] of a more sophisticated sensor, such as a geophone [71]. This type of accelerometer presents several advantages, as they are cheaper, capable of withstanding shock, have a good frequency response, need a low power input and produce little signal noise [41].

3.5.2. Case Studies

Khairallah et al. [47] used accelerometers to measure the vertical dynamic behavior of a railway track. To achieve this, accelerometers were placed under a sleeper and at the top of a bituminous sub-ballast layer with the aim to compare the differences in levels acceleration between a conventional section and a section with a bituminous sub-ballast layer.

Milne et al. [71] demonstrated how MEMS can be used to successfully obtain displacements from acceleration data measurements, through a double filter-integration. The accelerometers tested were the ADXL335 and ADXL326, whose results were compared with those obtained with a geophone (a relatively more expensive sensor, as stated previously). Given that railway track deformations occur at low frequencies, high frequencies are less important for track monitoring, and thus can be filtered out with a low pass filter [14]. Both the accelerometers and the geophone were glued to the same sleeper as shown in Figure 12. Although this sensor type could output a noisier signal, it was found to be of sufficient quality to be used to obtain track displacements and quantify trends in track behavior.

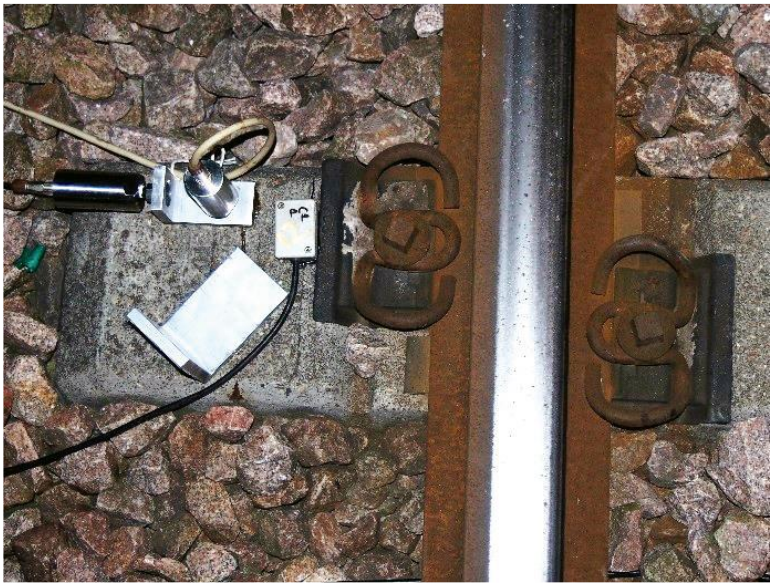

Figure 12. Accelerometer and geophone glued to the sleeper [72].

From the results of the case studies considered, if accelerometers and geophones are compared, it is possible to see that in spite of the geophones having a higher precision than the accelerometers, they are more expensive. Furthermore, accelerometers have a sufficient resolution to be used in railway tracks to measure accelerations and displacements, and they are less frequency-limited, compared to the geophones, which cannot operate below their natural frequency. Table 2 summarizes the main similarities and differences between these types of sensors.

Table 2. Comparison between geophones and accelerometers.

Characteristics	Geophone	Accelerometers
Acceleration and displacement measurement	✓	✓
Relatively low cost		✓
High frequency range operation		✓
High signal noise		✓
High measurement precision	✓	

4. Discussion

According to the aforementioned results, there are many sensors that offer the capability to be embedded in railway infrastructure, and that through their use it is possible to continually monitor the development of rail track failures. For this purpose, it is necessary to clarify which sensors are applicable to which failure type.

Assessing the data in Figure 13, in agreement with the case studies analyzed in the literature available, it is seen that permanent deformations have been traditionally evaluated through the direct measurement of the evolution of permanent or plastic deformations of the track bed under the passage of trains [29]. However, it must be noted that most of the previous research focused on temporally and geographically specific case studies, and therefore, would require devices with the ability to control such parameters through time and along the railway [13,22]. Similarly, this also happens when monitoring the transmission of vibrations, finding punctual investigations into specific problems related to this issue, using specialized instrumentation for punctual studies mainly measuring vibrations along the ground [68,69].

On the other hand, results show that the changes in the structural response of the track (such as changes in track stiffness, also influencing the previously cited failure modes) could be monitored through the measurement of different parameters, highlighting the variations in component oscillations (such as sleeper movements) or global track deflections over the rail [24], as well as

measuring the variations in the dynamic loads generated from wheel–rail interaction or impacts between the sleeper and ballast. Nonetheless, despite all these possibilities, traditional monitoring of these issues has focused on complex solutions, mainly applying loads over the rail and measuring track deflections with special vehicles [32–35]. Therefore, it could be interesting to design and implement smart sensors, with the capability to measure these properties continuously in real-time, to monitor the loads applied by traffic and quantify track deflections or oscillations and to avoid train line closures for structural health assessment.

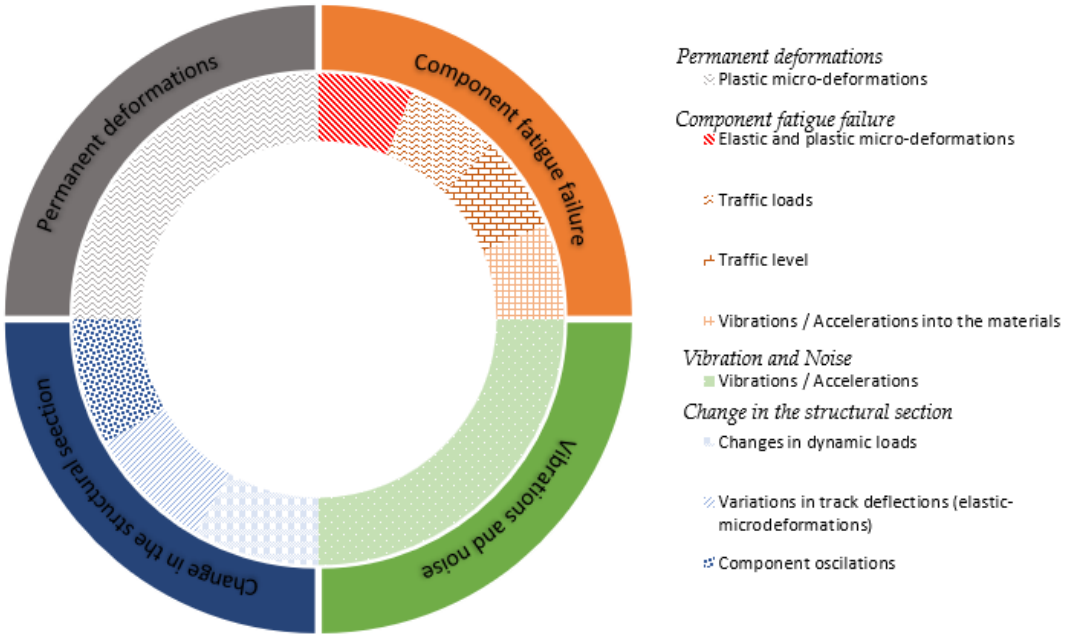

Figure 13. Variables to consider to monitor the main rail track failure modes.

In the same way, devices with the capacity to measure elastic and permanent micro-deformations in materials would monitor the evolution of the performance of components, which would also assist in monitoring the global track response. For the characterization of the life of the components, it would also be necessary to measure traffic conditions (load magnitude and frequency) that could modify the fatigue resistance of such components [28–31]. Furthermore, in previous years, the monitoring of material structure and state through the measurement of wave propagation into the components is gaining importance, requiring small and tailored devices to be included into the materials.

Therefore, it is seen that there are many sensor types available for continuous monitoring. However, not all sensors have the capability of measuring elastic and permanent micro-deformations. In this study, strain gauges, piezoelectric sensors, optical fibers, geophones and accelerometers have been considered since they were found to have been previously used for railway monitoring in the literature review. The placement of these sensors will depend on the variable that needs to be measured. Figure 14 represents the placement options for the different sensors usable for continuous monitoring, while Figure 15 relates the main variables that could be measured with each sensor to their relative cost per lineal meter of infrastructure.

While strain gauges have been widely used in rails, pads and bearing courses to measure elastic and plastic micro-deformations at a reasonable cost (in comparison with the other sensors), its application in sleepers could also be a viable way to measure the performance of this component and the evolution of its fatigue life. Nonetheless, it must be considered that this application has not been studied to date, and therefore, further study will be required [27,43–47]. Additionally, although these micro-deformations are normally correlated with fatigue failure, a strain gauge would also be able to identify other failures in an indirect way, such as traffic loads [43], by correlating the strain measured with the stress applied by using the Young's modulus and Poisson ratio of the material. Furthermore,

as it happens with all sensors, traffic conditions could be measured by considering the number of oscillations generated by the sensor (axel counting) or the time between two consecutive sensor readings along the railroad (train speed). Nonetheless, it must be kept in mind that strain gauges are affected by electromagnetic interferences when measuring the deformations, as opposed to the fiber-optic sensor, which reflects that this technology could be an interesting alternative to strain gauges [12,75].

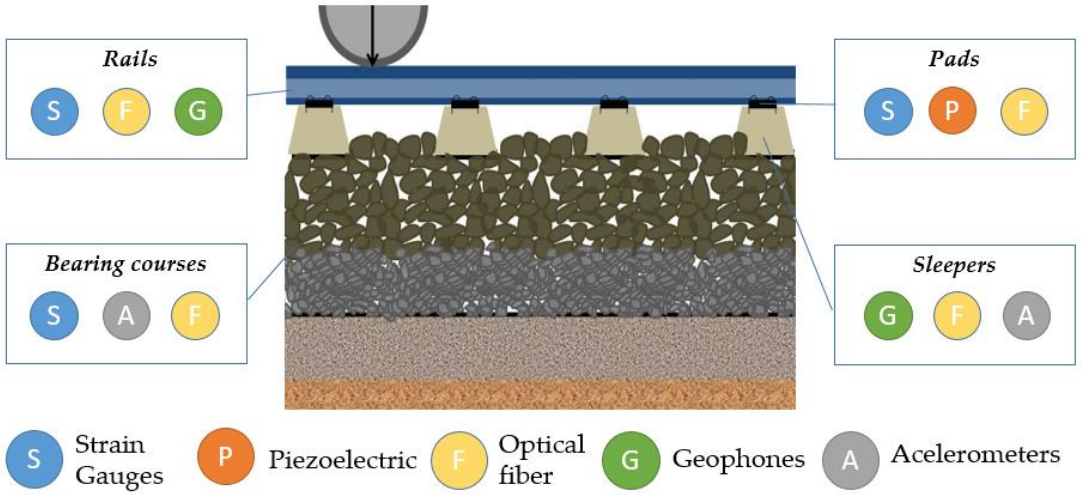

Figure 14. Sensor placements in the case studies reviewed.

Regarding piezolectric sensors, although they have demonstrated the potential to measure dynamic loads with a good linearity and a large bandwidth at a low price, there are not many case studies demonstrating their use [46]. However, this sensor could be a suitable solution for measuring different parameters, such as the loads transmitted by the trains and the vibrations of the railroad materials [49]. This could allow the monitoring of the number of trains that pass and their weight, as well as track performance such as bearing capacity or changes in track stiffness through determining if the components vibrate more in one section of the track than in other areas. Furthermore, as has been conducted in other fields, piezoelectrics could be studied for their application to detect fatigue failures of materials due to sudden changes in electric pulses generated. For all these purposes, it would be necessary to develop this technology, adapting it to the place where it going to be and also, encapsuling it when necessary to guarantee its operability. Therefore, despite the fact that further studies are still required before its wide application, these sensors show great potential due to their versatility and low cost.

In the same way, it is seen that the optical fiber sensor can be considered rather versatile, although its price is commonly higher than piezoelectrics. Nonetheless, due to such versatility, combined with the high development of this technology in the last years, this type of sensor has started to be used for railway monitoring, showing a great potential for its implementation in different parts of the section (Figure 14). Nowadays, there are studies that implement this technology in rails, pads, sleepers and also in bearing courses [34]. Furthermore, it presents certain advantages as it is immune to electromagnetic interference (which is present in railway lines and cannot be eliminated [75]), and it is the only sensor (studied in this review) that could measure temperature changes, being an important variable for understanding the longitudinal changes in the rails caused by dilation [47].

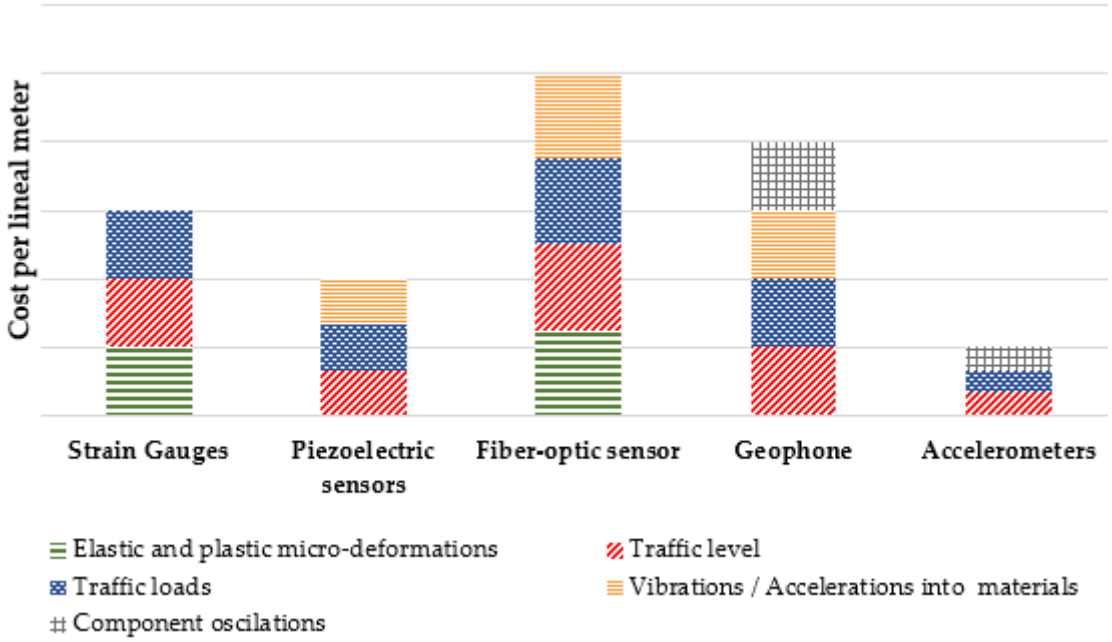

Figure 15. Difference in terms of cost per lineal meter and the main variables measured by each sensor.

With this technology (optical fiber), it is possible to identify changes in the rail track stiffness, by identifying the change in dynamic stresses and elastic micro-deformations (Figure 13). Some of the fatigue failure modes in railroad components (such as sleeper cracking or variations in the regularity of rails) could be studied through the transmission of vibrations into materials. Additionally, in addition to identifying the deformations of components, optical fibers can be used for other applications such as axle counting, vibration measurement and wheel condition monitoring [61–70]. However, although there are studies that use this technology, there is a need for further development to make it economically more competitive.

Finally, geophones and accelerometers can both be used to measure component oscillations. From these readings, it would then be possible to identify track displacements through mathematical analysis (e.g., the double integration of the signal). If both are compared, in spite of geophones having a higher accuracy than accelerometers, the latter are more economic and precise enough for this use [49]. Through their use, it is also possible to identify changes in the rail track stiffness, due to an increase in vibrations in the readings. Additionally, through the knowledge of the vibration amplitudes of the railway's component oscillations, and their frequencies, it is possible to identify certain fatigue problems related with the train's wheels, and the infrastructure's rails and sleepers [24]. On the other hand, although both sensors register vibrations, only the geophones have the capacity to register vibrations of the materials (similar to the piezoelectric and optical fiber sensors).

5. Conclusions

Predictive maintenance operations carried out with novel monitoring systems would provide a more in-depth, real-time and up-to-date knowledge of the railway track condition. In turn, this would decrease maintenance costs as interventions would only be carried out when they are really needed. In this way, it would be possible to achieve smarter, more efficient and more sustainable infrastructure by reducing the resources necessary for its maintenance. In this line, through the assessment of the main technologies available for railway track monitoring, it is possible to extract the following conclusions:

- The monitoring of the different main modes of failure of ballasted railway tracks can be carried out through advanced but simple sensors able to measure diverse parameters such as component deformations and vibrations, track oscillations and dynamic forces applied by traffic.

- In this sense, optical fiber sensors were demonstrated to be among the most versatile sensors since they can track diverse properties, such as deformations, stress levels, vibrations and temperature with a single sensor. Nonetheless, it must be considered that due to the high price of these sensors, in comparison with other alternatives, they would require further research and development to enable their widespread application.
- To cover this disadvantage, a strain gauge could be used as a simple device to track the micro-deformations in components. However, its use presents certain disadvantages, such as its fragility, while also being susceptible to electromagnetic interference and having a high dependence on temperature.
- On the other hand, it has also been seen that the state of the track could be monitored through measuring the transmission of stresses and vibrations, where various experiences demonstrated that piezoelectrics and accelerometers present a good potential for this application.
- This is especially highlighted in the case of piezoelectrics because of their diverse advantages, such as their high linearity and their low cost, while allowing for a clear recording of the dynamic loads (intensity and frequency).
- On the other hand, while piezoelectrics could be more appropriate for monitoring traffic loads, accelerometers are considered to be a promising technology to measure vibrations and deflections (to calculate stiffness changes, differential settlement, hanging sleepers, etc.) because of their high accuracy and lower prices compared to other devices, such as geophones.
- Therefore, it can be concluded that piezoelectric, accelerometer or fiber optic sensors are the most ideal for being embedded into a railway track's substructure (e.g., elastic elements, sleeper, bituminous sub ballast), while avoiding certain problems, such as stealing or vandalism.

Therefore, based on this study, it can be understood that there are currently various technologies available with the characteristics necessary for the continuous monitoring of a railway track's structural state. These sensors are capable of measuring different parameters, such as deflections, deformations, stresses or accelerations that would permit the tracking of various forms of degradation, such as railroad settlement, component fatigue, undesired vibrations or changes in the structural section. However, to continue advancing in this research line, it is essential to develop new systems, which are economically and technically viable, that could be used to support maintenance activities.

Author Contributions: Literature review and analysis, J.M.C.-M., M.S-S, F.M.-N., and M.C.R.-G.; writing—original draft preparation, J.M.C.-M and M.S-S.; writing—review and editing, J.M.C.-M, F.M.-N., and M.C.R.-G. All authors have read and agreed to the published version of the manuscript.

Funding: This research received no external funding.

Conflicts of Interest: The authors declare no conflicts of interest

References

1. Eurostat, Statistical Office of the European Communities. 2020.Retrieved from https://ec.europa.eu/eurostat/web/transport/data/database
2. Mesa, L.; Palacio, I.; Martín, S.; Manzano, G.; Domínguez, J. *Atlas of High Speed Rail in Spain, Madrid (España)*; Fundación de los Ferrocarriles Españoles: Madrid, Spain, 2017.
3. Calvo, F.; De Oña, J.; López, G.; Garach, L.; De Oña, R. Rail track costs management for efficient railway charges. *Proc. Inst. Civ. Eng. Transp.* **2011**, *166*, 325–335.
4. Williams, R. Improvement in Electric-Signaling Apparatus for Railroad. U.S. Patent US130661A, August 1872.
5. Kouroussis, G.; Kinet, D.; Moeyaert, V.; Dupuy, J.; Caucheteur, C. Railway structure monitoring solutions using fibre Bragg grating sensors. *Int. J. Rail Transp.* **2016**, *4*, 135–150.
6. Brzozowski, K.; Ryguła, A.; Maczyński, A. The use of low-cost sensors for air quality analysis in road intersections. *Transp. Res. Part D Transp. Environ.* **2019**, *77*, 198–211.
7. Chilamkuri, K.; Kone, V. Monitoring of varadhi road bridge using accelerometer sensor. *Mater. Today Proc.* **2020**, *33*, 367–371.

8. Xue, W.; Wang, L.; Wang, D.; Druta, C. Pavement Health Monitoring System Based on an Embedded Sensing Network. *J. Mater. Civ. Eng.* **2014**, *26*, 04014072.
9. Ribeiro, D.; Calçada, R.; Ferreira, J.; Martins, T. Measurement of the Dynamic Displacements of Railway Bridges Using Video Technology. *Matec Web Conf.* **2015**, *24*, 2007.
10. Murray, C.A.; Take, A.; Hoult, N.A. Measurement of vertical and longitudinal rail displacements using digital image correlation. *Can. Geotech. J.* **2015**, *52*, 141–155.
11. Gräbe, P.J.; Shaw, F.J. Design Life Prediction of a Heavy Haul Track Foundation. *Proc. Inst. Mech. Eng. Part F: J. Rail Rapid Transit* **2010**, *224*, 337–344.
12. Kouroussis, G.; Caucheteur, C.; Kinet, D.; Alexandrou, G.; Verlinden, O.; Moeyaert, V. Review of Trackside Monitoring Solutions: From Strain Gages to Optical Fibre Sensors. *Sensors* **2015**, *15*, 20115–20139.
13. Mishra, D.; Tutumluer, E.; Boler, H.; Hyslip, J. Instrumentation and Performance Monitoring of Railroad Track Transitions using Multidepth Deflectometers and Strain Gauges. In Proceedings of the 93rd Annual Meeting of the Transportation Research Board, Washington, DC, USA, 15 January 2014.
14. Bowness, D.; Lock, A.C.; Powrie, W.; Priest, J.A.; Richardson, D.J. Monitoring the dynamic displacements of railway track. *Proc. Inst. Mech. Eng. Part F J. Rail Rapid Transit* **2007**, *221*, 13–22.
15. Cornners, T. *Producing and Inspecting Railroad Crossties*; Department of Forestry, University of Kentucky—College of Agriculture: Lexington, Kentucky, 2008.
16. Ferdous, W.; Manalo, A.C. Failures of mainline railway sleepers and suggested remedies—Review of current practice. *Eng. Fail. Anal.* **2014**, *44*, 17–35.
17. Zeman, J.; Edwards, J.; Barkan, C.; Lange, D. Failure mode and effect analysis of concrete ties in North America. In Proceedings of the 9th International Heavy Haul Conference: Heavy Haul and Innovation Development, Shanghai, China, 22–25 June 2009.
18. Zi, G.; Moon, D.Y.; Lee, S.-J.; Jang, S.Y.; Yang, S.C.; Kim, S.-S. Investigation of a concrete railway sleeper failed by ice expansion. *Eng. Fail. Anal.* **2012**, *26*, 151–163.
19. Uranjek, M.; Štrukelj, A.; Lenart, S.; Peruš, I. Analysis of influential parameters for accelerated degradation of ballastrailway track. *Constr. Build. Mater.* **2020**, *261*, 19938.
20. Nurmikolu, A. *Degradation and Frost Susceptibility of Crushed Rock Aggregates Used in Structural Layers of Railway Track*; Tampere University of Technology: Tampere, Finland, 2005.
21. Indraratna, B.; Ngo, T.; Rujikiatkamjorn, C. Performance of Ballast Influenced by Deformation and Degradation: Laboratory Testing and Numerical Modeling. *Int. J. Géoméch.* **2020**, *20*, 04019138.
22. Berggren, E. Railway Track Stiffness: Dynamic Measurements and Evaluation for Efficient Maintenance. Ph.D. Thesis, Royal Institute of Technology KTH, Stockholm, Sweden, 2009.
23. Tanaka, H.; Matsumot, M.; Harada, Y. Application of axle-box acceleration to track condition monitoring for rail corrugation management. In Proceedings of the 7th IET Conference on Railway Condition Monitoring 2016 (RCM 2016), Birmingham, UK, 27–28 September 2016.
24. Connolly, D.; Kouroussis, G.; Laghrouche, O.; Ho, C.; Forde, M. Benchmarking railway vibrations—Track, vehicle, ground and building effects. *Constr. Build. Mater.* **2015**, *92*, 64–81.
25. Nielsen, J.; Johansson, A. Out-of-roun railway wheels- a literature survey. *Proc. Inst. Mech. Eng. Part F J. Rail Rapid Transit* **2000**, *214*, 79–91.
26. Remennikov, A.M.; Kaewunruen, S. A review of loading conditions for railway track structures due to train and track vertical interaction. *Struct. Control. Health Monit.* **2008**, *15*, 207–234.
27. Mueller-Boruttau, F.; Breitsamter, N.; Molzberger, H.; Buchmann, A. Detection of Brake Type and Tread Surface Quality of Passing Trains Based on Rail-Sleeper-Force Measurment. In Proceedings of the 10th International Workshop on Railway Noise, Nagahama, Japan, 18–22 October 2010.
28. Pita, A.L.; Teixeira, P.F.; Robuste, F. High speed and track deterioration: The role of vertical stiffness of the track. *Proc. Inst. Mech. Eng. Part F J. Rail Rapid Transit* **2004**, *218*, 31–40.
29. Hunt, G. EUROBALT optimises ballasted track. *Rail-Way Gaz. Int.* **2000**,156, 813–816.
30. Nielsen, J.; Li, X. Railway track geometry degradation due to differential settlement of ballast/subgrade—Numerical prediction by an iterative procedure. *J. Sound Vib.* **2018**, *412*,441–456.
31. Puzavac, L.; Popovic, Z.; Larevic, L. Influence of track stiffness on track behavior under vertical load. *Promet-Traffic Transp.* **2012**, *24*, 405–412.
32. Hildebrand, G.; Rasmussen, S. *Development of High Speed Deflectograph*; Road Directorate, Danish Road Institute: *Roskilde*, Denmark, **2002**.

33. Wang, P.; Wang, L.; Chen, R.; Xu, J.; Xu, J.; Gao, M. Overview and outlook on railway track stiffness measurement. *J. Mod. Transp.* **2016**, *24*, 89–102.
34. Burrow, M.; Fonsenca-Teixeira, P.; Dahlberg, T.; Berggren, E. *Railway Transportation: Policies, Technology and Perspectives*; Chapter 10; Nova Science Pusblisher: Hauppauge, NY, USA, 2009.
35. Vilotijević, M.; Brajović, L.; Lazarević, L.; Mirković, N. Methods for track stiffness measurement-state of the art. In Proceedings of the New Horizons 2017 of transport and communications, Doboj, Bosnia-Herzegovina, 17–18 November 2017.
36. Woschitz, H. Development of a rail-strain-pad using FBG sensors. In Proceedings of the *5th International Conference on Structural Health Monitoring of Intelligent Infrastructure (SHMII-5)*, Cancún, Mexico, 11–15 December 2011.
37. Milne, D.; Masoudi, A.; Ferro, E.; Watson, G.; le Pen, L. An analysis of railway track behavior based on distributed optical fibre acoustic sensing. *Mech. Syst. Signal Process.* **2020**, *142*,106769
38. Du, C.; Dutta, S.; Kurup, P.; Yu, T.; Wang, X. A review of railway infaestructure monitoring using fiber optic sensor. *Sens. Actuators A Phys.* **2020**, *303*.
39. Ferrero, J.; Guijarro, E. *Instrumentacion Electrónica. Sensores*; Servicio de Publicaciones UPV:Valencia, Spain, 1994.
40. Azate, E.; Montes, J.; Silva, C. Medidores de deformación por resistencia: Galgas extensiométricas. *Sci. Tech. Año XIII* **2007**, *34*, 7–12.
41. Iskander, M. *Underground Sensing. Monitoring and Hazard Detection for Environment and Infrastructure*; Academic Press: Cambridge, MA, USA, 2018.
42. *Figliola-Beasley, Mediciones Mecánicas: Teoría y Diseño*; Alfaomega Grupo Editor: Mexico City, Mexico, 2003.
43. Askarinejad, H.; Dhanasekar, M.; Cole, C. Assessing the effects of track input on the response of insulated rail joints using field experiments. *Proc. Inst. Mech. Eng. Part F J. Rail Rapid Transit* **2012**, *227*, 176–187.
44. Palo, M.; Galar, D.; Nordmark, T.; Asplund, M.; Larsson, D. Condition monitoring at the wheel/rail interface for decision-making support. *Proc. Inst. Mech. Eng. Part F J. Rail Rapid Transit* **2014**, *228*, 705–715.
45. Ahmad, S.S.; Mandal, N.K.; Chattopadhyay, G.; Powell, J. Development of a unified railway track stability management tool to enhance track safety. *Proc. Inst. Mech. Eng. Part F J. Rail Rapid Transit* **2013**, *227*, 493–516.
46. Delprete, C.; Rosso, C. An easy instrument and methology for the monitoring and the diagnosis of a rail. *Mech. Syst. Signal Process.* **2008**, *23*, 940–956.
47. Khairallah, D.; Blanc, J.; Cottineau, L.M.; Hornych, P.; Piau, J.-M.; Pouget, S.; Hosseingholian, M.; Ducreau, A.; Savin, F. Monitoring of railway structures of the high speed line BPL with bituminous and granular sublayers. *Constr. Build. Mater.* **2019**, *211*, 337–348.
48. Barriera, M.; Pouget, S.; Lebental, B.; Van Rompu, J. In Situ Pavement Monitoring: A Review. *Infrastructures* **2020**, *5*, 18.
49. Zhang, S.; Koh, C.G.; Kuang, K.S.C. Proposed rail pad sensor for wheel-rail contact force monitoring. *Smart Mater. Struct.* **2018**, *27*, 115041.
50. Ferdinand, P. The evolution of optical fiber sensors technologies during the35 last years and their applications in structure health monitoring. In Proceedings of the 7th European Workshop on Structural Health Monitoring, Nantes, France, 8–11 July 2014.
51. Rogers, A. Distributed optical-fibre sensing. *Meas. Sci. Technol.* **1999**, *10*, R75–R99.
52. Cho, Y.T.; Alahbabi, M.N.; Brambilla, G.; Newson, T. Distributed Raman amplification combined with a remotely pumped EDFA utilized to enhance the performance of spontaneous Brillouin-based distributed temperature sensors. *IEEE Photon Technol. Lett.* **2005**, *17*, 1256–1258.
53. Minardo, A.; Porcaro, G.; Giannetta, D.; Bernini, R.; Zeni, L. Real-time monitoring of railway traffic using slope-assisted Brillouin distributed sensors. *Appl. Opt.* **2013**, *52*, 3770–3776.
54. Bao, X.; Chen, L. Recent Progress in Distributed Fiber Optic Sensors. *Sensors* **2012**, *12*, 8601–8639.
55. Speziale, S.; Marquardt, H.; Duffy, T. Brillouin Scattering and its Application in Geosciences. *Rev. Mineral. Geochem.* **2014**, *78*, 543–603.
56. Hartog, A. *An Introduction to Disbributed Optical Fibre Sensor*; CRC Press: Boca Raton, FL, USA, 2017.
57. Hill, D. Distributed Acoustic Sensing (DAS): Theory and Applications. *Front. Opt. 2014* **2015**, FTh4E.1.
58. Dou, S.; Lindsey, N.; Wagner, A.M.; Daley, T.M.; Freifeld, B.; Robertson, M.; Peterson, J.; Ulrich, C.; Martin, E.R.; Ajo-Franklin, J. Distributed Acoustic Sensing for Seismic Monitoring of The Near Surface: A Traffic-Noise Interferometry Case Study. *Sci. Rep.* **2017**, *7*, 1–12.

59. Rodriguez, G.; Casas, J.; Villalba, S. SHM by DOFS in civil engineering: A review. *Struct. Monit. Maint.* **2015**, *2*, 357–382.
60. Froggatt, M.; Moore, J. High-spatial-resolution distributed strainmeasurement in optical fiber with Rayleigh scatter. *Appl. Opt.* **1998**, *37*, 1735–1740.
61. Lee, K.; Lee, K.; Ho, S. Exploration fo using FBG sensor for derailment detector. *WSEAS Trasaction Syst.* **2004**, *3*, 2433–2439.
62. Alemi, A.; Corman, F.; Lodewijks, G. Condition monitoring approaches for the detection of railway wheel defects. *Proc. Inst. Mech. Eng. Part F J. Rail Rapid Transit* **2016**, *231*, 961–981.
63. Filograno, M.L.; Corredera, P.; Rodriguez-Plaza, M.; Andres-Alguacil, A.; Gonzalez-Herraez, M. Wheel Flat Detection in High-Speed Railway Systems Using Fiber Bragg Gratings. *IEEE Sens. J.* **2013**, *13*, 4808–4816.
64. Wei, C.; Xin, Q.; Chung, W.H.; Liu, S.-Y.; Tam, H.-Y.; Ho, S.L. Real-Time Train Wheel Condition Monitoring by Fiber Bragg Grating Sensors. *Int. J. Distrib. Sens. Netw.* **2012**, *8*, doi:10.1155/2012/409048.
65. Lai, C.; Kam, J.; Leung, D.; Lee, T.; Tam, A.; Ho, S.; Tam, H.; Liu, M. Development of a fiber-optic sensing system for train vibration and train weight measurements in Hon Kong. *J. Sens.2* **2012**, 2012, 365165.
66. Alexakis, H.; Franza, A.; Acikgoz, S.; Dejong, M. A multi-sensing monitoring system to study deterioration of a railway bridge. In Proceedings of the 9th International Conference on Structural Health Monitoring of Intelligent Infrastructure (SHMII-9), St. Louis, MO, USA, 4–7 August 2019.
67. Buggy, S.J.; James, S.W.; Staines, S.; Carroll, R.; Kitson, P.; Farrington, D.; Drewett, L.; Jaiswal, J.; Tatam, R.P. Railway track component condition monitoring using optical fibre Bragg grating sensors. *Meas. Sci. Technol.* **2016**, *27*, 055201.
68. Lai, C.C.; Au, H.Y.; Liu, M.S.Y.; Ho, S.L.; Tam, H.Y. Development of Level Sensors Based on Fiber Bragg Grating for Railway Track Differential Settlement Measurement. *IEEE Sens. J.* **2016**, *16*, 6346–6350.
69. Yoon, H.-J.; Song, K.-Y.; Kim, J.-S.; Kim, D.-S. Longitudinal strain monitoring of rail using a distributed fiber sensor based on Brillouin optical correlation domain analysis. *NDT E Int.* **2011**, *44*, 637–644.
70. Wheeler, L.; Take, W.; Hoult, N.; Le, H. The Use of Fiber Optic Sensing to Measure Distributed Rail Strains and Determine Rail Seat Forces Due to a Moving Train. *Can. Geotech. J.* **2019**, *56*, 1–13.
71. Milne, D.; le Pen, L.; Watson, G.; Thompson, D.; Powrie, W.; Hayward, M.; Morley, S. Proving MEMS Technologies for Smarter Railway Infraestructure. *Procedia Eng.* **2016**, *143*, 1077–1084.
72. Crespo-Chacón, I.; García-De-La-Oliva, J.L.; Santiago-Recuerda, E. On the Use of Geophones in the Low-Frequency Regime to Study Rail Vibrations. *Procedia Eng.* **2016**, *143*, 782–794.
73. Gao, R.; Zhang, L. Micromachined microsensors for manufacturing. *IEEE Instrum. Meas. Mag.* **2004**, *7*, 20–26.
74. Albarbar, A.; Badri, A.; Sinha, J.K.; Starr, A. Performance evaluation of MEMS accelerometers. *Measurement* **2009**, *42*, 790–795.
75. Coronado-Martínez, J. Análisis de las perturbaciones producidas por el sistema eléctrico de potencia de ferrocarriles de alta velocidad alimentados a frecuencia industrial. *Vía Libre-Técnica* **2014**, 8, 81–100.

Castillo-Mingorance, J.M.; Sol-Sánchez, M.; Mattinzioli, T.; Moreno-Navarro, F., Rúbio Gámez; ***Development of rail pads from recycled polymers for ballasted railway tracks.*** **Constr. Build. Mater. 337 (2022) 127479. (Índice de Impacto 7,4 en 2.023, Q1 en CIVIL ENGENIERING, MATERIALS SCIENCE (MULTIDISCIPLINARY), y CONSTRUCTION & BUILDING TECHNOLOGY en 2.023).**

https://doi.org/10.1016/j.conbuildmat.2022.127479

Development of rail pads from recycled polymers for ballasted railway tracks

Castillo-Mingorance, J.M.[1]; Sol-Sánchez, M. [1*]; Mattinzioli, T. [1]; Moreno-Navarro, F.[1]; Rubio-Gámez, M.C.[1]

jumacami@ugr.es (J.M. Castillo-Mingorance); msol@ugr.es (M. Sol-Sánchez); tmattinzioli@ugr.es (T. Mattinzioli); fmoreno@ugr.es (F. Moreno-Navarro); mcrubio@ugr.es (M.C. Rubio-Gámez)

[1]Laboratory of Construction Engineering at the University of Granada. C/ Severo Ochoa s/n, 18071, Granada, Spain.

*Corresponding author (msol@ugr.es)

Abstract

This article focuses on the study and design of rail pads from recycled plastics for their application in railway tracks, aiming to reduce environmental impacts produced from virgin materials. For this purpose, sustainable rail pads were designed and manufactured using two separate locally recycled plastics: high-density polyethylene from plastic boxes, and from a combination of polypropylene and low-density polyethylene from reclaimed geomembranes. A high-performance polymeric industrial resin was also used as a reference material. These separate plastics were also combined with different quantities and sizes of recycled crumb rubber from end-of-life tires. The results of this paper analyse the influence of pad composition and geometry on the mechanical performance of the pads, while also assessing the durability and environmental benefits of the most optimal solutions. Results found that the pads from high-density polyethylene presented values of static stiffness around 800 kN/mm while the low-density polyethylene led to values close to 150 kN/mm, where the reference industrial binder outputted intermediate values. In addition, the combination of different quantities and sizes of crumb rubber resulted in a range of viable solutions, in some cases reducing stiffness more than 50%. Additionally, both recycled plastics offered a reduced carbon footprint compared to conventional pads, although this did decrease with increasing amounts of crumb rubber. Nonetheless, it was found that the softer solutions led to higher plastic deformations during

fatigue tests, reducing the durability in comparison to the pads made from high-density polyethylene.

Keywords: recycling, plastic, out-of-life tires, rail pads, railway.

Highlights

- Rail eco-pads made from recycled polymers were designed.
- Waste plastics and end-of-life tyres were combined to modify pad stiffness.
- The influence of pad geometry on its stiffness was determined.
- The carbon footprint of the designs was determined.
- Recycled high density polyethylene-based pads were found to be the most durable.
- The net and gross carbon footprints of the pads were explored.

Abbreviation	
CR/R	Crumb Rubber, followed by particle size in mm.
ELT	End-of-Life Tire
R-HDPE	Recycled High-Density Polyethylene
R-PP/PE	Recycled Polypropylene/Polyethylene Mix
G	Pad Geometric Design
G’	Elastic or Storage modulus
G´´	Viscosity or Loss modulus
GHG	Greenhouse Gas

1. Introduction

Railway lines are under evermore pressure to respond to the rapidly advancing requirements set by current and future traffic needs [1-2]. Such needs include higher travel speeds and loading capacities, coupled with the need for safe and comfortable passenger transit. In response to these needs, elastic structural elements, such as rail pads, will likely play a fundamental structural role [3]. These elements link the rail to the sleeper and improve train transit by modifying the stiffness of the rail track and mitigating phenomena such as wave propagation, noise emission, and ballast liquefaction; where the pads can be manufactured with different stiffnesses, and thus different damping capacities depending on the rail line.

It is necessary to consider that these engineered pads respond to the infrastructure’s needs, and so the material used for rail pad manufacturing should have a specific stiffness, since otherwise, the degradation speed of the infrastructure could be expedited. A high rail pad stiffness could increase the dynamic loads and stresses on the substructure, whereas a low stiffness could cause damages in the rail track, increasing their stress state even more [4-6]; making the ideal stiffness dependant on the engineering requirements of the railway. For this reason, when studying rail pads,

different flexible materials should be considered in order to provide a wide range of solutions to adapt to the requirements of the infrastructure. These solutions need to also consider the impact of in-service factors like temperature (affecting material stiffness while deteriorating its durability due to thermal ageing), train speed and traffic conditions, amongst other factors that could modify material stiffness and fatigue resistance [7-9].

However, these elastic elements are mainly manufactured with virgin polymers, like high density polyethylene (HDPE), thermoplastic polyester elastomer (TPE), or ethylene vinyl acetate (EVA) [8, 10-11], which cannot be considered a sustainable long-term solution for the construction of railways and would not meet the requirement of Sustainable Development Goal 12 for sustainable consumption and production (UN, 2021). The global production of plastics increased twentyfold since the 1960's, reaching 322 million tonnes in 2015. In this same year, the European annual plastics demand was 49 million tonnes, where 19.7% was associated with the building and construction sector [12]. Furthermore, combustion and landfilling as traditional methods of polymer waste elimination have several disadvantages such as the formation of dust, and emissions of fumes and toxic gases in the air, as well as the pollution of underground water resources. Therefore, regarding energy consumption and environmental issues, polymer recycling is one of the most efficient ways to manage these waste materials, but due to variability in the composition of polymer wastes and difficult conditions during their service life, the performance of recycled compounds varies compared to virgin compounds, which needs to be improved [13].

End-of-life tires (ELTs), and its derivative product crumb rubber (CR), have presented themselves as one of the most popular recycled materials for infrastructure use, having been used in a multitude of civil engineering applications such as roads [14-15], ports [16] and railways [17-20]. Regarding railways, CR was found to be beneficial to reduce ballast particle degradation and, in turn, the maintenance frequency; increasing track durability when placed between the sleeper and the ballast [18]. Regarding its use for rail pads, Sol-Sánchez et al. [6, 17] showed the high potential of ELTs for structural use in railroad pads too, in term of stiffness and durability. Regarding other polymeric materials, limited previous research on the use of recycled plastics for rail pads can be found in literature. In other sectors, the use of recycled HDPE for polyethylene pipes was found to be viable, but largely depended on the quality of the recycled HDPE [21]. Where HDPE is one of the most used and in demand plastics, both generally and in construction. Magnusson and Mácsik [22] studied the environmental impacts for different materials for an artificial turf field, where it was found energy use and global warming potential (GWP) were highest for virgin thermoplastics (such as HDPE and PP), and the use of recycled materials (such as CR) could reduce energy use and GWP. Therefore, the use of

these recycled thermoplastics and their comparison with other recycled waste materials, both as a structural level and a GHG level, would be of great value.

Thus, based on the current potential for increasing the sustainability of these elastic elements, the aim of this paper was to assess the viability of novel eco-pads in railway tracks manufactured with various recycled plastics. To achieve this aim, pads composed of CR, recycled thermoplastics (i.e., HDPE and PP) and an industrial polyurethane resin (as a reference material) manufactured at various stiffnesses were considered. For this purpose, the methodology consisted of, firstly, studying and analysing different material compositions, and considering the influence of crumb rubber content and size in the mix. Following on, the geometric influence of the rail pads was studied. Once this was known, the analysis of the durability of the recycled pads was carried out. Finally, a carbon footprint analysis of the eco-rail pads was carried out.

2. Methodology

2.1. Materials

Four different materials were involved in the manufacture of the rail pads. Three of them were used as a binder material (R-HDPE, R-PP/PE and Resin), which were mixed with different sizes and levels of crumb rubber (CR) from waste end-of-life car tyres. The CR was used to modify the stiffness of the pads. There are previous studies that demonstrated that the inclusion of CR can be used to modify the general railway structure's stiffness, for example, through the stone-blowing process [19].

The binder materials used are described as follows:

- R-HDPE. This material was sourced from end-of-life, recycled industrial plastic boxes, which are abundant all around the world. Its density was around 980 kg/m^3. The recycling process for this material consisted of its collection, cleaning, and grinding into particles of around 5 mm.
- R-PP/PE. This material came from the residue of geomembranes used for waterproofing applications, whose density was 930 kg/m^3. This material is composed of two different layers. The waterproof layer is mainly formed by low density polyethylene (LDPE), but also contains other polymers such as polypropylene (PP). Furthermore, the geomembrane also contains polyester fibres (white particles), for protective purposes. On top of these materials, it is possible to also find different additives like dyes, antioxidants, and thermal and UV radiation stabilizers within the membrane. The use of R-PP/PE was selected given the abundant presence of this waste material in the authors' local area, and thus its recycling would be more prominent.
- Resin. A bi-component polymeric industrial resin composed of polyurethane, with tough-elastic properties was used. This material had a shore hardness of 60 at 7 days (DIN 53505) and an abrasion resistance of 65 mg at 14 days (ASTM D

4060). This material was selected to act as an industrial reference material, which would be able to validate the performance of the recycled materials.

Meanwhile, the crumb rubber from waste car tyres, used as stiffness modifier, was implemented at three different granulometries. Specifically, at 0.6 mm (R0.6), between 0.6-2 mm (R2), and 2-4 mm (R4) width. Figure 1 shows the crumb rubber's granulometric curves. This material had a mean density of 1,170 kg/m^3.

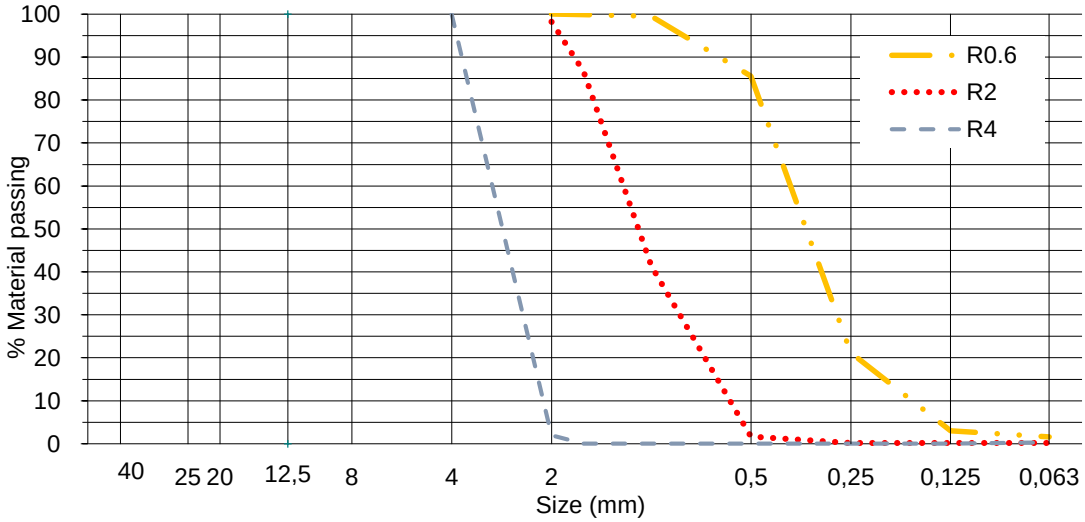

Figure 1. Grading curves of crumb rubber particles

The visual appearance of the different materials used as part of this study can be compared in Figure 2.

Figure 2. Visual appearance of the materials used for the manufacturing of sustainable pads.

The manufacturing process was determined after some previous experimental trials carried out in the laboratory to define the best procedure to obtain pads from the recycled materials with appropriate physical and mechanical properties. Specifically, the rail pads made from both the R-HDPE and R-PP/PE were manufactured by melting the recycled plastics (previously grounded up to particles with 5 mm of size) at a temperature of around 180°C. In the case of the pads which included crumb rubber, the CR was homogenously mixed with the melted plastic, using an automatic mixer in laboratory during 60 seconds. After that, the plastic mass was placed into rectangular metallic moulds with different superficial texture designs. These textures were applied on the bottom surface of the mould to provide pads with various geometries depending on the desired rail pad characteristic (Section 2.2.2). Once the material was in the mould, a load of 15 kN was applied in order to compact the material and obtain a high-quality finish without imperfections in the pads.

On other hand, the pads made from the resin were manufactured by mixing its two constituent components (liquid at room temperature, which solidify when mixed) and pouring them into the appropriate mould to obtain the required geometry. In the same way, in the cases where CR was added (Section 2.2.1), these materials were mixed before being poured into the moulds at laboratory temperature, without requiring the compaction step.

2.2. Testing plan and methods

Table 1 shows the testing plan carried out for this paper. The research was divided into four main steps: (1) analysis of the composition of the different materials used; (2) study of the influence of rail pad geometric design; (3) study of the material durability; (4) study of the carbon footprint of the pads.

Table 1. Testing plan

Study step	Step	Materials	Study variable(s)	Tests
(1) Influence of material composition	1.1 Material type influence	R-HDPE Resin R-PP/PE	Material type	- Static stiffness 20/95 -Dynamic stiffness -Damping capacity -Tensile test
	1.2 Percentage of crumb rubber influence	R-HDPE + R2 R-PP/PE + R2 Resin + R2	Crumb rubber percentage -0% -25% -50% -75%	
	1.3 Crumb rubber size influence	R-HDPE + 25/50/75% CR	Crumb rubber size -R0.6 -R2 -R4	
(2) Geometric design definition	2.1 Superficial design influence	R-HDPE + 50% R2	-Geometry 1 -Geometry 2 -Geometry 3 -Geometry 4	-Static stiffness 20/95 -Dynamic stiffness
	2.2 Superficial design influence in different materials	R-HDPE + 50% R2 R-HDPE + 50% R4 Resin + 50% R2 R-PP/PE + 50% R2	Less influential geometry	- Static stiffness 20/95 -Dynamic stiffness -Impact attenuation
			Most influential geometry	
(3) Study of the material durability	3.1 Fatigue Resistance *Geometry 1*	R-HDPE + 50% R2 R-HDPE + 50% R4 Resin + 50% R2 R-PP/PE + 50% R2	Material type	-Fatigue process
(4) Carbon footprint analysis	4.1 Gross and net footprint analysis	R-HDPE (25, 50, 75% CR) Resin (50,75% CR) PP-LDPE (25, 50, 75% CR)	Material type	-Cradle-to-Gate carbon footprint analysis

2.2.1. Influence of material composition

To study the influence of the binder material type, three rail pads of 140 x 180 x 7 mm were manufactured using 100 percent of R-HDPE, resin and R-PP/PE; the standard dimensions used in a rail track lines with a UIC 54 rail [23].

Once these materials were analysed, with the aim of expanding the range of the possibilities, further alternatives were studied by mixing the different binders with particles of crumb rubber looking for to adapt the stiffness of these initial pads. For this purpose, the influence of the volumetric crumb rubber percentage (0%; 25%; 50%; 75%) into these materials were characterized for rail pads manufactured with R-HDPE, resin and R-PP/PE as a binder. For this, the intermediate crumb rubber size was selected to explore this variable. Similarly, the influence of crumb rubber size (R0.6; R2; R4) was also studied. For this, the R-HDPE was selected due to it being the most rigid material, and thus the one which would most benefit from modifying the stiffness.

For this purpose, static and dynamic stiffness tests (UNE-EN 13146-9) were carried out to evaluate how these parameters (materials, crumb rubber percentage and crumb rubber size) influenced the material's performance. For the static test, three compressive load-unload cycles were carried out with loads between 20 kN and 95 kN. The loading speed was 15 kN/min (1st and 2nd cycle), while the discharge was at 50 kN/min. In the 3rd cycle, in which is static stiffness was calculated, the loading speed was at 5 kN/min. For the dynamic test, 1,000 load cycles at 4 Hz were applied over the rail pads, where the stress and strain in the axial direction was measured for each of the loads. Both static and dynamic stiffness (measured as kN/mm) was calculated as the relation between the load amplitude (75 kN) and the vertical displacement amplitude (in mm) recorded between 20 kN and 95 kN.

On the other hand, using a mechanical analyser (DMA) (Figure 3a), the damping capacity of the materials were studied. For this, prismatic specimens were manufactured with the follow dimensions: 50 x 7 x 7 mm. For this purpose, sinusoidal displacement of 10 µm at different frequencies (from 1 to 16 Hz) were applied in the middle of the specimens, as can be seen in the figure, obtaining the viscous, or Loss, modulus (G´´) and the elastic, or Storage, modulus (G´). The damping of the material is given by the G´´/G´ ratio. For a high knowledge of the material performance, this test was carried out at different temperatures, from 35ºC to 80ºC.

Finally, the tensile stress-strain properties were analysed through the tensile test (Figure 3b), according to the UNE-ISO 37. For this, specimens with a halter shape were manufactured and tested by applying a tensile load controlled by a displacement of 500 mm/min.

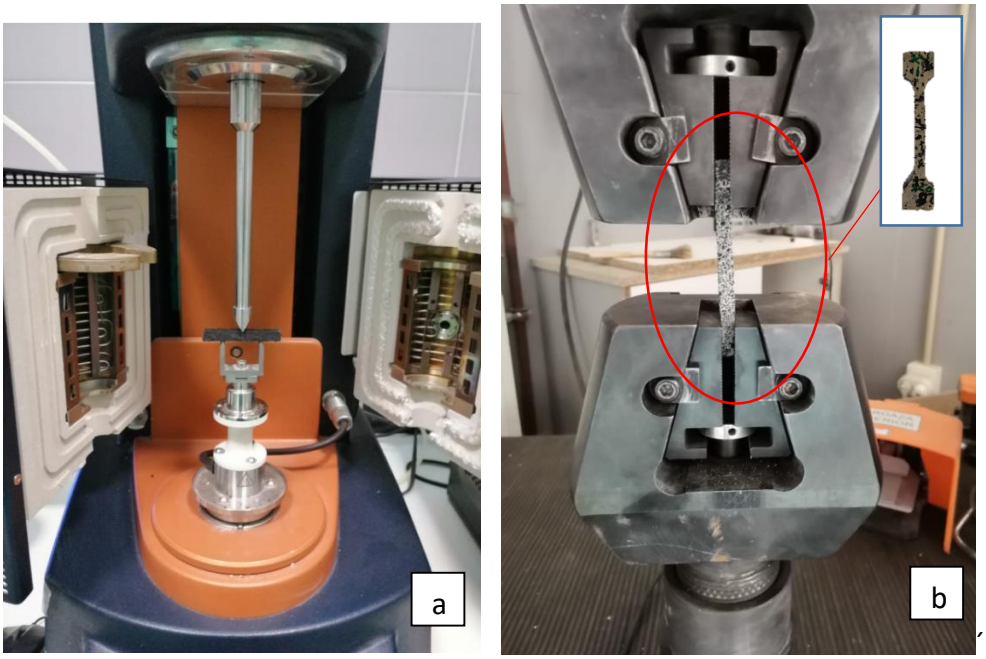

Figure 3. The DMA test (a) and the Tensile test (b).

2.2.2. Geometric design definition

Once the material designs for the pads were known, the influence of the surface configuration of the pads was also studied. This was considered due to previous studies demonstrating its influence on rail pad stiffness [5, 24]. The rail pads, manufactured with recycled materials, were designed according to the dimensions required for a rail track with a UIC 54 rail [23]. The dimensions were the same as in the previous section (140 x 180 x 7 mm), which are in compliance with the UNE-EN 13146. For their manufacture, different moulds were used to obtain the required geometry. In total, four different geometries were tested (Figure 4):

- Geometry 1 (G1): Rail pads without protrusion, used as a reference.
- Geometry 2 (G2): Pattern used in many of the Spanish high-speed lines, with oblong shaped protrusions in the upper side [24-25].
- Geometry 3 (G3): Prototype. Rail pads with lineal protrusions on the upper side, with 2 mm depth, and 6.60 mm wide, separated at this same distance. In the central part, a protrusion of 54 mm was used.
- Geometry 4 (G4): Prototype. Rail pad with lineal protrusions on the upper side, following the geometry 3 pattern. On the bottom, lineal protrusions with 2 mm of depth and separated 10 mm between them, respecting the central protrusion dimensions of geometry 3 too.

G1 and G2 were selected as standard geometries commonly used in the manufacturing of these elements, while G3 and G4 were studied as a prototype aiming to reduce the superficial pad area aiming to vary pad stiffness to provide a range of solutions.

Figure 4. Different rail pad geometries tested.

As detailed in Table 1, static and dynamic tests were carried out to evaluate how the surface configuration influenced the stiffness of a pad design with an intermediate CR content (R-HDPE + 50% R2). Once the difference in stiffness per geometry was found for this material combination, different rail pads were then also manufactured with the other binder materials (resin; R-PP/PE) for the selected geometries (i.e., G1 and G4), which had the highest and lowest stiffnesses. These were characterized for an intermediate crumb rubber size (R2), with 50/50 volumetric proportion with the binder, through their static and dynamic stiffness. Also, in order to know the effect of the crumb rubber size on the rail pad's behaviour when the geometry changed, rail pads manufactured with R-HDPE and R4 crumb rubber were studied too.

Furthermore, to determine the effect of G1 and G4 recycled rail pads (i.e., R-HDPE with R2 and R4; resin and R-PP/PE with R2) on the superstructure against irregular impact loads, such as those produced by wheel or rail imperfections, the impact attenuation capacity test was carried out. The impact attenuation capacity test was carried out according with the UNE-EN 134146-3 standard. For this purpose, a vertical preload of 50 kN was applied over the rail-sleeper and subsequently, without removing this preload, an impact load of 100 kN is applied to the rail by a free-falling mass. As part of this test, the deformations at the upper and lower parts of the sleeper were registered. Before the test, ten impacts were applied to ensure the perfect seating of the clamping. After that, the impact attenuation capacity was calculated according with Eq. (1), which compares top and bottom deformations of the sleeper against a reference pad (REF-PAD) with a static stiffness higher than 2,500 kN/mm.

$$a_{top}\ (\%) = 100\left(1 - \frac{\varepsilon_{top}}{\varepsilon_{RE,top}}\right)\%;\ a_{bottom} = 100\left(1 - \frac{\varepsilon_{bottom}}{\varepsilon_{RE,bottom}}\right);\ a = \frac{(a_{top} + a_{bottom})}{2}\ \%$$

(1)

where:

a_{top} and a_{bottom} are the attenuation ratios measured at the top and bottom of the sleeper, respectively;

ε_{top} and ε_{bottom} are the deformation values measured at the top and bottom of the sleeper, respectively, when using the tested pad;

$\varepsilon_{RE,top}$ and $\varepsilon_{RE,bottom}$are the deformation values measured at the top and bottom of the sleeper, respectively, when using the reference stiff pad;
a is the mean attenuation ratio.

2.2.3. Study of material durability

Rail pads must be designed to guarantee a good operativity during their service life. For this reason, the fatigue test was carried out to predict the long-term behaviour of the rail pads created. In this way, it was possible to experimentally determine the variation of the characteristics and the behaviour of an elastic rail pad when subjected to a cyclical loading simulation over a long period; as that which happens under normal conditions of rail track operation. With the aim to compare the behaviour of the materials, R-HDPE + 50% R2, R-HDPE + 50% R4, Resin + 50% R2 and R-PP/PE + 50% R2 rail pads were studied, which assessed the influence of the binder material type and the crumb rubber size in the rail pad durability. In this case, G1 was chosen for this study step, since this geometry was the one with the lowest decrease in rail pad stiffness. The R-HDPE was selected for testing both the R2 and R4 as it was the stiffest material, and thus most affected by the crumb rubber particle size.

The fatigue test (UNE-EN 13146-4) undertaken consisted of the application of $3x10^6$ load cycles (between 5 kN and 83 kN) on a rail piece (0.5 m long) placed over half a concrete sleeper (i.e., representing one side of the railway line). The angle of the load actuator was equal to 33° from the vertical direction of the rail (Figure 5). Before and after the 3 million of cycles, 10 static cycles were carried out (at a speed of 100 kN/mm), measuring the rail head and rail foot displacements, and calculating the differences between the movements before the fatigue process and those at the end of the test. Also, once a fatigue test was carried out, the static stiffness (according with the above-mentioned test) was studied, with the aim to understand how the fatigue process affects the rail pad performance.

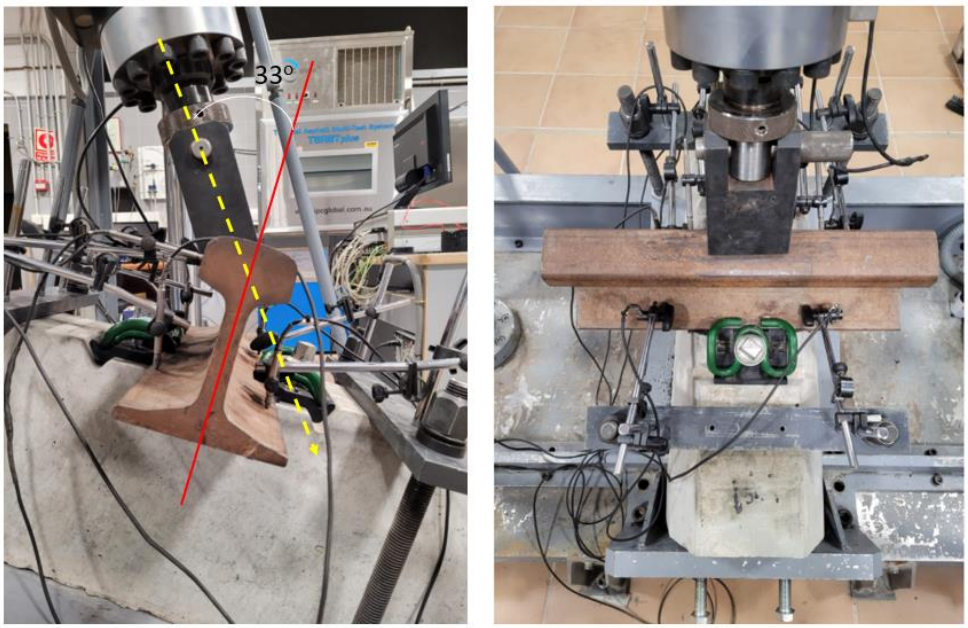

Figure 5. Fatigue test

2.2.4. Study of the rail eco-pad environmental footprints

To determine the environmental burdens of the eco-rail pads tested, a carbon footprint analysis was undertaken. This analysis considered the impacts associated to obtaining the recycled materials and the manufacture of the pads in the laboratory (stages A1 and A3 according to the EN 15804). The life-cycle inventory for 11 pad permutations was considered, as shown in Table 1. The resulting environmental footprints of the pads considered were compared to the production of a conventional rail pad. The functional unit for the study was 1 km of a single rail carriageway, requiring a total of 6,667 pads per double-track railway line (with a 0.6m sleeper separation).

A summary of the sources used for calculating the carbon footprint can be seen in Table 2. For the recycled materials both their gross and net carbon footprints were considered. This approach better identifies the resulting environmental benefits achieving through recycling the waste materials. For the resin, only the gross impacts were reported. As mentioned previously, the manufacture of the recycled pads requiring their heating and mixing to 180°C. The mixing was excluded from this analysis, due to being a manual process. For the heating process, the GHG emissions were calculated for heating the recycled materials for 6 hours in a 2,000 W laboratory furnace. The carbon footprint was calculated for the Spanish electricity grid mix [26], with emissions data from Ecoinvent [27]. The carbon footprint of the conventional reference rail pad was based on that of Pons et al. [28], where the rail pad is made with rigid foam polyurethane (HDPE).

Table 2. References used for the calculation of the pad carbon footprints.

Product	Modelled Process	Reference
R-HDPE	1. Treatment at primary recycling facility	

R-PP/PE	2. Transport 3. Re-processing and disposal of rejects	[29] – separate for recycled HDPE, PP and LDPE
Resin	Based on a reactive resin: 1. Resin production 2. Addition of hardening agents	[30]
Crumb Rubber	1. Grinding, with material separation 2. Crushing, with material separation	[31]

3. Results and Discussion

3.1. Definition of material composition

Figure 6 shows the results from the static (Figure 6a) and dynamic (Figure 6b) testing of the rail pads manufactured with different binder materials. According to the results, three distinct solutions could be derived from this study. Regarding the static stiffness values (used for the mechanical characterization of these components, which are used for track stiffness calculation), the pads manufactured with R-PP/PE presented a stiffness of around 100 kN/mm, while in the other cases, the stiffness increased considerably, reaching values of 800 kN/mm in R-HDPE rail pads and 500 kN/mm in resin pads.

To understand the applicability of these pads, Figure 6a also shows the range of static stiffness values commonly defined to differentiate between soft-medium pads and hard pads. These limits have been assigned according to various sources [32 - 34] where it could be said that the soft-medium pads (C_{stat} < 250 kN/mm) are mainly applied in conventional, high speed and transit lines, which corresponds in this study to the case of R-PP/PE pads. On the other hand, the hard pads (C_{stat} > 200 kN/mm) are currently limited to heavy haul freight or industrial lines.

Nonetheless, it must be noticed that such values are marked as general references to obtain a global track stiffnesses close to 50-80 kN/mm in standard ballasted lines, but different applications or classifications of the pads can be found in literature depending on different factors like the design and characteristics of track section, degradation grade of the line, radius of curves, transition zones, etc. In fact, literature [9] states that soft pads are mainly appropriate for slab tracks and modern ballasted tracks requiring a reduction in stress over sleepers and foundation layers. Also, these pads are used in lines which require a decrease in rail corrugation (particularly in urban areas or with a low curve radius), and in ballast vibration, as well as those with an abrupt change of stiffness along the line (mainly under frequent transition zones). On the other hand, stiff pads like the R-HDPE could be appropriate for heavy freight lines, and in for cases requiring a decrease in rail deflection and movement and vibration of the rail from passing traffic.

Regarding the dynamic stiffness (Figure 6b), the values found were considerably higher than those from the static results, which must be associated with a marked rheological performance of the recycled plastics, which stiffen when increasing load speed. Nonetheless, the dynamic/static stiffness ratio was close to 3.5, which is in consonance with previous studies [35]. This value of dynamic stiffness is mainly studied to understand the pad stiffening under dynamic loads, but it must be noticed that the characteristic parameter of the rail pads is the vertical static stiffness; being the one used to calculate the global track stiffness.

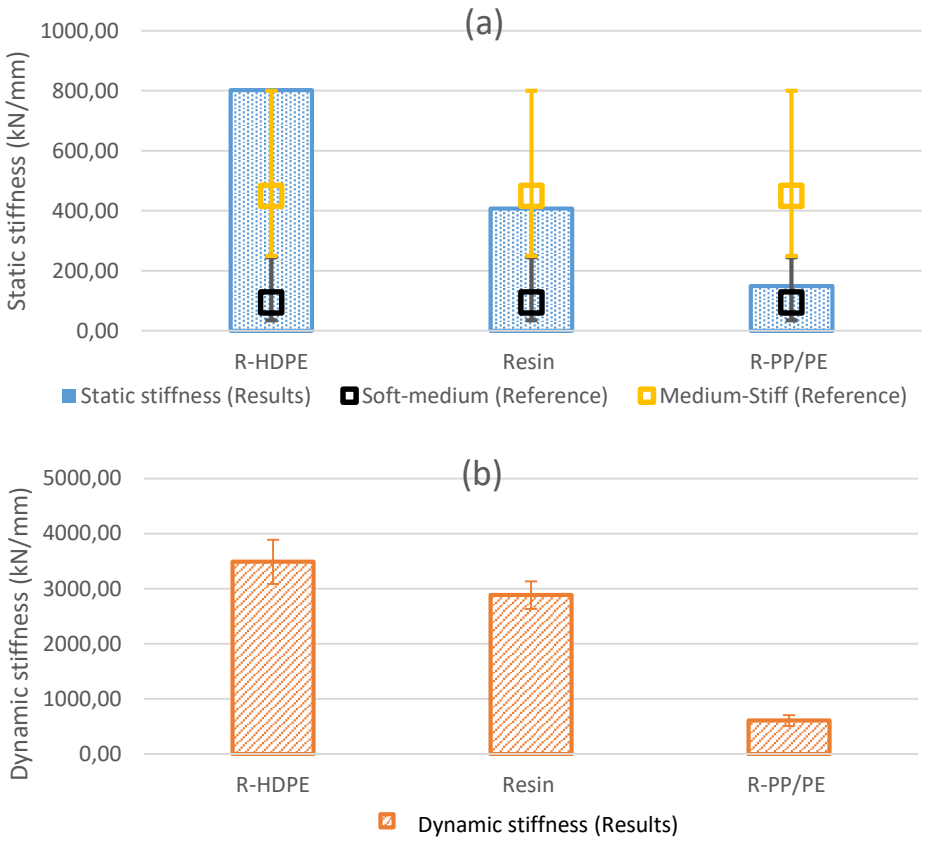

Figure 6. Vertical static and dynamic stiffness of rail pads manufactured with binder materials.

For a deeper study of the influence of pad material on its performance under traffic loads, Figure 7 shows the average curves for force-vertical displacement registered during the static tests. Results reflect that all pads showed a non-linear performance as expected for these materials, but with different trends. The R-HDPE pad presented the highest stiffening effect (higher curve slope) under a higher force level. Reproducing a similar phenomenon to that seen for other rail pads manufactured from other polymers like rubber [5, 11]. On the other hand, the Resin and R-PP/PE pads showed a slight tendency to creep under high force levels, leading to a greater plastic performance. This behaviour leads to higher plastic deformations that could limit the applicability of these type of pads.

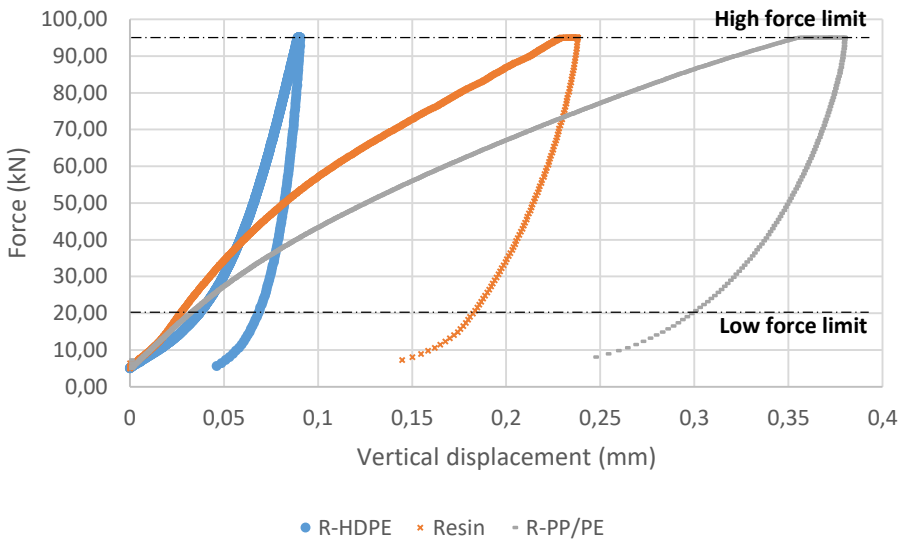

Figure 7. Representative curves of force-displacement for the pads manufactured with different binder materials.

Figure 8a displays the influence of the crumb rubber quantity (per volume), over the total for each of the binder materials, with a size between 0.6 and 2 mm (R2). Also, for one of them (the stiffest), the influence of crumb rubber size is shown. For the analysis of rubber size, the R-HDPE was selected since this binder provided the highest stiffness values (and therefore, required the highest increase in flexibility by including crumb rubber particles) while presenting a more appropriate performance under loads.

From the results, it is seen that, although the stiffness of the three materials changed with the inclusion of the CR, for R-PP/PE this was found to be at a lesser extent, even increasing the stiffness slightly. This could be related to the fact that both materials (the binder and the rubber) could present quite a similar stiffness value, and therefore, limiting the effect of rubber when combined with R-PP/PE. In other hand, if the R-HDPE and resin are compared, it is possible to observe how the latter has a higher susceptibility to decreasing its stiffness with the incorporation of rubber. With 50 percent of crumb rubber, “R2”, it was possible to reduce the static stiffness by 25% and 85% in R-HDPE and resin pads, respectively. These changes indicate that the rubber has a stronger impact in the pads with resin, where the behaviour is determined by the rubber while such effect is more limited when using R-HDPE due to the higher stiffness of this plastic, and therefore, requiring the effect of the rubber.

In this sense, it was demonstrated that the crumb rubber size could optimize the rail pad stiffness. Focusing on the rail pads manufactured with R-HDPE, it was possible to observe that as the size of the crumb rubber increases, the greater increase in pad stiffness. For example, for the pad with 50% percent crumb rubber (R0.6), it was possible to decrease the stiffness by around 20%. Meanwhile, if the rubber size was increased to 2-4 mm (R4), it was possible to decrease the stiffness twice that of the R0.6 (i.e., around

40%), passing from rigid to medium pads to be used in railway tracks requiring this type of softer elements.

Figure 8b shows the relationship between static and dynamic stiffnesses. As mentioned previously, as seen in literature there are studies that consider a dynamic-static stiffness ratio close to 3.5 appropriate for flexible rail pads [35]. Both R-HDPE and R-PP/PE demonstrated a ratio close to this value. However, the rail pads manufactured with resin were found to have a higher ratio, of around 7.5, which denotes an important stiffening of this material due to its marked rheological performance, whose elastic modulus depends on parameters like load speed, as seen by this type of materials [36]. The crumb rubber size was not found to have a significant influence on this ratio due to the three solutions tested presenting a similar dynamic-static stiffness ratio (around 5), when considering the dynamic stiffness modulus of the rail pads manufactured with R-HDPE with the different sizes of crumb rubber.

According to these results, it could be seen that by using different combinations of CR it is possible to obtain a wide range of solutions which could be used in a railway line. Where this would be more accentuated in the case of the resin for low stiffness values, and HDPE for higher values.

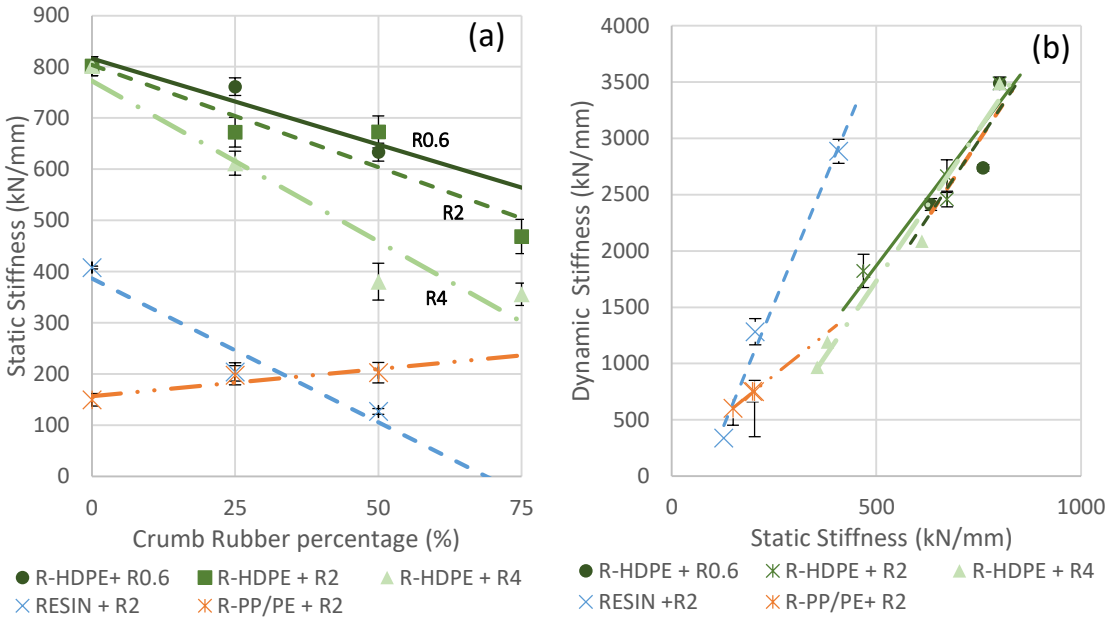

Figure 8. Vertical static stiffness for different materials (a) and stiffness correlations for different materials (b).

In the same way, Figure 9a demonstrates the results for how the crumb rubber affected the tensile strength of the materials tested. In this figure, it is possible to observe how the R-HDPE has the highest tensile strength, since it was the stiffer material. However, a fragile break occurred during testing, and for this reason it was the material that dissipated the least energy during the test (Figure 9b). Also, this material is the most affected by the addition of crumb rubber particles, decreasing it by more than 70

percent, with a composition of 50 percent of CR. This implies that the CR could provide reinforcement for the plastic, resulting in a tough matrix (as done in other polymeric matrices) [37], but with a more brittle behaviour with a lower tensile strength due to higher volume of particle accumulation [38].

The least susceptible was R-PP/PE, as also found with the stiffness variation, where its tensile strength remains practically constant, independent of the crumb rubber percentage incorporated. Nonetheless, despite the crumb rubber size having an influence on the stiffness of the material, the same did not occur for the tensile strength. This was seen as similar values were obtained for the rail pads manufactured with R-HDPE with different crumb rubber sizes (R0.6; R2; R4).

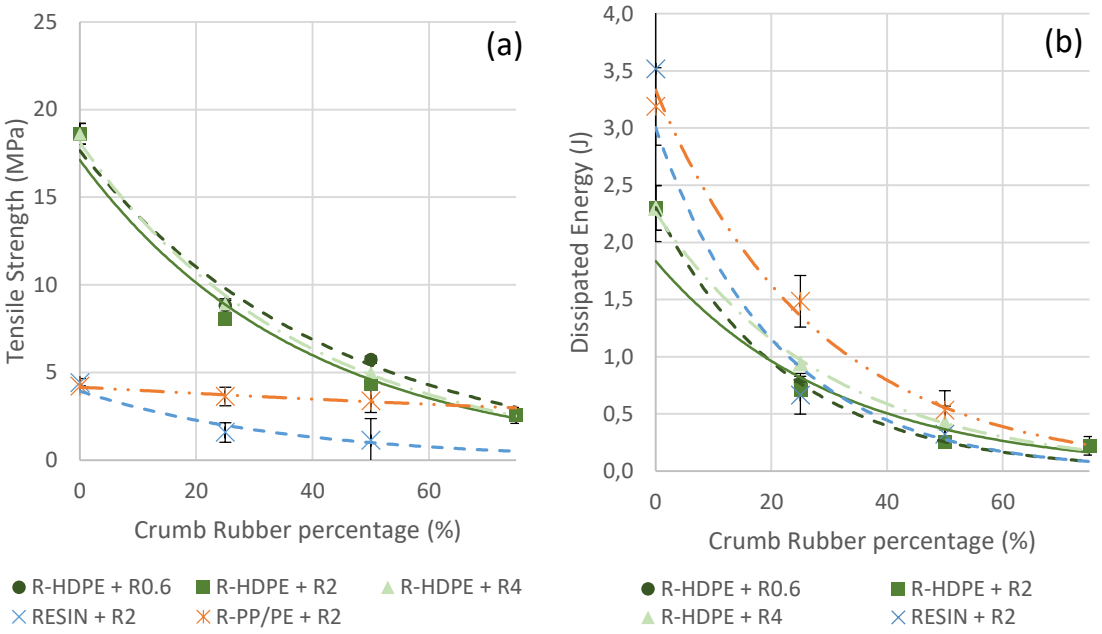

Figure 9. Tensile test results

Similarly, regarding the results for the influence of the binder types measured through the dynamic mechanical analysis (DMA test), Figure 10 displays how the temperature and the frequency affected the damping capacity of the material. Both the R-HDPE and R-PP/PE presented a similar behaviour at the different temperatures and frequencies studied, indicating low susceptibility to changes due to variations in test conditions, which could result in pads with low sensitivity to in-service conditions. However, the resin was found to have a different performance. Despite presenting a high damping capacity at low temperatures, as the temperature increased, the value of damping ratio decreased, as well as the influence of the frequency. This is in agreement with the stiffening of the pad observed during the dynamic stiffness tests as well as with the susceptibility of this material to change the behaviour when including rubber.

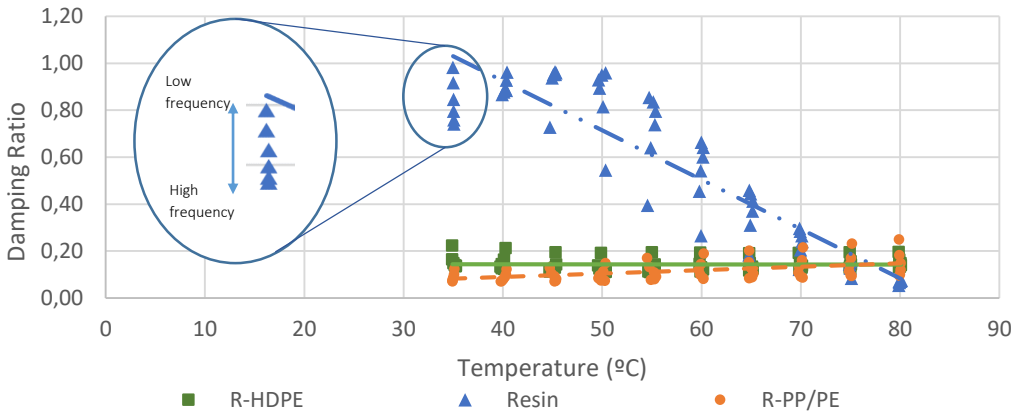

Figure 10. Damping ratio at different temperatures for the binding materials tested by DMA test.

Additionally, to understand the impact of the rubber quantity and size on the pad performance, Figure 11 displays the results of the damping ratio at 5 Hz on the R-HDPE pads (selected as an example given it requires rubber to decrease its stiffness) with different CR concentrations (0-75% at R2 size) and with different sizes (0.6-4R at 50% volume). Independent of the crumb rubber amount, the capacity of energy dissipation increased with the temperature. Also, this occurred in more accelerated way as the crumb rubber concentration decreased due to the rubber having a higher specific heat than the high-density polyethylene [39]. Furthermore, with the increase in crumb rubber concentration it was possible to improve the damping capacity of the material. For example, for a temperature of 60ºC, using 75% of crumb rubber increased the damping ratio by 70%. Conversely, as was found for the tensile stress-strain test, no significant differences were found for the crumb rubber particle size variation in the damping ratio of the materials.

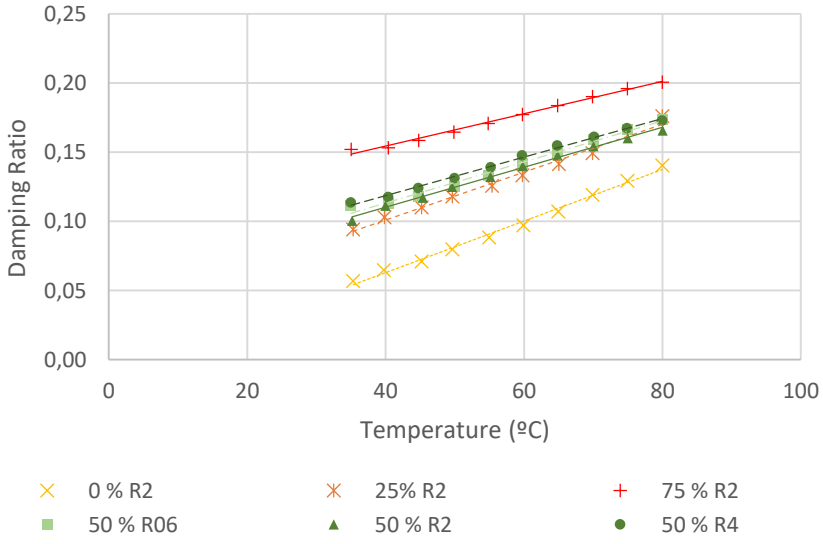

Figure 11. Damping ratio for different crumb rubber percentages and sizes mixed with R-HDPE

3.2. Geometric design definition

Once the possible materials to be used in the sustainable rail pads were characterized, different geometries were tested. For this purpose, considering an intermediate case, the influence of the pad geometry on the stiffness for the R-HDPE + 50% R2 mixture was studied. Figure 12 shows the static and dynamic stiffness for the main geometries analysed. From these results, it is possible to appreciate how surface area decreases, so does the stiffness. This occurred for both the static and dynamic stiffness. If G1 and G4 are compared, it is possible to observe a stiffness reduction of close to 50% and 70% in the static and dynamic stiffnesses, respectively. Therefore, this states that one of the most influential parameters in the geometrical design of the pad is the superficial area in contact with rail, and thus, the variation of this property could considerably affect the element stiffness.

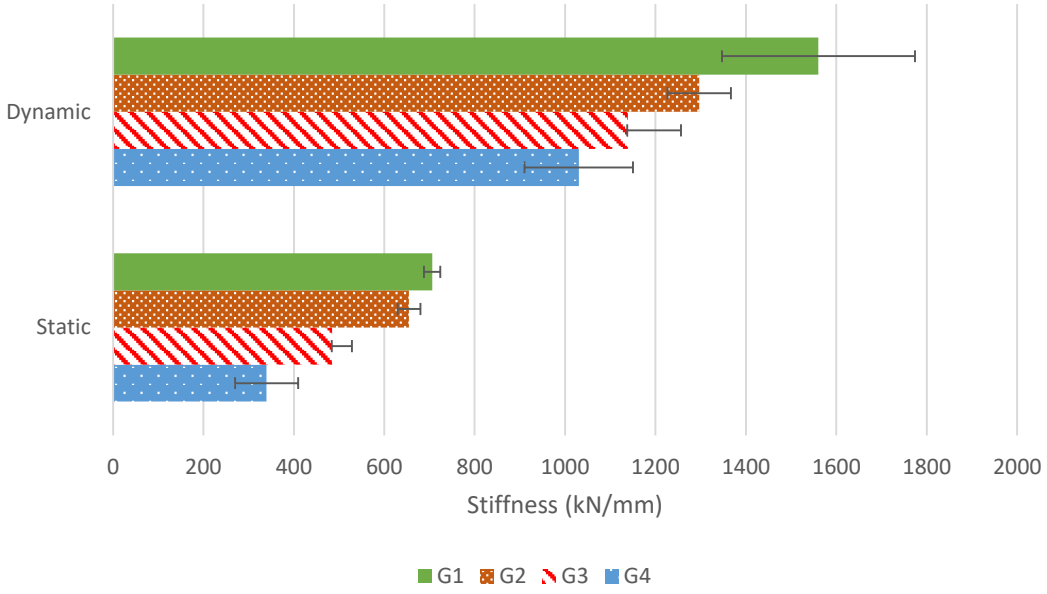

Figure 12. Static and dynamic stiffness depending on the superficial geometry of pad.

Focusing on the most and least influential geometries, Table 2 shows the results obtained for the static modulus at different loads, as well as, the dynamic modulus for the rail pads with geometry one and four for the different materials. The change in the rail pad's surface configuration was found to change the static and dynamic stiffness. Specifically, as the contact surface decreased, it was possible to reduce the rail pad's stiffness. For example, in the case of the rail pad manufactured with R-HDPE + 50% R2, it is possible to decrease the static stiffness (at 20/95 kN) by around 50 percent. This ratio decreased even more when the crumb rubber particle size increased, and therefore resulted in softer pads which could be used in a wider range of railway tracks requiring this type of solution.

Nonetheless, it should be noted that the rail pads manufactured with R-PP/PE + 50% R2, despite obtaining a low static stiffness (compatible with their use in high-speed lines), were not found to have a sufficient bearing capacity while presenting higher plastic performance as seen in Figure 7. During the static stiffness tests, the pads with geometry 4 were highly deformed, losing their original geometry. So, this solution cannot be considered for high-speed lines or lines subjected to high loads.

Table 2. Influence of geometry on the rail pad stiffness

Material	Geometry	Static Stiffness 20/95 (kN/mm)	Dynamic Stiffness (kN/mm)
R-HDPE + 50% R2	G1	706	1560
	G4	339	1030
	Reduction ratio (%)	52	34
R-HDPE + 50% R4	G1	380	1191
	G4	297	627
	Reduction ratio (%)	22	47
RESIN + 50% R2	G1	127	338
	G4	64	277
	Reduction ratio (%)	50	18
R-PP/PE + 50% R2	G1	203	750
	G4	145	-
	Reduction ratio (%)	29	-

Figure 13 shows a comparative plot for the impact attenuation capacity of the different materials tested. All of them met the requirements set by the local standard, which establishes a minimum value of 25% [23]. For both the Resin + 50% R2 and R-PP/PE + 50% R2 pads their geometry did not affect their impact attenuation resistance, obtaining values of 85 and 78%, respectively. However, in the rail pads manufactured with R-HDPE the same did not occur. The change in the geometry influenced, just as with the stiffness (Figure 11), the rail pad attenuation capacity too. The change in the rail pad geometry improved it by 30% in R-HDPE+ 50% R2 pad, and 10% in R-HDPE+50 % R4 pad. Also, it was demonstrated how the use of a higher crumb rubber particle size increased the impact attenuation capacity. If R-HDPE + 50% R2 and R-HDPE + 50% R4 are compared, it is possible to increment the pad's resistance by around 50% and 25% for G1 and G4 with the use of R4, respectively.

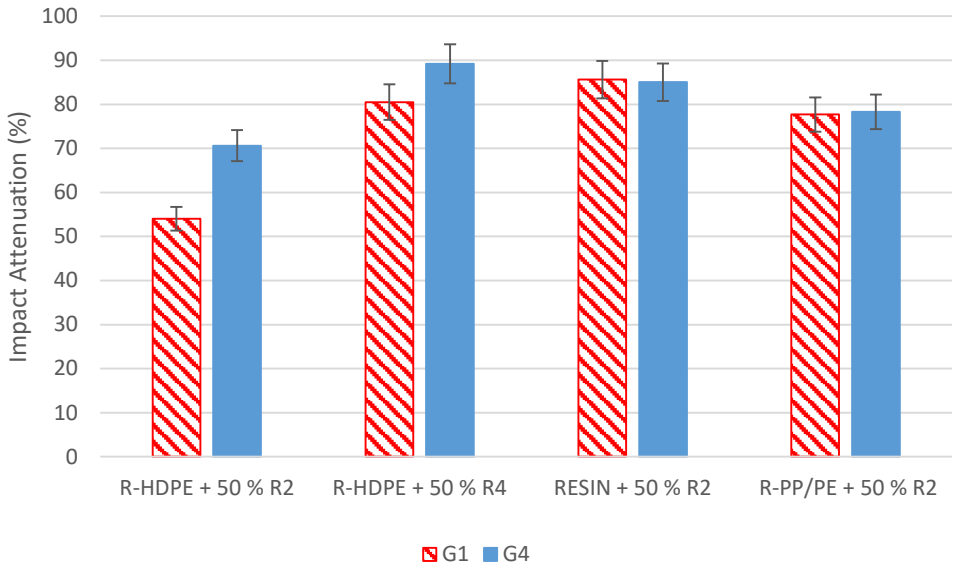

Figure 13. Rail pad impact attenuation capacity

3.3. Study of material durability

Figure 14 presents the rail displacement variation caused by the fatigue test carried out according to the UNE-EN 13146-4. The results are obtained for Fmax (maximum force equal to 83 kN) and for Fmin (minimum force equal to 5 kN). In general, the displacement found for both the railhead and railfoot means they would be compatible for use in high-speed lines, according to the Spanish regulation [23], except for the rail pads manufactured with R-PP/PE + 50% R2. In this last case, for Fmax, the displacement exceeds the standard values by around 20% in the railhead and 6% in the railfoot; thus, not making its use compatible for Spanish high-speed lines due to its plastic peformance, according to the Spanish standard.

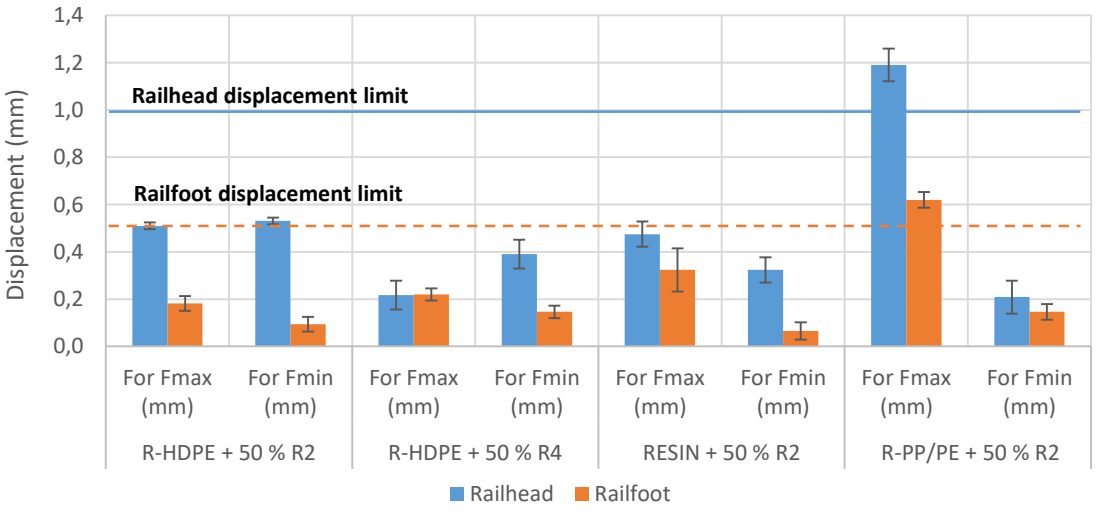

Figure 14. Rail displacement caused by fatigue process

Furthermore, with the aim to evaluate the durability of the rail pads, static tests were carried out before and after the fatigue process. Figure 15 shows the static stiffness variation as a result of the fatigue processes. In the rail pad manufactured with R-HDPE, both R-HDPE + 50% R2 and R-HDPE + 50% R4, the static stiffness decreased slightly, probably due to the possible degradation of the material. On the other hand, in the rail pads manufactured with the resin, the pad was found to increase in stiffness, as a result of cyclic loading that the rail pad was subjected to. In this case, the static stiffness increased by 12%, with respect to the value obtained before the fatigue process; with a limit of 25% [23]. Finally, the rail pads manufactured with R-PP/PE + 50% R2 suffered high deformations, which mean they cannot be considered for use in high-speed railways.

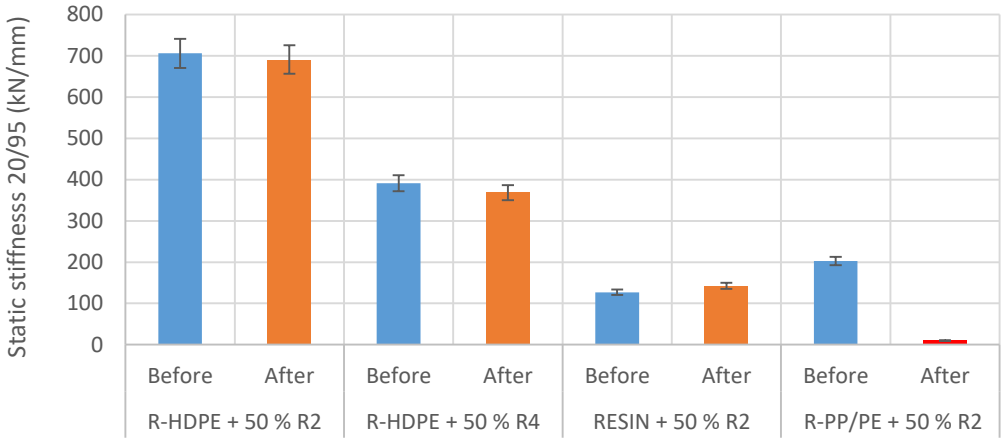

Figure 15. Static stiffness before and after fatigue process

3.4. Study of the rail eco-pad environmental footprints

Figure 16 display the results from the carbon footprint analysis for the 11 pad types. From these results, the use of recycled polymers can be considered to provide a positive environmental benefit. Meanwhile, the use of the polymeric resin, whose manufacture required more complex and chemical process, was found to have a comparatively large environmental footprint; 12.6 times more for 100% resin compared to a conventional rail pad, and 1.5 times more with 50% CR.

Comparing the gross and net impacts of the recycled polymers, it was found that both recycled polymers provided a net environmental saving. This can be associated with the fact that the material extraction stage for the recycled plastics (i.e., waste processing) is less impacting than the extraction of the constituent components of HDPE (methylene diphenyl diisocyanate, pentane and polyol). Furthermore, there impacts of the pads produced in the lab were different to the mass-produced inventory for the conventional pad (close to four times more).

Considering the net emissions for the recycled materials (i.e., the total GHG emissions including avoided primary production) it can be seen that for both the R-HDPE and R-PP/PE significant savings were made. However, this trend was seen to decrease with the increasing addition of CR in the pads: down 3-7% for gross impacts and 29-40% for net impacts.

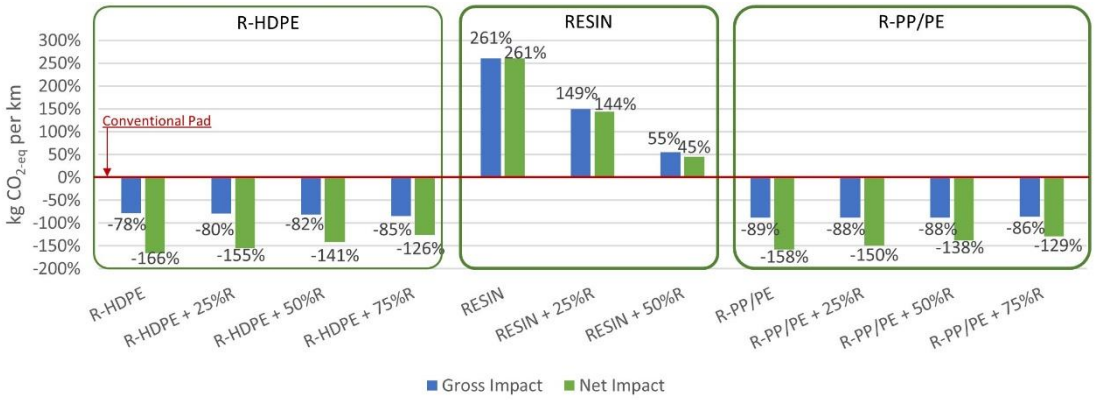

Figure 16. Carbon footprint results for the rail pad types tested in this study.

4. Conclusions and prospects

This paper studied the viability of using different recycled polymers for the development of sustainable rail pads for railway lines. The rail pads were manufactured with recycled binders obtained from recycled high-density polyethylene from waste plastic boxes and geomembrane residues. A polymeric resin was used as a reference material. These were combined with crumb rubber particles in different sizes and concentrations, from which a wide range of sustainable structural solutions were obtained. The research was conducted in four stages: (i) analysis of the composition of the different materials used; (ii) study of the influence of rail pad geometric design; (iii) study of the material durability; (iv) study of the carbon footprint of the materials. According to the results obtained in the different stages, the following conclusions were determined:

- Results demonstrated that binder type had a strong impact on pad properties. HDPE provided stiffer and more brittle pads, while the PP/PE led to softer pads.
- In general, an increase in crumb rubber percentage decreased the rail pad stiffness. Conversely, for the rail pad with R-PP/PE it increased slightly. However, this did cause a decrease in tensile strength due to discontinuities found between the materials. The use of higher particle sizes was found to also decrease the static and dynamic stiffness of the rail pads.
- Consequently, through the addition of crumb rubber, it was possible to adapt the stiffness of the rail pads, obtaining a broad range of pad solutions (with different stiffnesses) and an increase the damping capacities of the materials.
- The pad geometry played a special role in the manufacture of the rail pads. It was demonstrated that through changing the surface configuration of the rail

pads, it was possible to modify the stiffness of the rail pads, decreasing it by more than 50% in some cases.

- The use of geometries with a low superficial contact (G4) could negatively affect the behaviour of the rail pads for some materials. In rail pads manufactured with R-PP/PE, the plastic deformations was found to be high, such that the bearing capacity of this material could not be guaranteed.
- With regards to the durability, the rail pads manufactured with stiffer materials showed a higher resistance, obtaining acceptable results in the fatigue test. Meanwhile, the pads made with the softer material gave rise to excessive deformations, being more accentuated in the geometries in which the distance between protrusions increased.
- Finally, considering the carbon footprints of the solutions, the pads manufactured from the recycled polymers (R-HDPE and R-PP/PE) were found to both provide gross and net environmental benefits when compared to a conventional rail pad, reducing the CO_2 emissions by around 78-89% and 126-166%, respectively. However, these emissions saving decreased at higher crumb rubber contents.

Based on these conclusions, it can be said that the use of recycled plastics like R-HDPE in the manufacturing of rail pads could lead to environmental benefits (i.e., reduced waste and GHG emissions) and provide viable alternative materials with appropriate physical and mechanical performance for this application. Nonetheless, from these conclusions, further research will be carried out to optimize the design of these sustainable pads, evaluating key factors like ageing, thermal and chemical stability, among others, while aiming to include sensors for real-time track monitoring.

5. Acknowledgments

The present study has been conducted within the framework of the ECO-Smart Pads (Smart and Sustainable Resilient Pads for the Railway of the Future, RTI2018-102124-J-IOO) research project, funded by the Ministry of Economy and Competitiveness of Spain.

6. Bibliography

[1] S. Bressi, G. D´Angelo, J. Santos, M. Guinta. Environmental performance analysis of bitumen stabilized ballast for railway track-bed using life-cycle assessment. Constr. Build. Mater. 188 (2018) 1050-1064. https://doi.org/10.1016/j.conbuildmat.2018.08.175

[2] S. Kaewunruen, A. Remmennikov, Sensitivity analysis of free vibration characteristics of an in situ railway concrete sleeper to variations of rail pad parameters. J. Sound Vib. 298 (2020) 453-461. https://doi.org/10.1016/j.jsv.2006.05.034

[3] M. Sol-Sánchez, L. Pirozzolo; F. Moreno-Navarro, M.C. Rubio-Gámez, Advanced characterisation of bituminous sub-ballast for its application in railway tracks: The

influence of temperature. Constr. Build. Mater. 101 (2015) 338 - 346. https://doi.org/10.1016/j.conbuildmat.2015.10.102
[4] X. Lei and B. Zhang, Analysis of Dynamic Behavior for Slab Track of High-Speed Railway Based on Vehicle and Track Elements. Journal of Transportation Engineering, 137, 4 (2011).
[5] M. Sol-Sánchez, F. Moreno-Navarro, M.C Rubio-Gámez, Viability analysis of deconstructed tires as material for rail pads in high-speed railway. Mater. Des. 64 (2014) 407-414. https://doi.org/10.1016/j.matdes.2014.07.071
[6] M. Sol-Sánchez, L. Pirozzolo, F. Moreno-Navarro, M.C. Rubio-Gámez, 2016. A study into the mechanical performance of different configurations for the railway track section: A laboratory approach. Eng. Struct. 119 (2016) 13 - 2315. https://doi.org/10.1016/j.engstruct.2016.04.008
[7] S. Kaewunruen, A.M. Remennikov, A.M., 2007. Response and Prediction of Dymanic Characteristics of Worn Rail Pads Under Static Preloads. Proceedings of the 14th International Congress on Sound and Vibration, Australia.
[8] S. Kaewunruen, P. Liao, 2020. Sustainability and recyclability of composite materials for railway turnout systems. J. Clean. Prod. 285, 124890. https://doi.org/10.1016/j.jclepro.2020.124890
[9] M. Sol-Sánchez, F. Moreno-Navarro, M.C. Rubio-Gámez, The use of elastic elements in railway tracks: A state of the art review. Constr. Build. Mater. 75 (2015) 293-305. https://doi.org/10.1016/j.conbuildmat.2014.11.027
[10] S. Zhang, C. Koh, K. Kuang, 2018. Proposed rail pad sensor for wheel-rail contact force monitoring. Smart. Mater. Struct. 27, 115041. https://doi.org/10.1088/1361-665X/aadc8d
[11] J. Sainz-Aja, I. Carrascal, D. Ferreño, J. Pombo, J. Casado, S. Diego, 2020. Influence of the operational conditions on static and dynamic stiffness of rail pads. Mech. Mater. 148, 103505. https://doi.org/10.1016/j.mechmat.2020.103505
[12] European Commission, A European Strategy for Plastics in a Circular Economy 2020, 2020. https://www.europarc.org/wp-content/uploads/2018/01/Eu-plastics-strategy-brochure.pdf
[13] A.Fazli, D. Rodrigue, Waste Rubber Recycling: A Review on the Evolution and Properties of Thermoplastic Elastomers. Materials. 13 (2020) 1-31. https://doi.org/10.3390/ma13030782
[14] M. Sol-Sánchez, A. Jiménez del Barco-Carrión, A. Hidalgo-Arroyo, F. Moreno-Navarro, L. Saiz, M.C. Rubio-Gámez, 2020. Viability of producing sustainable asphalt mixtures with crumb rubber bitumen at reduced temperatures. Constr. Build. Mater. 265, 120154. https://doi.org/10.1016/j.conbuildmat.2020.120154
[15] S.M.A. Qaidi, Y.Z. Dinkha, J.H. Haido, M.H. Ali, B.A. Tayeh, 2021. Engineering properties of sustainable green concrete incorporating eco-friendly aggregate of crumb rubber: a review. J. Clean. Prod. 324, 129251.
[16] M. Sol-Sánchez, F. Moreno-Navarro, M. Hidalgo, V. Pérez, M.C. Rubio-Gámez, 2020. Laboratory study on asphalt mixtures for application in port pavements. Constr. Build. Mater. 235, 117513. https://doi.org/10.1016/j.conbuildmat.2019.117513
[17] M. Sol-Sánchez, F. Moreno-Navarro, M.C. Rubio-Gámez, The use of deconstructed tire rail pads in railroad tracks: Impact of pad thickness. Mater. Des. (2014) 198-203. https://doi.org/10.1016/j.matdes.2014.01.062

[18] M. Sol-Sánchez, F. Moreno-Navarro, G. Martínez-Montes, M.C. Rubio-Gámez, An alternative sustainable railway maintenance technique based on the use of rubber particles. J. Clean. Prod. 142 (2017) 3850-3858. https://doi.org/10.1016/j.jclepro.2016.10.077
[19] M. Sol-Sánchez, F. Moreno-Navarro, L. Saiz, M.C. Rubio-Gámez, 2020. Recycling waste rubber particles for the maintenance of different states of railway tracks through a two-step stoneblowing process. J. Clean. Prod. 244, 118570. https://doi.org/10.1016/j.jclepro.2019.118570
[20] M. Koohmishi and A. Azarhoosh, Degradation of crumb rubber modified railway ballast under impact loading considering aggregate gradation and rubber size. Canadian Geotechnical Journal, 2021.
[21] R. Juan, C. Domínguez, N. Robledo, B. Paredes, R. García-Muñoz, 2020. Incorporation of recycled high-density polyethylene to polyethylene pipe grade resins to increase close-loop recycling and Underpin the circular economy. J. Clean. Prod. 276, 124081. https://doi.org/10.1016/j.jclepro.2020.124081
[22] S. Magnusson, J. Mácsik, Analysis of energy use and emissions of greenhouse gases, metals and organic substances from construction materials used for artificial turf. Resour. Conserv. Recycl. 122 (2017) 362-372. https://doi.org/10.1016/j.resconrec.2017.03.007
[23] ADIF (Spanish Railway Infrastructures manager). ET 03.360.570.0 PLACAS ELÁSTICAS DE ASIENTO PARA SUJECIÓN VM, Renfe. Mantenimiento de Infraestructura, Dirección Técnica, Spain,2005.
[24] D. Ferreño, J. Sainz-Aja, I. Carrascal, M. Cuartas, J. Pombo, J. Casado, S. Diego, 2021. Prediction of mechanical properties of rail pads under in-service condition through machine learning algorithms. Adv. Eng. Softw. 151, 102927. https://doi.org/10.1016/j.advengsoft.2020.102927
[25] I. Carrascal, A. Pérez, J. Casado, S. Diego, J. Polanco, J. Martín, Experimental study of metal cushion pads for high speed railways. Constr. Build. Mater. 182 (2018) 273-283. https://doi.org/10.1016/j.conbuildmat.2018.06.134
[26] R.E.D. España, The Spanish Electricity System. Preliminary Report 2018, Madrid, Spain, 2019. https://www.ree.es/en/datos/publications/annual-system-report/spanish-electricity-system-preliminary-report-2019
[27] Ecoinvent. Ecoinvent 3.6. , 2019. https://www.ecoinvent.org/home.html
[28] J.J. Pons, I. Villalba Sanchis, R. Insa Franco, V. Yepes, 2020. Life cycle assessment of a railway tracks substructures: Comparison of ballast and ballastless rail tracks. Environ. Impact Assess. Rev. 85, 106444. https://doi.org/10.1016/j.eiar.2020.106444
[29] D.A. Turner, I.D. Williams, S. Kemp, Greenhouse gas emission factors for recycling of source-segregated waste materials. Resour. Conserv. Recycl. 105 (2015) 186-197. https://doi.org/10.1016/j.resconrec.2015.10.026
[30] FEICA, Environmental Product Declaration: Reactive resins based on polyurethane or SMP, filled or aqueous, solvent-free, Association of the European Adhesive and Sealant Industry, Brussels, Belgium , 2016 https://epd-online.com/PublishedEpd/Download/8011
[31] Ecopneus, Evaluation of the carbon footprint of the production of crumb rubber from end-of-life tires. Draft (in Italian), Italy, 2013.

[32] EN 13146-9:2011. Railway applications. Track. Test methods for fastening systems. Part 9: Determination of stiffness. European Committee for Standardization. Brussels, 2009.
[33] B.V. Dyk, 2016. Fastening system stiffness measurement and influence on railway track. In Proc. Int. Crosstie and Fastening System Symp. Urbana, IL.
[34] N. Hassan, 2019. Rail Pad Stiffness and Classification System. American Society of Civil Engineers.
[35] P. Bouvet, N. Vincent, 1998. Laboratory characterization of rail pad dynamic properties, Vibratec report. 450.1998.004.RA.05.A.
[36] L.D. Eiras-Pereira, M. Pereira Couto Neto, R. Guimaraes Pereira, L.F.J. Schneider, Influence of resin matrix on the rheology, translucency, and curing potential of experimental flowable composites for bulk-fill applications. Dental Materials 37 (2021) 1046-1053. https://doi.org/10.1016/j.dental.2021.03.003
[37] K. Padmanabhan, Mechanical behaviour of Kevlar fibre/epoxy matrix composites. Lambert Academic Publishers, Germany, 2012. ISBN-10 3659266124.
[38] K.W. Kwok, Z.M. Gao, C.L. Choy, X.G. Zhu, 2003. Stiffness and Toughness of Polypropylene/Glass Bead Composites. Polymer composites, 24, 1. https://doi.org/10.1002/pc.10005
[39] J. Wen, Physical Properties of Polymers Handbook, Springer, Cincinnati, 2007.

Sol-Sánchez, M.; Castillo-Mingorance, J.M.; Moreno-Navarro, F.; Rubio-Gámez, M.C. ***Smart rail pads for the continuos monitoring of sensored railway tracks: Sensor analysis.*** **Autom. Constr. 132 (2021) 103950. (Índice de Impacto 9,6 en 2.023, Q1 en CIVIL ENGENIERING y CONSTRUCTION & BUILDING TECHNOLOGY en 2.023).**

https://doi.org/10.1016/j.autcon.2021.103950

Smart Rail Pads for the Continuous Monitoring of Sensored Railway Tracks: Sensors Analysis

Sol-Sánchez, M.*[,1]; Castillo-Mingorance, J.M.[1]; Moreno-Navarro, F.[1]; Rubio-Gámez, M.C.[1]

msol@ugr.es (M. Sol-Sánchez); jumacami@ugr.es (J.M. Castillo-Mingorance); fmoreno@ugr.es (F. Moreno-Navarro); mcrubio@ugr.es (M.C. Rubio-Gámez)

[1]Laboratory of Construction Engineering at the University of Granada. C/ Severo Ochoa s/n, 18071, Granada, Spain.

*Corresponding author (msol@ugr.es)

Abstract

The inclusion of sensors in railway track components will permit the automated and real-time monitoring of track behaviour and traffic conditions; necessary for adopting preventive maintenance strategies. In this sense, this paper assesses the applicability of three different sensor types, commonly used for engineering applications, to be included into rail pads to thus provide smart components with sensing properties to monitor railway tracks. Various types of accelerometer, piezoresistive and piezoelectric sensors were evaluated to determine their viability for smart rail pads. Results demonstrated that piezoelectric devices showed a linear correlation between signal output and stress levels on pads, in contrast to piezoresistive panels which presented a logarithmic response, and clearer signal pulses than the other sensors to detect changes in loading conditions or track response. Therefore, piezoelectrics presented the highest implementation potential for this application, considering its low cost and clearer ability to monitor variations in traffic and/or track state.

Keywords: smart materials; automated railways; sensors; rail pads; monitoring.

Highlights

- Sensorised smart rail pads were tested for continuous track monitoring
- Accelerometers, press panels and piezoelectrics were embedded in rail pads
- Variations in traffic conditions and track state were monitored by sensored pads
- Piezoelectrics showed the best potential for monitoring load changes on pads
- Piezoelectrics had a linear correlation between stress level and signal output

1. Introduction

To maintain railway line track quality, frequent maintenance operations are needed. Currently, palliative corrections are the most common solution, instead of preventive maintenance, despite the latter showing a higher potential for reducing economic and

social impacts (Odolinski and Boysen, 2019; Sasidharan et al., 2020). The understanding of the evolution of track degradation over time, due to key factors like traffic conditions and track vertical oscillations under traffic loads, would be essential for the early detection of potential problems (i.e., preventative maintenance). This is in agreement with most of the current political goals and guidelines focusing on continuous monitoring to predict failures and carry out preventive maintenance operations (Zoeteman and Esveld, 2004; ISO 2014).

Nonetheless, most predictive models are based on mathematical approaches, with limited consideration for data provided by real-time monitoring systems on an infrastructure's condition (Peng et al., 2011; Macedo et al., 2017). So far, railway track monitoring has been mainly carried out for research purposes on specific sections in the short-term, due to the complex installations and data analysis needed. However, continuous real-time monitoring would be required to better evaluate structures, to make maintenance decisions sooner or to revise designs for future sections. To solve this limitation, inspection techniques are being developed to evaluate rail track conditions (Cantero and Basu, 2015; Benedetto et al., 2017; Jing et al., 2021); which are traditionally distinguished into onboard and wayside monitoring systems.

Thanks to the great advances in sensors in the last years (Tian et al., 2016; Lei et al., 2020), there is a greater potential for the wider application of these technologies. Through their inclusion into materials or components of the railway track, these components can monitor essential factors like load distribution along the track and/or oscillation levels of components under train passage. This trend for smart materials could provide an alternative or complementary solution to current pilot monitoring initiatives that currently require the special installation of sensors and complex electronic devices (at present being both expensive and over-track, thus susceptible to damage or theft) (Hu et al., 2020). In contrast, the philosophy of smart materials indicates that sensors are implanted into components that are essential for the structural section of the railway. Thus, these smart components could be used along the track as well as in specific singular points (like switches, crosses, transition areas, etc.) or control sections to understand traffic and track states to calibrate predictive models, among other applications.

Nonetheless, it must be considered that these smart materials must be specifically designed according to their application in the type of infrastructure to be monitored (e.g. railway tracks in this study), and using the most appropriate components to ensure they are precise enough for the desired application. Particularly, this article focuses on the inclusion of sensors into rail pads since they are in direct contact with traffic loads (transmitted from the rail to the sleeper through the pads) and are able to evaluate the oscillation of the superstructure over the ballast layer under such loads (Sol-Sánchez et al., 2016). Regarding the sensors, according to literature review (Castillo-Mingorance et al., 2020) and the authors' previous experience, devices like strain gauges (Dos Reis et al., 2018) and radio frequency identification tags (RFID) (Zhao et al., 2018) have been used as health monitoring devices for structures (i.e. bridges and tunnels), but not as specific sensors for global railway tracks where they could present limited sensitivity to failures (Hu et al., 2020). Meanwhile, innovative sensors like fibre-optics (Tan et al, 2016) are considered to provide complex data outputs for analysis and are expensive, among other drawbacks. On top of the limitations discussed, the aforementioned sensors do not provide adequate dimensional characteristics for their inclusion within the rail pad. In contrast, simple devices like accelerometers or piezoceramic materials have been

shown (Hu et al., 2020) to be appropriate for flexible sensor arrays applied on wayside monitoring systems. These benefits, coupled with their physical dimensions, make them ideal for a rail pad.

Thus, this study aims to analyze the viability and potential applicability of different sensors to be included into rail pads in order to provide smart railway components with real-time sensing properties, as an alternative to standard wayside monitoring systems. Particularly, different types of accelerometers, press panels (piezoresistive sensor) and standard piezoelectrics were assessed, which represent sensors with appropriate sizes and characteristics to be included into rail pads while offering easier to implement devices. Thus, this article will contribute to the exploration of sensors to be used into rail pads for the development of innovative monitoring components specifically designed and studied for application in railway tracks. To achieve this aim, this paper 1) calibrated each type of sensor for use in railway pads, 2) assessed their applicability to monitor traffic and track conditions through laboratory tests under realistic traffic loads and track sections with diverse capacities to deform, 3) evaluated the durability of the selected sensors when applied on the pads under repeated loads simulating train passing, in order to select the most appropriate devices for rail pad application.

2. Methodology

2.1 Materials

2.1.1. Sensors

The type of sensors to be included in the rail pads were selected after studying smart sensor literature (Castillo-Mingorance et al., 2020), focusing on small devices with appropriate dimensions to be added into the pads while presenting the potential for monitoring key parameters, like changes in superstructure displacement and/or load level and distribution. For this purpose, three types of sensors were selected (Figure 1): 1) accelerometers to control changes in oscillations; 2) press panels (piezoresistive sensor) to measure changes in the level of stress on the pads; 3) a piezoelectric to control changes in track performance by measuring the variations in wave transmissions into the material.

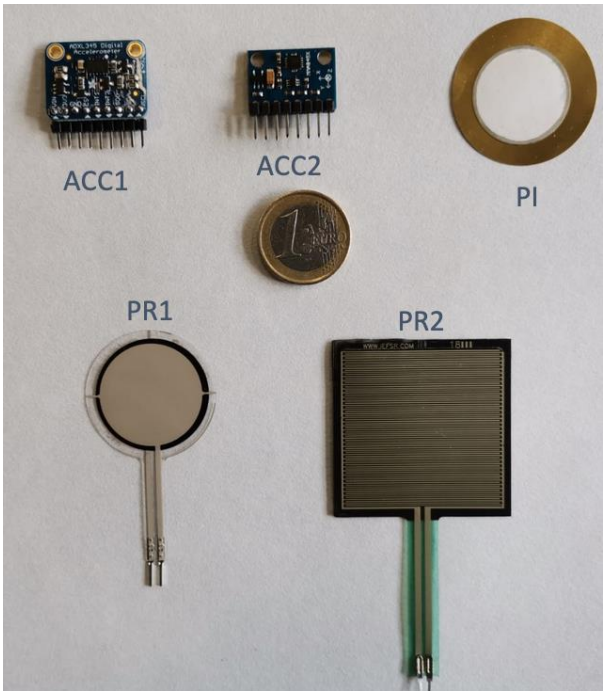

Figure 1. Visual appearance of the sensors studied in this article.

Two accelerometer models were selected (Figure 1), commonly applied in industrial instrumentation as well as in personal navigation devices, medical instrumentation, gaming, etc. They were selected according to the size and characteristics provided by the manufacturer (size, range of measurement, resolution, etc.). The first one (referred in this study as ACC1) was a small and thin 3-axis accelerometer with high resolution (13-bit) and capacity to measure up to ±16g, including an embedded memory management system. The second one (ACC2) was also a 3-axis device with 14-bit of resolution and with capacity to control from ±2g up to ±8g. The size for the ACC1 was of 25 mm x 19 mm x 3.1 mm, while the ACC2 had 20.5 mm x 14.5 mm x 2.8 mm. The price of the ACC1 was around 20€, while that of the ACC2 was close to 5€. The data from both sensors was collected from an Arduino microcontroller, according to the diagram shown in Figure 2 (configuration of smart rail pads per type of sensor, connected to PC through a microcontroller) and Figure 3 (connection of each type of sensor to the microcontroller).

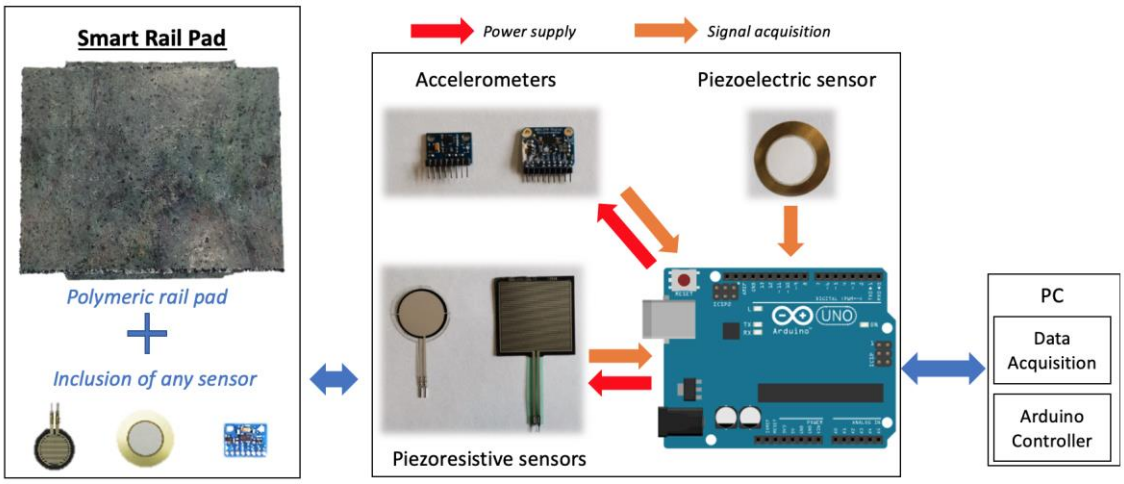

Figure 2. Smart Rail Pad concept and the configuration for data acquisition from the sensors.

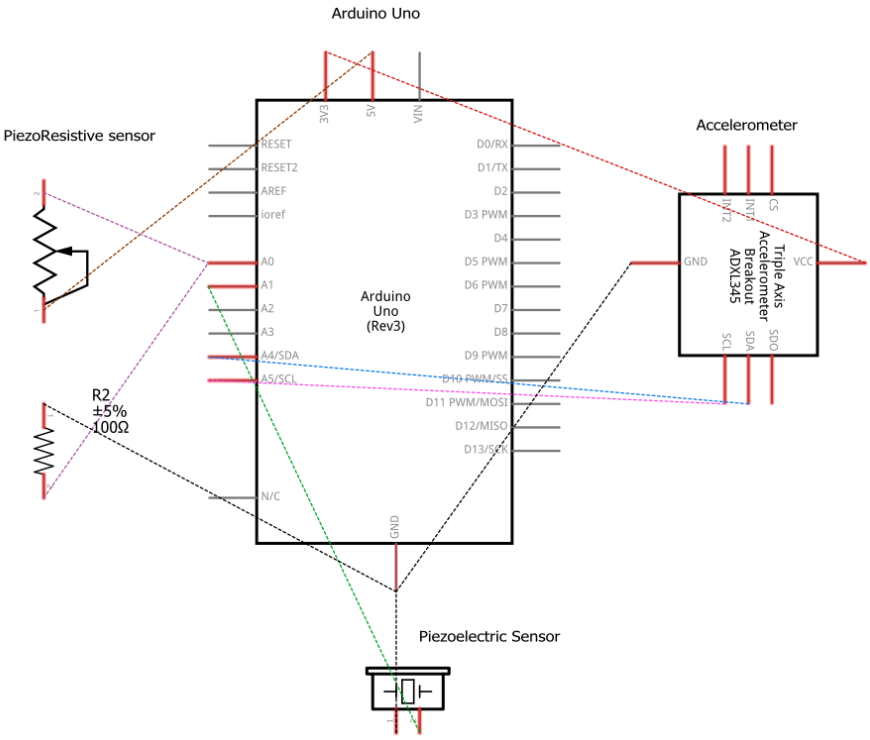

Figure 3. Diagram of connections between each type of sensor and the Arduino microcontroller.

Two different types of piezoresistive sensors were assessed in this study (Figure 1). The first one (PR1) was a circular flat device manufactured with polyester, and had a thickness of 0.208 mm and a sensing area with a diameter of 25.4 mm, costing around 25€. The force capacity recommended by the manufacturer ranged between around 0-30 kN, which could be increased by varying the resistance used in the measurement circuit. Then, it was calibrated, with values from 1 kΩ to 10 kΩ as recommended by the manufacturer. Regarding the second type of press sensor (PR2), it was a square, flat resistive sensor 0.42 mm thick, 43.7 mm wide, and 43.7 mm long. The price of this second PR sensor was close to 10€. As it will be seen in next section, both types of PR (piezoresistive) sensors had to be calibrated with different resistances by using Arduino as the microcontroller (Figures 2 and 3).

The piezoelectric used in this study had a cost close to 0.10€. It had a circular section with a total diameter of 35 mm of the metallic base and 24 mm of the quartz sheet, with a total thickness of 0.35 mm. This device was connected to the Arduino microcontroller (Figures 2 and 3), measuring the voltage generated by the piezoelectrics due to vibrations in the surface of the material where they are placed (rail pad in this study).

2.1.2 Rail pads

A series of railway track pads were used in this study for the testing of the sensors. The pads were manufactured from different polymers with the aim of assessing the applicability of the sensors on pads with varying properties, like the static stiffness (characteristic parameter of these elements). Specifically, 3 square pads (100 mm x 100 mm with 7 mm of thickness) were first used to evaluate the ability of the sensors to be included in different materials. These pads were composed of HDPE (High Density Polyethylene), a combination of PP/PE (Polypropylene and low-density Polyethylene), and a polymeric industrial resin composed of polyurethane with tough-elastic properties.

With these materials, the pads presented values of static stiffness (according to the Standard EN 13146-9) around 575 kN/mm for the HDPE, 250 kN/mm for the PP/PE, and close to 150 kN/mm for the resin, which could qualified as stiff, medium and soft, respectively (Sol-Sánchez et al., 2014).

Additionally, two other rail pads (140 mm x 180 mm x 7 mm) were employed in this study. These pads had the appropriate geometrical design for rail pad application. These pads, manufactured from HDPE and resin (stiff and soft ones), were applied in the tests simulating different tracks to determine the ability of the sensors to monitor diverse track and traffic conditions. Figure 4 shows an example of the pad with a standard superficial geometry while including sensors: (a) example of piezoresistive sensor on pad surface; (b) piezoelectric device embedded in a hole drilled into the bottom surface.

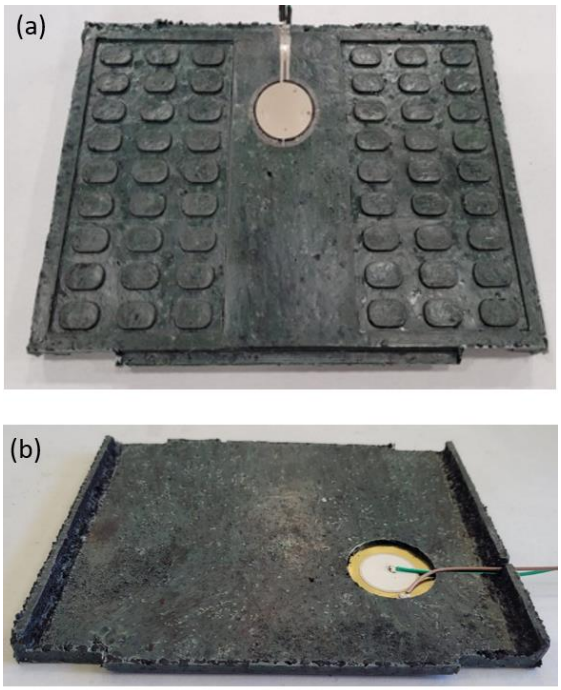

Figure 4. Example of visual representation of the smart pads. (a) piezoresistive sensor on surface; (b) piezoelectric embedded in the bottom surface.

2.2. Testing plan and methods

Table 1 lists the testing plan that was carried out in this study, which consists of 3 main study steps: (i) calibration of the sensors in correlation with the main parameter to be controlled in railway tracks, and selection of the most appropriate devices for next steps; (ii) study of sensor response when included in different types of pads, composed of diverse materials that result in pads with various stiffness values; (iii) assessment of the ability of sensors to monitor different track states and traffic conditions; (iv) evaluation of the durability of the sensors in the pads under repeated loads.

Table 1. Testing plan.

Study step	Variable of study	Sensor	Rail pad	Tests
	Displacements	Accelerometer 1 (ACC1)	--	Vertical displacements at

1. Sensor calibration and selection		Accelerometer 2 (ACC2)		different amplitudes and frequencies
	Load	Piezoresistive 1 (PR1) Piezoresistive 2 (PR2)		Vertical loads at different stress levels and frequency
		Piezoelectric (PI)		
2. Use of sensors in different types of pads	Type of pad material	ACC1 PR1 PI	Stiff Medium Soft	Application of different levels of stress on pads including the sensors
3. Study of sensors for monitoring different track performance	Simulation of different tracks	ACC1 PR1 PI	Stiff Soft	Simulation of train passage
	Traffic load level			
4. Assessment of sensor durability	Resistance to fatigue under repeated train loads	PR1 PI	Stiff	Fatigue test under repeated inclined loads simulating train passing

2.2.1 Sensor calibration

As seen in the testing plan, it was first necessary to calibrate the diverse sensors in correlation with their measurements to measure the loads in the railway superstructure; mainly changes in displacement due to oscillations of the rail-sleeper block over the ballast, and the loads transmitted through this block. Despite most sensors being typically calibrated by the manufacturer, the sensors were recalibrated for the loading ranges expected for this study, while also ensuring a high-quality output for the signal recorded by each sensor.

Particularly, the accelerometers (ACC1 and ACC2) were subjected to different levels of displacement oscillations, with amplitudes between 0-2.5 mm. These were considered expected conditions (Stark and Wilk, 2015; Sol-Sánchez et al., 2016; Ferro et al., 2020) for the passage of different types of trains over diverse tracks (in various structural states, leading to different oscillations), at a series of train speeds that generate load pulses on the sleeper with a frequency range from 0 to 10 Hz. The frequency applied was calculated to be a representative range for passing trains, calculated from train speed and the reference distance between bogies (the principal waves affecting track performance) (Milne et al., 2020). Nonetheless, as higher frequencies can occur in railway tracks due to different phenomenon, further research and calibration could be required before its application in real tracks.

For the test, each accelerometer was fixed to the actuator of a laboratory hydraulic machine (commonly used for materials testing), and sequences of 1,000 oscillation waves were applied for each testing conditions (at different amplitudes and frequencies). It must be noted that these tests were focused on the Z-axis of the accelerometers, given that the displacements were predominantly expected to be in this plane during its application for monitoring railway track performance and structural state.

To calibrate the piezoresistive sensors (PR1 and PR2), they were glued to a metallic pad of 150 mm x 150 mm and 50 mm thick, and a series of load pulses were applied over the

sensor at different amplitudes (stress levels from 0 to 5,000 kPa, which cover that expected under the rail) and frequencies (from 0 to 10 Hz) (Standard EN 13146-9; Milne et al., 2020; Ferro et al., 2020).

Similarly, a series of loads were applied over a resin pad (100 mm x 100 mm x 7 mm) with a piezoelectric (PI) glued to the surface. In this case, unlike the piezoresistive sensors, for the calibration of the piezoelectrics the load was not applied directly over the sensor in order to avoid breaking the quartz sheet, but it was applied through a rectangular actuator (40 mm x 60 mm) on the resin pad at a distance of 1 cm from the piezoelectric. Thus, the capacity of these devices to monitor the vibrations transmitted through the material was measured (Tian et al., 2016).

2.2.2 Use of sensors in different types of pads

With the aim of assessing the measurements recorded by the sensors (ACC1, PR1 and PI) in different pads considered (with different composition and mechanical properties), a series of tests were carried out with the rail pads incorporated into a system simulating the railway track applying diverse load ranges.

The system (Figure 5) consisted of a rubber sheet (150 mm x 150 mm x 4.5mm, with a stiffness around 300 kN/mm) to simulate the deflections in the subgrade, as done by other researchers like Ferro et al., 2020; a concrete block of 150 mm x 150 mm x 150 mm to simulate the sleeper; an I-shaped metal profile to simulate the rail with a base of 100 mm x 100 mm; and a series of rail pads (100 mm x 100 mm x 7 mm) embedded with sensors, being made from different materials (HDPE, PP/PE and Resin) and qualified as stiff, medium and soft, respectively.

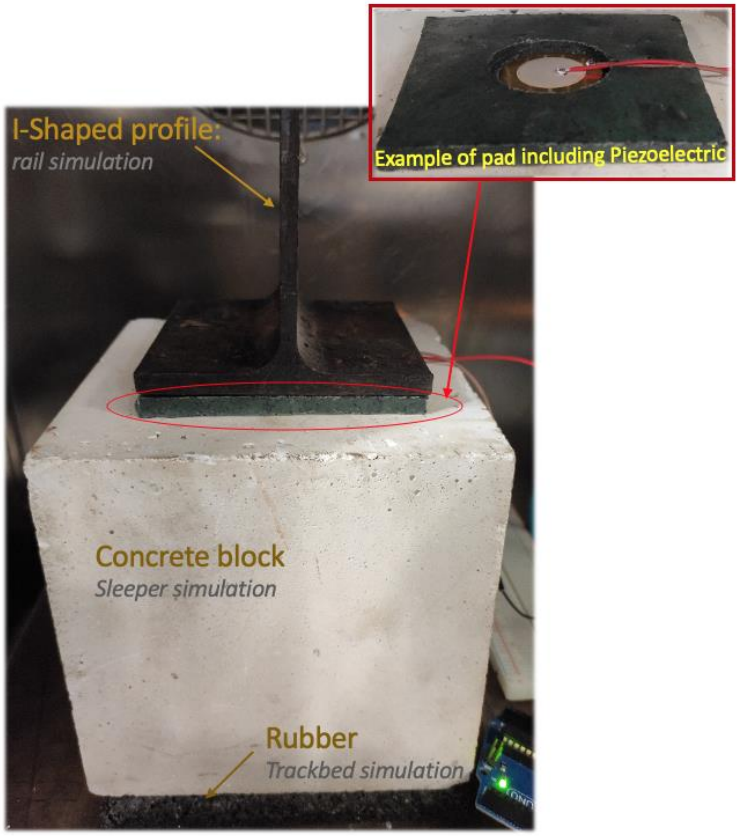

Figure 5. Example of the simulated track system, including a pad with sensors (piezoelectric in this example).

For the case of the PR sensor, it was directly glued to the surface of the pad, and therefore, the sensor was directly in contact with the base of the metal profile as would happen in real tracks under the rail. However, for the cases of the accelerometer and piezoelectric, these were included in a hole drilled in the bottom side of each pad (Figure 4) in order to avoid damaging the sensors, by protecting them from the direct contact within the rail and the sleeper, which could crush the sensors. The hole in the pads was created with appropriate dimensions (35 mm of diameter and 3.5 mm deep) to embed the devices and provide an adequate place for them to function properly.

The tests were carried out by applying a series of loads over the metal profile (as would happen in real tracks where a train transmits the loads to the rail), and recording the measurements provided by the different sensors. The loads (1,000 cycles) ranged from 0 to 2,000 kPa stress levels at 5 Hz over the pads including the sensors, which were considered appropriate testing conditions in consonance with those expected in the central sleeper under train bogie passing over the railway track. This fact was fixed considering that rail pads in real tracks (with dimensions of 140 mm x 180 mm) can be subjected to loads per wheel around 95 kN, with distribution close to 50-60% over the central sleeper because of the division of loads through the rail to a different number of sleepers (Standard EN 13146-9; Wilk et al., 2015; Sussman, 2017).

2.2.3 Study of sensors for monitoring different track performance

This study step focused on assessing the ability of the sensors to monitor diverse track states through measuring the changes in some of the main parameters, such as the level of traffic and the variation in the capacity of the track to deform under such traffic loads. For this study, one sensor of each type (ACC1, PR1 and PI) was included in two rail pads with different compositions and stiffnesses, aiming therefore to assess the capacities of the sensors for various types of pads: a soft pad made of resin and a stiff pad composed of HDPE.

For this purpose, two configurations for the track section were simulated (Figure 6), both consisting of an I-shaped metal profile (simulating a track rail) with a base of 100 mm x 100 mm, the rail pads including the sensors and a concrete block (150 mm x 150 mm x 150 mm). These were placed over two solutions with diverse capacity to deform under loading: (i) a medium base made of a rubber sheet (150 mm x 150 mm x 4.5mm) that permits deflections of around 1 mm at 2,000 kPa; (ii) a soft base composed of a rubber mat (150 mm x 150 mm x 10 mm) with deflections close to 2.5 mm.

For the evaluation of the ability of each type of sensor to identify different track performances, a sequence of forces (Figure 6) simulating train passage was applied over each system (over rubber sheet and rubber mat) with each type of pad including the various sensors. For the pads with the accelerometer, Figure 6 displays the loading sequence used to generate different oscillations on the system. For the cases with the press panel (piezoresistive sensor) and piezoelectric sensors, a sequence of different deformation levels were applied on each system (Figure 6), which required diverse stress levels on the pad to be detected with the mentioned sensors.

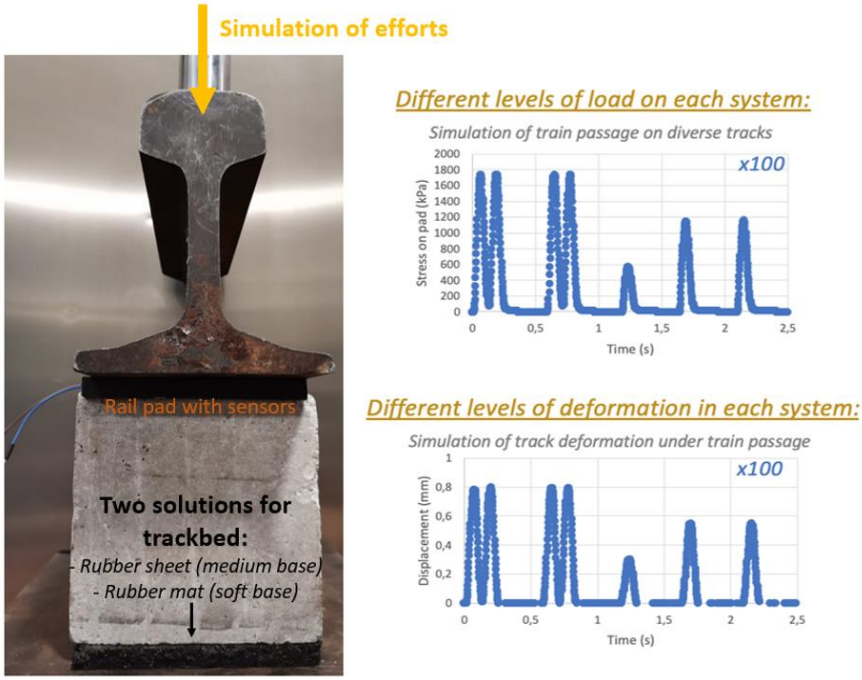

Figure 6. Scheme of the simulation of different track systems (over different bases), to be subjected to different loading conditions, simulating the passage of trains.

Firstly, a loading sequence consisting of a series of loads with stresses between 0-2,000 kPa was applied (the same level of loading expected on rail pads for a singular section under the central sleeper), with the capacity to produce different states of deformation in each system, to be detected by the accelerometers. This could be appropriate for monitoring variations in track deflections under various traffic conditions over a constant section, or changes in sleeper movements under a same load level because of different configurations/states of the system, like those associated with the "hanging sleeper" phenomenon (increasing the sleeper oscillation accelerations) or abrupt stiffness changes, among others (Stark and Wilk, 2015; Wilk et al., 2015). Figure 7 shows a representation of some examples of the phenomena that could vary the oscillations in a track, which can be detected by the sensors.

On the other hand, a sequence of different displacements (between 0 and 0.8 mm) was applied over each system in order to evaluate the ability of the sensors to measure the variations in stress levels under the various configurations. With the simulation of different systems with varying vertical strength, different loads were required to achieve such deformations, which were detected by the piezoresistive sensors and piezoelectrics. This focused on measuring changes in track support depending on their strength and state (Figure 5 shows some examples). For example, soft track substructures are expected to generate lower levels of stress on the rail pad than stiff ones (Sussman, 2017), because of a longer distribution of loads within different sleepers. Similarly, phenomena such as differential settlement, or hanging sleepers, are expected to vary the level of pressure in rail pads due to different gap heights under sleepers (Stark and Wilk, 2015; Sol-Sánchez et al., 2017).

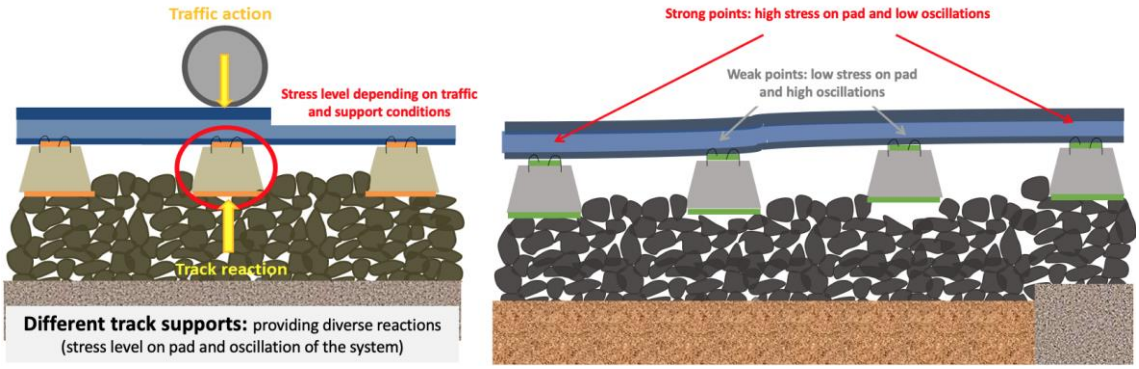

Figure 7. Scheme representing different examples of track conditions to be detected by the sensors through variations in stress on pad and/or oscillation of superstructure. Left: tracks with different bearing capacity; Right: differential settlement.

2.2.4 Assessment of sensor durability

Once the ability of the different sensors was studied to monitor traffic and track conditions, the durability of the most appropriate sensors was evaluated; where these were selected according to the results of the previous study steps. For this purpose, a fatigue test simulating repeated loads from trains passing through curved sections (considered the most unfavorable testing condition) on a pad including the selected sensors was carried out (in this case, using the stiff pad as example). The test was adapted from the Standard EN 13146-4 to focus on determining the durability of the sensors. The test consisted of applying 1.5 x 10^6 cycles at 5 Hz with amplitude between 5 kN and 83 kN, under a load angle of 33° from the vertical direction over the head of a rail section mounted on the system pad-fastening-sleeper. To determine the durability of the sensors, the signal amplitude was measured before and after the fatigue process by applying a series of 100 cycles at stress amplitudes ranging from 0-2,000 kPa at 5 Hz over the rail-pad-sleeper system.

3. Analysis of results

3.1 Sensor calibration and selection

Figure 8a displays the acceleration amplitudes recorded by ACC1 and ACC2 under different oscillation amplitudes (displacements in mm) at various frequencies (1, 5, 10 Hz). Figure 8b shows an example of the wave signals collected by each sensor (ACC1 in the left, and ACC2 in the right) in comparison with their displacements, for a medium case of 1.5 mm at 5 Hz, generated by the hydraulic actuator of the testing machine.

Both the accelerometer models showed a lineal correlation between the signal measured in Z-axis and the amplitude of oscillation applied, leading to higher values of acceleration when increasing the displacement and/or the frequency of the oscillation, being the values in consonance with those measured in previous field studies (Wang and Markine, 2019; Khairallah et al., 2019). In this sense, it is remarkable the fact that at low displacements, the differences between the frequencies were small, while it was also noted that at low frequency (as those expected as dominant ones under bogie traffic), there were no differences between the diverse oscillation amplitudes.

All this must be considered when using them for monitoring since it could limit the detection of small track variations, and therefore, being appropriate for only considerable changes in track performance (like hanging sleepers or component breakages). Where in

this case, it has been seen in previous field studies (Stark and Wilk, 2015; Wang and Markine, 2019) that higher values of acceleration are expected. Besides, as the signals are dependent on both parameters (displacements and frequencies), knowing the load frequencies may be required to be able to distinguish the changes in displacements for detecting variations in the performance of the infrastructure.

Assessing the quality of the signals measured by each accelerometer (Figure 8b), it could be said that the ACC1 showed a good correlation between the accelerations and the displacement waves, being able to distinguish the different pulses. However, in the case of the ACC2 the signal was poorer, showing higher number of peaks at different frequencies, and thus, offering a worse correlation with the waves applied by the testing machine. This led to discarding this sensor for the rest of the study, since it would not be appropriate for the application desired in this paper. This demonstrates that all devices could be not suitable for the track monitoring, and also requiring the previous step of calibration and study of the properties in relation to that aim.

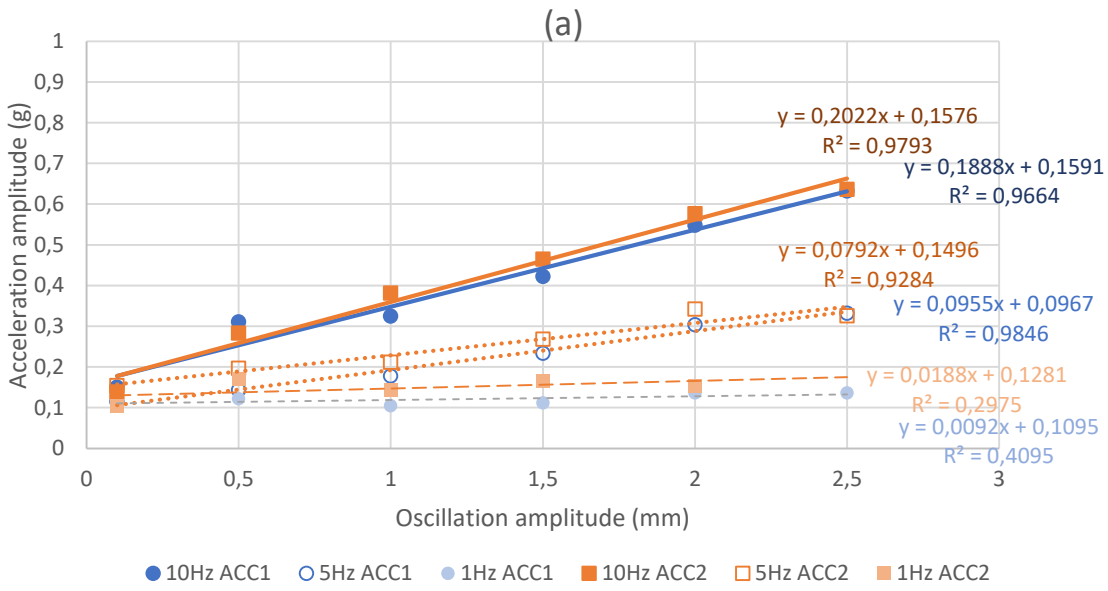

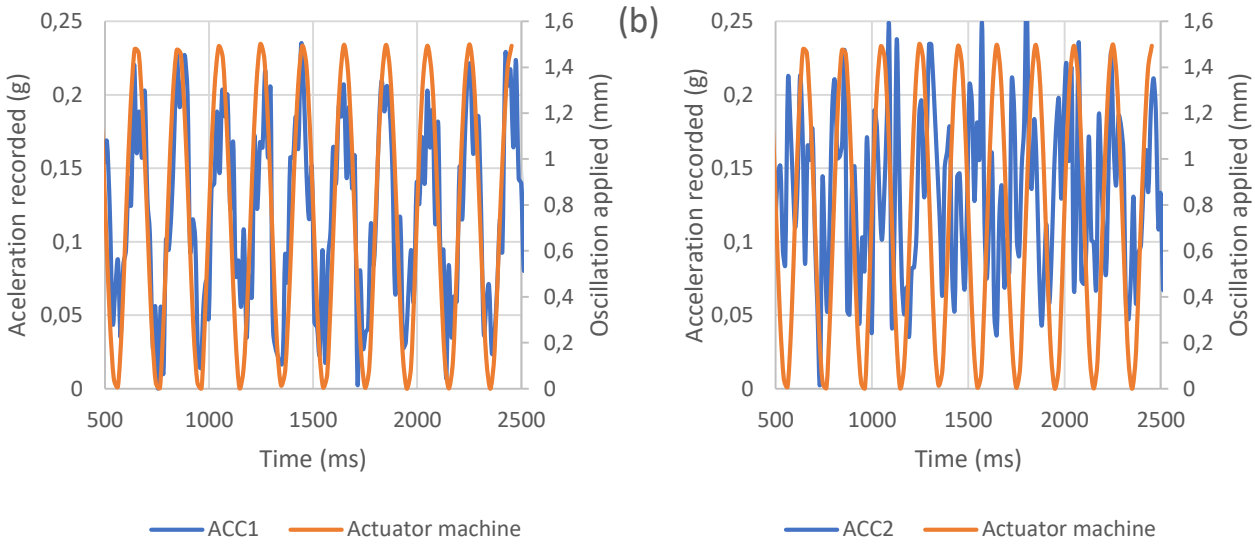

Figure 8. Results from the calibration of the accelerometers. (a) correlation between acceleration amplitudes collected and oscillations applied; (b) waves signals from the accelerometers in comparison with waves applied.

In the case of the piezoresistive sensors, as the signal of those depended on the resistance used in the microcontroller, Figure 9 represents the results for PR1 and PR2 for diverse values of resistances (measured in kΩ), in consonance with the recommendations from manufacturers. Results showed that for both cases, the reduction in resistance value led to lower values of voltage amplitude measured under the different levels of stress applied on the surface of each device. A logarithmic correlation between the voltage and stress was obtained, with a higher capacity to distinguish the changes in stress when reducing the resistance. Generally, it was seen that for a same value of resistance (1 kΩ) the PR2 led to higher values of voltage, which could limit its range of applicability because of the reduction of capacity to measure high levels of stress.

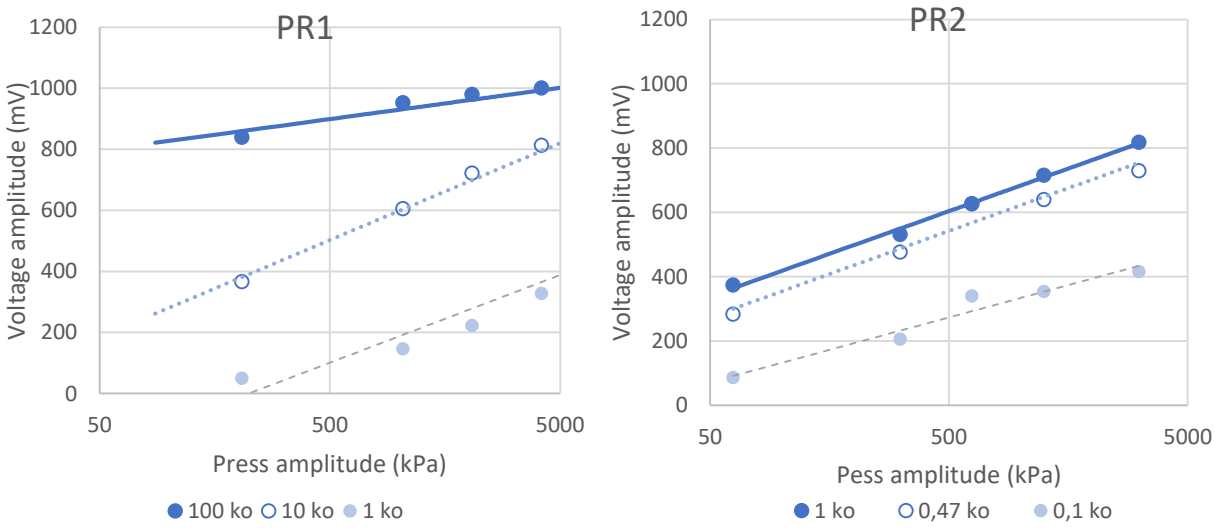

Figure 9. Influence of resistance used in the measurement system for the piezoresistive sensors calibration.

In fact, Figure 10a (which represents the correlation of the signal of each sensor, in milli volts, with the level of stress amplitude applied at different load frequencies), confirms the higher results for the PR2 than the case with the PR1 for a same level of stress. Also, it is seen that the signals measured by the sensor number one (PR1) were independent of

the load frequency (at least, for those studied in this article), while a small increase in voltage was collected by PR2 when increasing the load frequency, particularly at high levels of stress. This fact could limit the application of PR2 because of the higher difficulty to interpret the changes collected by this sensor during monitoring, being dependent on the level of stress (main variable to control for monitoring the changes in stress under the rail due to variations in track performance), but also its frequency (varying with train speed, for example).

Because of this, joined with the quality of the signals in comparison with the frequencies applied by the testing machine (where Figure 10b shows an example for the case of 5 kN over the sensors at 5 Hz), the PR1 was selected for its application to the rail pads since clearer signals were obtained with little deviation from the load frequency.

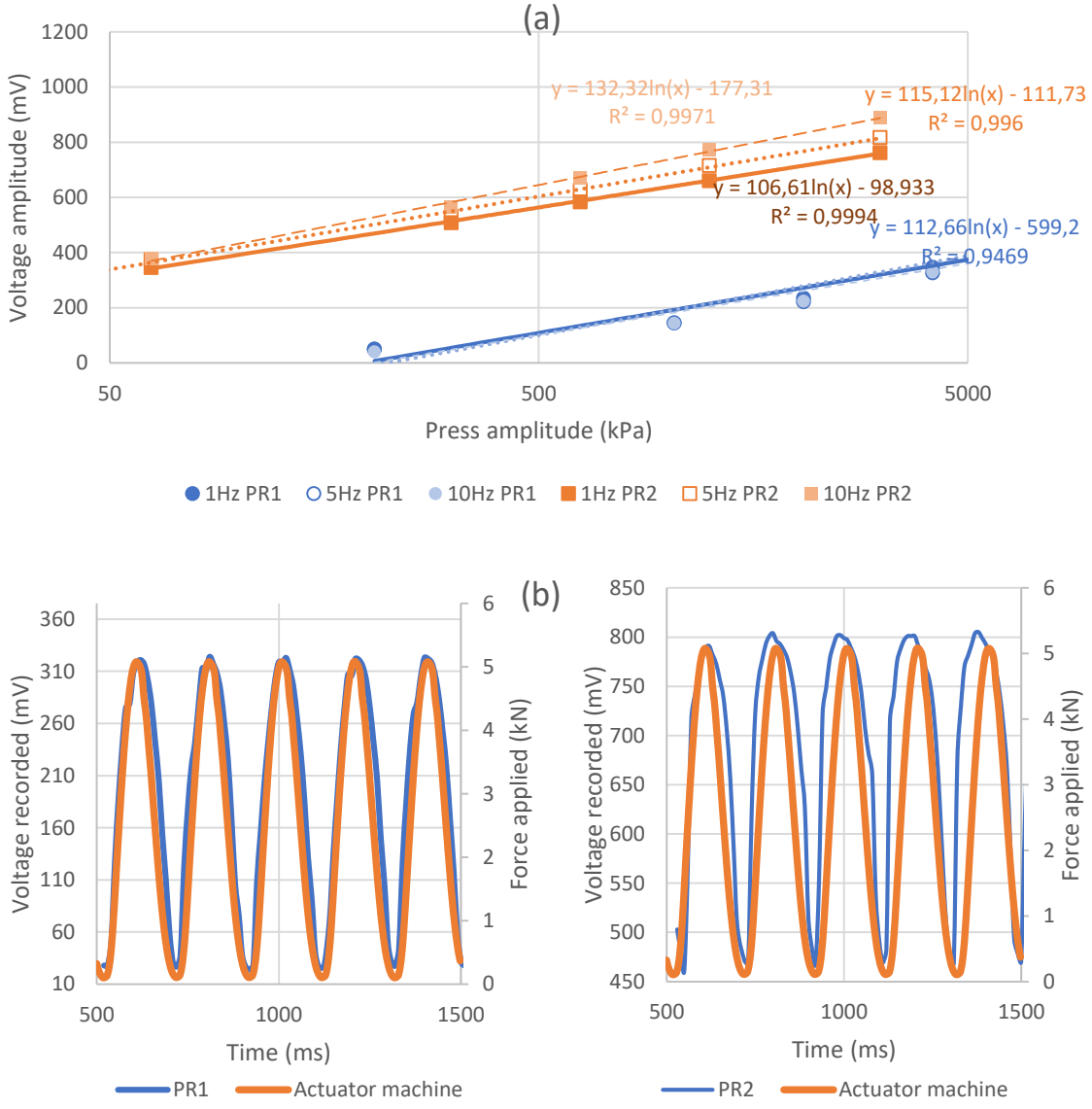

Figure 10. Results from the calibration of the press sensors. (a) correlation between voltage measured and compressive force applied; (b) signals collected versus waves of force applied.

Figure 11a displays the results (measured in milli volts) for the calibration for the piezoelectric under different levels of stress applied over a pad including such device, at different frequencies, while Figure 11b shows an example of the signal measured by the

piezoelectric under a load of 5 kN at 5 Hz. In contrast with the piezoresistive sensors, the signals of the piezoelectric showed a linear correlation with the level of stress, which could lead to a clearer distinction of the variations in loads at high loading levels. This is in consonance with previous studies that reflected the linear correlation of the measurement of this type of sensors (Song et al., 2017; Zhang et al., 2018). Besides, similar to PR1, the piezoelectric also presented little dependence with the pulse frequency, at least for the cases studied in this paper, while further calibration could be required for application in real tracks; higher frequencies may be present, this would need to be verified through consultation with railway agencies. This could be appropriate for clearer monitoring of the evolution of stress in components, regardless of train speed. On the other hand, Figure 11b indicated that the quality of the signal was acceptable to distinguish the different pulses, showing clearly the correlation between the voltage and the load waves applied with the testing machine.

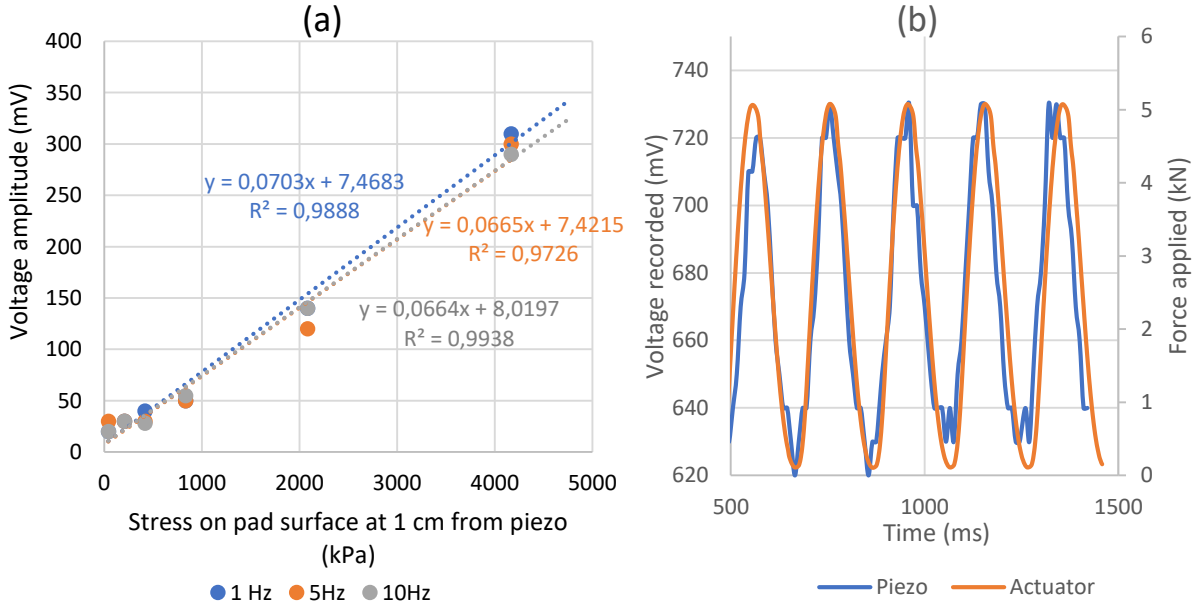

Figure 11. Results from calibration of piezoelectrics. (a) correlation voltage-stress; (b) waves measured by piezoelectric versus wave forces applied by machine actuator.

3.2 Use of sensors in different types of pads

With the aim of proving the applicability of accelerometers in different types of rail pads, Figure 12 represents the values of acceleration amplitudes measured by the ACC1 under various levels of stress (between 0-2,000 kPa at 5Hz) generating diverse ranges of vertical displacements over the system (rail-sleeper) including three types of pads under the rail (soft, medium and stiff). Results showed little differences between the two systems including the various pads, since the accelerations were only dependent on the level of oscillation displacement generated when varying the range of stress over the system, recording small variations depending on the pad.

Therefore, the accelerometers could be used in different types of pads, with no differences in the signal recorded. Nonetheless, it is important to keep in mind that the magnitudes collected by these devices are dependent on the oscillation amplitude (parameter to control in track monitoring), but also vary with the frequency, which could complicate the interpretation of the results, combined with the small variations generated by the

ranges expected in railway tracks, as can be seen in Figure 12, and in agreement with the calibration results (Figure 8a).

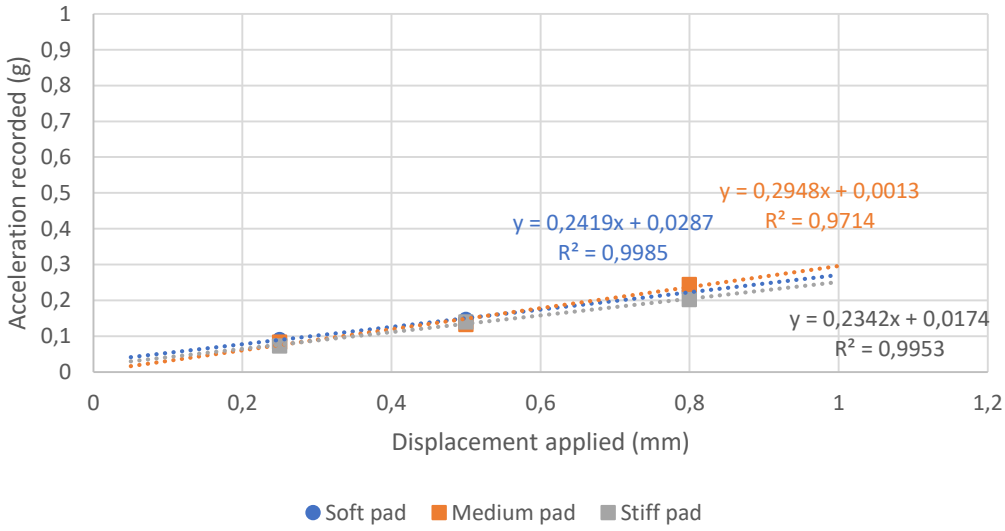

Figure 12. Influence of type of pad on the measurements collected by ACC1 under different displacement oscillations.

For the press sensor (PR) and piezoelectric (PI) case studies, different types of pads were included into the system simulating the railway track. Figure 13 represents the results of the signal measured by these devices (in milli volts) under various stress levels when using three pads with different compositions and properties (stiff pad made of HDPE; medium one from PP/PE; and soft pad from resin).

Results confirm that piezoelectrics offer a linear correlation with level of stress while PR showed a logarithmic relationship, which could limit its applicability to distinguish variations at high stress levels. Assessing the influence of the pad, it was seen that higher values were recorded by both PR and PI for the stiff one while the lowest values were measured when using the soft pad. This could be associated with the higher density and stiffness of the pad made of HDPE (stiff), facilitating therefore the propagation of waves into the material (increasing the measurements from PI) while presenting a higher concentration of stress on surface (leading to higher values on PR) (Zhang et al., 2018). Therefore, this states the importance of the material used in the manufacturing of the pad to include these sensors, or in other words, it is important to assess and calibrate these types of sensors depending on the pad properties where they are to be included.

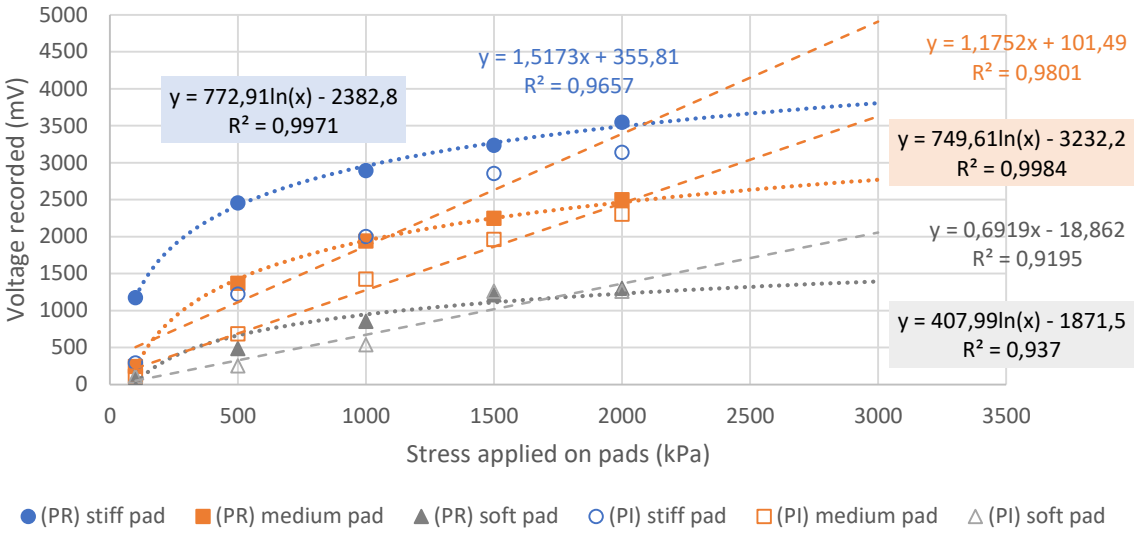

Figure 13. Influence of the type of material on the signal measured by PR and PI.

3.3 Use of sensors for monitoring track performance

For the analysis of the functionality of each type of sensor to identify different track behaviours, Figure 14 shows the signal measured by the accelerometer included in two different pads (soft and stiff from different compositions) into two different systems simulating railway tracks over various supports (medium and soft track-bed base).

Results are expressed as the acceleration amplitude (Figure 14a) measured from pulses reproducing various levels of loads deforming the track. Figure 14b represents an example of the evolution of such measurements during one sequence of train passage, in comparison with the displacements measured by standard instrumentation (LVDTs in this case). Similarly, Figure 15 and Figure 16 show the results measured from the piezoresistive sensor and the piezoelectric when each track system was subjected to various levels of deformation, simulating various stress conditions to be monitored. Before the analysis, it was important to keep in mind the different sensors reading types. The maximum and minimum values from the accelerometers were out of phase with the force or displacement peaks, since the minimum accelerations occur at the maximum displacement value of the actuator. This is due to the fact that such displacement peaks represent a change in load direction (from increasing pad compression to reducing it), and therefore, leading to values of minimum acceleration. In contrast, the press panel peaks correspond to those from actuator load, and the piezoelectric peaks were recorded as electrical pulses caused by vibration propagation.

Results demonstrate that the accelerometer was able to identify the different stress levels applied by traffic (simulating trains with different weights), while also distinguishing the differences between systems, since higher accelerations were measured for the soft base where higher movements were expected. These results are in consonance with those expected for the changes in accelerations in field for tracks with varying performances (differential settlement for example), as those measured in previous studies (Stark and Wilk, 2015; Wang and Markine, 2019). Besides, it was confirmed that the type of pad presented little influence as a support for the accelerometer.

However, it must be noticed that the quality of the signal under the pulses (Figure 14b) was lower than the other cases using the PR and PI (Figures 15b and 16b), respectively. This is in agreement with the previous results where it was seen that the variations to be recorded by the accelerometers could be small, and therefore, presenting some limitations that could affect their suitability.

On the other hand, as previously indicated, the use of the piezoresistive sensor and piezoelectric did allow for a clear identification of the pulses, showing waves similar to those collected by the standard instrumentation of testing machine, which states the potential applicability of these technologies to monitor track performance under train passage. Both sensors (PR and PI) identified the different stress levels required to reproduce the different displacements (Figures 15a and 16a), while allowing for a clear distinction between the type of track system (over a medium or soft base). This last fact was clearer for the case of piezoelectric where signal reductions were greater than 50% when passing from medium to soft base, while the PR showed smaller changes. Besides, it is important to note that, in agreement with previous results, the values depended on the type of pad used to include the sensors, obtaining higher values for the pad composed of HDPE with a stiff surface (for the PR sensor) and with probably a clearer transmission of waves for the PI.

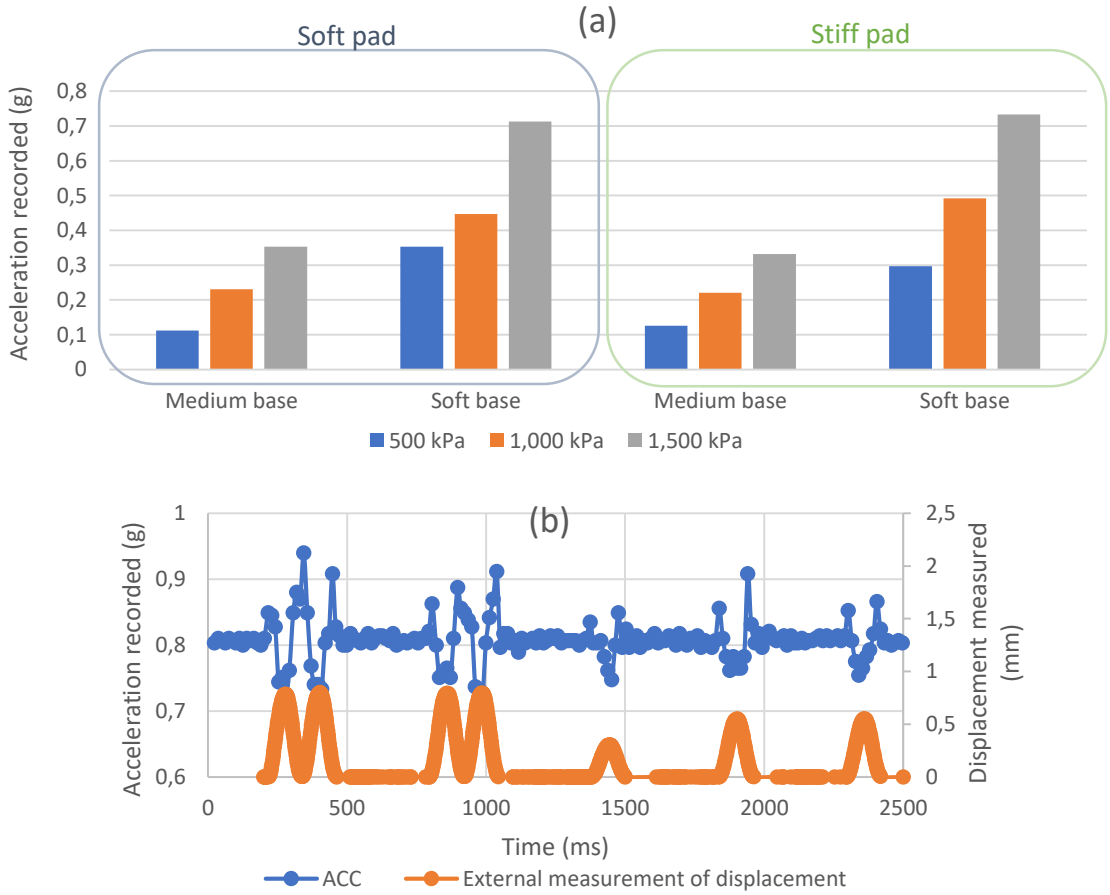

Figure 14. Results of accelerometers in the different pads used in the track testing system over different bases. (a) influence of system configurations under diverse load levels; (b) example of correlation between acceleration measurements and displacements generated under a load sequence.

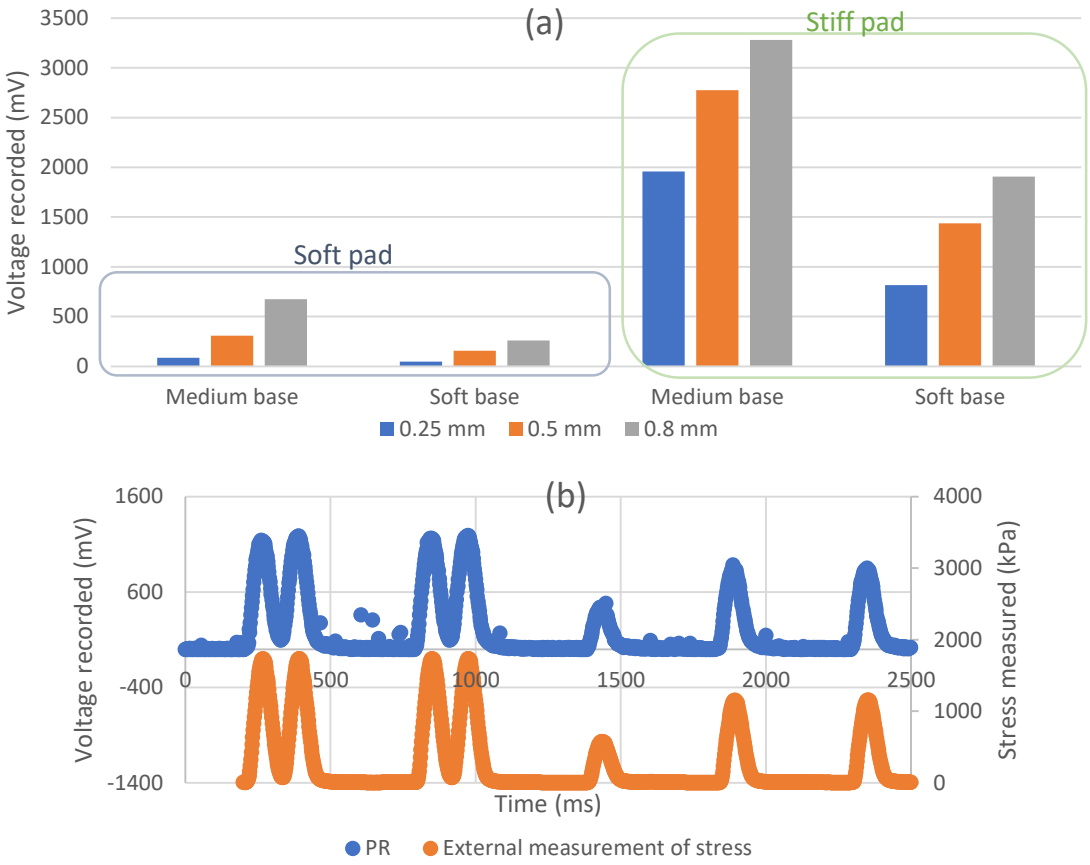

Figure 15. Results of PR in different pads used in the different track testing systems over different bases. (a) detecting different stress levels required to produce various displacement amplitudes on different systems; (b) example of correlation between PR signals and stress required for the testing machine to simulate the displacements.

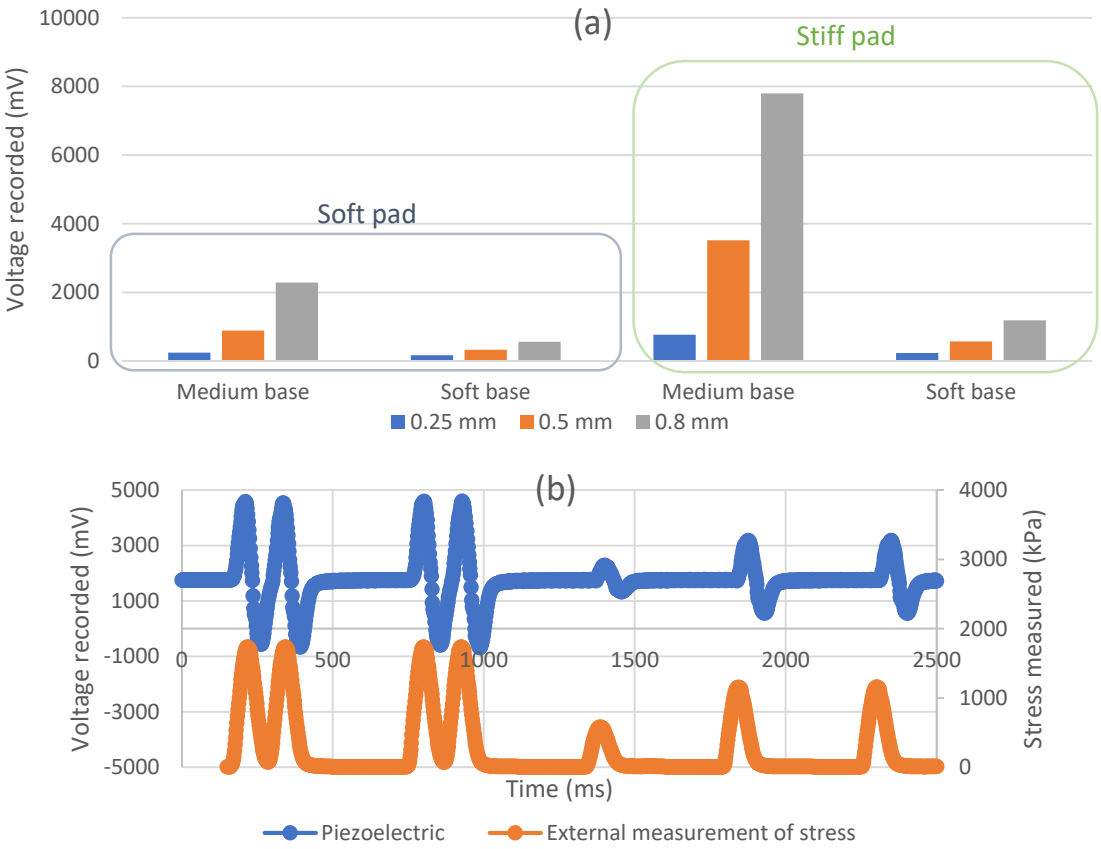

Figure 16. Results for the piezoelectric in the track testing systems subjected to diverse loads to generate various displacement levels (a); and correlation between PI signals and stress measured by the testing machine (b).

For a deeper understanding of the functionality of the PR and PI sensors (seen to be the technologies with highest potential for use in smart track monitoring), Figure 17 represents examples of changes in track performance monitored by PR and PI sensors through variations in the recorded voltage when used in the stiff pad, for example. Particularly, axis X represents the variations in the stress applied on the pad due to changes in track support (soft trackbed or hanging sleepers are expected to decrease the stress on the central sleeper under train wheel) (Stark and Wilk, 2015; Sussman, 2017) or due to variation in traffic loads. On the other hand, axis Y represents how such variations (from 1,700 kPa to 850 kPa due to traffic load reduction; and from 1,700 kPa to 250 kPa due to a reduction in support strength) are detected by varying the voltage recorded by the PR and PI.

It can be seen how a variation in load level in a track (associated with changes like the value of train weight, the presence of dents in wheels or irregularities in the rail etc.) (Wang and Markine, 2019) could be clearly identified by both types of sensors, which shows the potential use of these technologies to detect track failures as done with other devices in previous studies (Song et al., 2017; Khairallah et al., 2019). For example, it was seen that a variation in stress from around 1,700 kPa to 850 kPa led to the reduction in voltage recorded by both sensors. Nonetheless, it must be noted that this variation was higher for the PI (from around 7,800 mV to 3,500 mV) than for the PR (from around 3,250 mV to 2,750 mV), which indicates the piezoelectric would be more suitable, due to its linear relationship between the voltage measurements and the stress level (Song et al., 2017; Zhang et al., 2018).

Similarly, it is seen that both sensors identified a change in track performance under the conditions modelled to represent the reduction in support strength or the appearance of the hanging sleeper phenomenon, leading to a lower concentration of stress on the pad including the sensor (Wang and Markine, 2019). This is because of the higher deformability of the system (simulating higher distribution of loading along the track), and therefore, lower values of voltage recorded by the sensors. Again, particularly in the case of the piezoelectric, a higher variation in stress was identified when passing from a deformability of 0.2 mm to 0.8 mm.

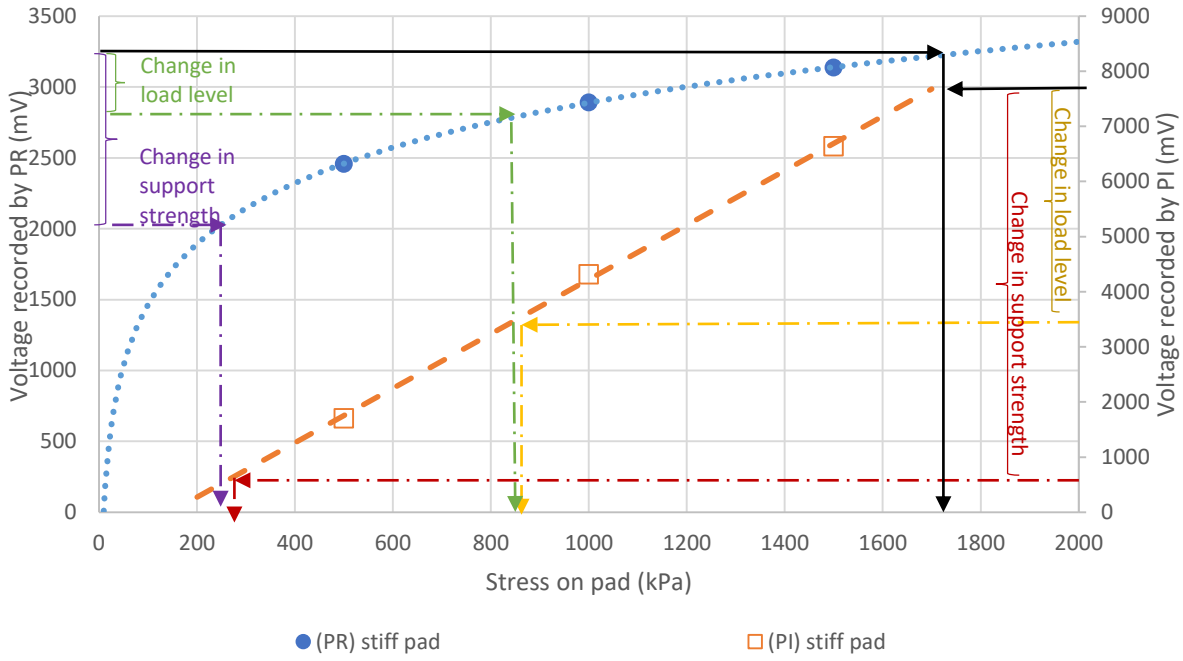

Figure 17. Correlation between measurements of PR (left) and PI (right) with the variations of stress on pad due to diverse testing conditions.

3.4 Assessment of sensor durability

In order to evaluate the durability of the PI and PR1 sensors (those selected as most applicable for smart pads, based on the previous results), Figure 18 shows the values of the signal amplitude of the sensors before and after the fatigue process. Results reflect that the PR failed during the fatigue process since the signal amplitude was reduced to null after the repeated loads, which could be due to sensor breakage as a result of frictional efforts during the test. Therefore, for the application of this type of sensor (which needs direct contact with the loads) further research would be required in order to protect the device.

On the other hand, it was seen that the piezoelectric (whose monitoring capacity is based on wave propagations) continued measuring after the fatigue process, but obtained lower values than those collected before the repeated loads. Nonetheless, it must be considered that the percentage of signal variation from PI due to changes in load level was quite similar to that measured before the fatigue process, thus conserving the capacity to detect changes in load level.

In addition, Figure 19 displays the evolution of the PI signal during the test, in comparison with the rail displacements measured through LVDTs during the fatigue process (as indicated in the Standard EN 13146-4). It is seen that the PI signal had quite a similar evolution to that found for the rail displacements, obtaining considerable variations at the beginning of the test (which could be due to the adjustment of rail and fastening system), but later presenting stable performance.

Therefore, it could be said that the PI showed an adequate durability since it conserved its capacity to detect changes in load level, while presenting stable performance during the fatigue test (comparable to that measured by standard sensoring devices used in laboratory tests). Nonetheless, further assessments in real tracks could be required for a deeper understanding of the durability and accuracy of these smart pads (including common piezoelectric devices).

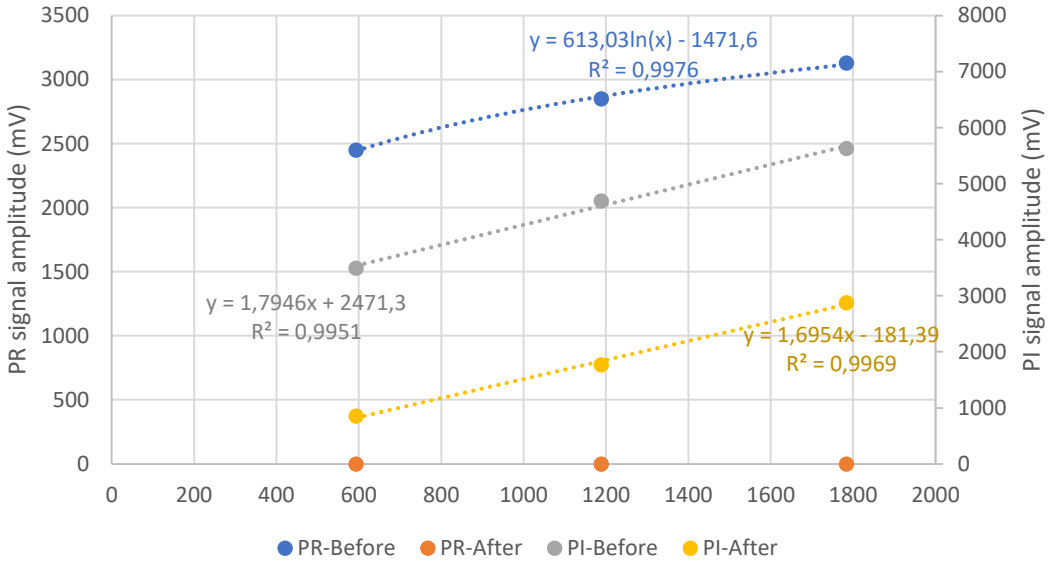

Figure 18. Signal of PR and PI sensors before and after a fatigue process from repeated inclined train loads.

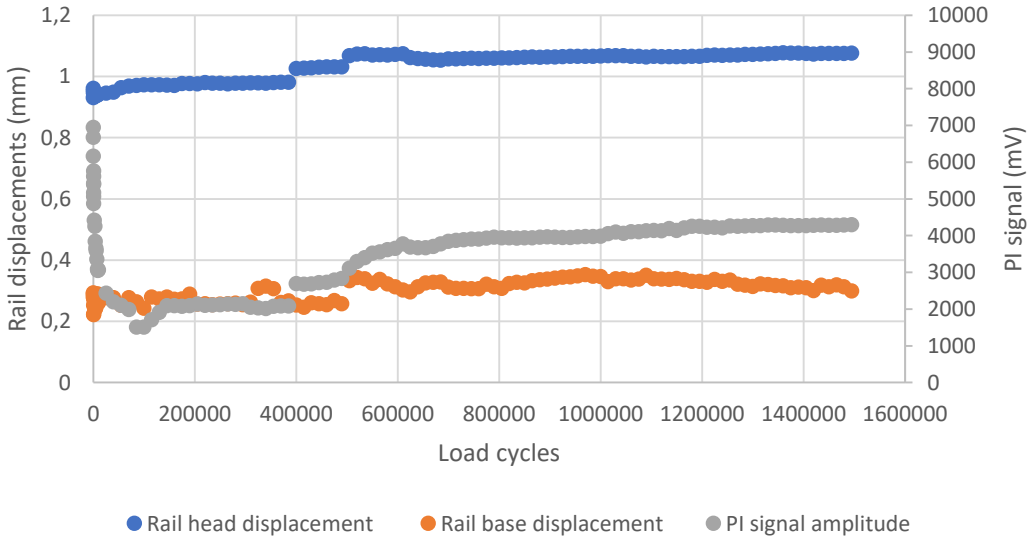

Figure 19. Evolution of PI signal during the fatigue tests, in comparison with rail displacements.

4. Conclusions

This article aimed to enhance the current state of knowledge on real-time railway track monitoring through studying rail pads, a key railway structural component, equipped with different types of sensors to monitor the structural performance of the track and also detect changes traffic levels and loading conditions. Through these tests, the goal was to determine the most appropriate sensors to be used in rail pads. The study focused the calibration of different types of accelerometers, press panels (piezoresistive sensor) and piezoelectrics, assessing also the applicability of these sensors on different types of rail pads manufactured from different polymers, and evaluating the potential ability to measure changes in essential parameters defining the state of railway tracks under different traffic conditions. From this study, the following conclusions were drawn:

- Results from the calibration of the sensors demonstrated that not all devices are suitable to provide sensitive rail-pad monitoring systems. Thus, the calibration and selection of the most appropriate sensors is required before their application.
- Accelerometers and piezoelectric sensors showed a linear relationship between the signal and track response, but the first one detected changes in oscillation magnitude while the second one focused on the level of stress on the pad. However, the press panels (piezoresistive) showed a logarithmic relationship, which could limit their capacity to detect oscillation changes under higher loading levels expected in rail pads under traffic.
- Signals from accelerometers showed to be independent on the type of pads while those from piezoelectric and press panel depended on the type of pad where they were embedded, obtaining higher amplitude signals on stiff pads, which have a higher capacity to propagate the waves (in the case of the piezoelectrics) and with higher stress concentrations (in the case of the piezoresistive panels).
- Regardless of the type of pad, the accelerometers were able to identify the changes in oscillations due to variations in traffic load or strength of the support simulating the railway track. Nonetheless, it must be considered that the quality of the signals from the accelerometers due to train passage was poorer than those from the piezoresistive sensor and the piezoelectric. Hence, further research into accelerometers for this application may be required.
- The piezoresistive sensor and piezoelectric showed the best ability to detect changes in track performance due to variations in traffic conditions or the strength of track support, particularly when using a stiff pad.
- Furthermore, the piezoelectrics provided the clearest signal outputs when measuring track performance. Also, in contrast to the press sensor, the piezoelectric device showed adequate durability after fatigue testing.

Therefore, based on the results, it could be said that the piezoelectric sensors presented the highest implementation potential for this application, particularly considering its low cost in comparison with other standard sensors. Nonetheless, further studies will be required to continue the development of this technology. Particularly, a deeper analysis on the durability of the pads and the sensors, mainly under environmental and fatigue conditions, while also defining an optimized design (possibly considering sensor encapsulation) for the smart rail pads; as the removal of material would intuitively affect its structural capacity. Finally, the study of the sensors' responses in laboratory testing boxes, reproducing different track conditions (i.e. hanging sleeper phenomenon, harsh

environmental conditions), would also be required to establish a range of measurements per sensor, to later be more prepared to apply these technologies in field experiences.

Acknowledgments

The present study has been conducted within the framework of the ECO-Smart Pads (Smart and Sustainable Resilient Pads for the Railway of the Future, RTI2018-102124-J-IOO) and HP-RAIL (Smart technologies & high performance materials for the next railway generation, RTC-2017-6510-4) research projects, funded by the Ministry of Science, Innovation and University of Spain and the Ministry of Economy and Competitiveness of Spain, respectively.

References

Benedetto, A.; Tosti, F.; Ciampoli, L.B. et al. (2017) Railway ballast condition assessment using ground-penetrating radar – an experimental, numerical simulation and modelling development. Construction and Building Materials, 140, pp. 508-520. https://doi.org/10.1016/j.conbuildmat.2017.02.110

Cantero, D.; Basu, B. (2015) Railway infrastructure damage detection using wavelet transformed acceleration response of traversing vehicle. Structural Control Health Monitoring, 22, pp. 62-70. https://doi.org/10.1002/stc.1660

Castillo-Mingorance, J.M.; Sol-Sánchez, M.; Moreno-Navarro, F.; Rubio-Gámez, M.C. (2020) A critical review of sensors for the continuous monitoring of smart and sustainable railway infrastructures. Sustainability, 12 (22), 9428. https://doi.org/10.3390/su12229428

Dos Reis, J.; Oliveira Costa, C.; Sá da Costa, J. (2018) Strain gauges debonding fault detection for structural health monitoring. Structural Control Health Monitoring, 25 e2264. https://doi.org/10.1002/stc.2264

Ferro, E.; Harkness, J.; Le Pen, L. (2020) The influence of sleeper material characteristics on railway track behaviour: concrete vs composite sleeper. Transportation Geotechnics, 23, 100348. https://doi.org/10.1016/j.trgeo.2020.100348

Hu, P.; Wang, H.; Tian, G.; Liu, Y.; Li, X.; Spencer, B. (2020) Multifunctional flexible sensor array-based damage monitoring for switch rail using passive and active sensing. Smart Materials and Structures, 29, 095013. https://doi.org/10.1088/1361-665X/ab9e0f

ISO – International Standardization Organisation (2014) ISO 55000:2014. Asset management – overview, principles and terminology. https://www.iso.org/obp/ui/#iso:std:iso:55000:ed-1:v2:en (last access, 23 August, 2021)

Jing, G.; Siahkouhi, M.; Qian, K.; Wang, S. (2021) Development of a field condition monitoring system in high speed railway turnout. Measurement, 169, 108358. https://doi.org/10.1016/j.measurement.2020.108358

Khairallah, D.; Blanc, J.; Cottineau, L.M.; Hornych, P.; Piau, J.; Pouget, S.; Hosseingholian, M.; Ducreau, A., Savin, F. (2019) Monitoring of railway structures of the high speed line BPL with bituminous and granular sublayers. Construction and Building Materials, 211, pp. 337-348. https://doi.org/10.1016/j.conbuildmat.2019.03.084

Lei, Y.; Li, R.; Chen, R. et al. (2021) A high-precision two-dimensional micro-accelerometer for low-frequency and micro-vibrations. Precision Engineering, 67, pp. 419-427. https://doi.org/10.1016/j.precisioneng.2020.10.011

Macedo, R.; Benmansour, R.; Artiba, A.; Mladenovic, N.; Urosevic, D. (2017) Scheduling preventive railway maintenance activities with resource constraints. Electron Notes Discrete Mathematics, 58, pp. 215-222. https://doi.org/10.1016/j.endm.2017.03.028

Milne, D.; Masoudi, A.; Ferro, E.; Watson, G.; Le Pen, L. (2020) An analysis of railway track behaviour based on distributed optical fibre acoustic sensing. Mechanical Systems and Signal Processing, 142, 106769. https://doi.org/10.1016/j.ymssp.2020.106769

Odolinski, K. and Boysen, H.E. (2019) Railway line capacity utilization and its impact on maintenance costs. Journal of Rail Transport Planning and Management, 9, pp. 22-33. https://doi.org/10.1016/j.jrtpm.2018.12.001

Peng, F.; Kang, S.; Li, X.; Ouyang, Y. (2011) A heuristic approach to the railroad track maintenance scheduling problem. Computer-Aided Civil and Infrastructure Engineering, 26 (12), pp. 129-145. https://doi.org/10.1111/j.1467-8667.2010.00670.x

Sasidharan, M.; Burrow, M.P.N.; Ghataora, G.S. (2020) A whole life cycle approach under undertainty for economically justifiable ballasted railway track maintenance. Research in Transportation Economics, 80, 100815. https://doi.org/10.1016/j.retrec.2020.100815

Sol-Sánchez, M.; Moreno-Navarro, F.; Rubio-Gámez, M.C. (2014) The use of deconstructed rite rail pads in railroad tracks: impact of pad thickness. Materials & Design, 58, pp. 198-203. https://doi.org/10.1016/j.matdes.2014.01.062

Sol-Sánchez, M.; Pirozzolo, L.; Moreno-Navarro, F.; Rubio-Gámez, M.C. (2016) A study into the mechanical performance of different configurations for the railway track section: a laboratory approach. Engineering Structures, 119, pp. 13-23. https://doi.org/10.1016/j.engstruct.2016.04.008

Sol-Sánchez, M.; Moreno-Navarro, F.; Martínez-Montes, G.; Rubio-Gámez, M.C. (2017) An alternative sustainable railway maintenance technique based on the use of rubber particles. Journal of Cleaner Production, 142, pp. 3850-3858. https://doi.org/10.1016/j.jclepro.2016.10.077

Song, S.; Hou, Y.; Guo, M.; Wang, L. (2017) An investigation on the aggregate-shape embedded piezoelectric sensor for civil infrastructure health monitoring. Construction and Building Materials, 131, pp. 57-65. https://doi.org/10.1016/j.conbuildmat.2016.11.050

Stark, T. and Wilk, S. (2015) Root case of differential movement at bridge transition zones. Proceedings of the Institution of Mechanical Engineers Part F, Journal of Rail and Rapid Transit, 230(4). https://doi.org/10.1177/0954409715589620

Sussman, T (2017) Field conditions observed at a site with concrete tie base abrasion. Railway Engineering, Conference at Edinburg, 2017. https://doi.org/10.25084/raileng.2017.0113

Tan, C.; Shee, Y.; Yap, B.K.; Adikan, F.M. (2016) Fiber Bragg grating based sensing system: early corrosion detection for structural health monitoring. Sensors Actuators A: Physical, 246, pp. 123-128. https://doi.org/10.1016/j.sna.2016.04.028

Tian, B.; Liu, H.; Yang, N. et al. (2016) Design of a piezoelectric accelerometer with high sensitivity and low transverse effect. Sensors, 16 (10), 1587. https://doi.org/10.3390/s16101587

Wang, H. and Markine, V. (2019) Dynamic behaviour of the track in transitions zones considering the differential settlement. Journal of Sound Vibrations, 459, 114863. https://doi.org/10.1016/j.jsv.2019.114863

Wilk, S.; Stark, T.; Rose, J. (2015) Evaluating tie support at railway bridge transitions. Proceedings of the Institution of Mechanical Engineers Part F, Journal of Rail and Rapid Transit, 230 (4). https://doi.org/10.1177/0954409715596192

Zhang, S.L.; Koh, C.G.; Kuang, K.S.C. (2019) Proposed rail pad sensor for wheel-rail contact force monitoring. Smart Materials and Structures, 27, 115041. https://doi.org/10.1088/1361-665X/aadc8d

Zhao, A.; Tian, G.Y.; and Zhang, J. (2018) IQ signal based RFID sensors for defect detection and characterization. Sensors Actuators A: Physical, 269, pp. 14-21. https://doi.org/10.1016/j.sna.2017.11.008

Zoeteman, A. and Esveld, C. (2004) State of the art in railway maintenance management: planning systems and their application in Europe. IEEE International Conference on Systems, Man and Cybernetics, 5, pp. 4165-4170. https://doi.org/10.1109/ICSMC.2004.1401184

Sol-Sánchez, M.; Castillo-Mingorance, J.M.; Moreno-Navarro, F.; Mattinzioli, T.; Rubio-Gámez, M.C. ***Piezolectric-sensored sustainable pads for smart railway traffic and track state monitoring: Full-scale laboratory test. Constr. Build. Mater.*** **301 (2021) 124324. (Índice de Impacto 7,4 en 2.023, Q1 en CIVIL ENGENIERING, MATERIALS SCIENCE (MULTIDISCIPLINARY), y CONSTRUCTION & BUILDING TECHNOLOGY en 2.023).**

https://doi.org/10.1016/j.conbuildmat.2021.124324

Piezoelectric-sensored sustainable pads for smart railway traffic and track state monitoring: full-scale laboratory tests

Sol-Sánchez, M.*[,1]; Castillo-Mingorance, J.M.[1]; Moreno-Navarro, F.[1]; Mattinzioli, T.[1]; Rubio-Gámez, M.C.[1]

msol@ugr.es (M. Sol-Sánchez); jumacami@ugr.es (J.M. Castillo-Mingorance); fmoreno@ugr.es (F. Moreno-Navarro); tmattinzioli@ugr.es (T. Mattinzioli); mcrubio@ugr.es (M.C. Rubio-Gámez)
[1]Laboratory of Construction Engineering at the University of Granada. C/ Severo Ochoa s/n, 18071, Granada, Spain.
*Corresponding author (msol@ugr.es)

Abstract

The present paper focuses on an initial assessment into the applicability of sensored sustainable pads, made from recycled polymers and embedded with commonly-accessible piezoelectrics. These sensing devices were used as smart rail pads and inside bituminous sub-ballast to monitor traffic and track state by measuring the stress variations in the components. A series of full-scale laboratory tests were carried out simulating train passage under diverse traffic scenarios and varying track section conditions in a testing box. Results indicated that the smart sustainable pads in both components showed the capacity to detect traffic load variations by measuring relative changes in signal amplitude of the sensor. Nonetheless, the smart rail pads presented higher accuracy to monitor axle loads, while the signals from the sub-ballast were influenced by the position of the sensor, and so a higher potential to monitor track performance, rail-sleeper load distribution, and detecting phenomena like hanging sleepers.

Keywords: railway; smart materials; infrastructure monitoring; sensors; piezoelectrics.

1. Introduction

Railways play a vital role in modern transportation and social economy, providing efficient mobility for passengers and freight, which has led to the development of various political targets (such as the EU Mobility Strategy) [1]. Nonetheless, as a result of the required rail traffic increase, coupled with the continuous development of high-speed trains and the aim to increase the railway transportation of cargo, there is a need for the development of novel solutions to ensure the safety and real-time monitoring of track state and traffic level to better manage and conserve infrastructure services [2, 3].

The track circuit invented by William Robinson in 1872 [11] can be considered as the first railway monitoring approach to prevent accidents. Since then, a variety of sensing techniques and devices have been developed for both vehicles and track sections with the aim of monitoring traffic and infrastructure conditions, including widely used sensors like accelerometers, strain gauges, digital image correlation, geophones, magnetic sensors and deflectometers, among others [12]. Nonetheless, most of these conventional sensors are not practical for long-term railway monitoring because of either complex configuration, lack of accuracy and stability under specific conditions or their high cost, among others. However, the degradation of railway tracks is a progressive process, and therefore, long-term railway monitoring is required through the use of a sensor network.

For this purpose, sensors with electrical properties like Force Sensing Resistors (FSR) or piezoelectric sheets have been demonstrated to be appropriate for monitoring transportation infrastructures. These work by measuring the voltage changes due to variations in the stress levels to which they are subjected. In this sense, various successful previous experiences have proven their capacity to monitor structural performance [13] or road pavement deflection [14] or damage [15] by developing specific sensors from piezoelectric devices [16, 17]. Furthermore, in the railway field, literature also collects some examples of these devices in elastic elements, aggregates or sub-ballast, showing their feasibility and potential for monitoring parameters like wheel-rail contact [6, 7, 18].

Therefore, in light of the promising potential of embedding sensors into railway components for monitoring [3, 7, 12, 19], the present paper aims to contribute to their study and development. Particularly, this work focuses on the assessment of the ability of pads made from recycled polymers to be equipped with conventional and low-cost commercial piezoelectric devices to monitor both traffic and track conditions/states. Specifically, this study focused on the use of these innovative pads as (a) a replacement of standard rails pads to provide an elastic track component with sustainable and smart characteristics and (b) a sensoring device where the pads work as protective capsules for the piezoelectrics in the bituminous sub-ballast. Thus, this paper aims to contribute to the development of integrated smart solutions for track components; combining both structural and sensoring properties.

This paper analyses the calibration factors and measurements of the sensors under different scenarios according to their application in both rail pads and bituminous sub-ballast. Specifically, the paper assesses and compares, through full-scale tests in a laboratory box, the ability of each of these solutions to monitor traffic conditions

through measuring train weight and wheel-rail contact, as well as the state of the superstructure through measuring the stress on sleepers (assessing the strength of their support). In particular, the paper focused on monitoring parameters like number of loads applied, detection of flat or irregular train wheels, or train weight (particularly in rail freight lines), and the evolution of section degradation by measuring phenomenon like hanging sleepers due to differential settlements (particularly appropriate for transition zones), or distribution of loads along the track. This would enable the continuous monitoring of track and traffic state, making it possible to predict future track failures and maintenance needs.

2. Methodology

2.1 Materials

This study focuses on the assessment of common piezoelectric devices (typically used in different industries at a low cost) embedded as sensors into pads made from recycled polymers, to be used as smart rail pads and as sensor devices for smart bituminous sub-ballast. Figure 1 displays the design of each type of smart and recycled pad considered in this study, showing also their applications as rail pads and when embedded into bituminous sub-ballast.

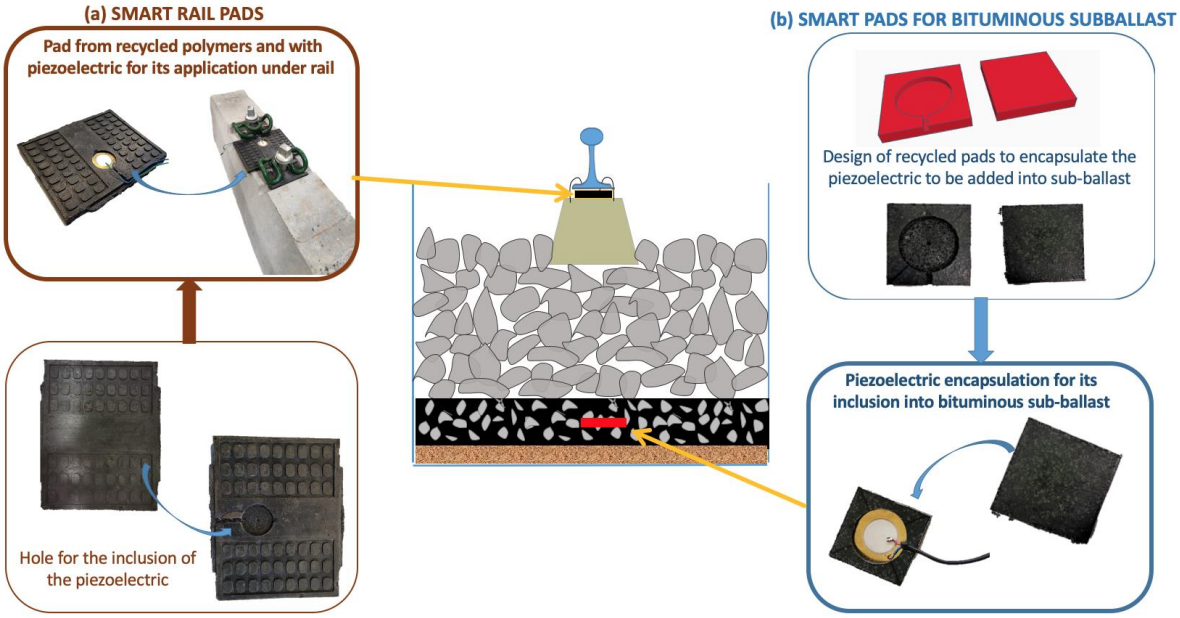

Figure 1. Design of the smart rail pads and the pads with sensor to be included in bituminous sub-ballast.

2.1.1 Piezoelectrics

With the aim of using economic and readily-available sensors, commercial piezoelectrics commonly used in diverse applications (industry, music, sensoring, etc.) were selected for this study. The sensors used were composed of a metallic circular base with a diameter of 35 mm and a quartz sheet with 24 mm diameter. The total thickness of these devices was around 0.35 mm, which makes them appropriate to be embedded in different track elements, as done for example in this study with rail pads and bituminous sub-ballast. To measure the electrical changes due to variations in infrastructure/traffic characteristics, they were connected to a data logger with the capacity to directly measure the voltage generated by the piezoelectrics.

2.1.2 Smart and sustainable rail pad

The rail pads were manufactured from a volumetric combination of 50% of recycled HDPE (High Density Polyethylene from recycled industrial plastic boxes) and 50% of recycled rubber particles from waste tires, with size ranging 2-4 mm, resulting in medium-stiff pads with a static stiffness around 250 kN/mm, according to EN 13146-9 [20]. The rail pads had a size of 140 mm x 180 mm with a thickness of 7 mm, being appropriate to be used in standard concrete sleepers commonly used in Spanish railway lines. The manufacturing process consisted of melting the recycled HDPE (with a 5 mm particle size) at 180°C and mixing it with crumb rubber (size 2-4mm), followed by pouring the materials into a mould. Once the material was in the mould, a load of 15 kN was applied in order to compact the material and obtain a high-quality finish without imperfections in the pads.

One piezoelectric device was included in a hole drilled in the recycled rail pad (Figure 1a), with the purpose of avoiding damage to the electrical devices from direct contact with the rail or the sleeper, which could crush the quartz sheet of the sensor. The hole had a diameter of 35 mm and depth of 3.5 mm, which was considered appropriate to embed the devices.

2.1.3 Smart pads into bituminous sub-ballast

For the case of the smart bituminous sub-ballast, the piezoelectric sensor was encapsulated by two polymeric pads made from recycled HDPE combined with 50% of waste crumb rubber (2-4 mm), following the same manufacturing process to that described for the rail pads. This was required since the piezoelectrics were embedded into the bituminous sub-ballast during the compaction of the asphalt at around 160°C; which at such temperatures could damage the sensors. The encapsulation system consisted of: (a) a bottom pad with dimensions of 50 mm x 50 mm x 7 mm, with a hole (35 mm diameter and 3.5 mm thick) drilled in the centre to fit a piezoelectric; (b) and a upper pad with same dimensions but without the hole, which was glued to the bottom pad to obtain the protective capsule for the sensor. Figure 1b shows the visual appearance of the encapsulation system for the piezoelectric.

The bituminous sub-ballast consisted of a dense asphalt mixture type AC22S (EN 13108-1) [21], manufactured from limestone aggregates (with fractions of 18/25mm, 12/18mm, 6/12mm, and 0/6mm), with appropriate characteristics for this application according to the requirements for this type of mixture. The filler (with dosage around 5% aggregate weight) was cement type CEM II/B-L 32.5 N and the bitumen was a conventional B 50/70, using a bitumen content of 4.25% per total weight of the mixture. The design characteristics of the asphalt mixture are shown in Table 1.

Table 1. Properties of the asphalt mixture used as sub-ballast.

Properties	**Standard**	**Bituminous sub-ballast**
Bulk Density (Mg/m^3)	EN 12697-6	2.52
Air Voids (%)	EN 12697-8	3.4
Marshall Stability (kN)	EN 12697-34	10.5
Marshall Flow (mm)	EN 12697-34	3.2
Index of retained tensile strength after water action (%)	EN 12697-12	86.0
Stiffness at 20°C (MPa)	EN 12697-26	5,079

2.2 Testing plan and methods

With the aim of assessing the viability of the piezoelectric-sensored sustainable pads to be used as smart components in railway tracks (rail pads and bituminous sub-ballast) for monitoring traffic and infrastructure conditions, the testing plan consisted of three key study steps: (a) assessment of the piezoelectric signals in the components, evaluating the different possible scenarios for each solution in order to calibrate the sensors for this application; (b) analysis of the ability of the smart components to monitor traffic conditions (mainly, load level/train weight, and detection of impacts due to irregular wheel-rail contact); (c) study of the ability to monitor the track performance by measuring the variations in load distribution in the superstructure. Table 2 summarises the testing plan carried out, showing the three study steps, the main variables analysed and the smart material employed, as well as the laboratory tests used in the assessment.

Table 2. Testing plan.

Study step	Solution	Variable	Test
Study of piezoelectrics in the track component	Piezoelectric in the recycled rail pad	Influence of support strength	Diverse sinusoidal load levels
	Sensored pad in the bituminous subballast	Influence of load distance	Loads at different distances from sensor
		Effect of sensor depth into subballast layer	Sensors at different depth from surface
Ability of sensored components to measure traffic loads	Piezoelectric in: -Recycled rail pad -Recycled pad in Subballast	Train weight Irregular contact rail-wheel	Simulation of diverse sequence of train loads
Ability of sensored components to control superstructure performance	Piezoelectric in the recycled rail pad	Stress distribution on sleepers	Simulation of traffic loads over a system of 3 sleepers: -all supported sleepers -central hanging sleeper
		Supported sleeper Vs hanging sleeper	

2.2.1 Study of piezoelectrics in track components

The first step focused on the measurement of the signal recorded by sensored sustainable pad when reproducing different scenarios that could take place during their application as smart rail pads and as sensor into bituminous sub-ballast. The aim of this stage was to assess the aptitude of each solution to measure different load levels, assessing also the influence of different factors that could modify the signal recorded by the sensor.

In the case of the smart rail pad, the effect of the strength of the support under the sleeper was assessed, since this factor is expected to modify the stress on the pad depending on the deformability of such support. For this purpose, a laboratory test was carried out applying different load states on the system composed of a rail (type UIC-54, 25 cm long), the smart rail pad, and a prestressed concrete sleeper (type AI-VE commonly used in Spanish railway lines, 85 cm long), while using three different supports under such a system, reproducing different conditions for the substructure. Specifically, the three following support types were used: a very stiff metallic support; a

medium-stiff rubber mat with dynamic bending modulus of 0.24 N/mm^3 (DIN 45673-5); and a soft rubber mat with a bending modulus of 0.15 N/mm^3 (DIN 45673-5) [22].

The test consisted of applying a series of load sequences under displacement control mode, with the aim of reproducing different load levels on the pad to be identified by the sensor. As seen in Figure 2, the displacement values were fixed at 0.1 mm, 0.5 mm, 0.9 mm, 1.3 mm, 1.7 mm and 2.1 mm (which are values expected in railway tracks) [4, 23, 24]; different force levels are required depending on the type of support simulated, which also generates different stress states to be monitored by the smart pad. The dynamic loads were applied directly on the head of the rail (which transmits the stress to the rail pad and the sleeper) at a frequency of 5 Hz.

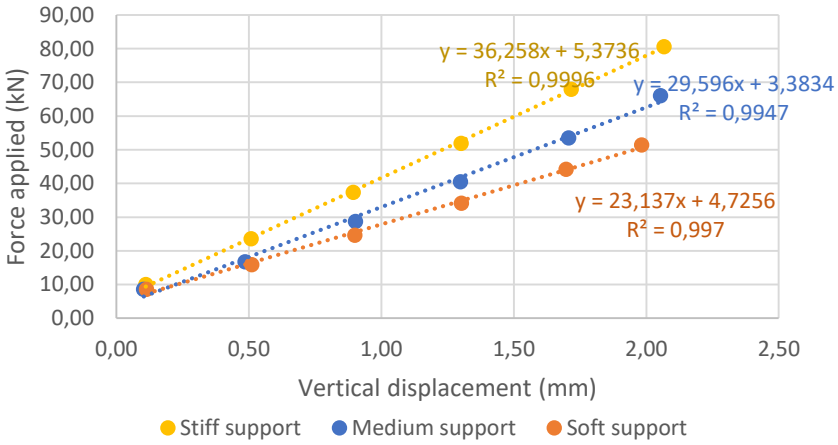

Figure 2. Force values applied on rail to obtain similar deformations with different supports for the sleeper.

Regarding the application of the piezoelectric-sensored and sustainable pads in the sub-ballast, the signal recorded by the sensors was measured depending on two main factors that could influence their functionality: depth of the sensor in the bituminous layer, and distance between the application of the load and the sensor. It is important to note that, in this application, the devices will receive the load from the ballast layer, thus, the load point could vary and not always be on the sensor placement line.

To test the encapsulated sensors, four square specimens (300 mm in length and 120 mm thick) of bituminous sub-ballast were manufactured in the laboratory, including in each specimen two sensors (piezoelectric encapsulated in the aforementioned polymeric pads) at different depths, as seen in Figure 3a. Two specimens of each case were manufactured, assessing twice the values of 2 cm, 4 cm, 8 cm and 10 cm of sensor depth from the surface.

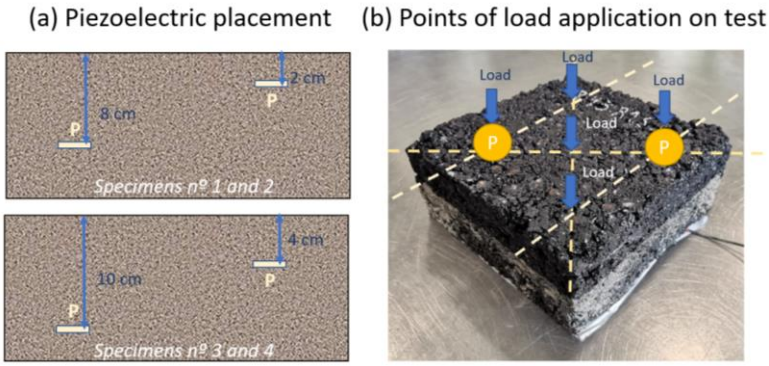

Figure 3. Specimens of smart bituminous sub-ballast: (a) placement of piezoelectric-sensored pads at different depths; (b) scheme of the application of loads at diverse distances from the sensors.

In order to evaluate the influence of the depth and the distance of the sensor from the loads on the specimen surface (simulating the loads transmitted by the ballast layer to the sub-ballast), a series of tests were carried out applying series of 100 load cycles at 5 Hz with amplitudes of 1 kN, 2 kN, 3 kN, 4 kN, 5 kN and 6 kN through an actuator with a flat square section (100 mm x 100 mm), which correspond to stress levels of 100 kPa, 200 kPa, 300 kPa, 400 kPa, 500 kPa and 600 kPa, respectively. This is in accordance with maximum values expected for the sub-ballast layer (according to other researchers) [25], while also assessing a wide range of stress values, to obtain a trend. As seen in Figure 3b, the load application was carried out on different points of the specimen's surface, evaluating the influence of distance from load centre to the sensor, at 0 cm (load applied directly on the vertical line of the placement of the sensor), 10, 15 and 20 cm.

2.2.2 Application of smart components to monitor different traffic conditions

For this study step, a series of tests were carried out on a full-scale railway section, reproduced in a laboratory testing box that allowed for the inclusion of the smart components with the sensors while simulating trains passing.

The testing box was 2 m long, 1 m wide and 60 cm high, and the track section was reproduced through: (i) a granular layer of 8 cm simulating the track subgrade, with elastic modulus higher than 80 MPa (which is in accordance with real tracks), according to the plate bearing test (EN 103807) [26]; (ii) a layer of 12 cm of bituminous sub-ballast (including the piezoelectric at a depth of 4 cm from the layer surface, placed on the area under the sleeper); (iii) a ballast layer of 30 cm composed of ophitic aggregates with appropriate properties for this application according to EN 13450 [27]; (iv) a section of concrete sleeper (85 cm of length) commonly used in Spanish railway lines; (v) a fastening system, of type VM, commonly used for concrete sleepers, including the rail pad with the sensor; (vi) a rail section type UIC 54, 25 cm long.

With the aim of evaluating the ability of the smart components to monitor traffic conditions, loads were applied on the head of the rail at a sequence simulating the passage of a standard train; in this instance, a standard train circulating on the Spanish railway network. Figure 4 represents a diagram of load per axle of such a train (Figure 4a), and the values of loads applied by the testing machine (Figure 4b), reproducing the passage of a train at a speed close to 100 km/h. The train speed was fixed to this value

in this study to obtain a clear understanding of the influence of variable load application from the testing machine in the laboratory according to the various train load levels defined in this paper, to prove the ability to detect changes in train-track contact. Also, it is important to note that the load applied corresponded to 25% of that applied by a train bogie (as seen in Figure 6, of a diagram of train loads) because of the consideration of load per wheel (50% of the load per axle) and the concentration of stress on a central sleeper, where it was considered that the load on the sleeper under the wheel is close to 50% of the total, which is in agreement with [20, 28, 29].

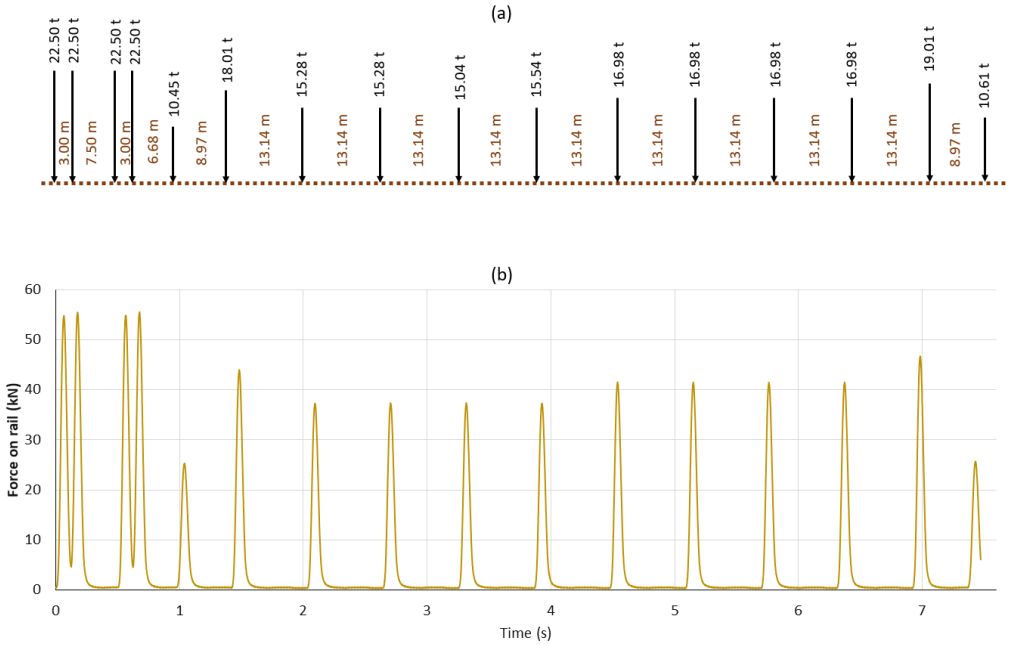

Figure 4. Diagram of axle loads of the simulated train: (a) distribution of load per axle; (b) simulation of load per wheel on the test.

With this sequence of loads, under the aim of assessing the ability of the smart components to identify diverse conditions of train loads, two main factors were studied:

- Ability to monitor the weight of train freight. For this, eight trains with different load levels were simulated. Figure 5 represents the load value for the different wheels (a total of 16) for each train, varying from 50% (train number 1) to 130% (train number 8) of the original train represented in Figure 4. The loads of all the wheels were modified since the main objective of this step was to evaluate the ability and accuracy of each solution to detect a wide range of load variations.

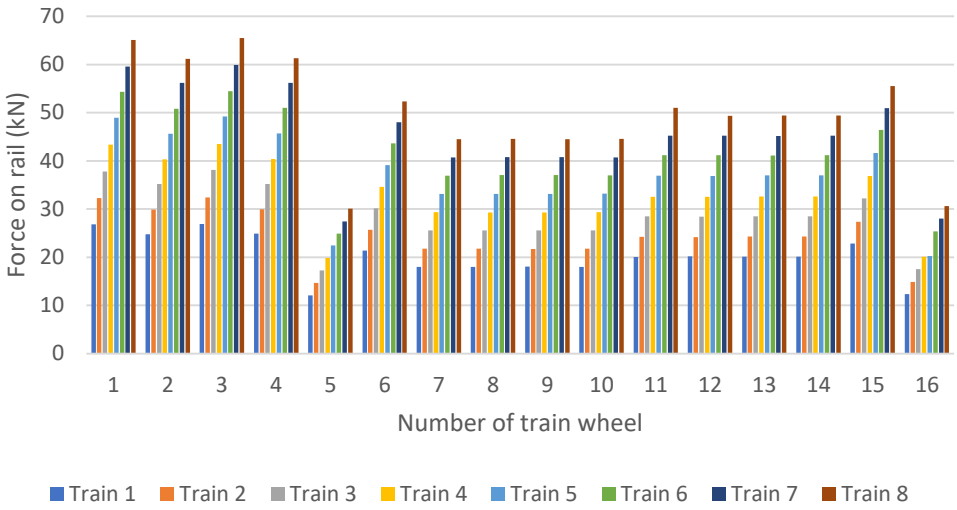

Figure 5. Load per wheel of diverse simulated trains with different levels of load on rail.

- Ability to monitor the presence of irregularities in the wheel-rail contact, which generally leads to a considerable increase in the load transmitted to the track. This was simulated by reproducing the loads of the train number 1 (Figure 4), but increasing the load level in the wheels number 7 and 10 (as examples of simulation of the presence of flats in such wheels), close to 3 times the original load under regular contact. Figure 6 displays the level of load applied on the two comparative cases (simulation of regular and irregular contact), aiming to analyse the accuracy of the smart components to detect such traffic conditions.

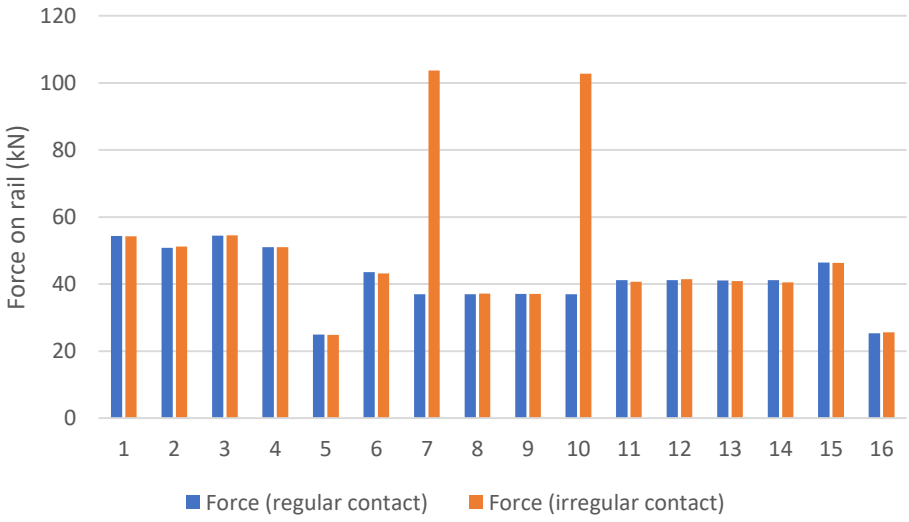

Figure 6. Simulation of regular and irregular wheel-rail contact (example of impacts on axles 7 and 10)

2.2.3 Ability of sensors to identify changes in track performance

This step focused on studying the ability of the sensor to measure changes in track performance through the variations in the level of stress on the smart rail pad. For this step, the rail pad was used as a monitoring device since the present assessments focused on the determination of load distribution on the central and adjacent sleepers, as well

as the simulation of hanging sleepers due to differential settlements on the central sleeper.

For this purpose, the testing box described in the previous step was employed, but in this case, three sleepers were used (equipped with smart rail pads) and all connected to a rail section with a length of 1.75 m, and a spacing of 0.6 m between sleepers, as commonly used in railway tracks. Figure 7 displays the visual appearance of the configuration of the testing box for this study step, where Figure 7a shows the smart rail pads before the placement of the rail over the three-sleeper system, and Figure 7b after.

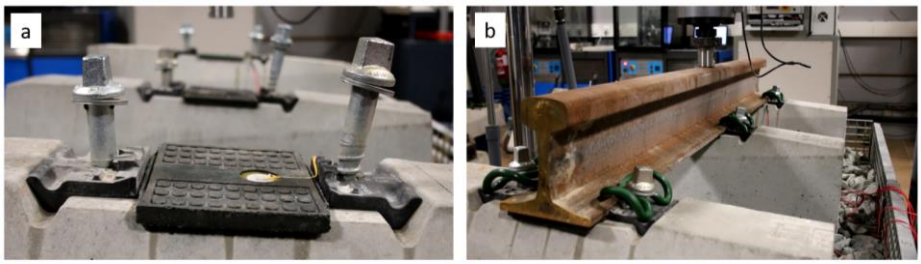

Figure 7. Three-sleeper test to monitor track performance: (a) smart rail pads on sleepers; (b) test configuration.

To evaluate the ability of the smart pads to monitor the load distribution on the sleepers (which could be appropriate to evaluate changes in stiffness, differential settlement, calibration of sensor settlement models to predict track failure, etc.), a series of trains were simulated (1, 2, 3, 4 and 5, from Figure 5) to obtain a range of loads to be detected by the sensors of each sleeper (where the load was applied to the central one).

Additionally, to assess the influence of differential sleeper settlement, a gap of various millimetres under the central sleeper was created, with the aim of obtaining higher oscillations in this element; thus, reducing the level of stress on the smart pad due to a weaker support, and therefore, assessing the ability of the rail pads to be used as sensors to detect such changes due to this track failure type. For this, as previously seen, the passage of trains 1, 2, 3, 4 and 5 were simulated over this setup, and the results were compared to those obtained in a section with a good support for all the sleepers (previous paragraph).

3. Analysis of results

3.1 Study of piezoelectric signal in track components

Figure 8 represents the values of the signals measured by the piezoelectric-sensored and sustainable pads employed as smart rail pads, when different forces were applied on the rail-sleeper system over different supports, qualified as stiff, medium and soft. Results demonstrate that these devices are able to identify the variations in force applied on the rail, obtaining a good linear correlation. This is in agreement with previous studies [6] using piezoelectric sheets in special panels to monitor wheel-rail contact, and therefore, proving that this solution, with common piezoelectrics, embedded into recycled rail pads, is also able to correctly monitor load variations.

Nonetheless, results show that the test configuration led to a slight variation in the signal recorded, obtaining lower values when using a softer support. This could be

related to the damping capacity of the rubber mat used to simulate the track sub-structure. Therefore, according to these laboratory results, the smart rail pads could be required to be calibrated according to field conditions since the boundary conditions could influence them.

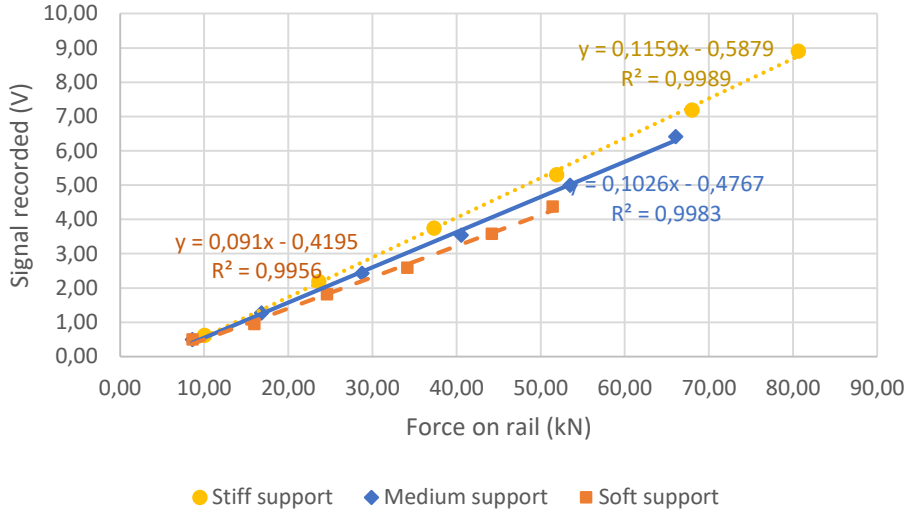

Figure 8. Signal recorded by the smart rail pad under diverse level of loads applied on the system over different supports.

Regarding the use of the sensors on bituminous sub-ballast, Figure 9 displays the influence of the depth of the sensors from the surface of the layer under different levels of stress on the sub-ballast. Results clearly show that the design of the layer plays an essential role, obtaining lower values and a lower capacity (in absolute terms) to distinguish load levels with an increasing depth of the encapsulated sensor. In this sense, for the stress level expected on the sub-ballast layer (around 100-200 kPa according to field studies) [25], low signal values could be expected, particularly when increasing the depth of the sensor. Therefore, for this application, more superficial sensors could be appropriate in order to provide clearer absolute changes in signal responses due to load variations; for example, as a consequence of irregular wheel-rail contact.

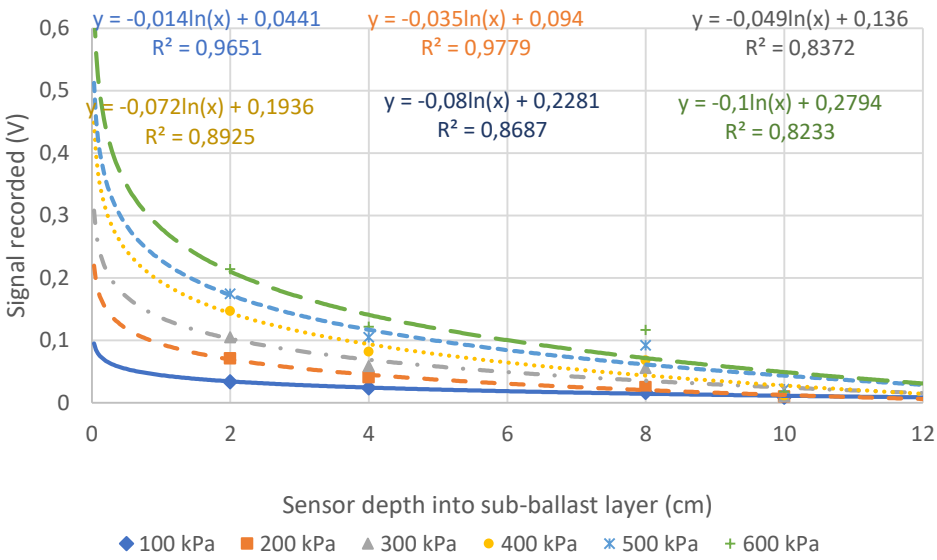

Figure 9. Influence of sensor depth into sub-ballast layer on the recorded signal.

Also, Figure 10 evaluates the influence of the distance from the load application to the sensor, showing as an example the cases for 200 kPa loading as a reference magnitude expected in railways for this smart material. Results state that this parameter also has a strong influence on the signal recorded, obtaining a remarkable decrease in values when increasing the distance of the applied load to the sensor's position. This fact was particularly noted for the case of the sensor at a depth of 2 cm, where at distances around 5 cm the decrease in signal was close to 70%, while more than 20 cm were needed to obtain such reduction when the sensor was at 10 cm of depth. Therefore, the more superficial the sensor, the higher the signals recorded, but also more susceptible to the variation of the distance from load application to sensor position.

This is clearly related to the load distribution through the specimen thickness, and therefore, the placement of the sensor at a depth of 2 cm could be recording only the loads when applied practically on the vertical line of the sensor, while depths higher than 4 cm are shown to be less susceptible to load distance. For this reason, together with the consideration that the greater the depth of sensor, the lower the signal recorded, for the next study steps, the sensors were placed at a depth of 4 cm in the sub-ballast layer constructed in the testing box.

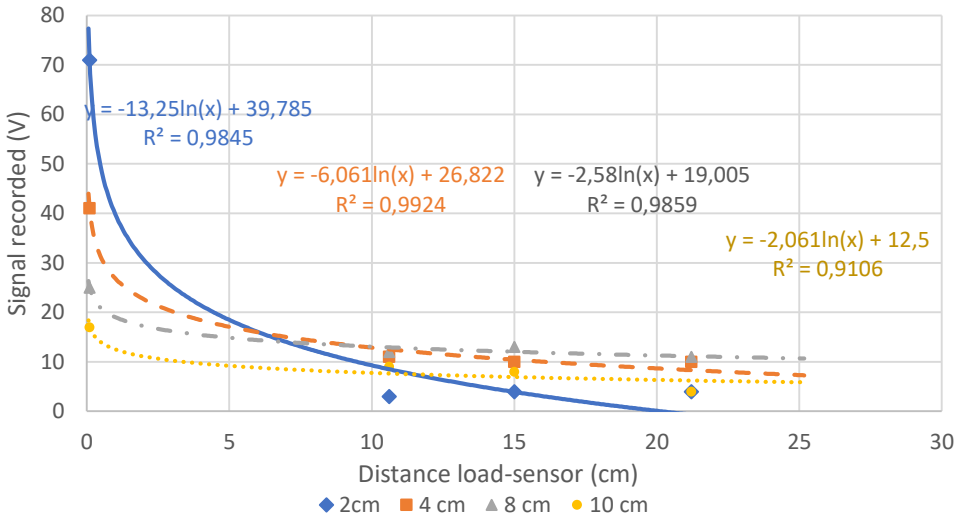

Figure 10. Effect of distance between load application point and sensor placement.

3.2 Analysis of the ability of sensored components to control traffic loads

Firstly, Figure 11 displays the signals measured by each smart component (rail pads in Figure 11a, and bituminous sub-ballast in Figure 11b) when simulating the diverse train axles represented in Figure 4. Both solutions are able to record the diverse train axles, thus identifying the changes in load level and showing the sequence of pulses according to those applied from the testing machine. Both cases recorded the signals as electrical pulses, where not only the maximum value changes were measured, but also the minimum ones, and thus, the appropriate evaluation of the loads through the measurement of signal amplitudes. This agrees with previous studies [6, 7] showing the potential of rail pads and bituminous sub-ballast to include sensors to monitor passing trains, where in this study this was validated using alternative devices (i.e., common piezoelectrics) to obtain smart components with embedded sensors.

Comparing the signals from each component, it is clear that the inclusion of piezoelectrics in rail pads led to higher signal values, since higher stress and oscillation levels are expected in this material. In fact, the signals in the rail pad proved to be generally 20 times higher than those in the sub-ballast. This means that this type of smart component could be more appropriate for identifying the train loads, obtaining also a better sequence of loads when referring to those of Figure 4. Nonetheless, it is important to note that the smart bituminous sub-ballast also proved to be effective to measure train loads, but with lower output signal values.

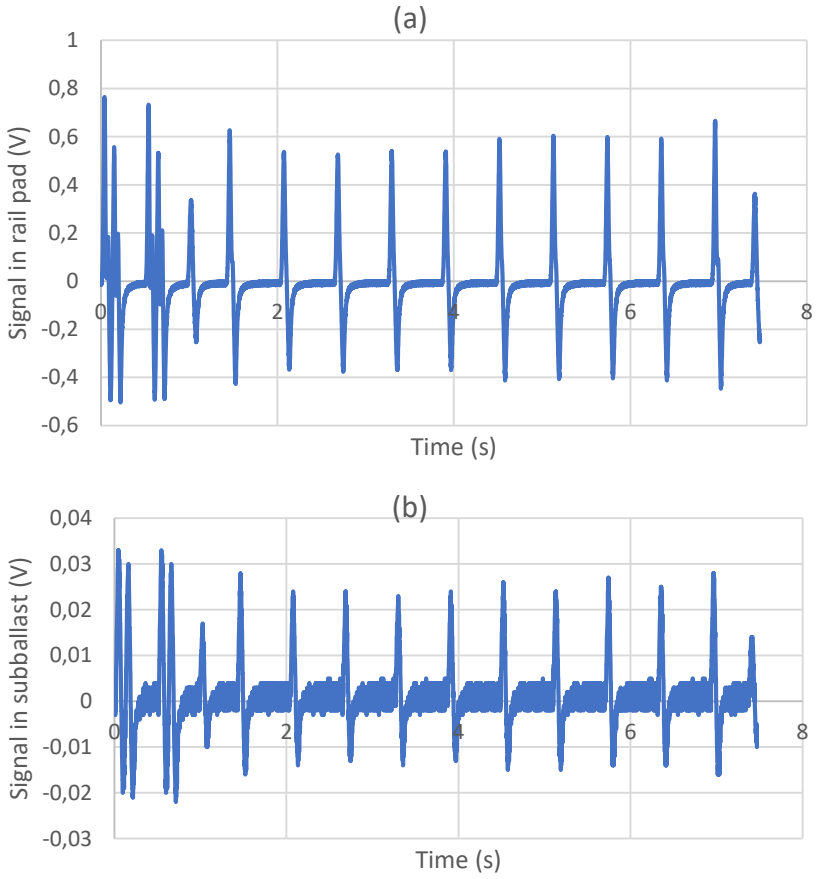

Figure 11. Diagram of recorded signals by the (a) smart rail pad, and (b) smart bituminous sub-ballast; under train load simulation.

This finding is in accordance with the results displayed in Figure 12, where the signals recorded from the simulation of each axle for the different trains with diverse range of loads is represented, where Figure 12a shows rail pad signals and Figure 12b those for bituminous sub-ballast. These results confirm that the smart rail pad measured higher values than the bituminous sub-ballast encapsulated piezoelectrics, showing also a clearer distinction between trains, since a gradual variation in signals was obtained from the gradual change in loads from the different train simulations.

This could be appropriate for the identification of the characteristics of train wheel loads, permitting the real-time measurement of bogie loads and weights, which could be particularly appropriate in freight railway lines, for example. Nonetheless, it is important to note that the signal values measured for the different force levels (ranging from around 10 kN in axle number 5 of train 1, to 65 kN in axle 1 of train 8) are lower than those expected from the results in Figure 8, which confirms the effect of the boundary conditions on the piezoelectric signals, and therefore, the need for their calibration when absolute values are required. Nevertheless, most of the desired applications could be carried out through relative values like the increase in signal due to the passing of heavier trains, the signal variation due to the weakening of the support, etc.

In the case of the smart sub-ballast, lower variations in signals regarding the diverse trains were found, particularly from those with lower load level. This is in accordance

with previous results in Figure 9, where it was seen that the sensitivity of this smart component was reduced with decreasing stress levels. Nonetheless, this solution also allowed for the identification of the characteristics of train load, particularly for the heavier bogies.

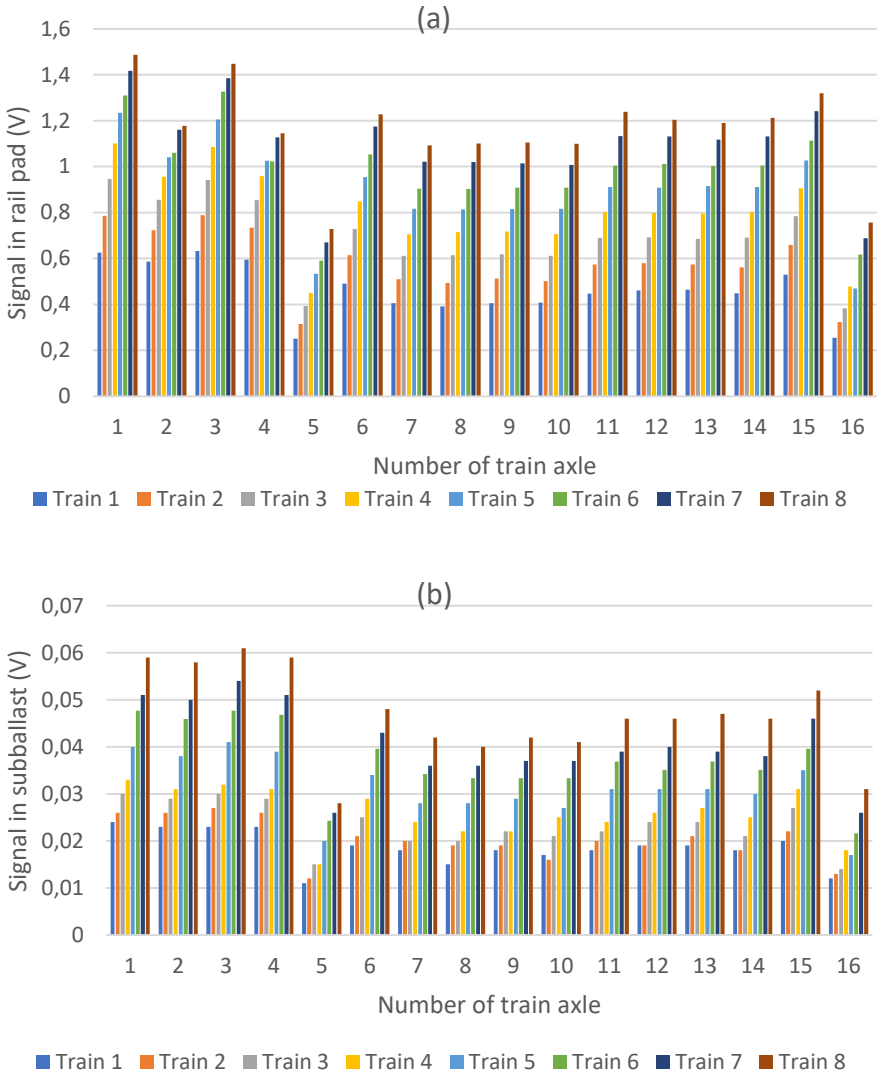

Figure 12. Results of monitoring variations on train load level by using (a) smart rail pad; (b) smart bituminous sub-ballast.

In fact, Figure 13 shows a good correlation between the train load and signal measured by the sensors, demonstrating that these smart components could be appropriate for the identification of load level from their electrical signal, which could facilitate the continuous traffic monitoring with diverse purposes (axle counting, train weight, load recording for predictive models, etc.). In addition, for a deeper study of the sensitivity of these sensors, Figure 14 represents the variations (in %) of the applied loads relative to the original train simulations (Figure 4) versus the signal changes collected by the sensors.

Results confirm the good accuracy of the smart rail pad, as seen from the good linear correlation and similar values of percentage change from the loads (seen from the

superposition of the signal line to that from theoretical changes). Regarding the case of the sub-ballast, a good correlation for load variations was also recorded, but the values at low stress levels (negative values of percentage force change) were lower than those expected from the theoretical line, due to the cited reduction in accuracy of the smart sub-ballast technology for low train loads. This could limit the application of this solution when accurate load detection values are required, although further field studies would be required for this solution under different boundary conditions.

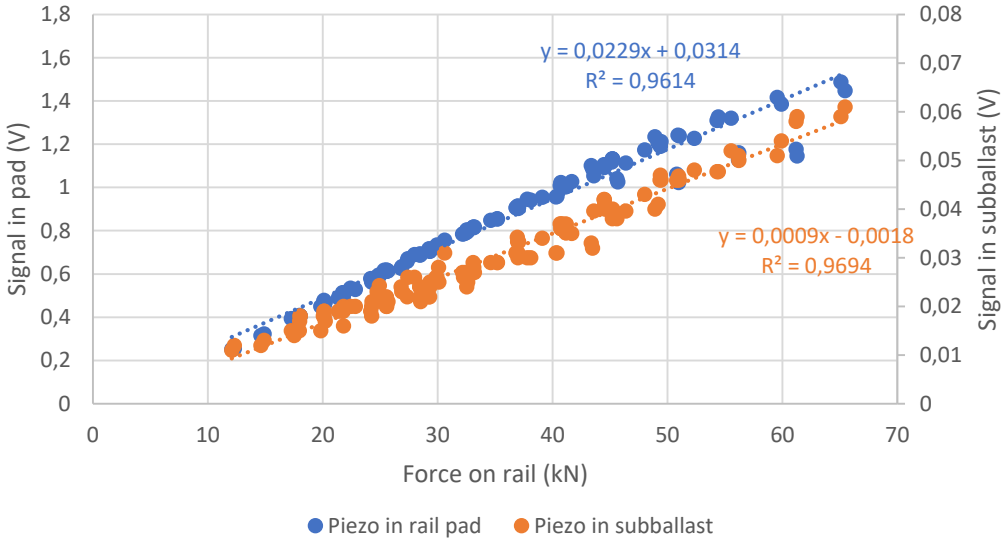

Figure 13. Correlation between train load on rail and signals recorded by the smart components.

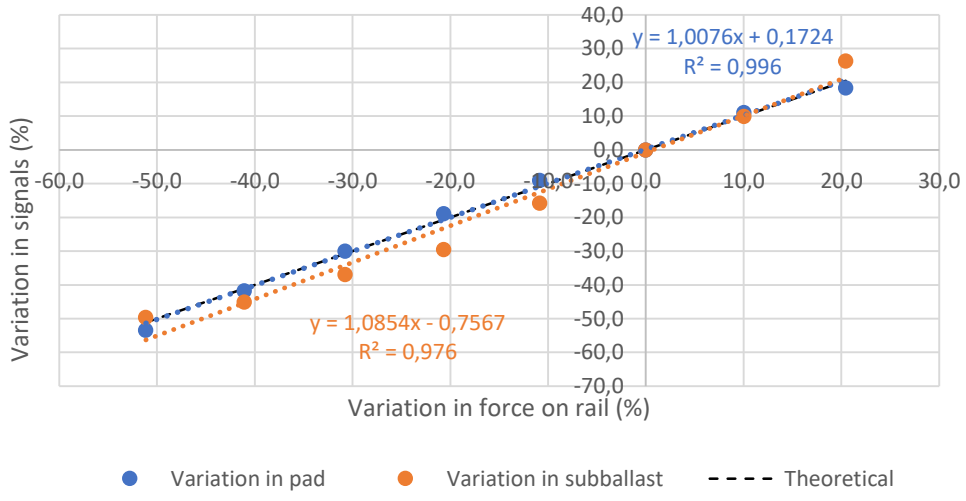

Figure 14. Correlation between train load change and the variations recorded by the sensors.

Figure 15 represents the values measured when simulating both the regular and irregular rail-wheel contact, where higher impact loads were applied on axles 7 and 10, as an example of flats in the wheels (identified by the sensors). It is seen that both piezoelectric solutions clearly detected the presence of such higher loads, and therefore, demostrated the potential applicability of smart components for monitoring traffic conditions, and load characteristics.

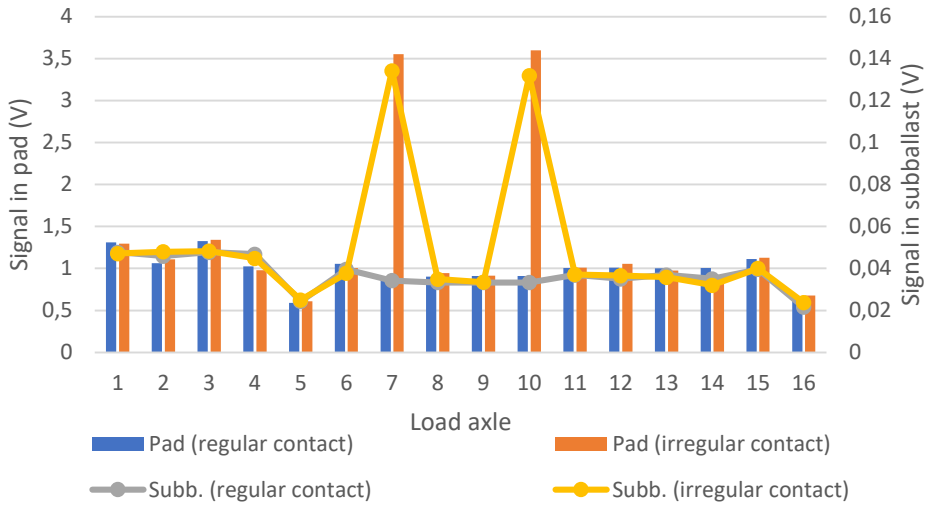

Figure 15. Results of monitoring irregular wheel-rail contact.

3.3 Application of sensored components to measure superstructure performance

For the study of the applicability of the smart rail pads to monitor superstructure performance, Figure 16 displays the signals measured by such components when applying different load levels, and using sensors on both central and adjacent sleepers under the load application. The figure shows two study cases: when all sleepers were properly laid on the ballast layer (all supported), and when the central sleeper was hanging from the adjacent ones (central one unsupported).

Results reflect how the use of the smart rail pads could clearly monitor load distributions along the sleepers when simulating train passage, obtaining in the adjacent sleeper values from around 40 to 70% lower than those measured in the central sleeper, which lead to load distributions close to 25-50-25% and 17.5-65-17.5%, respectively, across the sleepers. These values are in accordance with those measured in field studies [28, 29], particularly considering that the rail pads can be qualified as medium-stiff ones, which leads to higher load concentration at the central sleeper.

Regarding the effect of the hanging sleeper (due to, for example, differential ballast settlement), it is seen that the smart rail pad detected the reduction in stress concentration in the pad over the hanging sleeper while increasing the values measured in each adjacent sleeper. This is due to the gap existing under the hanging sleeper (in this study being simulated in the central sleeper), causing higher load oscillations because of weaker supports, thus distributing applied loads to the adjacent sleepers; also in agreement with previous studies [9]. Therefore, this confirms that this solution could be appropriate for monitoring both traffic and track conditions, as well as the evolution of differential track settlements, for example.

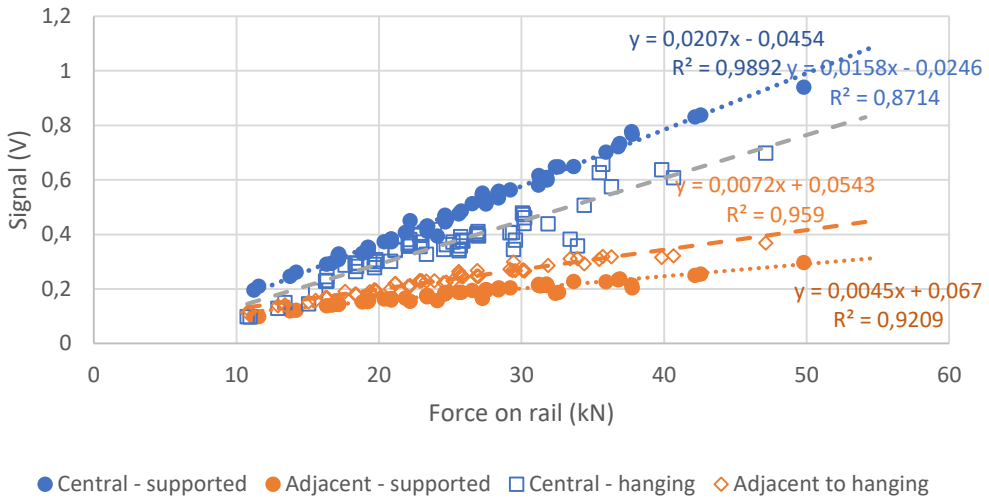

Figure 16. Results from smart rail pad monitoring rail load distribution on different sleepers, and detecting hanging sleepers.

In addition, Figure 17 compares the signals measured by the central sleeper when properly laid on the ballast layer and in the case of a hanging sleeper, representing the signals under similar loads at a constant frequency of 5 Hz for a clearer analysis. Results denote that not only was the load level reduced in the case of the hanging sleeper, but also the signal wave form varied from the reference case (supported sleeper), obtaining a more irregular signal.

Therefore, the results of the analysis for this phenomenon could be used in conjunction with those for the detection of this problem on railway tracks through the use of the smart rail pads. In particular, Figure 18 proves that the case with the hanging sleeper led to lower values of signal amplitude, while reducing also the frequency between the maximum and minimum value of each wave (flatter waves).

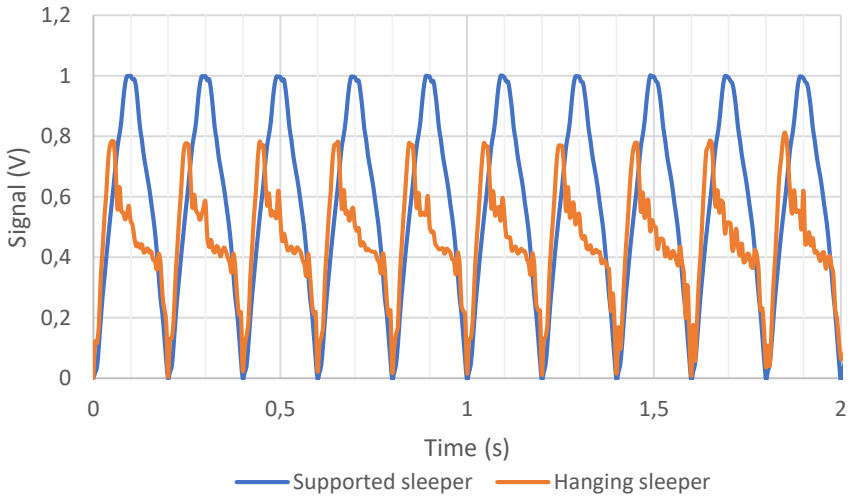

Figure 17. Waves recorded by the smart rail pad for supported and hanging sleepers.

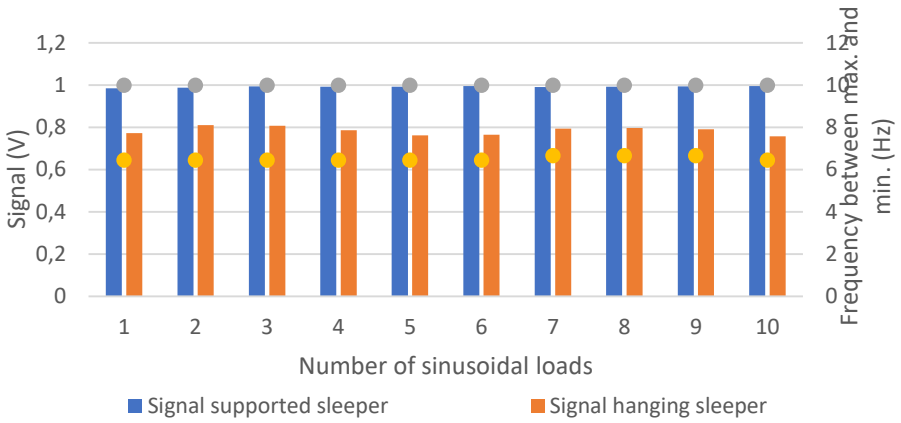

Figure 18. Results of monitoring hanging sleeper versus properly seated sleeper.

4. Conclusions

The present paper focused on studying the ability of sensored sustainable pads, made from recycled polymers and containing standard piezoelectric devices, to be used as both smart rail pads and sensoring devices in bituminous sub-ballast to monitor railway traffic and track state by detecting changes in load transmission from wheels through track components. For this purpose, a series of full-scale laboratory tests were carried out to simulate train passage under different scenarios, varying mainly the level of axle loads (with and without the simulation of irregular rail-wheel contact loads) and the conditions of track configuration (reproduced in a testing box). From this study, the following conclusions can be drawn:

- From the study of the calibration and design of the smart components (smart rail pads and smart bituminous sub-ballast), it was seen that the track configuration or boundary conditions can influence the signal recorded by the smart rail pads, obtaining lower values of voltage amplitude when reducing the strength of the sleeper support. This means that sensor calibration would be needed in field applications, when absolute signal values are required.
- The higher the depth of a piezoelectric sensor in a sub-ballast layer, the lower the signal measured, but the lower the susceptibility to the horizontal distance of detection between load application and sensor placement. This could be related to the load distribution and wave propagation of the load into the material, which could also require field calibration for the implementation of this solution, when absolute values are needed.
- Nonetheless, both smart solutions demonstrate their capacity to detect traffic variations by measuring the relative change in sensor signals recorded. Smart rail pads showed a clearer capacity to monitor load variations from the simulation of trains with different axle loads, while the smart bituminous sub-ballast showed a higher dependence on stress level magnitude; detecting changes more accurately at high load ranges.
- The smart components, including standard piezoelectrics, were shown to provide an appropriate solution for measuring traffic conditions and irregularities in the wheel-rail contact (due to different causes like flats in wheels

or impacts in crossings). In particular, smart pads presented a higher accuracy in this context, which was also demonstrated for their use in detecting vehicle weight.
- In addition, the smart rail pads showed a good potential to be used for monitoring track performance by recording changes in load distribution through the superstructure.
- This paper demonstrates the capacity of the piezoelectric sensors to measure load distributions from the rail on various sleepers, being able to detect changes in load concentration due to phenomena like the hanging sleeper. This monitoring solution recorded the reduction of stresses on the hanging sleeper (in a full-scale three-sleeper setup), while varying the form of the electrical signal measured, increasing the frequency between the peaks of wave amplitude, among other factors that could be measured to predict track failure.

Based on these results, it could be said that the smart components studied in this article, using common and affordable piezoelectric devices, could provide an alternative monitoring system for the continuous measurement of traffic conditions and irregularities in the wheel-rail contact (due to different causes like flats in wheels or impacts in crossings), as well as measuring changes in load transmission through the track. This could be used, for example, in control sections or problematic points along the railway line for continuous monitoring. Nonetheless, further research is still required to assess different issues like the durability of the smart components, possibility of obtaining a wireless sensor network, and in-field experiences, among other future works.

5. Acknowledgments

The present study has been conducted within the framework of the ECO-Smart Pads (Smart and Sustainable Resilient Pads for the Railway of the Future, RTI2018-102124-J-IOO) and HP-RAIL (Smart technologies & high performance materials for the next railway generation, RTC-2017-6510-4) research projects, funded by the Ministry of Science, Innovation and University of Spain and the Ministry of Economy and Competitiveness of Spain, respectively.

6. References

[1] EC-European Comission. https://ec.europa.eu/transport/themes/mobilitystrategy_en (last access on 04/05/2021)

[2] C. Chen, T. Xu, G. Wang, B. Li, 2020. Railway turnout system RUL prediction based on feature fusion and genetic programming, Measurement. 151, 107162.

[3] A. Kampczyk, K. Dybel, 2021. Integrating surveying railway special grid pins with terrestrial laser scanning targets for monitoring rail transport infrastructure, Measurement. 170, 108729.

[4] M. Strach, A. Kampczyk, 2011. Surveys of geometry of rail track facilities and railway tracks in the infrastructure of rail transport, Rep. Geod. 1, 429–437.

[5] M. Nordlindh, M. Berg. Implementing Internet of Things in the Swedish Railroad Sector: Evaluating Design Principles and Guidelines for E-Infrastructures, Uppsala University, Uppsala, Sweden, 2012.

[6] S.L. Zhang, C.G. Koh, K.S.C. Kuang, 2019. Proposed rail pad sensor for wheel-rail contact force monitoring, Smart Mater. Struct. 27, 115041.

[7] D. Khairallah, J. Blanc, L.M. Cottineau, P. Hornych, J. Piau, S. Pouget, M. Hosseingholian, A. Ducreau, F. Savin, 2019. Monitoring of railway structures of the high speed line BPL with bituminous and granular sublayers, Constr Build Mater. 211, 337-348.

[8] A. Sabato, C. Niezrecki, 2017. Feasibility of digital image correlation for railroad tie inspection and ballast support assessment, Measurement 103, 93–105.

[9] T. Stark, S. Wilk, 2016. Root case of differential movement at bridge transition zones. Proc Inst Mech Eng F J Rail Rapid Transit. 230, 1257-1269.

[10] H. Wang, V. Markine, 2019. Dynamic behaviour of the track in transitions zones considering the differential settlement, J. Sound Vib. 459, 114863.

[11] A.R.A.S. Section, H.S. Balliet, The Invention of the Track Circuit: the History of Dr. William Robinson's Invention of the Track Circuit, the Fundamental Unit Which Made Possible Our Present Automatic Block Signaling and Interlocking Systems: Signal Section, American Railway Association, New York, 1922.

[12] C. Du, S. Dutta, P. Kurup, T. Yu, X. Wang, 2020. A review of railway infrastructure monitoring using fiber optic sensors. Sens. Actuators, A 303, 111728

[13] P. Jiao, K-J. Egbe, Y. Xie, A. Nazar, 2020. Piezoelectric sensing techniques in structural health monitoring: a state-of-the-art review. Sensors, 20 (13): 3730.

[14] R. Huff, C. Berthelot, B. Daku, 2005. Continuous primary dynamic pavement response system using piezoelectric axle sensors. Canadian Journal of Civil Engineering, 32(1), 260-269.

[15] A. Alavi, H. Hasni, N. Lajnef, K. Chatti, 2016. Continuous health monitoring of pavement systems using smart sensing technology. Construction and Building Materials, 114, 719-736

[16] S. Song, Y. Hou, M. Guo, L. Wang, An investigation on the aggregate-shape embedded piezoelectric sensor for civil infrastructure health monitoring. Constr Build Mater. 131 (2017) 57-65.

[17] Q. Zhao, L. Wang, K. Zhao, H. Yang, 2019. Development of a novel piezoelectric sensing system for pavement dynamic load identification. Sensors, 19(21):4668.

[18] J.M. Castillo-Mingorance, M. Sol-Sánchez, F. Moreno-Navarro, M.C. Rubio-Gámez, 2020. A critical review of sensors for the continuous monitoring of smart and sustainable railway infrastructures. Sustainability 12 (22) 9428.

[19] S.J. Lee, D. Ahn, I. You, D.Y. Yoo, Y.S. Kang, 2020. Wireless cement-based sensor for self-monitoring of railway concrete infrastructures. Autom. Constr. 119, 103323.

[20] EN 13146-9. Railway applications. Track. Test methods for fastening systems. Part 9: Determination of stiffness. European Committee for Standardization. Asociación Española de Normalización y Certificación, Spain, 2011.

[21] EN 13108-1. Bituminous mixtures - Material specifications - Part 1: Asphalt Concrete. European Committee for Standardization. Asociación Española de Normalización y Certificación, Spain, 2007.

[22] DIN 45673-5. Mechanical vibration. Resilient elements used in railway tracks. Part 5: Laboratory test procedures for under-ballast mat. Berlin, Germany, 2010.

[23] M. Sol-Sánchez, L. Pirozzolo, F. Moreno-Navarro, M.C Rubio-Gámez, 2016. A study into the mechanical performance of different configurations for the railway track section: a laboratory approach, Eng. Struct. 119, 13-23.

[24] E. Ferro; J. Harkness, L. Le Pen, 2020. The influence of sleeper material characteristics on railway track behaviour: concrete vs composite sleeper. Transp. Geotech. 23, 100348.

[25] L. Bryson, J. Rose, Pressure Measurements and Structural Performance of Hot Mixed Asphalt Railway Trackbeds. Bearing Capacity of Roads, Railways and Airfields. 8th International Conference (BCR2A'09), Champaign IL, United States, 2009.

[26] EN 103807. Plate loading test of soils by means of dynamic plate. Part 2: Rigid plate, diameter 2r=300 mm, Method 2. European Committee for Standardization. Asociación Española de Normalización y Certificación, Spain, 2008.

[27] EN 13450. Aggregates for railway ballast. European Committee for Standardization. Asociación Española de Normalización y Certificación, Spain, 2003.

[28] S. Wilk, T. Stark, J. Rose, 2016. Evaluating tie support at railway bridge transitions, Proc Inst Mech Eng F J Rail Rapid. 230, 1336-1350.

[29] T. Sussman, Field conditions observed at a site with concrete tie base abrasion. Railway Engineering, Conference at Edinburg, 2017.